Propriétés analytiques des solutions de viscosité des équations integro-différentielles : visualisation et restauration d'images par mouvements de courbure

Adina Ciomaga

ECOLE NORMALE SUPERIEURE DE CACHAN
DOCTORAL SCHOOL OF PRACTICAL SCIENCES

P H D T H E S I S

to obtain the title of

DOCTOR OF PHILOSOPHY
Specialty : MATHEMATICS

Defended by

Adina CIOMAGA

Analytical Properties of Viscosity Solutions for Integro-Differential Equations. Image Visualization and Restoration by Curvature Motions

Supervisors: Guy BARLES and Jean-Michel MOREL

Jury :

Reviewers :	Vicent CASELLES	-	Universitat Pompeu Fabra, Barcelona
	Hitoshi ISHII	-	Waseda University, Tokyo
	Takis SOUGANIDIS	-	University of Chicago
Supervisors :	Guy BARLES	-	LMPT, Université de Tours
	Jean-Michel MOREL	-	CMLA, ENS Cachan
Examinators :	Antonin CHAMBOLLE	-	CMAP, Ecole Polytechnique
	Benoît PERTHAME	-	Université Pierre et Marie Curie.

April 29, 2011

ECOLE NORMALE SUPERIEURE DE CACHAN

ECOLE DOCTORALE SCIENCES PRATIQUES

T H E S E DE D O C T O R A T

pour obtenir le grade de

DOCTEUR DE L'ECOLE NORMALE SUPERIEURE DE CACHAN
Specialité : MATHEMATIQUES

Présentée par

Adina CIOMAGA

Propriétés Analytiques des Solutions de Viscosité des Equations Integro-Différentielles. Visualisation et Restauration d'Images par Mouvements de Courbure

Directeurs de thèse: Guy BARLES and Jean-Michel MOREL

Jury :

Reviewers :	Vicent CASELLES	-	Universitat Pompeu Fabra, Barcelona
	Hitoshi ISHII	-	Waseda University, Tokyo
	Takis SOUGANIDIS	-	University of Chicago
Supervisors :	Guy BARLES	-	LMPT, Université de Tours
	Jean-Michel MOREL	-	CMLA, ENS Cachan
Examinators :	Antonin CHAMBOLLE	-	CMAP, Ecole Polytechnique
	Benoît PERTHAME	-	Université Pierre et Marie Curie.

29 Avril, 2011

Abstract

The present dissertation has two independent parts.

Viscosity solutions theory for nonlinear Integro-Differential Equations

We consider nonlinear elliptic and parabolic Partial Integro-Differential Equations (PIDES), where the nonlocal terms are associated to jump Lévy processes. The present work is motivated by the study of the *Long Time Behavior of Viscosity Solutions for Nonlocal PDEs, in the periodic setting*. The typical result states that the solution $u(\cdot,t)$ of the initial value problem for parabolic PIDEs behaves like $\lambda t + v(x) + o(1)$ as $t \to \infty$, where v is a solution of the stationary ergodic problem corresponding to the unique ergodic constant λ. In general, the study of the asymptotic behavior relies on two main ingredients: regularity of solutions and the strong maximum principle.

We first establish *Strong Maximum Principle* results for semi-continuous viscosity solutions of fully nonlinear PIDEs. This will be used to derive Strong Comparison results of viscosity sub and super-solutions, which ensure the up to constants uniqueness of solutions of the ergodic problem, and subsequently, the convergence result. Moreover, for super-quadratic equations the strong maximum principle and accordingly the large time behavior require Lipschitz regularity.

We then give *Lipschitz* estimates of viscosity solutions for a large class of nonlocal equations, by the classical Ishii-Lions's method. Regularity results help in addition solving the ergodic problem and are used to provide existence of periodic solutions of PIDEs.

In both cases, we deal with a new class of nonlocal equations that we term *mixed integro-differential equations*. These equations are particularly interesting, as they are degenerate both in the local and nonlocal term, but their overall behavior is driven by the local-nonlocal interaction, e.g. the fractional diffusion may give the ellipticity in one direction and the classical diffusion in the complementary one.

Image Visualization and Restoration by Curvature Motions

The role of curvatures in visual perception goes back to 1954 and is due to Attneave. It can be argued on neurological grounds that the human brain could not possible use *all* the information provided by states of simulation. But actually human brain registers *regions where color changes abruptly (contours), and furthermore angles and peaks of curvature*. Yet, a direct computation of curvatures on a raw image is impossible. We show how curvatures can be *accurately estimated, at subpixel resolution,* by a direct computation on level lines after their independent smoothing.

To perform this programme, we build an image processing algorithm, termed *Level Lines (Affine) Shortening*, simulating a *sub-pixel* evolution of an image by mean curvature motion or by affine curvature motion. Both in the analytical and numerical framework, LL(A)S first extracts all the level lines of an image, then independently and simultaneously smooths all of its level lines by curve shortening (CS) (respectively affine shortening (AS)) and eventually reconstructs, at each time, a new image from the evolved level lines.

We justify that the Level Lines Shortening computes explicitly a viscosity solution for the *Mean Curvature Motion* and hence is equivalent with the clasical, geometric Curve Shortening.

Based on simultaneous level lines shortening, we provide an accurate visualization tool of image curvatures, that we call *an Image Curvature Microscope*. As an application we give some illustrative examples of image visualization and restoration: noise, JPEG artifacts, and aliasing will be shown to be nicely smoothed out by the subpixel curvature motion.

Résumé

Le manuscrit est constitué de deux parties indépendantes.

Propriétés des Solutions de Viscosité des Equations Integro-Différentielles.

Nous considérons des équations intégro-différentielles elliptiques et paraboliques non-linéaires (EID), où les termes non-locaux sont associés à des processus de Lévy. Ce travail est motivé par l'étude du *Comportement en temps long des solutions de viscosité des EID, dans le cas périodique.* Le résultat classique nous dit que la solution $u(\cdot, t)$ du problème de Dirichlet pour EID se comporte comme $\lambda t + v(x) + o(1)$ quand $t \to \infty$, où v est la solution du problème ergodique stationaire qui correspond à une unique constante ergodique λ. En général, l'étude du comportement asymptotique est basé sur deux arguments: la régularité de solutions et le principe de maximum fort.

Dans un premier temps, nous étudions le Principe de Maximum Fort pour les solutions de viscosité semi-continues des équations intégro-différentielles non-linéaires. Nous l'utilisons ensuite pour déduire un résultat de comparaison fort entre sous et sur-solutions des équations intégro-différentielles, qui va assurer l'unicité des solutions du problème ergodique à une constante additive près. De plus, pour des équations super-quadratiques le principe de maximum fort et en conséquence le comportement en temps grand exige la régularité Lipschitzienne.

Dans une deuxieme partie, nous établissons de nouvelles estimations *Hölderiennes et Lipschitziennes* pour les solutions de viscosité d'une large classe d'équations intégro-différentielles non-linéaires, par la méthode classique de Ishii-Lions. Les résultats de régularité aident de plus à la résolution du problème ergodique et sont utilisés pour fournir existence des solutions périodiques des EID.

Nos résultats s'appliquent à une nouvelle classe d'équations non-locales que nous appelons *équations intégro-différentielles mixtes.* Ces équations sont particulièrement intéressantes, car elles sont dégénérées à la fois dans le terme local et non-local, mais leur comportement global est conduit par l'interaction locale - non-locale, par example la diffusion fractionnaire peut donner l'ellipticité dans une direction et la diffusion classique dans la direction orthogonale.

Visualisation et Restauration d'Images par Mouvements de Courbure

Le rôle de la courbure dans la perception visuelle remonte à 1954, et on le doit à Attneave. Des arguments neurologiques expliquent que le cerveau humain ne pourrait pas possiblement utiliser *toutes* les informations fournies par des états de simulation. Mais en réalité on enregistre *des régions où la couleur change brusquement (des contours) et en outre les angles et les extremas de courbure.* Pourtant, un calcul *direct* de courbures sur une image est impossible. Nous montrons comment les courbures peuvent être *précisément évaluées, à résolution sous-pixelique* par un calcul sur les lignes de niveau après leur lissage indépendant.

Pour cela, nous construisons un algorithme que nous appelons *Level Lines (Affine) Shortening,* simulant une évolution *sous-pixelique* d'une image par mouvement de courbure moyenne ou affine. Aussi bien dans le cadre analytique que numérique, LLS (respectivement LLAS) extrait toutes les lignes de niveau d'une image, lisse indépendamment et simultanément toutes ces lignes de niveau par *Curve Shortening*(CS) (respectivement *Affine Shortening* (AS)) et reconstruit une nouvelle image. Nous montrons que LL(A)S calcule explicitement une solution de viscosité pour le *le Mouvement de Courbure Moyenne* (respectivement Mouvement par Courbure Affine), ce qui donne une équivalence avec le mouvement géométrique.

Basé sur le raccourcissement de lignes de niveau simultané, nous fournissons un outil de visualisation précis des courbures d'une image, que nous appellons *un Microscope de Courbure d'Image.* En tant que application, nous donnons quelques exemples explicatifs de visualisation et restauration d'image: du bruit, des artefacts JPEG, de l'aliasing seront atténués par un mouvement de courbure sous-pixelique.

Acknowledgments

I would like to express my warmest thanks to my advisors, Guy Barles and Jean-Michel Morel. Their expert guidance on the topics of this work has proved invaluable for my research. I am grateful for their constant support and careful suggestions, that helped me advance during my thesis. It has been an honor to work with them and a pleasure to discover them as professors of great character.

I address my warmest thanks to all the members of my jury. I thank professors Vicent Casselles, Hitoshi Ishii and Takis Souganidis, for accepting to report my thesis. Some previous works of each of them had an important role during the elaboration of my thesis and I am therefore extremely honored by their presence and interest. I sincerely thank professors Antonin Chambolle and Benoît Berthame to have agreed to take part in the jury.

Along the years I had the opportunity to exchange ideas and have many fruitful discussion with various researchers. I would like to express my admiration for professor Yves Meyer and thank him for his support and very interesting scientific conversations. I am grateful to Emmanuel Chasseigne, Cyril Imbert and Pascal Monnase, for precious advice that helped me overcome several difficulties and improve my results. It has always been a pleasure and fruitful to discuss with Antonin Chambolle, Pierre Cardaliaguet, Lionel Moisan, Francesca Da Lio, Jean-Fançois Aujol, Jerôme Darbon, Filippo Santambrogio.

I am greatful to Luis Caffarelli for his kind support and several interesting discussions. I have always admired his perspective and vision on mathematics. I thank Luis Silvestre for helping me understand some of the undertakings in regularity problems, and I greatly appreciate his kind advice.

I express my consideration and appreciation to my previous professors and mentors: Viorel Barbu, Ioan Vrabie and Cătălin Lefter, who have constantly supported me and thanks to whom I have made my carrier in mathematics. My gratitude goes as well as to Elena Adam, who instilled in me the passion for mathematics at an early age.

***

J'aimerais bien évidemment remercier toutes les personnes qui m'ont accompagné au quotidien pendant cet thèse. Les conditions de travail au CMLA ont été excellentes et j'en remercie à tous les membres! Un grand merci pour leur gentillesse et leur bienveillance à Carine, Véronique, Micheline, Virginie et Sandra. Merci aussi à Christophe et Pascal, nos informaticiens. Le monitorat que j'ai effectué au département de mathématiques de l'ENS Cachan a été une expérience très enrichissante et je remercie specialement à Jean-Michel. Merci également à Frédéric Pascal, Sylvie Fabre, Claudine Picaronny, Alain Trouvé et Filippo Santambrogio.

Je remercie spécialement à tous les doctorants et postdoctorants du CMLA : Aude, Ayman, Benjamin, Eric, Enric, F.-X., Frédéric, Frédérique, Gabrielle, Gaël, Jean-Pascal, Jérémie, Julie, Julien, Mathieu, Mauricio, Morgan, Neus, Nicolas C., Nicolas L., Pascal G., Rachel, Rafa, Saad, Vincent, Yohann, Yves, Zhongwei, et aussi à ceux qui ont été de passage par le CMLA : Alex,

Hugo, Mauricio C., Magalie, Mariano, Mariella, Sira, Yaxin et Yifei. Je remercie particulièrement à Julie et Eric pour les conversations intéressantes sur la culture française, à Neus et Aude pour les magnifiques recettes de cuisine, à Bruno et Nicolas C. pour les discussions cinéfiles, à Nicolas L. pour ses nombreux conseils en informatique, à Rafa et Gabrielle pour m'introduire en Megawave. Un grand merci à Hugo, avec qui j'ai appris Matlab. Merci également à Nick Chriss pour ses spéciaux cours d'anglais.

***

Un merci de tout mon coeur à mes amis qui ont été pratiquement ma famille en France et avec qui j'ai passé des moments inoubliables: Oana et Sergiu, Karin et Jorge, Chiara et Labib, Birte et Isa. Merci à Brittany pour les interessantes conversations d'anglais (et roumain).

***

Truly great friends are hard to find and impossible to forget. My warmest thanks go to Sys (Oana), whose kind encouragements meant so much to me, and to Elena, Laura and Larisa, who have been unconditionally supportive and understanding, despite the distance.

***

Last but not least, I would like to express all my gratitude to my parents, whose enthusiasm for my projects encouraged me on the way. I am especially grateful to Daniel, whose care and advice, confidence and patience have not only been inestimable but helped me find harmony in life.

to Vera and Jan,
to Daniel

Contents

CHAPTER 1

Introduction

If I have been able to see further, it was only because I stood on the shoulders of giants.
Isaac Newton (1643 - 1727)

Abstract: This chapter provides a detailed outline of the manuscript. We briefly describe the main contributions of the present disertation. The thesis has two independent parts: viscosity solutions theory for nonlinear integro-differential equations and image visualization and restoration by curvature motions. We present each in turn.[1][2]

Résumé : Ce chapitre est un sommaire détaillé du manuscrit, où nous présentons les principales contributions. Le manuscrit est constitué de deux parties indépendantes : la premiere porte sur sur la théorie de solutions de viscosité pour des équations integro-différentielles non-linéaires et la seconde traite de l'utilisation des mouvements par courbure pour la visualisation et la restauration des images numériques. Nous présentons chacune à son tour.

Keywords: nonlinear integro-differential equations, Strong Maximum Principle, Hölder and Lipschitz regularity, viscosity solutions, Lévy processes; mean curvature motion, affine curvature motion, curve shortening, affine shortening, level lines, topographic maps.

[1] For the sake of clarity, the contributions of the thesis are listed dryly. Rigouros assumptions, bibliographic notes and comparisons will be extensively given in the following chapters.

[2] Paragraphs herein will be largely used for the introductions of the corresponding chapters.

Contents

1.1 Viscosity Solutions Theory for Integro-Differential Equations

Nonlocal equations occur in the theory of Lévy jump-diffusion processes and have an extensive range of applications (e.g. physics, engineering, ecology and economics). Throughout this work, we mainly refer to equations of the type

$$u_t + F(x,t,Du,D^2u,\mathscr{I}[x,t,u]) = 0 \text{ in } \Omega \times (0,T) \tag{1.1}$$

and their stationary variant, where $\mathscr{I}[x,t,u]$ is a nonlocal operator

$$\mathscr{I}[x,t,u] = \int_{\mathbb{R}^d} (u(x+z,t) - u(x,t) - Du(x,t)\cdot z 1_B(z))\mu_x(dz), \tag{1.2}$$

$1_B(z)$ denotes the indicator function of the unit ball B and $\{\mu_x\}_{x\in\Omega}$ a family of Lévy measures, or a Lévy-Itô operator of the form

$$\mathscr{J}[x,t,u] = \int_{\mathbb{R}^d} (u(x+j(x,z),t) - u(x,t) - Du(x,t)\cdot j(x,z) 1_B(z))\mu(dz) \tag{1.3}$$

with μ a Lévy measure and $j(x,z)$ the size of the jumps at x.

The theory of viscosity solutions has been extended for a rather long time to Partial Integro-Differential Equations (PIDEs). Some of the first papers are due to Soner [Son86a], [Son86b], in the context of stochastic control jump diffusion processes. Following his work, existence and comparison results of solutions for *first order PIDEs* were given by Sayah in [Say91a] and [Say91b]. When these equations involve *bounded integral operators*, general existence and comparison results for semi-continuous and unbounded viscosity solutions were found by Alvarez and Tourin [AT96].

Jakobsen and Karlsen in [JK06] used the original approach due to Jensen [Jen88], Ishii [Ish89], Ishii and Lions [IL90], Crandall and Ishii [CI90] and Crandall, Ishii and Lions [CIL92]

for proving comparison results for viscosity solutions of nonlinear degenerate elliptic integro-partial differential equations with second order nonlocal operators. Parabolic versions of their main results were given in [JK05]. They give an analogous of Jensen-Ishii's Lemma, a keystone for many comparison principles, but they are restricted to *sub-quadratic solutions*.

The viscosity theory for general PIDEs has been recently revisited and extended to *solutions with arbitrary growth at infinity* by Barles and Imbert [BI08]. The authors provided as well a variant of Jensen-Ishii's Lemma for general integro-differential equations. We refer in our work to viscosity solutions as they were defined by Barles and Imbert [BI08].

Motivation: Long Time Behavior of Viscosity Solutions[3]

Our work on regularity of viscosity solutions and the strong maximum principle for (mixed) nonlocal equations was motivated by the study of long time behavior of viscosity solutions.

Recast shortly, the asymptotic behavior as $t \to \infty$ of *periodic* solutions of integro-differential equations is this. Under suitable assumptions on the nonlinearity F, it is possible to show that the solution of the initial value problem

$$\begin{cases} u_t + F(x, Du, D^2u, \mathscr{I}[x,t,u]) = 0, & \text{in } \mathbb{R}^d \times (0,+\infty) \\ u(x,0) = u_0(x), & \text{in } \mathbb{R}^d \end{cases} \tag{1.4}$$

with $u_0 \in C^{0,\alpha}(\mathbb{R}^d)$ / $Lip(\mathbb{R}^d)$ and periodic, satisfies

$$u(x,t) - \lambda t - v(x) - m \to 0, \text{ as } t \to \infty, \text{ uniformly in } x, \tag{1.5}$$

where v is a periodic solution of the stationary ergodic problem with ergodicity constant λ

$$F(x, Dv, D^2v, \mathscr{I}[x,v]) + \lambda = 0, \text{ in } \mathbb{R}^d \tag{1.6}$$

and m is a constant. This type of behavior has been established in a series of papers in the local case. The closest approach to our work is the one described by Barles and Souganidis in [BS01] for *space-time periodic solutions of quasilinear parabolic equations*. However, similar results for parabolic equations were developed with other techniques, such as degree theory (see for example [NR97]).

There are two types of results to be proved when studying the long time behavior of solutions.

1. **The existence of a unique λ and of a $C^{0,\alpha}$ or $Lipschitz$ periodic solution of the stationary ergodic problem (1.6).**

   Theorem 1.1.1. *There exists a unique λ such that the cell problem (1.6) has a periodic viscosity solution $v \in C^{0,\alpha}(\mathbb{R}^d)$ / $Lip(\mathbb{R}^d)$. In addition, when $v \in Lip(\mathbb{R}^d)$, the solution is unique up to constants.*

   The ergodic problem does not have in general a unique solution even up to an additive constant. Instead, when $v \in Lip(\mathbb{R}^d)$, *applying Strong Maximum Principle for the linearized equation*, we get uniqueness up to constants.

[3] work in progress, out of scope of this PhD thesis.

For proving the uniqueness and existence of λ and the existence of v one uses the classical argument introduced by Lions, Papanicolau and Varadhan in [LV] and considers small perturbations of the equation, of the form $F+\varepsilon u$. Therefore it shall be necessary at some point to show the compactness of the approximate solutions. This requires in particular *regularity of solutions* and if/when possible *uniform gradient bounds*.

2. **The convergence as $t\to\infty$ of the solution $u(x,t)$ of (1.4)**, whose proof relies heavily on the *strong maximum principle*.

Theorem 1.1.2. *For every initial data $u_0 \in Lip(\mathbb{R}^d)$, $\mathbb{Z}^d$ - periodic in x, there exists a unique solution $u \in Lip(\mathbb{R}^d \times [0,\infty))$ of (1.4), $\mathbb{Z}^d$ - periodic in x. In addition*

$$u(x,t) - \lambda t - v(x) - \overline{m} \to 0, \ \text{as } t\to\infty \tag{1.7}$$

where $v \in Lip(\mathbb{R}^d)$ is a bounded $\mathbb{Z}^d$-periodic viscosity solution of the stationary ergodic problem (1.6) with ergodic constant λ, and $\overline{m}$ is a constant.

We give below a brief insight into the proof, in order to see how we employ Strong Maximum Principle. Remark that $u(x,t)$ and $v(x)+\lambda t$ are both solutions in $\mathbb{R}^d\times(0,\infty)$ of the evolution equation (1.4). By standard comparison arguments we would have

$$m(t) = \max_{x\in\Pi}\big(u(x,t)-\lambda t - v(x)\big) \searrow \overline{m} \text{ as } t\to\infty. \tag{1.8}$$

It is possible to show that for the of $\mathbb{Z}^d$-periodic functions $w(x,t)=u(x,t)-\lambda t$ there exist a sequence $(w(\cdot,\cdot+t_n))_{n\geq 0}$ converging uniformly to a function in $C(\mathbb{R}^d\times[0,\infty))$

$$w(x,t+t_n)\to\overline{w}(x,t), \text{ as } t_n\to\infty.$$

The limit $\overline{w}$ is, by the stability properties of the viscosity solutions, a $\mathbb{Z}^d$-periodic viscosity solution of

$$\begin{cases} \overline{w}_t + F(x,D\overline{w},D^2\overline{w},\mathscr{I}[x,t,\overline{w}]) + \lambda = 0, & \text{in } \mathbb{R}^d\times(0,+\infty) \\ \overline{w}(x,0) = \overline{v}(x), & \text{in } \mathbb{R}^d. \end{cases} \tag{1.9}$$

Passing to the limit for $t_n\to\infty$ in $m(t+t_n) = \max_{x\in\Pi}\big(w(x,t+t_n)-v(x)\big)$ and using the uniform convergence of the sequence $(w(\cdot,\cdot+t_n))_{t_n}$ we obtain that

$$\overline{m} = \max_{x\in\Pi}\big(\overline{w}(x,t)-v(x)\big), \forall\, t>0.$$

At his point we use Strong Maximum Principle to get that $\overline{w}(x,t) = v(x)+\overline{m}$. We then show that the whole sequence converges to the same limit.

All in all, the study of the asymptotic behavior relies on two key ingredients: regularity results and the strong maximum principle.

1.1.1 Lévy Processes and Integro-Differential Equations (Chapter 2)

We give a brief overview of Lévy processes and and present their connection with integro-differential operators. In the second part we present some recent developments for Partial Integro-Differential Equations involving nonlocal terms associated to Lévy processes.

1.1.2 Strong Maximum Principle (Chapter 3)

Our study began with an investigation of the Strong Maximum Principle for viscosity solutions of second-order non-linear parabolic integro-differential equations [Cio]. It is worth mentioning that Strong Maximum Principle for linear elliptic equations goes back to Hopf in the 20s and to Nirenberg in 1953.

We study separately the propagation of maxima in the horizontal component of the domain and the local vertical propagation in simply connected sets of the domain. For horizontal propagation of maxima we give two types of results: one coming from the structure of the nonlocal operator and the other as the natural extension of the classical results of local propagation of maxima. We point out that we do not restrict ourselves to the periodic setting.

To be more precise, by the Strong Maximum Principle for equation (1.1) in an open set $\Omega \times (0,T)$ we mean the following.

SMaxP: *Any* $u \in USC(\mathbb{R}^d \times [0,T])$ *viscosity subsolution of (1.1) that attains a maximum at* $(x_0,t_0) \in \Omega \times (0,T)$ *is constant in* $\Omega \times [0,t_0]$.

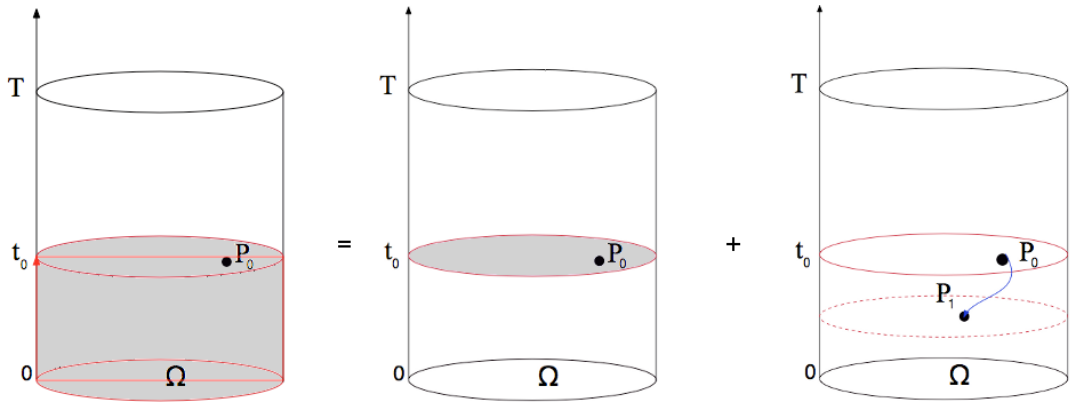

Figure 1.1: Strong Maximum Principle follows from the horizontal and vertical propagation of maxima.

Similar to smooth solutions of parabolic PDEs, Strong Maximum Principle consists of

- *horizontal propagation of maxima:* if the maximum is attained at some point (x_0,t_0) then the function becomes constant in the connected component $C(P_0)$ of the domain $\Omega \times \{t_0\}$ which contains the point (x_0,t_0) , and
- *local vertical propagation:* if the maximum is attained at some point (x_0,t_0) then at any time $t < t_0$ one can find another point (x,t) where the maximum is attained.

The propagation of maxima in $\Omega \times (0,t_0)$ then follows by standard covering arguments.

The horizontal propagation of maxima requires two different perspectives.

Translations of measure supports. Using the structure of the nonlocal operator, we show that *Strong Maximum Principle* holds whenever the whole domain (not necessarily connected) can be covered by translations of measure supports, starting from a maximum point. Under quite general assumptions on the nonlinearity F, we show that

Theorem 1.1.3. *If u attains a global maximum at $(x_0, t_0) \in \mathbb{R}^d \times (0,T)$, then u is constant on $\overline{\bigcup_{n\geq 0} A_n} \times \{t_0\}$ with*

$$A_0 = \{x_0\}, \quad A_{n+1} = \bigcup_{x\in A_n} (x + supp(\mu_x)). \tag{1.10}$$

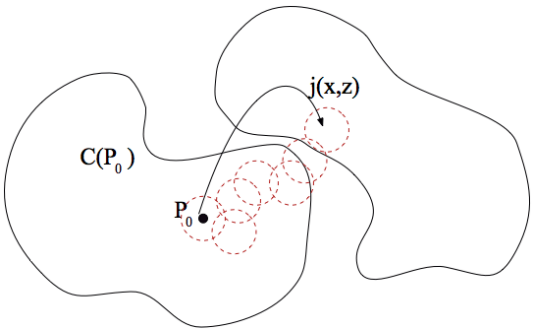

Figure 1.2: Horizontal propagation of maxima by translations of measure supports.

This is the case for example of a pure nonlocal diffusion

$$u_t - \mathscr{I}[x,t,u] = 0 \text{ in } \mathbb{R}^d \times (0,T) \tag{1.11}$$

where $\mathscr{I}$ is an isotropic Lévy operator of form (1.2), integrated against the Lévy measure associated with the fractional Laplacian $(-\Delta)^{\beta/2}$:

$$\mu(dz) = \frac{dz}{|z|^{d+\beta}}.$$

Nevertheless, there are equations for which maxima do not propagate just by translating measure supports, such as pure nonlocal equations with nonlocal terms associated with the fractional Laplacian, but whose measure supports are defined only on half space.

Non-degeneracy assumptions. However, we manage to show that the propagation of maxima holds, under suitable *non-degeneracy and scaling* assumptions on the nonlinearity F.

We deal with *non-degenerate Levy measures*, in the sense given by following assumption

(*N*) For any $x \in \Omega$ there exist $1 < \beta < 2$, $0 \leq \eta < 1$ and a constant $C_\mu(\eta) > 0$ such that the following holds on $\mathscr{C}_{\eta,\gamma}(p) = \{z;\ (1-\eta)|z||p| \leq |p\cdot z| \leq 1/\gamma\}$, with $p \in \mathbb{R}^d$, $0 < |p| < R$

$$\int_{\mathscr{C}_{\eta,\gamma}(p)} |z|^2 \mu_x(dz) \geq C_\mu(\eta)\gamma^{\beta-2}, \forall \gamma \geq 1$$

Theorem 1.1.4. *If a viscosity subsolution u attains a maximum at $P_0 = (x_0, t_0)$, then u is constant (equal to the maximum value) in the horizontal component of the domain, passing through point P_0.*

This applies for example to a pure nonlocal diffusion (1.11) where $\mathscr{I}$ is an isotropic Lévy operator of form (1.2), integrated against the Lévy measure associated with the fractional Laplacian $(-\Delta)^{\beta/2}$, and *with support in half hyperplane*

$$\mu(dz) = 1_{\{z_1 \geq 0\}} \frac{dz}{|z|^{d+\beta}}.$$

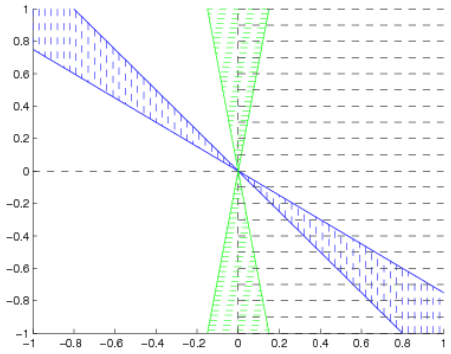

Figure 1.3: Non-degeneracy: measures charge cones $\mathscr{C} = \{z;\ (1-\eta)|z||p| \leq |p \cdot z| \leq 1/\gamma\}$.

Mixed integro-differential equations

$$u_t - \mathscr{I}_{x_1}[u] - \frac{\partial^2 u}{\partial x_2^2} = 0 \text{ in } \mathbb{R}^2 \times (0,T) \tag{1.12}$$

i.e. equations for which local diffusions occur only in certain directions and nonlocal diffusions on the orthogonal ones *cannot be handled by simple techniques.*

This is particularly interesting since the equations are degenerate both in the local and nonlocal term, but the overall behavior is driven by their interaction (the two diffusions cannot cancel simultaneously). We recall that the diffusion term gives the ellipticity in the direction of x_2, while the nonlocal term gives it in the direction of x_1

$$\mathscr{I}_{x_1}[u] = \int_{\mathbb{R}} (u(x_1 + z_1, x_2) - u(x) - \frac{\partial u}{\partial x_1}(x) \cdot z_1 1_{[-1,1]}(z_1)) \mu_{x_1}(dz_1).$$

In this case, *the non-degeneracy argument applies with respect to the variable x_1*, which is shown to be a sufficient condition for the mixed equation above to satisfy the Strong Maximum Principle.

Local vertical propagation of maxima occurs under softer assumptions on the non-degeneracy and scaling conditions. We establish the following result, under some specific assumptions on F.

Theorem 1.1.5. *Let $u \in USC(\mathbb{R}^d \times [0,T])$ be a viscosity subsolution of (1.1) that attains a maximum at $P_0 = (x_0, t_0) \in Q_T$. Then any rectangle $\mathscr{R}_0(x_0,t_0) = \{(x,t) || x^i - x_0^i| \leq a^i, t_0 - a_0 \leq t \leq t_0\}$ contains a point $P \neq P_0$ such that $u(P) = u(P_0)$.*

As an application, we use the Strong Maximum Principle to prove a *Strong Comparison Result* of viscosity sub and supersolution for integro-differential equations of the form (1.1) with the Dirichlet boundary condition

$$u = \varphi \text{ on } \Omega^c \times [0,T] \tag{1.13}$$

where φ is a continuous function. Namely, for certain nonlinearities we have the sequel result.

Theorem 1.1.6 (Strong Comparison Principle)**.** *Assume the Lévy measure μ satisfies assumption (N) with $\beta > 1$. Let $u \in USC(\mathbb{R}^d \times [0,T])$ be a viscosity subsolution and $v \in LSC(\mathbb{R}^d \times [0,T])$ a viscosity supersolution of (1.1), with the Dirichlet boundary condition (1.13). If $u - v$ attains a maximum at $P_0 = (x_0, t_0) \in \Omega \times (0,T)$, then $u - v$ is constant in $C(P_0)$.*

Each of these results hold under suitable assumptions on the nonlinearity F, that we make precise in each chapter. We mention that they extend to parabolic integro-differential equations the results obtained by Da Lio in [DL04] for fully nonlinear degenerate elliptic equations, as well as the maximum principle for nonlocal operators generated by nonnegative kernels obtained by Coville in [Cov08].

1.1.3 Regularity of Solutions (Chapter 4)

There are two approaches for proving the Hölder regularity of *viscosity solutions* of integro-differential equations:

- either by Harnack inequalities (see Silvestre [Sil06] Caffarelli and Silvestre [CS09])
- or by Ishii-Lions's method [IL90] (see Barles, Chasseigne and Imbert [BCI11]).

Recently there have been many papers dealing with $C^{0,\alpha}$ estimates and regularity of solutions (not necessarily in the viscosity setting) for fully nonlinear PIDEs and the literature has been considerably enriched. We give an overview of the existent results in the ongoing chapter, but send the reader to Chapter 2 for further details on the references.

The two above methods do not cover the same class of equations and each of it has its own advantages. The powerful Harnack approach for *strictly elliptic fully nonlinear equations* leads in general to further regularity such as $C^{1,\alpha}$, but requires some integrability condition of the measure at infinity. On the other hand, viscosity methods apply under weaker ellipticity assumptions and therefore deal with a large class of *degenerate, fully nonlinear equations*, in particular with *super-linear gradient growth*, allow measures which are only bounded at infinity, but do not seem to yield further regularity.

We refer in the sequel to the direct viscosity method, introduced by Ishii and Lions in [IL90]. According to it, in order to establish Lipschitz or Hölder regularity of the solution u, we shift the function u and show that the corresponding difference can be uniformly controlled by some radial function $\phi(|z|) = L|z|^\alpha$, for $\alpha \in (0,1]$.

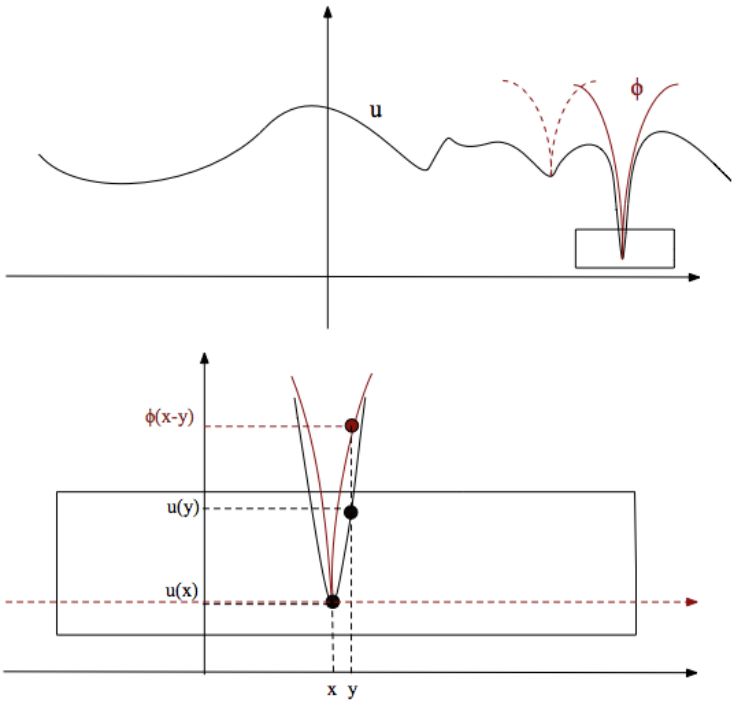

Figure 1.4: Uniformly controlling the shift of u by $\phi(|x-y|) = L|x-y|^\alpha$, for all $\alpha \in (0,1]$.

This simple method, closely related to classical viscosity solutions theory, was recently explored by Barles, Chasseigne and Imbert in [BCI11] in order to prove $C^{0,\alpha}$ estimates of solutions of PIDEs. They were able to deal with a large class of integro-differential equations as well as a general class of nonlocal operators, satisfying proper assumptions. The authors prove that the solution is α-Hölder continuous for any $\alpha < \min(\beta, 1)$, where β characterizes the singularity of the measure associated with the integral operator. However, in the case $\beta \geq 1$ the ad-literam estimates do not yield Lipschitz regularity.

In addition, they assume the equation is elliptic in a generalized sense, i.e. at each point of the domain, the ellipticity comes either from the second order term, or from the nonlocal term. We realized when studying the Strong Maximum Principle that another type of ellipticity might arise: at each point, the nonlinearity is *degenerate individually in the second-order term, and in the nonlocal term*, but *the combination of the local and the nonlocal diffusions renders the nonlinearity uniformly elliptic*. We recall that we termed this type of equations *mixed integro-differential equations* since for example the diffusion term might give the ellipticity in one direction, whereas the nonlocal term in the complementary direction. For this type of non-degeneracy, the assumptions in [BCI11] are not satisfied and we provide new Hölder and Lipschitz regularity results in this framework.

The simplest example of mixed integro-differential equations is given by

$$-\Delta_{x_1} u + (-\Delta_{x_2} u)^{\beta/2} = f(x).$$

In this case local diffusions occur only in x_1-direction and nonlocal diffusions in x_2-direction.

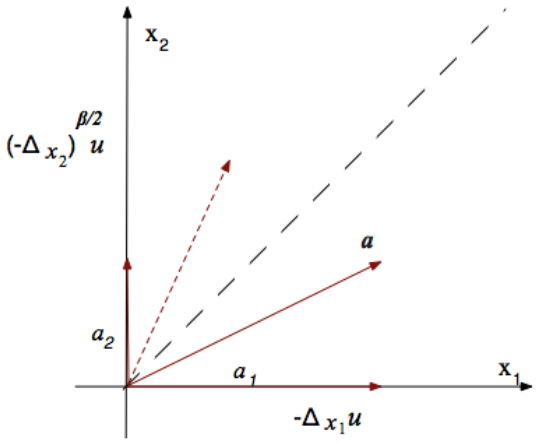

Figure 1.5: Mixed integro-differential equation: classical diffusion occurs in x_1 direction and fractional diffusion in the complementary direction x_2.

Using Ishii-Lions's viscosity method, we are able to establish both *Hölder and Lipschitz regularity results* of viscosity solutions for a *general class of mixed integro-differential equations* of the type

$$\begin{aligned} &F_0(u(x), Du, D^2u, \mathscr{I}[x,u]) + \\ &\quad F_1(x_1, D_{x_1}u, D^2_{x_1x_1}u, \mathscr{I}_{x_1}[x,u]) + F_2(x_2, D_{x_2}u, D^2_{x_2x_2}u, \mathscr{I}_{x_2}[x,u]) = f(x) \end{aligned} \tag{1.14}$$

where we employ directional integro-differential operators

$$\mathscr{I}_{x_2}[x,u] = \int_{\mathbb{R}^{d_2}} (u(x_1, x_2 + j(x_2,z)) - u(x_1,x_2) - D_{x_2}u(x)\cdot j(x_2,z)1_B(z))\mu(dz).$$

The three nonlinearities must satisfy suitable strict ellipticity and growth conditions, that we omit here for the sake of simplicity, but can be illustrated on the following example:

$$-a_1(x_1)\Delta_{x_1}u - a_2(x_2)\mathscr{I}_{x_2}[x,u] - \mathscr{I}[x,u] + b_1(x_1)|D_{x_1}u_1|^{k_1} + b_2(x_2)|D_{x_2}u|^{k_2} + |Du|^n + cu = f(x)$$

where the nonlocal term $\mathscr{I}_{x_2}[x,u]$ is non-degenerate (satisfying (N)), of fractional exponent $\beta \in (0,2)$ and $a_i(x_i) > 0$, for $i = 1,2$.

When $\beta > 1$, we show that the solution is Lipschitz continuous for mixed equations with gradient terms $b_i(x_i)|D_{x_i}u|^{k_i}$ having a natural growth $k_i \le \beta$ if b_i bounded. If in addition b_i are τ-Hölder continuous, then the solution remains Lipschitz for gradient terms up to growth $k_i \le \tau + \beta$. When $\beta \le 1$, the solution is α-Hölder continuous for any $\alpha < \beta$. An open problem is the Lipschitz continuity of solutions in the critical case $\beta = 1$.

In particular, for the advection fractional diffusion equation

$$u_t + (-\Delta u)^{\beta/2} + b(x)\cdot Du = f$$

we obtain that the solution is Lipschitz continuous in the subcritical case $\beta > 1$, with b bounded and is Hölder continuous in the supercritical case $\beta \le 1$, whenever b is $C^{1-\beta+\tau}$, where $\tau > 0$. Recently, Silvestre obtained similar results to ours by Harnack techniques [Sila]. In addition to our results, he showed [Silb] that in the supercritical case the solution becomes $C^{1,\tau}$, with τ as before.

With this type of nonlinearities in mind, we establish Lipschitz and Hölder regularity results at several stages. For the sake of precision, we illustrate them on the previous general example.

Partial regularity. We first give regularity estimates of the solution with respect to each of its variables, in which case we use classical regularity arguments in one set of variables, and uniqueness type arguments in the other variables. Then the following holds.

Theorem 1.1.7. *Any periodic continuous viscosity solution u*

(a) is Lipschitz continuous in the x_2 variable, if $\beta > 1$ and $k_2 \le \beta$, $k_1 = 1$, $n \ge 0$;

(b) is $C^{0,\alpha}$ continuous with $\alpha < \frac{\beta - k_2}{1-k_2}$, if $\beta \le 1$ and $k_2 < \beta$, $k_1 = 1$, $n \ge 0$.

The Lipschitz/Hölder constant depends on $||u||_\infty$, on the dimension of the space d and only on the constants associated to the Lévy measures and on the functions a_2 and b_2.

If we want to extend the regularity result with respect to *all* its variables, the uniqueness requirements seem rather restrictive, as gradient terms are restrained to sublinear growth.

A priori estimates. Nevertheless, the regularity results can be extended to superlinear cases, by a gradient cut-off argument. Roughly speaking, one should look at the approximated equations with $|Du|$ replaced by $|Du| \wedge R$, for $R > 0$ and remark that their solutions are Lipschitz continuous, with the Lipschitz norm independent of R, thus the solution obtained by this approximation is Lipschitz continuous.

Global regularity then follows by interchanging the roles of x_1 and x_2. Subsequently, we can deal with gradient growths of orders respectively $k_1 = 2$, $k_2 \le \beta$.

Theorem 1.1.8. *Any periodic continuous viscosity solution u of (1.14)*

(a) is Lipschitz continuous, if $\beta > 1$ and $k_2 \le \beta_i$, $k_1 \le 2$, $n \ge 0$;

(b) is $C^{0,\alpha}$ continuous with $\alpha < \frac{\beta_2 - k_2}{1-k_2}$, if $\beta \le 1$ and $k_2 < \beta_i$, $k_1 \le 2$, $n \ge 0$.

We provide the detailed proof of the regularity result for periodic viscosity solutions of elliptic integro-differential equations. In a separate section, we give the extensions to *the non-periodic setting*, *parabolic case* as well as *fully nonlinear Bellman - Isaacs equations*, pointing out each time the main differences that occur in the proof.

1.1.4 Work in Progress and Future Plans

Long time Behavior of Viscosity Solutions, in the Periodic Setting[4]

The arguments are classical up to the point of solving the stationary ergodic problem. To prove the uniqueness and existence of λ and v we use the classical argument introduced by Lions, Papanicolau and Varadhan in [LV] and consider the approximated equations

$$F(x, Dv_\varepsilon, D^2 v_\varepsilon, \mathscr{I}[x, v_\varepsilon]) + \varepsilon v_\varepsilon = 0, \quad \text{in } \mathbb{R}^N. \tag{1.15}$$

and pass to the limit as $\varepsilon \to 0$. Therefore it is necessary to show some compactness for this family of functions and this requires in particular *equicontinuity*, if posible *uniform* $C^{0,\alpha}$ *estimates*. The inconvenient is that the gradient bound depends in general on the L^∞ norm of the solution. Sometimes, it is possible to establish gradient bounds independent of the L^∞ norm of the solution (see for example the work of Barles and Souganidis [BS01]). In the nonlocal case, we show that the renormalized functions $\tilde{v}_\varepsilon(x) = v_\varepsilon(x) - v_\varepsilon(0)$ are uniformly bounded, thus they are equicontinuous. We argue by contradiction and combine Hölder estimates and the Strong Maximum Principle for the equations satisfied by the renormalized functions $w_\varepsilon = \frac{\tilde{v}_\varepsilon}{||\tilde{v}_\varepsilon||_\infty}$. The proof is different though for the superlinear and sublinear case. So far, the sublinear case is completed.

Almost Periodic Framework

We would like to consider in near future the stationary ergodic problem in almost periodic domains. There have been some recent developments [Sch] and [GS] in this direction but to the best of our knowledge, their study concerns only a particular family of nonlinear equations and nonlocal operators.The ergodic problem is related both to the homogenization and to the long time behavior of solutions. The case of fully nonlinear degenerate second-order PDEs in almost periodic environment has been studied by Lions and Souganidis in [LS05], where they assume the ellipticity has the same order as the space oscillation. We would like to investigate if similar techniques can be adapted to nonlocal equations.

Regularity Theory for Fully Mixed Jump Diffusion Equations

An interesting problem would be the extension of the regularity results to the more general case of *Mixed Jump Diffusion Equations*

$$-a(x)\Delta_{x_1} u + b(x)(-\Delta)^{\alpha/2}_{x_2} u = 0. \tag{1.16}$$

We have been already working on the approach given by classical viscosity methods, where we have obtained partial regularity of solutions: the problematic case seems to be when the gradient forms a $\pi/4$ angle with the x_i-axis. At the same time, we are interested in the approach given by Harnack inequalities and ABP estimates, when $a(x)$ and $b(x)$ are bounded above and below but not necessarily continuous. We expect that similar estimates to those given by Caffarelli and Silvestre in [CS09] can be obtained.

[4] work in progress with Guy Barles, Emmanuel Chasseigne and Cyril Imbert

1.2 Image Restoration and Visualization by Curvature Motions

The role of curvatures in visual perception goes back to the 50s and one of the first important contributions is due to Attneave [Att54]. Attneave argued on neurological grounds that the human brain could not possible use *all* the information provided by states of simulation, and showed that the important information, that *stimulated the retina*, is located at *regions where color changes abruptly (contours), and furthermore at angles and peaks of curvature.*

This explains why, in one of the first serious attempts to cope with this numerical challenge, Asada and Brady [AB86] introduced the concept of *multiscale curvature.* This paper led to increasingly sophisticated attempts to analyze planar shapes by their curvatures.

The subject has required a fairly elaborate series of mathematical contributions, among which image smoothing by geometric curvature motions, such as the *Mean Curvature Motion*

$$\frac{\partial u}{\partial t} = |Du|\text{curv}(u) \tag{MCM}$$

or its affine variant the *Affine Curvature Motion*

$$\frac{\partial u}{\partial t} = |Du|\text{curv}(u)^{1/3}. \tag{ACM}$$

These equations are of great interest in image processing since they can be axiomatically obtained from the image multiscale theories, as the partial differential equations satisfying some invariance properties: *causality*, *locality*, *isometry* and *contrast invariance*, and in the case of (ACM) *affine invariance* as well. This characterization was given in '93 by Alvarez, Guichard, Lions and Morel in [AGLM93].

The PDEs above describe the evolution of a hypersurface (curve in 2D) moving according to its mean curvature. Osher-Sethian defined and studied in [OS88] the level set method for the motion of fronts by (mean) curvature, for which Chen-Giga-Goto [CGG91] and Evans-Spruck [ES91] provided rigorous justifications. Their arguments are based on the notion of viscosity solution of Crandall and Lions [CL83], that allows one to give a suitable meaning to the (MCM) and (ACM) equations, in the class of uniformly continuous functions. The undertaking is analytically subtle principally because the mean curvature evolution equation is nonlinear, degenerate, and even undefined at points where $Du = 0$. Their approach, recast slightly, is this. Given the initial curve Σ_0 as above, select some function u_0 such that

$$\Sigma_0 = \{x;\ u_0(x) = 0\}.$$

Solve then the Dirichlet problem for the parabolic (MCM) or (ACM) with initial condition u_0, which gives the solution $u(x,t)$ and define the evolution of Σ_0 as

$$\Sigma_t = \{x;\ u(x,t) = 0\}.$$

The evolution is shown to be geometric, in the sense that it is uniquely defined and independent of the choice of the initial function $u_0 \in BUC(\Omega)$. However, for semi-continuous initial data, may be *more than one solution* of the initial value problem as pointed out by Soner in

[Son93]. In fact, this is the case whenever the level set develops a nonempty interior or becomes 'fat'. This difficulty was explained by Barles, Soner and Souganidis in [BSS93].

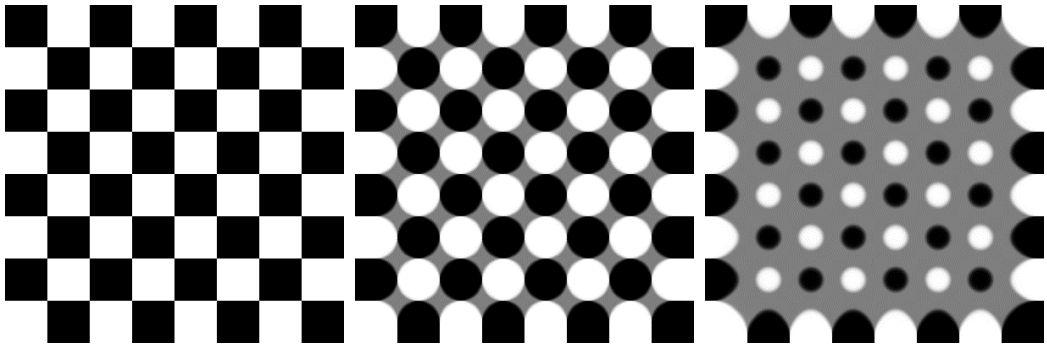

(a)

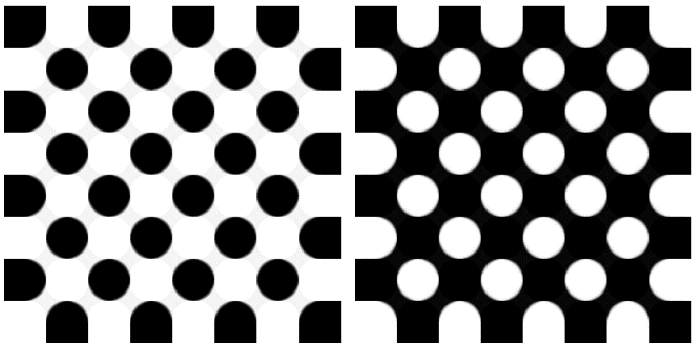

(b)

Figure 1.6: Checkerboard image (upper-left corner) evolving by mean curvature motion. (a) For bounded uniformly continuous initial data, the level set is uniquely defined. (b) For semi-continuous functions, the fattening phenomena discards uniqueness of solutions.

On the other hand, these geometric evolutions have been long studied using parametric methods of differential geometry. Curve smoothing by intrinsic heat equation, also called *Curve Shortening*

$$\frac{\partial \mathbf{x}}{\partial t} = \kappa(\mathbf{x}). \tag{CS}$$

was one of the first versions of curve analysis proposed by Mackworth and Mokhtarian in [MM86]. Rigorous proofs were given by Gage and Hamilton for convex Jordan curves [GH86] and later extended to embedded curves by Grayson [Gra87]. The *Affine Shortening* equation

$$\frac{\partial \mathbf{x}}{\partial t} = \left(|\kappa|^{-2/3}\kappa\right)(\mathbf{x}) \tag{AS}$$

is a surprising variant of curve shortening introduced by Sapiro and Tannenbaum [ST93a]. A remarkably fast and geometric algorithm for affine shortening was given by Moisan in [Moi98]. It was used for shape identification algorithms in the works of Cao, Lisani, Musé, Sur, [CLM+08]. Following the works of Mackworth and Mokhtarian [MM86] on curve smoothing and shape extraction, Caselles et al. realized the potential of using directly the image level

lines instead of its edges. They proposed to perform contrast invariant image analysis directly on the set of level lines, or *topographic map* [CCM96]. A fast algorithm computing the topographic map was developed by Monasse and Guichard in [MG98].

1.2.1 Algorithms for Curvature Motions (Chapter 5)

All sound shape smoothing algorithms in the computer vision literature perform curve shortening or affine curve shortening. But the numerical variety of the underlying numerical algorithms is worth noticing. In the first part, we present a review, analysis and comparison of the main classes of curvature algorithms. We discuss their history, implementation, advantages and drawbacks. There are three kinds of initial data for the algorithms: digital curves, digital sets, or digital images. We shall examine each in turn.

1.2.2 From Curve Shortening to Image Curvature Motion (Chapter 6)

We were first intrigued to find out if an explicit connection can be given between the geometric approach for *Curve/Affine Shortening* and the viscosity approach for the *Mean/Affine Curvature Motion*. This lead us to set forth in [CMM10] a new image processing numerical chain, that we termed *Level Lines (Affine) Shortening*. This image processing pipeline yields in practice subpixel evolutions of images by mean, respectively affine curvature, but it also gives an *accurate curvature estimate*, based on a direct computation on the level lines. It, hopefully, advances Attneave's program and proves that computer vision can get close enough to human vision. This was one reason ahead to rigorously justify that the Level Lines Shortening, and its Affine variant, computes explicitly a viscosity solution for the *Mean Curvature Motion*, respectively Affine Curvature Motion.

Evans and Spruck checked in [ES91] the consistency of the level set approach with the classical motion by mean curvature. More precisely, they showed that the mean curvature motion agrees with the classical motion, if and as long as the latter exists. The result applies for a smooth hypersurface, given as the connected boundary of a bounded open set. Their arguments are based on comparison techniques with lower barriers for the approximated mean curvature motion and strongly use the fact that the hypersurface is the zero level set of its (signed) distance function. However, the result does not describe the complete behavior of *all* the level lines of a Lipschitz function. Namely, if we are given a Lipschitz function u_0 which evolves by mean curvature in the viscosity sense, are all of its level lines evolving independently by curve shortening? For dimension $n \geq 3$ the result is not true, since hypersurfaces can develop singularities and possible change topology. Thanks to Grayson's theorem, the 2D case has a very peculiar structure which we will take advantage of and show that evolving independently and simultaneously by curve shortening *all* the level lines of a function is equivalent to applying directly a mean curvature motion to the functions itself.

The *Level Lines Shortening (LLS)* builds on the previous mentioned contributions and connects explicitly the geometric approach for curve shortening evolutions and the viscosity framework for curvature motions. Both in the continuous and the discrete case, Level Lines (Affine) Shortening is defined as an operator which first extracts all the level lines of an image, then it independently and simultaneously smooths all of its level lines by curve shortening

(CS) (respectively affine shortening (AS)) and eventually reconstructs, at each step, a new image from the evolved level lines. The chain is based on a topological structure, the inclusion tree of level lines as a full and non-redundant representation of an image [CM10a], and on a topological property, the monotonicity of curve shortening with respect to inclusion. Therefore, the hierarchy of the level lines is maintained while performing the smoothing. Thus, the chain realizes the commutative diagram:

$$\begin{array}{ccc} u_0(\cdot) & \xrightarrow{\quad level\ lines\ extraction \quad} & \{\Sigma_0^{\lambda,i}\}_{\lambda,i} \\ \Big\downarrow MCM/ACM{=}LLS/LLAS & & \Big\downarrow CS/AS \\ u(\cdot,t) & \xleftarrow{\quad reconstruction \quad} & \{\Sigma_t^{\lambda,i}\}_{\lambda,i}. \end{array}$$

We prove that the image reconstructed from the evolved level lines is a viscosity solution of the mean curvature motion (MCM) (resp. affine curvature motion (ACM)) provided that the level lines at almost all levels evolve by curve shortening (resp. affine shortening).

Theorem 1.2.1. *Let $u_0 \in \mathcal{VS}(\Omega)$. Then the Level Lines Shortening evolution of the function u_0,*

$$u(\mathbf{x},t) = LLS(t)\,u_0(\mathbf{x}), \forall \mathbf{x} \in \mathbb{R}^2, \forall\, t \in [0,\infty)$$

is a viscosity solution for the mean curvature PDE, with the initial data u_0

$$\begin{cases} u_t = curv(u)|Du|, & in\ \mathbb{R}^2 \times [0,\infty) \\ u(\cdot,0) = u_0, & on\ \mathbb{R}^2. \end{cases} \tag{MCM}$$

A similar result holds for LLAS and the affine curvature PDE with initial condition u_0.

The initial image will be considered as an element of a particular space of functions $\mathcal{VS}(\Omega)$ that we term space of *very simple* functions and is related to fattening phenomena for Lipschitz continuous functions. This class corresponds to bilinearly interpolated images defined on a rectangle Ω whose topographic maps contain only Jordan curves. The set of very simple functions arises naturally in image processing, since level lines corresponding to noncritical levels are sufficient to grant an exact reconstruction of the digital image.

In this way, the described chain corresponds exactly to its numerical implementation [CMMM] and has the advantage of satisfying both numerically and analytically all the invariance properties required by the scale space in question. Then, by stability properties of viscosity solutions and density arguments, the result is immediately extended to Lipschitz functions.

1.2.3 Level Lines Shortening Algorithm (Chapter 7)

The next chapter describes the discrete *Level Lines Shortening (LLS)* Algorithm and its variant the *Level Lines Affine Shortening (LLAS)*.

Digital images are given in discrete sampled forms on a rectangle Ω. The underlying substratum is assumed to be continuous and interpolated as such on Ω. Among the possible interpolations, the bilinear interpolation presents two advantages: it is the most local of continuous

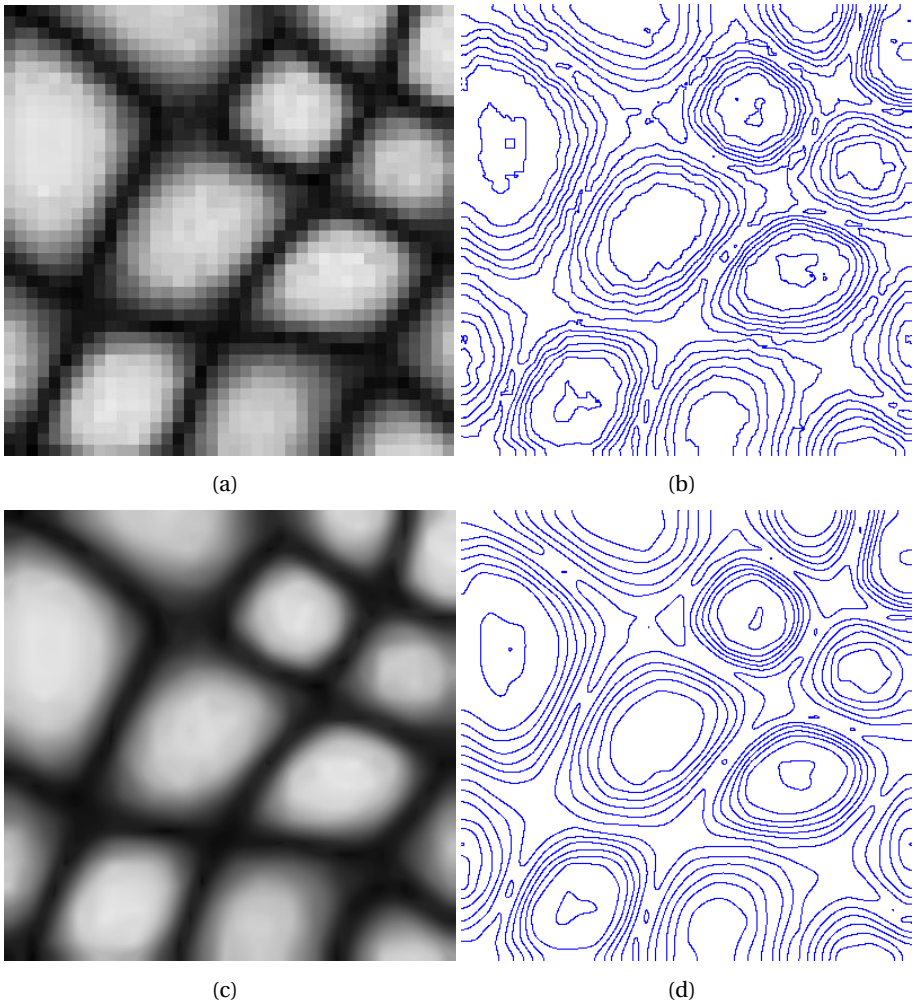

(a) (b)

(c) (d)

Figure 1.7: Illustration of the LL(A)S numerical chain. (a) Original image. (b) Bilinear level lines extraction. (d) Simultaneous and independent smoothing of level lines by affine shortening. (c) Image reconstructed from shortened level lines.

interpolations, and it preserves the order between the gray levels of the image. For this reason, we deal with level lines in bilinearly interpolated images.

Level Lines Shortening. The discrete algorithm is performed in three steps

1. it first extracts all the *bilinear level lines* of a digital image, with a number of levels sufficient to grant an exact reconstruction of the initial image
2. then it independently and simultaneously smooths all of its level lines by *discrete* curve shortening (CS) (resp. affine shortening (AS)).
3. the evolved image is eventually reconstructed from its evolved level lines.

One of the difficulties in image processing was until recently the extraction of the contours at subpixel accuracy. In '98, Monasse and Guichard gave a fast algorithm [MG98]

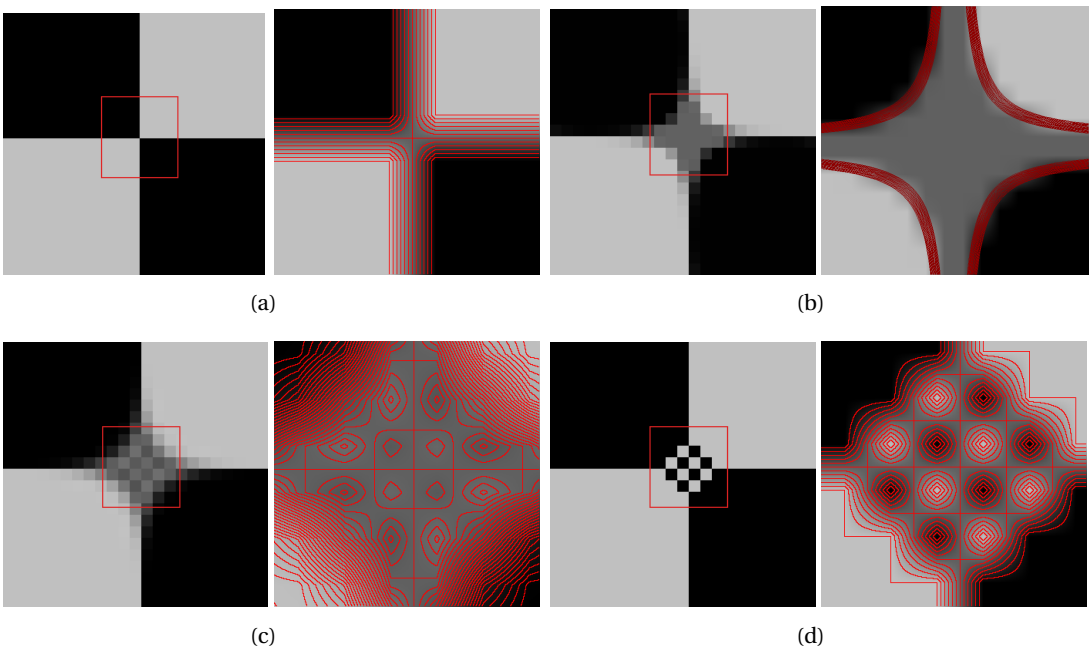

Figure 1.8: The four pairs present various implementations of the mean curvature motion on a checkerboard image (left column) and zooms at an X-junction, with its level lines overprinted on the image (right). From top to bottom : (a). original image (the zoom is by bilinear interpolation), (b). Level lines shortening, (c). Finite difference scheme, (d) FDS stack filter. Only LLS does not create new extrema.

for computing the tree of shapes of an image and accordingly, the topographic map. Caselles and Monasse describe in their recent work [CM10a] a direct extraction algorithm for the tree of bilinear level lines. But surprisingly, no algorithm for the inverse reconstruction *at subpixel accuracy* was given. We complete their work with a fast algorithm of image reconstruction from an *arbitrary* family of Jordan curves given at subpixel resolution, provided it is embedded in a tree structure.

Accurate evolution. The order preserving property or *inclusion principle* is the main structural requirement of LL(A)S algorithm. It basically prevents the crossing of two different level curves and therefore permits the construction of a unique image having a prescribed set of level lines. Some level lines may present multiple crossings at saddle points, in which case the level lines shortening develops a non-empty interior. Performing classical Finite Difference Schemes (FDSs) for mean curvature spurious diffusions occur around the image extrema and at *T-junctions* or *X-junctions*. At saddle points FDSs algorithms create new extrema, and therefore spurious level lines. Only LLS resolves this issue, by separately evolving the level lines and then reconstructing the image.

An Image Curvature Microscope. Furthermore, we show that Level Lines Shortening yield *accurate curvature estimates*, based on direct computation on the level lines. Most of curvature algorithms have a common drawback: they are based on finite difference schemes (FDS) for the second order differential operator curv(u). In this case, the cur-

vature depends on the gray values of the neighbor pixels and consequently, high oscillations along transverse level lines appear. Noise and aliasing effects render direct methods of curvature computation on a raw image practically impossible.

However, whenever we talk about curvatures in a digital image, we actually refer to the curvatures of the level lines associated to the image. Therefore, the curvature must be computed as a 1D differential operator, directly on level lines. After short time smoothing the pixelized level lines become accurate and we deal with curves, having sub-pixel control points, whose curvature can be faithfully computed. The striking difference between an FDS result and an LLS result is displayed in Figure 7.11.

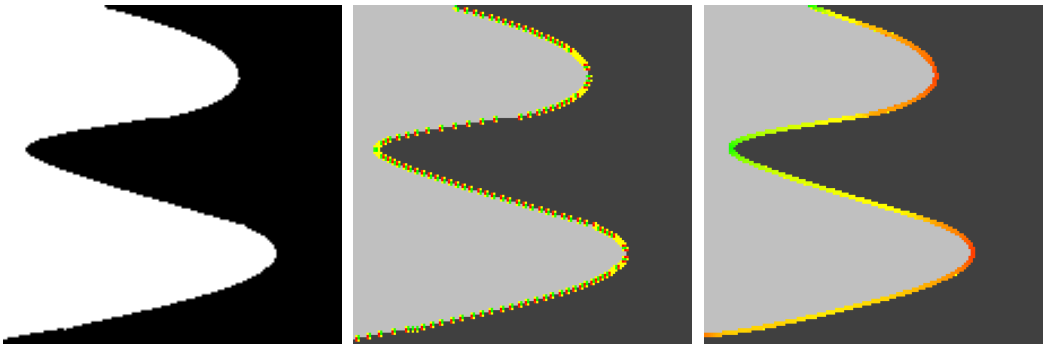

(a) Original image (b) Curvatures by FDS (c) Curvatures by LLS

Figure 1.9: The curvature color display rule. Zero curvatures are displayed in yellow, positive curvatures are shown in a gradation from yellow to red, and negatives from yellow to green. The initial image (a) had its curvatures computed in two different ways: by a FDS (b), and by LLS (c). In the first case the curvature presents oscillations, whereas the second result is coherent with our perception.

Range of Applications. In the last part we give a wide range of illustrative examples of image restoration and visualization.For example, in Fig.7.25 we display bacterial morphologies and the corresponding curvature map. In this case, the curvature is an intrinsic geometrical descriptor, useful for shape discrimination. An accurate curvature filter permits to make curvature statistics.

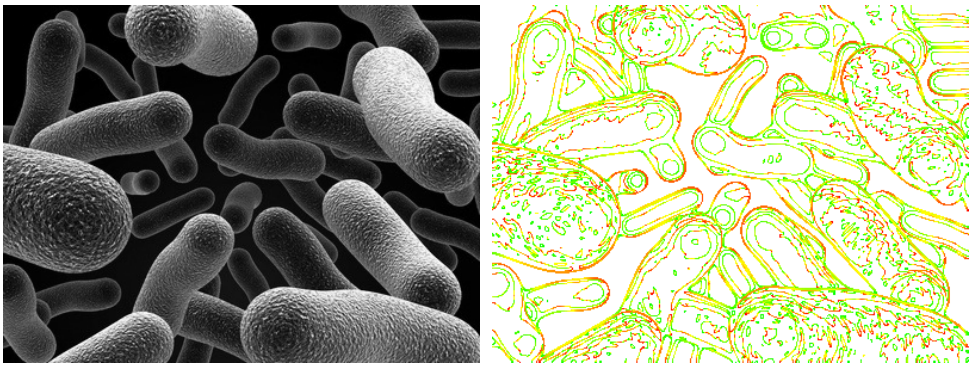

Figure 1.10: (a). Original image (b). Curvature Map

The algorithm can be tested on line and many examples of all kinds are provided.[5]

1.2.4 Work in Progress and Future Plans

Simultaneous Erosion and Dilation[6]

The Level Lines Shortening approach remains true for any increasing function of the curvature. When the power of the curvature goes to zero, we obtain the so called erosion-dilation filter, which is described by the following equation

$$\frac{\partial \mathbf{x}}{\partial t} = |\boldsymbol{\kappa}|^{-1}\boldsymbol{\kappa}(\mathbf{x}(t)). \tag{GCS}$$

This equation solves the famous problem never fixed in Mathematical Morphology: *simultaneous erosion and dilation*. Erosions correspond to the minus sign (the case where $\boldsymbol{\kappa}$ points towards the interior of the curve) in the above equation, and dilation to the plus sign in the above equation. Therefore the above equation solves the long dilemma unsatisfactorily replaced by the so called *alternate filters*, which perform alternate tiny erosions followed by tiny dilations, and iterate to attain a final joint "erosion-dilation".

Variational Framework[7]

We analyze the previous evolution, written in the form

$$\frac{\partial u}{\partial t} = \text{sgn}(\text{curv(u)})|Du| \tag{GCS}$$

as a limit in the viscosity sense of an iterative time-discrete perimeter minimization problem. We address the same question to more general cases.

In a first phase we look for class of convex functions F such that the iterative minimization of energy functional

$$\mathscr{F}(E;E_h^n) = \int_\Omega |\nabla \chi_E| + \int_{E\Delta E_h^n} (\partial F)_*(\frac{1}{h}\text{dist}(\cdot, E_h^n)) \tag{1.17}$$

has good compactness and regularity properties, using techniques similar to those in [ATW93], [Cha04] and [CN08]. We then prove that the discrete evolutions converge to a viscosity solution of the differential inclusion

$$u_t \in |Du|\partial F^*(\text{div}(\frac{Du}{|Du|})). \tag{1.18}$$

The arguments are similar up to some point to those explored by Caffarelli and Cordoba in [CC93], Caffarelli, Roquejoffre and Savin in [CRS10]for flatness properties of minimal surfaces.

[5] http://www.ipol.im/pub/algo/cmmm_image_curvature_microscope/

[6] work in progress with Sira Ferradans and Rachel Saffar

[7] work in progress with Antonin Chambolle and Gilles Thouroude

1.3 Publications related to the thesis

Journal Articles

- *Long Time Behavior of Periodic Viscosity Solutions for Integro-Differential Equations* joint work with G. Barles, E. Chasseigne, and C. Imbert - work in progress.
- *Lipschitz regularity of viscosity solutions for Mixed Integro-Differential Equations* - in preparation.
- *On the Strong Maximum Principle for Second Order Nonlinear Parabolic Integro - Differential Equations* - A. Ciomaga, submitted to Differential and Integral Equations.
- *A proof of equivalence between Level Lines Shortening and Curvature Motion in image processing* - A. Ciomaga, J.M. Morel, submitted to SIAM J. on Mathematical Analysis.
- *Image Visualization and Restoration by Curvature Motions* - A. Ciomaga, P. Monasse, J.M. Morel, to appear in SIAM Multiscale Modeling and Simulation.

Image Processing On Line (IPOL) Journal - the ANSI C implementations and online demo

- *An Image Curvature Microscope* - A. Ciomaga, P. Monasse, L. Moisan J.M. Morel. `http://www.ipol.im/pub/algo/cmmm_image_curvature_microscope/`
- *Finite Differences Schemes for Mean Curvature Motion and Affine Morphological Scale Space* - A. Ciomaga, M. Mondelli, accepted for publication. `http://www.ipol.im/pub/algo/cm_fds_mcm_amss/`

Conference Proceedings - related to IPOL algorithms

- *Level Lines Shortening yields an Image Curvature Microscope* - A. Ciomaga, P. Monasse, J.M. Morel, IEEE Proceedings of International Conference on Image Processing, 2010.
- *On the Finite Differences Schemes for Curvature Motions* - M. Mondelli, A. Ciomaga, Proceedings of International Student Conference on Pure and Applied Mathematics, 2010.

Part I

Nonlinear Integro-Differential Equations

CHAPTER 2

Levy Processes. Integro-Differential Equations

Employ your time in improving yourself by other mens' writings, so that you shall gain easily what others have labored hard for.

Sōkrátēs (470-399 B.C.E)

Abstract: We give a brief introduction to the class of Lévy processes and and present their connection with integro-differential operators. In the second part we present some recent developments for partial integro-differential equations involving nonlocal terms associated to Lévy processes. [1]

Résumé : Nous introduisons les processus de Lévy et nous présentons leur rapport avec des opérateurs intégro-différentiels. Dans la deuxième partie nous présentons quelques résultats récents sur les équations integro-différentielles, impliquant des termes nonlocaux associés aux processus de Lévy.

Keywords: Lévy processes, integro-differential equations, comparison principles, regularity of solutions

[1] This chapter is State of the Art on Lévy processes and on Partial Integro-Differential Equations.

Contents

2.1 Introduction

Throughout this work we refer to *nonlocal equations* that occur in the theory of *Lévy jump-diffusion processes*. Recently, there has been a great revival of interest in these processes, due to novel applications in mathematical finance and quantum field theory. Viscosity solutions approach has been extended for the last twenty years to Partial Integro-Differential Equations.

2.2 Lévy processes [2]

The basic theory of stochastic processes was extensively established in the last century. Intuitively, a stochastic process aims to model the interaction of chance with time. The tools with which this was made precise were provided by Kolmogorov in the 1930s, who realized that probability can be rigorously founded on measure theory. Stochastic processes are not only mathematically rich objects, but they also have an extensive range of applications, e.g. physics, engineering, ecology and enconomics.

There is a limited amount that can be said about the general concept and much of both theory and applications focuses on specific classes of stochastic processes, that are endowed with additional structures, such as random walks, Markov chains, Lévy processes, semimartingales, measure-valued diffusions.

Lévy processes were first studied by Lévy in the 30s and are the simpliest class of processes whose paths consist of continuous motion interspersed with jump discontinuities of random size, apearing at random times. Their structure was understood in the 40s and much is due to Lévy, Khintchine and Itô.

[2] Section entirely based on D. Appelbaum's book *Lévy Processes and Stochastic Calculus [App09]* and survey article *Lévy Processes - From Probability to Finance and Quantum Groups [App04]*.

2.2.1 The Structure of Lévy processes. Lévy-Khintchine Formula

A stochastic process is a family of fandom vairables $(X(t))_{t\geq 0}$ defined on a probability space $(\Omega, \mathscr{F}, P)$ and taking values in a measurable space, here $\mathbb{R}^d$.

Definition 2.2.1. *A Lévy processes $X = \big(X(t)\big)_{t\geq 0}$ is a stochastic process satisfying*

(1) X has independent and stationary increments;
(2) $X(0) = 0$ (a.s.);
(3) X is stochasticly continuous, i.e. for all $\varepsilon > 0$ and for all $s \geq 0$

$$\lim_{t\to s} P(|X(t) - X(s)| > \varepsilon) = 0.$$

Of these axioms, the first one is the most important. It refers to the increments

$$\big\{X(t) - X(s);\ 0 \leq s \leq t < \infty\big\}.$$

Stationarity means that the distribution of $X(t) - X(s)$ is invariant undeer shifts

$$P\big(X(t) - X(s) \in A\big) = P\big(X(t-s) - X(0) \in A\big), \forall\, A \text{ Borel sets.}$$

Independence means that given any finite ordered sequence of times $0 \leq t_1 \leq t_2 \leq \ldots \leq t_n < \infty$, the random variables

$$X(t_1) - X(0), X(t_2) - X(t_1), \ldots, X(t_n) - X(t_{n-1})$$

are independent. The second axiom is a convenient renormalization. The continuity is a technical, but important assumption that enables to perform rigorous analysis.

The structure of a generic Lévy processes can be understood by means of Fourier analysis. The key formula from which many results flow, is the Lévy-Khintchine formula, which says that any Lévy process has a specific form of its characteristic function. More precisely, for the *characteristic function* of $X(t)$, i.e. the mapping $\phi_t : \mathbb{R}^d \to \mathbb{C}$ defined by

$$\phi_t(\xi) = \mathbb{E}(e^{i\xi\cdot X(t)}) = \int_{\mathbb{R}^d} e^{i\xi\cdot z} p_t(dz)$$

where p_t is the distribution of $X(t)$and $\mathbb{E}$ denotes the expectation, the following holds.

Theorem 2.2.1 (Lévy Khintchine formula)**.** *If $X = \big(X(t)\big)_{t\geq 0}$ is a Lévy process, then $\phi_t(\xi) = e^{t\eta(\xi)}, \forall\, t \geq 0, \forall\, x \in \mathbb{R}^d$ where*

$$\eta(\xi) = ib\cdot\xi - \frac{1}{2}\xi\cdot A\xi + \int_{\mathbb{R}^d_*} \Big(e^{i\xi\cdot z} - 1 - i\xi\cdot z 1_B(z)\Big)\mu(dz) \tag{2.1}$$

for some $b \in \mathbb{R}^d$, A a nonnegative definite symmetric $d\times d$ matrix, μ a Borel measure for which

$$\int_{\mathbb{R}^d_*} \min(1, |z|^2)\mu(dz) < \infty.$$

Conversely, given a mapping η of the form (2.1) we can always construct a Lévy process X for

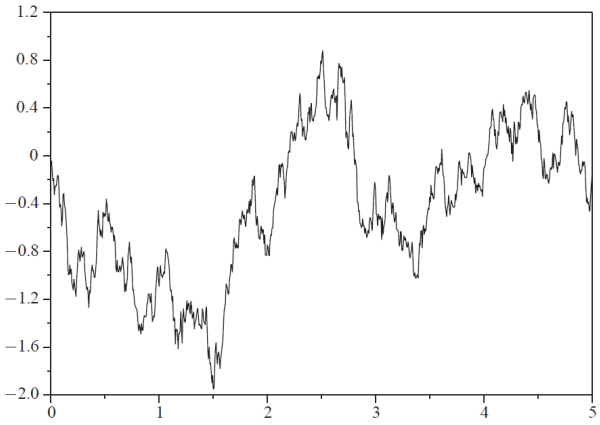

Figure 2.1: Standard Brownian motion. The path is continuous but nowhere differentiable.

which $\phi_t(\xi) = e^{t\eta(\xi)}$. *The mapping* $\eta : \mathbb{R}^d \to \mathbb{C}$ *is called the* characteristic exponent *of* X. *The tripe* (b, A, μ) *is called the* characteristic *of* X. *The measures* μ *are called* Lévy measures.

2.2.2 Examples of Lévy Processes

2.2.2.1 Brownian motion and Gaussian processes

A Brownian motion[3] in $\mathbb{R}^d$ is a Lévy process $B = \big(B_A(t), t \geq 0\big)$ with characteristics $(0, A, 0)$. Thus it has mean zero and covariance A. If A is positive definite, then each $B_A(t)$ has a normal distribution with density

$$f(x) = \frac{1}{(2\pi)^{\frac{d}{2}} \det(A)^{\frac{1}{2}}} e^{-\frac{1}{2t} x A^{-1} x}.$$

Standard Brownian motion was rigorously constructed by N. Wiener in the 1920s as a family of functionals on the space $C = C_0([0,\infty), \mathbb{R})$ of real valued continuous functions on $[0,\infty)$ that vanish at zero. In so doing, he equipped the infinite dimensional space C with a Gaussian measure that is now called Wiener measure (in his honor). It follows that the paths $t \mapsto B_A(t)(\omega)$, where $\omega \in C$ are continuous. In the 1930s Wiener, together with Paley and Zygmund showed that the paths are nowhere differentiable (w.p.1).

2.2.2.2 Brownian motion with drift

A Brownian motion with drift is a Lévy process $C = \big(C_{b,A}(t), t \geq 0\big)$ with characteristics $(b, A, 0)$. Each $C_{b,A}(t)$ is a Gaussian random variable having mean vector tb and covariance matrix tA.

[3] Brownian motion is named after the botanist R. Brown who first observed in 1820s the irregular motion of pollen grains immersed in water. By the end of nineteenth century the phenomenon was understood by means of kinetic theory as a result of molecular bombardement. In 1905 A. Einstein predicted its existence from purely theoretical considerations. Five years later, L. Bachelier had employed it to model the stock market, where the analogue of the molecular bombardement is the interplay of the myriad of individual market decisions that determine the market price.

In fact the process can be writen as

$$C_{b,A}(t) = tb + B_A(t).$$

A Lévy process has continuous sample paths (w.p.1) iff is a Brownian motion with drift.

2.2.2.3 The Poisson Process

A Poisson process $N = \big(N_\lambda(t), t \geq 0\big)$ with intensity λ is a Lévy process with characteristics $(0, 0, \lambda\delta_1)$ where δ_1 is a Dirac mass concentrated at 1. N takes non-negative integer values and we have the Poisson distribution

$$P(N_\lambda(t) = n) = \frac{e^{-\lambda t}(\lambda t)^n}{n!}$$

The paths of N are piecewise constant on finite intervals, with jumps of size 1 at each of the random times $t_n = \inf\big\{t \geq 0, N_\lambda(t) = n\big\}$.

2.2.2.4 The Compound Poisson Process

Let $\big(Y_n\big)_{n\geq 0}$ be a sequence of independent identically distributed random variables with common law ν and let N_λ be an independent Poisson process. The compound Poisson process[4] is the Lévy process

$$Z_\lambda(t) = \sum_{j=1}^{N_\lambda(t)} Y_j.$$

It has characteristic exponent

$$\eta(\xi) = \int_{\mathbb{R}^d} \Big(e^{i\xi\cdot z} - 1\Big)\lambda\nu(dz).$$

The sample paths of Z are piecewise constant on finite intervals with jump discontinuities at the random times $\big(t_n\big)_{n\geq 0}$, only this time the size of the jumps is itself random, and the jump at t_n can take any value in the range of the random variable Y_n.

2.2.2.5 Interlacing processes

Given a Browninan motion with drift $C_{b,A}$ and a compound Lévy process Z_λ, de can define an interlacing process by

$$X(t) = C_{b,A}(t) + Z_\lambda(t)$$

provided the two summands are independent. It has characteristic exponent

$$\eta(\xi) = ib\cdot\xi - \frac{1}{2}\xi\cdot A\xi + \int_{\mathbb{R}^d} \Big(e^{i\xi\cdot z} - 1\Big)\lambda\nu(dz). \tag{2.2}$$

The paths are piecewise continuous on finite intervals, interlaced with random jumps occuring at random times. The form if the characteristic exponent (2.2) is quite close to the general

[4] Poisson process (with $d = 1$) can be used to model the takings at a till in a supermarket, where $N_\lambda(t)$ is the number of customers in the queue at time t and Y_j is the amount paid by the j-th customer.

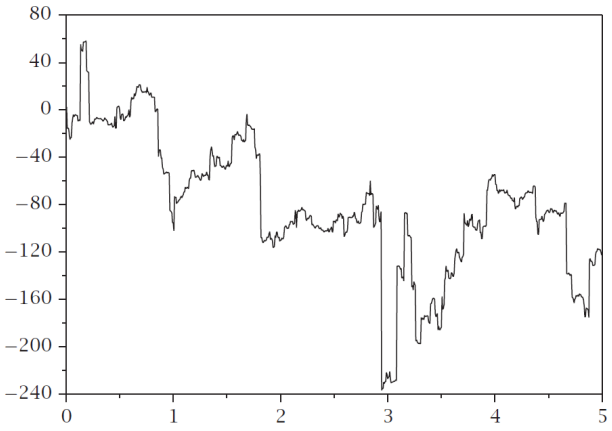

Figure 2.2: Stable Lévy process. Jump discontinuities are represented by vertical lines. This process is self similar: the path has a fractal nature.

form (2.1). It was actually proposed as the most general form for η by B. de Finetti in the 1920s. His error was in failing to appreciate that the finite measure $\lambda\nu$ can be replaced by a $\sigma-$ finite measure μ. But if we do this, $e^{i\xi\cdot z}-1$ may not be μ-integrable and hence we must adjust the integrand. Probabilistically, this corresponds to a lack of convergence of a countable number of "small jumps". Although (2.2) is incorrect, the most general characteristic exponent can be obtained as a pointwise limit of terms of similar type, i.e.

$$\eta(\xi)=\lim_{\delta\to 0}\eta_\delta(\xi),$$

where each

$$\eta_\delta(\xi)=ib\cdot\xi-\frac{1}{2}\xi\cdot A\xi+\int_{\delta<|z|\leq 1}z\cdot\xi\mu(dz)+\int_{|z|\geq 1}\left(e^{i\xi\cdot z}-1\right)\lambda\nu(dz)+$$

From the above examples, one may think that a Lévy process is nothing but the interplay of Gaussian and Poisson measures. However, the Gaussian and Poisson measures are just extremes of all characteristic exponents; there are some interesting processes in between.

2.2.2.6 Stable Lévy processes

Stable random variables are those whose laws are stable. They are characterized by the property that if X_1 and X_2 are independent copies of a stable random variable X, then for each $c_1,c_2>0$, there exists $c_0>0$ and $c\in\mathbb{R}^d$ such that $cX+c_0$ has the same law as $c_1X_1+c_2X_2$. A Lévy process is stable if each $X(t)$ is stable in this sense. The characteristics of a stable Lévy process are either of the form $(b,A,0)$ (so it is a Brownian motion with drift) or $(b,0,\mu)$ where

$$\mu(dz)=C\frac{dz}{|z|^{d+\beta}},\ \text{with } \beta\in(0,2),\ \text{and } C>0.$$

β is called the *index of stability*. With the sole exception of the Brownian motions with drift, the random variables of a stable Lévy process all have infinite variance, and if $\beta \leq 1$, they also have infinite mean. One example of interest (in the case $d = 1$) for which $\beta = 1$ is the Cauchy process, which has the density

$$f_t(x) = \frac{t}{\pi(x^2 + t^2)}.$$

Figure 2.2 presents a simulation of its paths in which jump discontinuities are represented by vertical lines. When X is rotationally invariant, i.e. $P(X(t) \in OA) = P(X(t) \in A)$, $\forall O \in \mathcal{O}(d)$, $t \geq 0$ and Borel sets A, we obtain

$$\eta(\xi) = -\sigma^\beta |\xi|^\beta$$

Rotationally invariant stable processes are an important class of self-similar processes, i.e. $(X(ct), t \geq 0)$ and $(c^{\frac{1}{\alpha}} X(t), t \geq 0)$ have the same finite dimensional distributions (for each $c > 0$), and this is one reason why such processes are important in applications. Another reason, applying to general stable random variables X, is that they have "heavy tails", i.e. $P(X > y)$ behaves asymptotically like $y^{-\alpha}$ as $y \to \infty$ as opposed to the exponential decay found in the Gaussian case. Such behavior has been found in models of telecommunications traffic on the Internet.

2.2.2.7 Relativistic processes

In 1905 Einstein gave a quantum mechanical explanation of the photoelectric effect (which broght him the Nobel prize) and developed the special theory of relativity. According to it, a particle of rest mass m moving with momentum p has kinetic energy

$$E(p) = \sqrt{m^2c^4 + c^2|p|^2} - mc^2,$$

where c is the speed of light. If we define $\eta(p) = -E(p)$, then η is the characteristic exponent of a Lévy processes.

2.2.3 The Lévy-Itô Decomposition

Given a characteristic exponent, we can always associate to it a Lévy process whose paths are right continuous with left limits (w.p.1). It follows that this process X can only have jump discontinuities, and there are, at most, a countable number of these on each closed interval. We formally write

$$X(t) = X_c(t) + \sum_{0 \leq s \leq t} \Delta X(s)$$

where X_c has continuous paths (w.p.1) and $\Delta X(s) = X(s) - X(x-)$ is the "jump" at time s where $X(s-)$ is the left limit. We can describe X_c quite easily. It is a Brownian motion with drift

$$X_c(t) = bt + B_A(t)$$

(although this is by no means easy to prove). The second term is more problematic: in particular, the sum may not converge. Instead of dealing directly with the jumps, it is more convenient

to count the jumps up to time t that are in a given Borel set A and to introduce

$$N(t,A) = \#\{0 \le s \le t; \Delta X(s) \in A\}.$$

In any finite time, X can have only a finite number of jumps of size greater than 1. We can write this finite sum of jumps as $\int_{|z|>1} zN(t,dz)$. Similarly, the sum of all the jumps of size greater than $\frac{1}{n}$ but less than 1 is $\int_{\frac{1}{n}<|z|<1} zN(t,dz)$. However, the limit may not converge as $n \to \infty$. Lévy argued that the accumulation of a large number of very small jumps may be difficult to distinguish from bursts of deterministic motion, so one should consider

$$M_n(t) = \int_{\frac{1}{n}<|z|<1} z(N(t,dz) - t\mu(dz))$$

which is a sequence of square-integrable, mean zero martingales. The sequence converges in mean square to a martingale

$$M(t) = \int_{0<|z|<1} z\tilde{N}(t,dz).$$

where $\tilde{N}(t,dz) = (N(t,dz) - t\mu(dz))$ is called a compensated Poisson random measure. Lévy's intuition was made precise by K. Itô, to whom we owe the decomposition of sample paths of a Lévy process:

$$X(t) = bt + B_A(t) + \int_{|z|<1} z\tilde{N}(t,dz) + \int_{|z|\ge 1} zN(t,dz).$$

2.2.4 Integro-Differential Operators

Lévy processes are in particular Markov processes, thus their past and their future are independent at the present. More precisely, if we denote by $\mathscr{F}_t$ the smallest sub σ-algebra of $\mathscr{F}$ with respect to which all $\big(X(s)\big)_{0\le s\le t}$ are measurable, then the following must hold

$$\mathbb{E}\big(u(X(t+s)|\mathscr{F}_t)\big) = \mathbb{E}\big(u(X(t+s)|X(t))\big),\ \forall\, t,s \ge 0,\ \forall\, u \in B_b(\mathbb{R}^d)$$

where $B_b(\mathbb{R}^d)$ is the Banach space, with respect to the supremum norm, of all bounded measurable functions on $\mathbb{R}^d$. One can define a two-parameter family of linear contractions $\big(T_{s,t}\big)_{0\le s\le t<\infty}$ on $B_b(\mathbb{R}^d)$ by

$$(T_{s,t}u)(x) := \mathbb{E}\big(u(X(t)|X(s)=x\big) = \int_{\mathbb{R}^d} u(x+z)\,p_t(dz).$$

The Markov property implies that the family is an evolution, i.e. $T_{r,s}T_{s,t} = T_{r,t}$, for all $r \le s \le t$.

Lévy processes have two additional structural properties, which makes them a nice subclass of Markov processes. They are time-homogenenous $T_{s,t} = T_{0,t-s}$ for all $0 \le s \le t$. Thus, the one-parameter family $T_t = T_{0,t}$ forms a semigroup $T_sT_t = T_{s+t}$. In addition, they are Feller processes, i.e. preserves the Banach space $C_0(\mathbb{R}^d)$ of continuous functions, vanishing at infinity $T_t : C_0(\mathbb{R}^d) \mapsto C_0(\mathbb{R}^d)$ and

$$\lim_{t\to 0} ||T_tu - u|| = 0.$$

Therefore, $\big(T_t\big)_{t\ge 0}$ forms a contraction semigroup on $C_0(\mathbb{R}^d)$, which is strongly continuous,

and by the general theory of semigroup operators, T_t admits a generator

$$Au = \lim_{t\to 0} \frac{T_t u - u}{t}$$

for all u in some linear space dense in $C_0(\mathbb{R}^d)$.

2.2.4.1 The Structure of the Generator

The structure is then completely determined by the Lévy Khintchine formula and reads

$$Au(x) = \underbrace{\sum_{i=1}^{d} b_i \frac{\partial u}{\partial x_i}}_{drift} + \underbrace{\frac{1}{2}\sum_{i,j=1}^{d} a_{ij}\frac{\partial^2 u}{\partial x_i \partial x_j}}_{diffusion} + \underbrace{\int_{\mathbb{R}^d}\Big(u(x+z)-u(x)-\sum_{i=1}^{d} z_i \frac{\partial u}{\partial x_i} 1_B(z)\Big)\mu(dz)}_{jumps}.$$

In particular

- Brownian motions are generated by half-Laplacian $A = \frac{1}{2}\Delta$;
- Rotationally invariant β-stable processes by *fractional Laplacian* $A = -(-\Delta)^{\frac{\beta}{2}}$;
- Relativistic processes by the Schrödinger operator $-A = \sqrt{m^2c^4 - c^2\Delta} - mc^2$.

More generaly, this structure can be given for a wider class of Markov processes, when the generator is of the Courrège form

$$\begin{aligned} Au(x) \quad = \quad & c(x)u(x) + \underbrace{\sum_{i=1}^{d} b_i(x)\frac{\partial u}{\partial x_i}}_{drift} + \underbrace{\frac{1}{2}\sum_{i,j=1}^{d} a_{ij}(x)\frac{\partial^2 u}{\partial x_i \partial x_j}}_{diffusion} + \\ & \underbrace{\int_{\mathbb{R}^d}\Big(u(z)-u(x)-\sum_{i=1}^{d}(z_i-x_i)\frac{\partial u}{\partial x_i}K(x,z)\Big)\mu_x(dz)}_{jumps}. \end{aligned}$$

Note that the drift, diffusion and jumps are no longer fixed, but change from point to point. There is an additional term c, that corresponds to killling. The function K is a smoothed version of the indicator function that effects the cut-off between large and small jumps.

2.2.4.2 Types of Integro-Differential Operators

For each point $x \in \mathbb{R}^d$, the Lévy measure $\mu_x(dz)$ on $\mathbb{R}^d_* = \mathbb{R}^d \setminus \{0\}$ determines the integro-differential operator. Depending on the assumptions on the singularity at the origin of the Lévy measure, we may classify these integro-differential operators. To fix ideas, we refer to general nonlocal operators, of the form

$$\mathscr{I}[x,t,u] = \int_{\mathbb{R}^d}(u(x+z,t)-u(x,t)-Du(x,t)\cdot z 1_B(z))\mu_x(dz). \tag{2.3}$$

Integro-differential operators or order 0 (or bounded) have the expression

$$\mathscr{I}[x,u]=\int_{\mathbb{R}^d_*}\big(u(x+z)-u(x)\big)\mu_x(dz) \text{ with } \int_{\mathbb{R}^d_*}\mu_x(dz)<\infty.$$

since they make sense for bounded functions.

Integro-differential operators or order 1 have the expression

$$\mathscr{I}[x,u]=\int_{|z|<1}\big(u(x+z)-u(x)\big)\mu_x(dz) \text{ with } \int_{|z|<1}|z|\mu_x(dz)<\infty$$

since they make sense for bounded continuously differentiable functions.

Integro-differential operators or order 2 have the expression

$$\mathscr{I}[x,u]=\int_{|z|<1}\big(u(x+z)-u(x)-Du\cdot z1_B(z)\big)\mu_x(dz) \text{ with } \int_{|z|<1}|z|^2\mu_x(dz)<\infty$$

since they make sense for bounded twice-continuously differentiable functions.

For operators of order 1 or 2 the interesting part is the singularity of the measures at the origin, thus the *small jumps*. The region of integration $\{|z|<1\}$ can be replaced by any region of the form $\{|z|<\varepsilon\}$, with $\varepsilon>0$. On the other hand, for operators of order 0 the interest is on the integrability at infinity, thus *large jumps*. Similarly, one could replace the domain of integration by $\{|z|\geq\varepsilon\}$, with $\varepsilon>0$. For operators of form (2.5) both large and small jumps are comprised, and they will be often writen as

$$\mathscr{I}[x,u]=\mathscr{I}^1_\delta[x,u]+\mathscr{I}^2_\delta[x,u]$$

with

$$\begin{aligned}\mathscr{I}^1_\delta[x,u] &= \int_{|z|<\delta}\big(u(x+z)-u(x)-Du\cdot z1_B(z)\big)\mu_x(dz)\\ \mathscr{I}^2_\delta[x,u] &= \int_{|z|\geq\delta}\big(u(x+z)-u(x)-Du\cdot z1_B(z)\big)\mu_x(dz).\end{aligned}$$

2.3 Integro-Differential Equations

Prior to viscosity solutions theory there was the classical theory for second order, uniformly elliptic integro-differential equations. We will not discuss it here, but it is worth mentioning that a priori estimates, weak and strong maximum principles, existence and uniqueness results have been extended from elliptic partial differential equations to elliptic integro-differential equations. For results in the framework of Green functions and classical regular solutions we send the reader to the up-to-date book of Garroni and Menaldi [GM02] and the references therein.

Lately, there has been a great interest in extending viscosity solutions theory to Partial Integro-Differential Equations (PIDEs). The advantage of this theory is that is allows merely continuous functions to be solutions of fully nonlinear equations and it has a great flexibility

for passages to limits under quite general conditions. Moreover, general existence and uniqueness results can be provided, as well as regularity results. Many interesting developments were recently established for partial integro-differential equations and would be hard to cover them all. We will focus only on the main contributions that brought the theory of viscosity solutions for PIDEs at its present stage.

The theory of viscosity solutions applies today [BI08] to a wide class of integro-differential equations of the form

$$F(x,u,Du,D^2u,\mathscr{I}[x,u])=0 \text{ in } \Omega. \tag{2.4}$$

where the nonlinearity F satisfies a fundamental monotonicity condition, known in the literature as *degenerate ellipticity condition*, i.e.

$$F(...,X,l)\leq F(...,Y,l') \text{ if } X\geq Y,\ l\geq l',$$

for all $X,Y\in\mathbb{S}^{d_i}$ and $l,l'\in\mathbb{R}$.

The integro-differential operator $\mathscr{I}[x,u]$ is either general nonlocal operator of the type

$$\mathscr{I}[x,u]=\int_{\mathbb{R}^d}(u(x+z)-u(x)-Du(x)\cdot z1_B(z))\mu_x(dz), \tag{2.5}$$

where $1_B(z)$ denotes the indicator function of the unit ball B and $\left(\mu_x\right)_{x\in\Omega}$ a family of Lévy measures, i.e. non-negative, possibly singular, Borel measures on Ω such that

$$\sup_{x\in\Omega}\int_{\mathbb{R}^d}\min(|z|^2,1)\mu_x(dz)<\infty.$$

or a Lévy-Itô operator of the form

$$\mathscr{J}[x,u]=\int_{\mathbb{R}^d}(u(x+j(x,z))-u(x,t)-Du(x)\cdot j(x,z)1_B(z))\mu(dz) \tag{2.6}$$

with μ a Lévy measure and $j(x,z)$ the size of the jumps at x.

Although the nonlocal operator $\mathscr{I}$ is defined on the whole space, we consider equations on a bounded domain Ω. Therefore, we assume that the function $u=u(x)$ is a priori defined outside the domain Ω. The choice corresponds to prescribing the solution in Ω^c, as for example in the case of Dirichlet boundary conditions.

There are several definitions for viscosity solutions, among which the closest to the PDE framework is the following.

Definition 2.3.1 (Viscosity solutions)**.** *An usc function $u:\mathbb{R}^d\to\mathbb{R}$ is a* subsolution *of (3.1) if for any $\phi\in C^2(\mathbb{R}^d)$ such that $u-\phi$ attains a global maximum at $x\in\Omega$*

$$F(x,\phi(x),D\phi(x),D^2\phi(x),\mathscr{I}[x,\phi])\leq 0.$$

A lsc function $u:\mathbb{R}^d\to\mathbb{R}$ is a supersolution *of (3.1) if for any test function $\phi\in C^2(\mathbb{R}^d)$ such that $u-\phi$ attains a global minimum at $x\in\Omega$*

$$F(x,\phi(x),D\phi(x),D^2\phi(x),\mathscr{I}[x,\phi])\geq 0.$$

One of the first papers is due to Soner [Son86b], where the author is interested in the optimal control of jump processes with a state-space constraint. The deterministic counterpart of this problem is studied in [Son86a], and generalizations to a certain class of jump processes, namely *piecewise deterministic processes* is given in [Son86b]. Yet, the theory of viscosity solutions has required fairly elaborated works on the topic.

2.3.1 Existence and Comparison Results

Roughly speaking, uniqueness and comparisons principles in the viscosity solutions theory refer to one of the two statements below.

Comparison Principle on $\Omega = \mathbb{R}^d$. *If u is a bounded usc subsolution of (2.4) and v is a lsc supersolution of (2.4) then $u \le v$ in $\mathbb{R}^d$.*

Comparison Principle on Ω bounded. *If u is a bounded usc subsolution of (2.4), v is a lsc supersolution of (2.4) and $u \le v$ on $\partial\Omega$ then $u \le v$ in $\overline{\Omega}$.*

Following Soner's work, existence and comparison results of solutions for *first order PIDEs* were given by Sayah in [Say91a] and [Say91b]. The author studies the existence and uniqueness of viscosity solutions of the fully nonlinear first-order, integro-differential equation

$$F(x,u,Du,\mathscr{I}[x,u]) = 0 \text{ in } \mathbb{R}^d$$

where the integral term $\mathscr{I}[x,u]$ depends on a *family Lévy measures* $(\mu_x)_x$ *sufficiently regular* with respect to x, and F is continuous in all its variables and increasing with respect to u. Comparison results between bounded uniformly continuous, as well as semicontinuous, respectively unbounded subsolutions and supersolutions were given.

Second-order degenerate PIDEs are more complex and required careful studies, according to the nature of the integral operator (often reflected in the singularity of the Lévy measure against which they are integrated). When these equations involve *bounded integral operators*, general existence (by Perron's method) and comparison results for semi-continuous and unbounded viscosity solutions were found by Alvarez and Tourin [AT96]. They deal with Cauchy problems for nonlinear equations of the type

$$-u_t + F(x,t,u,Du,D^2u) - \int_{\mathbb{R}^d} K\big(u(x+z,t),u(x,t)\big)\mu_{x,t}(dz) = 0 \text{ on } \mathbb{R}^d \times (0,T)$$

where F is continuous, $(\mu_{x,t})_{x,t}$ is a bounded positive measure and K is continuous, nondecreasing with respect to the first variable. Amadori extended the existence and uniqueness results for a class of Cauchy problems for integro-differential equations, starting with initial data with exponential growth at infinity [Ama03] and proved a local Lipschitz regularity result.

Barles, Buckdahn and Pardoux deal in [BBP97] with systems of parabolic, second order integro-differential equations

$$-u_t^i - \frac{1}{2}\mathrm{tr}\big(\sigma(x)\sigma^*(x)D^2u^i\big) - b(x)Du^i - \mathscr{J}[x,u^i] - f^i(x,t,u,Du^i\sigma,B_i[x,u^i]) = 0$$

where $\mathscr{J}[x,u]$ is a *second order nonlocal operator*

$$\mathscr{J}[x,u]=\int_E \big(u(x+j(x,z)-u(x)-Du\cdot j(x,z))\big)\mu(dz)$$

and

$$B_i[x,u]=\int_E \big(u(x+j(x,z)-u(x))\big)\gamma_i(x,z)\mu(dz).$$

These systems were connected to backwards stochastic differential equations

$$dX_s=b(X_s)ds+\sigma(X_s)dW_s+\int_E j(X_s,z)\tilde{\mu}(ds,dz)$$

and existence and comparison results were established.

Pham connected the optimal stopping time problem in a finite horizon of a controlled jump diffusion process with a parabolic PIDE in [Pha98] and proved existence and comparison principles of uniformly continuous solutions. Existence and comparison results were also provided by Benth, Karlsen and Reikvam in [BKR01] where a singular stochastic control problem is associated to a nonlinear second-order degenerate elliptic integro-differential equation subject to gradient and state constraints, as its corresponding Hamilton-Jacobi-Bellman equation.

Jakobsen and Karlsen in [JK06] used the original approach due to Jensen [Jen88], Ishii [Ish89], Ishii and Lions [IL90], Crandall and Ishii [CI90] and Crandall, Ishii and Lions [CIL92] for proving comparison results for viscosity solutions of nonlinear degenerate elliptic integro-partial differential equations

$$F(x,Du,D^2u,\mathscr{I}[x,u])=0 \text{ in } \mathbb{R}^d \tag{2.7}$$

with second order nonlocal operators

$$\mathscr{J}[x,u]=\int_{\mathbb{R}^d}(u(x+j(x,z))-u(x)-Du(x)\cdot j(x,z)1_B(z))\mu(dz)$$

where μ is a Lévy measure and $j(x,z)$ is the size of the jumps at x. Parabolic versions of their main results were given in [JK05]. They give an analogous of *Jensen-Ishii's Lemma*, a keystone for many comparison principles, but they are restricted to *subquadratic solutions*

$$|u(x)|\le C(1+|x|^2).$$

The viscosity theory for general PIDEs has been recently revisited by Barles and Imbert [BI08] and extended to *solutions with arbitrary growth at infinity*

$$|u(x)|\le C(1+R(x))$$

for any given R, upper semicontinuous function.

The notion of viscosity solution in [BI08] generalizes the one introduced by Imbert in [Imb05] for first-order Hamilton Jacobi equations in the whole space and Arisawa in [Ari06], [Ari07] for degenerate integro-differential equations on bounded domains. It consists of re-

placing the solution by the test-function only around the singularity of the measure, in the nonlocal term.

Definition 2.3.2 (Viscosity subsolution)**.** *An usc function $u:\mathbb{R}^d\to\mathbb{R}$ is a* subsolution *of (2.7) if for any $\phi\in C^2(\mathbb{R}^d)$ such that $u-\phi$ attains a global maximum at x*

$$F(x,D\phi(x),D^2\phi(x),\mathscr{I}_\delta^1[x,\phi]+\mathscr{I}_\delta^2[x,D\phi(x),u])\le 0.$$

Similar definitions of viscosity sub(super)solutions were given by Caffarelli and Silvestre in [CS09]. They test the nonlocal operators in $C^{1,1}$ functions that touch the function u either from above or from below, and are only defined locally in a neighborhood of the touching point, their tails being completed by u itself.

Barles and Imbert provided as well a variant of *nonlocal Jensen Ishii's Lemma* for general integro-differential equations [Imb05]. A direct consequence is the following corollary, which is an extremely useful tool in uniqueness proofs (and shall be used in Chapters 3 and 4).

Theorem 2.3.1 (Corollary of Nonlocal Jensen Ishii's Lemma)**.** *Let u be an usc subsolution of (2.7), v be a lsc viscosity supersolution of (2.7) and $\varphi\in C(\mathbb{R}^{2d})$. If $(\bar x,\bar y)$ is a global maximum point of $u(x)-u(y)-\varphi(x,y)$, then for any $\delta>0$ there exists $\bar\alpha$ such that for $0<\alpha<\bar\alpha$*

$$\begin{aligned} F(\bar x,u(\bar x),p,X^\alpha,\mathscr{I}^{1,\delta}[\bar x,\varphi(\cdot,\bar y)]+\mathscr{I}^{2,\delta}[\bar x,p,u]+o_\alpha(1)) &\le 0\\ F(\bar y,u(\bar y),q,Y^\alpha,\mathscr{I}^{2,\delta}[\bar x,-\varphi(\bar x,\cdot)]+\mathscr{I}^{2,\delta}[\bar y,q,u]+o_\alpha(1)) &\ge 0 \end{aligned}$$

where $p=D_x\varphi(\bar x,\bar y)$, $q=-D_y\varphi(\bar x,\bar y)$ and

$$-\frac{1}{\alpha}I\le\begin{bmatrix}X^\alpha & 0\\ 0 & -Y^\alpha\end{bmatrix}\le D^2\varphi(\bar x,\bar y)+o_\alpha(1).$$

2.3.2 Regularity Theory for Fully Nonlinear Integro-Differential Equations

Regularity theory for *nonlocal evolution equations of variational type* with measurable kernels can be developed using the original ideas of De Giorgi [DG57] and Nash [Nas58] from the calculus of variations. In this setting, Caffarelli, Chan and Vaseur [CCV] show that solutions with initial data in L^2 become instantaneously bounded and Hölder continuous. Their arguments are closely related to the work of Kassmann [Kas09], Kassmann and Bass [BK05a], where the Moser approach for the stationary case is fully developed. Some results about Hölder estimates using probabilistic techniques can be found in [BL02] and [BK05b].

In the setting of viscosity solutions, there are essentially two approaches for proving Hölder or Lipschitz regularity of viscosity solutions: by ABP - Harnack inequalities and by Ishii-Lions's viscosity method.

Regularity theory of viscosity solutions for fully nonlinear integro-differential equations by ABP - Harnack inequalities was recently developed by Caffarelli and Silvestre in [CS09]. Under suitable assumptions that we discuss below, the authors show that the solution is $C^{0,\alpha}$ and give

the following Hölder estimates of solutions

$$||u||_{C^{0,\alpha}(B_{1/2})} \leq C(\sup_{\mathbb{R}^d} |u| + C_0).$$

Moreover, using the above estimates for the incremental quotients of the solution, they establish $C^{1,\alpha}$ regularity results

$$||u||_{C^{1,\alpha}(B_{1/2})} \leq C(\sup_{\mathbb{R}^d} |u| + C_0).$$

In their paper, the authors focus on equations obtained from purely jump processes (without diffusions or drifts), e.g.

$$\inf_{\gamma} \sup_{\delta} \mathscr{J}^{\gamma,\delta}[x,u] = 0$$

with $\mathscr{J}^{\gamma,\delta}$ comparable with the fractional Laplacian of exponent $\beta \in (0,2)$ and provide estimates that remain uniform as the degree of the equation approaches 2 (i.e. $\beta \to 2$), therefore the theory reaches naturally the second-order case. They intend to extend to the nonlocal case the existing theory for fully nonlinear second-order elliptic equations (see the self-contained notes by Cabré and Caffarelli [CC95] and the references therein).

Similar to second-order differential operators, they use extremal Pucci operators to define a replacement to the concept of *uniform ellipticity*. Thus, an elliptic operator $\mathscr{I}$ with respect to a class $\mathscr{L}$ of linear integro-differential operators must satisfy

$$M^-_{\mathscr{L}}[x,v] \leq \mathscr{I}[x,u+v] - \mathscr{I}[x,u] \leq M^+_{\mathscr{L}}[x,v]$$

where $M^-_{\mathscr{L}}$ and $M^+_{\mathscr{L}}$ are the maximal and minimal operators with respect to the class $\mathscr{L}$

$$\begin{aligned} M^-_{\mathscr{L}}[x,u] &= \inf_{L\in\mathscr{L}} Lu(x) \\ M^+_{\mathscr{L}}[x,u] &= \sup_{L\in\mathscr{L}} Lu(x). \end{aligned}$$

Regularity results are given for the class $\mathscr{L}_0$ of operators of the form

$$\mathscr{L}_0 u(x) = \int_{\mathbb{R}^d} (u(x+z) - u(x-z) - 2u(x))\, K(y)\, dy$$

with

$$(2-\beta)\frac{\lambda}{|y|^{d+\beta}} \leq K(y) \leq (2-\beta)\frac{\Lambda}{|y|^{d+\beta}}, \beta \in (0,2)$$

In this way, they can deal with *fully nonlinear operators* (and accordingly fully nonlinear equations), defined as the $supremum$ or as an $infsup$ over a collection of linear operators. In addition, the extremal operators allow to define solutions to *equations with bounded, measurable coefficients*.

The Lévy measure μ is given by a positive, symmetric kernel satisfying the *integrability assumption*

$$\int_{\mathbb{R}^d} \frac{|z|^2}{1+|z|^2} K(z)\, dz < \infty.$$

Hölder regularity results for viscosity solutions of fully nonlinear integro-differential equations were also provided by Barles, Chasseigne and Imbert [BCI11], using a direct viscosity method, initially introduced by Ishii and Lions in [IL90]. This method gives explicit $C^{0,\alpha}$ estimates

$$|u(x)-u(y)| \le L|x-y|^{\alpha}, \text{ if } |x-y| \le \delta$$

in terms of the nonlinearity F and the singular measure(s) μ_x appearing in the nonlocal term (L depends only on the constants and functions associated with F and μ_x). In addition, they can *identify the critical Hölder exponent* α and show that the solution is α-Hölder continuous, for any $\alpha < \beta$, where β characterizes the singularity of the measure associated to the nonlocal operator. Their results are given for *a general class of nonlocal equations* satisfying *suitable ellipticity and growth assumptions*. The results hold for a wide class of integro-differential operators, whose *singular measures depend on x and are only bounded at infinity*, uniformly with respect to x

$$\sup_{x\in\mathbb{R}^d}\int_{\mathbb{R}^d}\min(|z|^2,1)\mu_x(dz)<\infty.$$

Unlike the Harnack approach, the viscosity method requires *regularity of the coefficients*.

The authors deal with equations having both local and nonlocal terms, which are *strictly elliptic in a generalized sense*: for each point, the equation is either uniformly elliptic in the classical sense and (possibly) degenerate with respect to the nonlocal term, or conversely. In the example below

$$-\text{tr}(\sigma(x)\sigma^*(x)D^2u)-c(x)\mathscr{I}[x,u]+H(x,Du)=0$$

classical ellipticity in the second-order differential term means that $\sigma(x)\sigma^*(x)$ is positive definite and $c(x)$ might be zero. Precise computations show that we just need ellipticity in the gradient direction. When it comes to the *nonlocal* term, one has to translate in a proper way the ellipticity in the gradient direction. And this is reflected in a suitable *nondegeneracy condition with respect to the the family of Lévy measures*. Roughly speaking, the measures have to charge cones $C_{\eta,\delta}(p)$ in a ball of radius δ, with axis in the gradient direction p and aperture η, i.e.

$$\int_{\mathscr{C}_{\eta,\delta}(p)}|z|^2\mu_x(dz)\ge C(\eta)\delta^{2-\beta}$$

where β characterizes the singularity of the measure.

The *growth condition* allows to consider equations with superlinear growth of the gradient

$$-c(x)\mathscr{I}[x,u]+b(x)|Du|^k+|Du|^r=f(x),$$

in which case solutions are Hölder continuous for $k=\beta+\tau$, $r=\beta$ and $b\in C^{0,\tau}$.

Moreover, solutions of Bellman-Isaacs equations

$$cu+\sup_{\lambda\in\Lambda}\inf_{\gamma\in\Gamma}\Big\{-\frac{1}{2}\text{Tr}(\sigma_{\lambda,\gamma}(x)\sigma^*_{\lambda,\gamma}(x)D^2u)-b_{\lambda,\gamma}(x)\cdot Du-\mathscr{I}^{\lambda,\gamma}_{LI}[x,u]-f_{\lambda,\gamma}(x)\Big\}=0 \tag{2.8}$$

are Hölder continuous, if all the nonlocal operators have fractional exponents $\beta^{\lambda,\gamma} \geq \beta > 0$ and the coefficients are Hölder continuous, uniformly with respect to λ, γ.

2.4 Discussion

Although many comparison results were given, to the best of our knowledge, no strong maximum principle of viscosity solutions for integro-differential equations associated to jump-diffusion processes exists. We present some of our recent results in Chapter 3 This will be used to derive a strong comparison result between viscosity sub and supersolution.

Strong Comparison Principle on Ω open and bounded. *If u is a bounded usc subsolution of (2.4), v is a lsc supersolution of (2.4) such that $u(x_0) = v(x_0)$ for some $x_0 \in \Omega$ then $u \equiv v$ in $\overline{\Omega}$.*

As far as the regularity is concerned, the above methods do not cover the same class of equations and each of it has its own advantages. The powerful Harnack approach applies for *uniformly elliptic fully nonlinear equations*, with *rough coefficients* and leads in general to further regularity such as $C^{1,\alpha}$, but requires some integrability condition of the measure at infinity. On the other hand, viscosity methods apply under weaker ellipticity assumptions and therefore deal with a *large* class of *degenerate, fully nonlinear equations*, in particular with *super-linear gradient growth*, allow measures which are only bounded at infinity, but require Hölder continuous coefficients and do not seem to yield further regularity.

In Chapter 4 we extend to Lipschitz regularity the Hölder regularity results recently obtained by Barles, Chasseigne and Imbert. In addition, we deal with a new class of nonlocal equations that we term *mixed integro-differential equations*. In near future, we would like to address the Harnack approach for this type of equations. It would be also interesting to investigate the possibility of obtaining $C^{1,\alpha}$ estimates by direct viscosity methods.

CHAPTER 3

Strong Maximum Principle for Integro-differential Equations

All truths are easy to understand once they are discovered; the point is to discover them.
Galileo Galilei (1564 - 1642)

Abstract: This chapter is concerned with the study of the Strong Maximum Principle for semi-continuous viscosity solutions of fully nonlinear, second-order parabolic integro - differential equations. We study separately the propagation of maxima in the horizontal component of the domain and the local vertical propagation in simply connected sets of the domain. We give two types of results for horizontal propagation of maxima: one is the natural extension of the classical results of local propagation of maxima and the other comes from the structure of the nonlocal operator. As an application, we use the Strong Maximum Principle to prove a Strong Comparison Result of viscosity sub and supersolution for integro-differential equations.[1]

Résumé: Ce chapitre est dédié au Principe de Maximum Fort pour les solutions de viscosité semi-continues des équations intégro-différentielles nonlinéaires de second ordre. Nous étudions séparément la propagation horizontale de maxima, ainsi que la propagation verticale dans les domaines simplement connexes. En ce qui concerne la propagation horizontale de maxima, nous présentons deux types des résultats: une extension naturelle des résultats classiques de propagation locale de maxima et un résultat simple qui est donné par la structure de l' opérateur nonlocal. Dans la dernière partie, nous utilisons le Principe de Maximum Fort pour déduire un Résultat de Comparaison Fort entre sous et sur-solutions des équations intégro-différentielles.

Keywords: nonlinear parabolic integro-differential equations, strong maximum principle, viscosity solutions

[1] This work represents the article *On the Strong Maximum Principle for Second Order Nonlinear Parabolic Integro-Differential Equations*, submitted.

Contents

3.1 Introduction

We investigate the Strong Maximum Principle for viscosity solutions of second-order nonlinear parabolic integro-differential equations of the form

$$u_t + F(x,t,Du,D^2u,\mathscr{I}[x,t,u]) = 0 \text{ in } \Omega \times (0,T) \tag{3.1}$$

where $\Omega \subset \mathbb{R}^N$ is an open bounded set, $T > 0$ and u is a real-valued function defined on $\mathbb{R}^N \times [0,T]$. The symbols u_t, Du, D^2u stand for the derivative with respect to time, respectively the gradient and the Hessian matrix with respect to x. $\mathscr{I}[x,t,u]$ is an integro-differential operator, taken on the whole space $\mathbb{R}^N$. Although the nonlocal operator is defined on the whole space, we consider equations on a bounded domain Ω. Therefore, we assume that the function $u = u(x,t)$ is a priori defined outside the domain Ω. The choice corresponds to prescribing the solution in $\Omega^c \times (0,T)$, as for example in the case of Dirichlet boundary conditions.

The nonlinearity F is a real-valued, continuous function in $\Omega \times [0,T] \times \mathbb{R}^N \times \mathbb{S}^N \times \mathbb{R}$, ($\mathbb{S}^N$ being the set of real symmetric $N \times N$ matrices) and *degenerate elliptic*, i.e.

$$F(x,t,p,X,l_1) \le F(x,t,p,Y,l_2) \text{ if } X \ge Y,\ l_1 \ge l_2, \tag{3.2}$$

for all $(x,t) \in \overline{\Omega} \times [0,T]$, $p \in \mathbb{R}^N \setminus \{0\}$, $X, Y \in \mathbb{S}^N$ and $l_1, l_2 \in \mathbb{R}$.

Throughout this work, we consider integro-differential operators of the type

$$\mathscr{I}[x,t,u] = \int_{\mathbb{R}^N} (u(x+z,t) - u(x,t) - Du(x,t)\cdot z 1_B(z))\mu_x(dz) \tag{3.3}$$

where $1_B(z)$ denotes the indicator function of the unit ball B and $\{\mu_x\}_{x\in\Omega}$ is a family of Lévy measures, i.e. non-negative, possibly singular, Borel measures on Ω such that

$$\sup_{x\in\Omega}\int_{\mathbb{R}^N}\min(|z|^2,1)\mu_x(dz)<\infty.$$

In particular, Lévy-Itô operators are important special cases of nonlocal operators and are defined as follows

$$\mathscr{J}[x,t,u]=\int_{\mathbb{R}^N}(u(x+j(x,z),t)-u(x,t)-Du(x,t)\cdot j(x,z)1_B(z))\mu(dz) \tag{3.4}$$

where μ is a Lévy measure and $j(x,z)$ is the size of the jumps at x satisfying

$$|j(x,z)|\le C_0|z|,\ \forall x\in\Omega,\forall z\in\mathbb{R}^N$$

with C_0 a positive constant.

We denote by $USC(\mathbb{R}^N\times[0,T])$ and $LSC(\mathbb{R}^N\times[0,T])$ the set of respectively upper and lower semi-continuous functions in $\mathbb{R}^N\times[0,T]$. By Strong Maximum for equation (3.1) in an open set $\Omega\times(0,T)$ we mean the following.

SMaxP: *any $u\in USC(\mathbb{R}^N\times[0,T])$ viscosity subsolution of (3.1) that attains a maximum at $(x_0,t_0)\in\Omega\times(0,T)$ is constant in $\Omega\times[0,t_0]$.*

The Strong Maximum Principle follows from the horizontal and vertical propagation of maxima, that we study separately. By horizontal propagation of maxima we mean the following: if the maximum is attained at some point (x_0,t_0) then the function becomes constant in the connected component of the domain $\Omega\times\{t_0\}$ which contains the point (x_0,t_0). By local vertical propagation we understand that if the maximum is attained at some point (x_0,t_0) then at any time $t<t_0$ one can find another point (x,t) where the maximum is attained. This will further imply the propagation of maxima in the region $\Omega\times(0,t_0)$.

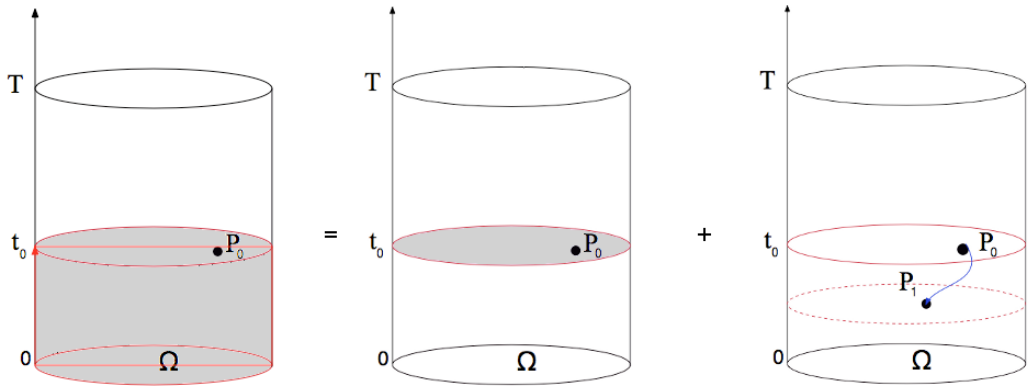

Figure 3.1: Strong Maximum Principle follows from the horizontal and vertical propagation of maxima.

We set $Q_T=\Omega\times(0,T]$ and for any point $P_0=(x_0,t_0)\in Q_T$, we denote by $S(P_0)$ the set of all points $Q\in Q_T$ which can be connected to P_0 by a simple continuous curve in Q_T and by $C(P_0)$ we denote the connected component of $\Omega\times\{t_0\}$ which contains P_0.

The horizontal propagation of maxima in $C(P_0)$ requires two different perspectives. An almost immediate result follows from the structure of the nonlocal operator. More precisely, we show that *Strong Maximum Principle holds for PIDEs involving nonlocal operators in the form (3.3) whenever the whole domain (not necessarily connected) can be covered by translations of measure supports, starting from a maximum point.* This is the case for example of a pure nonlocal diffusion

$$u_t - \mathscr{I}[x,t,u] = 0 \text{ in } \mathbb{R}^N \times (0,T) \tag{3.5}$$

where $\mathscr{I}$ is an isotropic Lévy operator of form (3.3), integrated against the Lévy measure associated with the fractional Laplacian $(-\Delta)^{\beta/2}$:

$$\mu(dz) = \frac{dz}{|z|^{N+\beta}}.$$

The result is the natural extension to PIDEs of the maximum principle for nonlocal operators generated by nonnegative kernels obtained by Coville in [Cov08].

Nevertheless, there are equations for which maxima do not propagate just by translating measure supports, such as pure nonlocal equations with nonlocal terms associated with the fractional Laplacian, but whose measure supports are defined only on half space. *Mixed integro-differential equations*, i.e. equations for which local diffusions occur only in certain directions and nonlocal diffusions on the orthogonal ones cannot be handled by simple techniques, as they might be degenerate in both local or nonlocal terms but the overall behavior might be driven by their interaction (the two diffusions cannot cancel simultaneously). We have in mind equations of the type

$$u_t - \mathscr{I}_{x_1}[u] - \frac{\partial^2 u}{\partial x_2^2} = 0 \text{ in } \mathbb{R}^2 \times (0,T) \tag{3.6}$$

for $x = (x_1, x_2) \in \mathbb{R}^2$. The diffusion term gives the ellipticity in the direction of x_2, while the nonlocal term gives it in the direction of x_1

$$\mathscr{I}_{x_1}[u] = \int_{\mathbb{R}} (u(x_1+z_1,x_2) - u(x) - \frac{\partial u}{\partial x_1}(x)\cdot z_1 1_{[-1,1]}(z_1))\mu_{x_1}(dz_1)$$

where $\{\mu_{x_1}\}_{x_1}$ is a family of Lévy measures. However, we manage to show that under some nondegeneracy and scaling assumptions on the nonlinearity F, *if a viscosity subsolution attains a maximum at $P_0 = (x_0,t_0) \in Q_T$, then u is constant (equal to the maximum value) in the horizontal component $C(P_0)$.*

We then prove the local propagation of maxima in the cylindrical region $\Omega \times (0,T]$ and thus extend to parabolic integro-differential equations the results obtained by Da Lio in [DL04] and Bardi and Da Lio in [BDL01] and [BDL03] for fully nonlinear degenerate elliptic convex and concave Hamilton Jacobi operators. For helpful details of Strong Maximum Principle results for Hamilton Jacobi equations we refer to [Bar94]. Yet, it is worth mentioning that Strong Maximum Principle for linear elliptic equations goes back to Hopf in the 20s and to Nirenberg, for parabolic equations [Nir53].

In the last part we use Strong Maximum Principle to prove a Strong Comparison Result of viscosity sub and supersolution for integro-differential equations of the form (3.1) with the Dirichlet boundary condition

$$u = \varphi \text{ on } \Omega^c \times [0,T] \tag{3.7}$$

where φ is a continuous function.

Nonlocal equations find many applications in mathematical finance and occur in the theory of Lévy jump-diffusion processes. The theory of viscosity solutions has been extended for a rather long time to Partial Integro-Differential Equations (PIDEs). Some of the first papers are due to Soner [Son86a], [Son86b], in the context of stochastic control jump diffusion processes. Following his work, existence and comparison results of solutions for *first order PIDEs* were given by Sayah in [Say91a] and [Say91b].

Second-order degenerate PIDEs are more complex and required careful studies, according to the nature of the integral operator (often reflected in the singularity of the Lévy measure against which they are integrated). When these equations involve *bounded integral operators*, general existence and comparison results for semi-continuous and unbounded viscosity solutions were found by Alvarez and Tourin [AT96]. Amadori extended the existence and uniqueness results for a class of Cauchy problems for integro-differential equations, starting with initial data with exponential growth at infinity [Ama03] and proved a local Lipschitz regularity result.

Jakobsen and Karlsen in [JK06] used the original approach due to Jensen [Jen88], Ishii [Ish89], Ishii and Lions [IL90], Crandall and Ishii [CI90] and Crandall, Ishii and Lions [CIL92] for proving comparison results for viscosity solutions of nonlinear degenerate elliptic integro-partial differential equations with second order nonlocal operators. Parabolic versions of their main results were given in [JK05]. They give an analogous of Jensen-Ishii's Lemma, a keystone for many comparison principles, but they are restricted to *subquadratic solutions*.

The viscosity theory for general PIDEs has been recently revisited and extended to *solutions with arbitrary growth at infinity* by Barles and Imbert [BI08]. The authors provided as well a variant of Jensen Ishii's Lemma for general integro-differential equations. The notion of viscosity solution generalizes the one introduced by Imbert in [Imb05] for first-order Hamilton Jacobi equations in the whole space and Arisawa in [Ari06], [Ari07] for degenerate integro-differential equations on bounded domains.

The chapter is organized as follows. In section §3.2 we study separately the propagation of maxima in $C(P_0)$ and in the region $\Omega \times (0,t_0)$. In section §3.3 similar results are given for Lévy Itô operators. Examples are provided in section §3.4. In section §3.5 we prove a Strong Comparison Result for the Dirichlet Problem, based on the Strong Maximum Principle for the linearized equation.

3.2 Strong Maximum Principle - General Nonlocal Operators

The aim of this section is to prove the local propagation of maxima of viscosity solutions of (3.1) in the cylindrical region Q_T. As announced, we study separately the propagation of maxima in

the horizontal domains $\Omega \times \{t_0\}$ and the local vertical propagation in regions $\Omega \times (0, t_0)$. Each case requires different sets of assumptions.

In the sequel, we refer to integro-differential equations of the form (3.1) where the function u is a priori given outside Ω. Assume that F satisfies

(E) F is continuous in $\Omega \times [0,T] \times \mathbb{R}^N \times \mathbb{S}^N \times \mathbb{R}$ and degenerate elliptic.

Results are presented for general nonlocal operators

$$\mathscr{I}[x,t,u] = \int_{\mathbb{R}^N} (u(x+z,t) - u(x,t) - Du(x,t)\cdot z 1_B(z))\mu_x(dz)$$

where $\{\mu_x\}_{x\in\Omega}$ is a family of Lévy measures. We assume it satisfies assumption

(M) there exists a constant $\tilde{C}_\mu > 0$ such that, for any $x \in \Omega$,

$$\int_B |z|^2 \mu_x(dz) + \int_{\mathbb{R}^N \setminus B} \mu_x(dz) \le \tilde{C}_\mu.$$

To overcome the difficulties imposed by the behavior at infinity of the measures $(\mu_x)_x$, we often need to split the nonlocal term into

$$\begin{aligned} \mathscr{I}^1_\delta[x,t,u] &= \int_{|z|\le\delta} (u(x+z,t) - u(x,t) - Du(x,t)\cdot z 1_B(z))\mu_x(dz) \\ \mathscr{I}^2_\delta[x,t,p,u] &= \int_{|z|>\delta} (u(x+z,t) - u(x,t) - p\cdot z 1_B(z))\mu_x(dz) \end{aligned}$$

with $0 < \delta < 1$ and $p \in \mathbb{R}^N$.

There are several equivalent definitions of viscosity solutions, but we will mainly refer to the following one.

Definition 3.2.1 (Viscosity solutions)**.** *An usc function $u : \mathbb{R}^N \times [0,T] \to \mathbb{R}$ is a* subsolution *of (3.1) if for any $\phi \in C^2(\mathbb{R}^N \times [0,T])$ such that $u - \phi$ attains a global maximum at $(x,t) \in \Omega \times (0,T)$*

$$\phi_t(x,t) + F(x,t,\phi(x,t),D\phi(x,t),D^2\phi(x,t),\mathscr{I}^1_\delta[x,t,\phi] + \mathscr{I}^2_\delta[x,t,D\phi(x,t),u]) \le 0.$$

A lsc function $u : \mathbb{R}^N \times [0,T] \to \mathbb{R}$ is a supersolution *of (3.1) if for any test function $\phi \in C^2(\mathbb{R}^N \times [0,T])$ such that $u - \phi$ attains a global minimum at $(x,t) \in \Omega \times (0,T)$*

$$\phi_t(x,t) + F(x,t,\phi(x,t),D\phi(x,t),D^2\phi(x,t),\mathscr{I}^1_\delta[x,t,\phi] + \mathscr{I}^2_\delta[x,t,D\phi(x,t),u]) \ge 0.$$

3.2.1 Horizontal Propagation of Maxima by Translations of Measure Supports

Maximum principle results for nonlocal operators generated by nonnegative kernels defined on topological groups acting continuously on a Hausdorff space were settled out by Coville in [Cov08]. In the following, we present similar results for integro-differential operators in the setting of viscosity solutions.

It can be shown that Maximum Principle holds for nonlocal operators given by (3.3) whenever the whole domain can be covered by translations of measure supports, starting from a maximum point, as suggested in Figure 3.2.2.

An additional assumption is required with respect to the nonlinearity F. More precisely we require that

(E') F is continuous, degenerate elliptic and for $x, p \in \mathbb{R}^N$ and $l \in \mathbb{R}$

$$F(x,t,0,O,l) \leq 0 \Rightarrow l \geq 0.$$

For the sake of precision, the following result is given for integro-differential equations defined in $\mathbb{R}^N$. We explain in Remark 3.2.2 what happens when we restrict to some open set Ω.

Theorem 3.2.1. *Assume the family of measures $\{\mu_x\}_{x\in\Omega}$ satisfies assumption (M). Let F satisfy (E') in $\mathbb{R}^N \times [0,T]$ and $u \in USC(\mathbb{R}^N \times [0,T])$ be a viscosity solution of (3.1) in $\mathbb{R}^N \times (0,T)$. If u attains a global maximum at $(x_0,t_0) \in \mathbb{R}^N \times (0,T)$, then $u(\cdot,t_0)$ is constant on $\overline{\bigcup_{n\geq 0} A_n}$, with*

$$A_0 = \{x_0\}, \quad A_{n+1} = \bigcup_{x\in A_n} (x + supp(\mu_x)). \tag{3.8}$$

Proof. Assume that u is a viscosity subsolution for the given equation. Consider the test-function $\psi \equiv 0$ and write the viscosity inequality at point (x_0,t_0)

$$F(x_0,t_0,0,O,\mathscr{I}_\delta^1[x_0,t_0,\psi] + \mathscr{I}_\delta^2[x_0,t_0,D\psi(x_0,t_0),u]) \leq 0.$$

This implies according to assumption (E'), that

$$\mathscr{I}_\delta^2[x_0,t_0,u] = \int_{|z|\geq\delta} (u(x_0+z,t_0) - u(x_0,t_0))\mu_{x_0}(dz) \geq 0.$$

But u attains its maximum at (x_0,t_0) and thus $u(x_0+z,t_0) - u(x_0,t_0)) \leq 0$. Letting δ go to zero we have

$$u(z,t_0) = u(x_0,t_0), \text{ for all } z \in x_0 + \text{supp}(\mu_{x_0}).$$

Arguing by induction, we obtain

$$u(z,t_0) = u(x_0,t_0), \forall z \in \bigcup_{n\geq 0} A_n.$$

Take now $z_0 \in \overline{\bigcup_{n\geq 0} A_n}$. Then, there exists a sequence of points $(z_n)_n \subset \bigcup_{n\geq 0} A_n$ converging to z_0. Since u is upper semicontinuous, we have

$$u(z_0,t_0) \geq \limsup_{z_n \to z_0} u(z_n,t_0) = u(x_0,t_0).$$

But (x_0,t_0) is a maximum point and the converse inequality holds. Therefore

$$u(z,t_0) = u(x_0,t_0), \forall z \in \overline{\bigcup_{n\geq 0} A_n}.$$

□

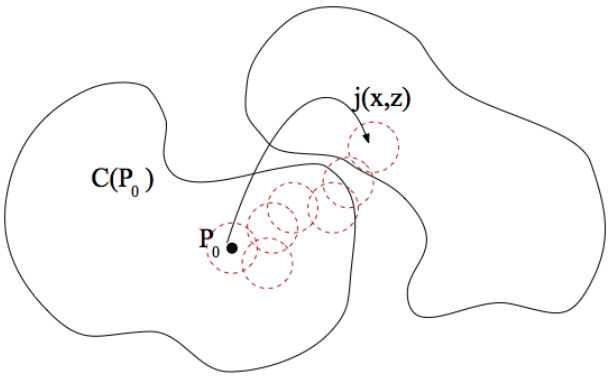

Figure 3.2: Horizontal propagation of maxima by translations of measure supports.

Remark 3.2.1. *In particular when $supp(\mu_x) = supp(\mu) = B$, with μ being a Lévy measure and B the unit ball, $\mathbb{R}^N$ can be covered by translations of $supp(\mu)$ starting at x_0*

$$\mathbb{R}^N = x_0 + \bigcup_{n\geq 0} \big(\underbrace{supp(\mu) + ... + supp(\mu)}_{n}\big).$$

and thus $u(\cdot, t_0)$ is constant in $\mathbb{R}^N$.

Remark 3.2.2. *Whenever the equation is restricted to Ω, with the corresponding Dirichlet condition outside the domain, then iterations must be taken for all the points in Ω, i.e.*

$$A_{n+1} = \bigcup_{x\in\Omega\cap A_n} (x + supp(\mu_x))$$

In particular, if $\Omega \subset \overline{\bigcup_{n\geq 0} A_n}$, then $u(\cdot, t_0)$ is constant in Ω.

Remark 3.2.3. *The domain Ω may not necessarily be connected and still maxima might propagate, since jumps from one connected component to another might occur when measure supports overlap two or more connected components.*

The previous result has an immediate corollary. If all measure supports have nonempty (topological) interior and contain the origin, strong maximum principle holds.

Corollary 3.2.1. *Let Ω be connected, F be as before and $u \in USC(\mathbb{R}^N \times [0,T])$ be a viscosity subsolution of (3.1) in $\Omega \times (0,T)$. Assume that $\{\mu_x\}_{x\in\Omega}$ satisfies (M) and in addition that the origin belongs to the topological interiors of all measure supports*

$$0 \in \overset{\circ}{\overbrace{supp(\mu_x)}}, \forall x \in \Omega. \tag{3.9}$$

If the solution u attains a global maximum at $(x_0, t_0) \in \Omega \times (0,T)$, then $u(\cdot, t_0)$ is constant in the whole domain Ω.

Proof. Consider the iso-level

$$\Gamma_{x_0} = \{x \in \Omega; u(x, t_0) = u(x_0, t_0)\}.$$

Then the set is simultaneously open since $0 \in \overset{\circ}{\overbrace{\text{supp}(\mu_x)}}$ implies, by Theorem 3.2.1, together with Remark 3.2.2 that for any $x \in \Gamma_{x_0}$ we have

$$\left(x + \overset{\circ}{\overbrace{\text{supp}(\mu_x)}}\right) \cap \Omega \subset \Gamma_{x_0}$$

and closed because for any $x \in \bar{\Gamma}_{x_0}$ we have by the upper-semicontinuity of u

$$u(x,t_0) \geq \limsup_{y \to x,\ y \in \Gamma_{x_0}} u(y,t_0) = \max_{y \in \Omega} u(y,t_0)$$

thus $u(x,t_0) = u(x_0,t_0)$. Therefore, $\Gamma_{x_0} = \Omega$ since Ω is connected and this completes the proof. □

3.2.2 Horizontal Propagation of Maxima under Nondegeneracy Conditions

There are cases when conditions (3.8) and (3.9) fail, such as measures whose supports are contained in half space or nonlocal terms acting in one direction, as we shall see in section §3.4.

However, we manage to show that, if a viscosity subsolution attains a maximum at $P_0 = (x_0,t_0) \in Q_T$, then the maximum propagates in the horizontal component $C(P_0)$, as shown in Figure 3.2.2. This result is based on *nondegeneracy* (N) and *scaling* (S) properties on the nonlinearity F:

(N) For any $\bar{x} \in \Omega$ and $0 < t_0 < T$ there exist $R_0 > 0$ small enough and $0 \leq \eta < 1$ such that for any $0 < R < R_0$ and $c > 0$

$$F(x,t,p,I - \gamma p \otimes p, \tilde{C}_\mu - c\gamma \int_{\mathscr{C}_{\eta,\gamma}(p)} |p \cdot z|^2 \mu_x(dz)) \to +\infty \text{ as } \gamma \to +\infty$$

uniformly for $|x - \bar{x}| \leq R$ and $|t - t_0| \leq R$, $R/2 \leq |p| \leq R$, where

$$\mathscr{C}_{\eta,\gamma}(p) = \{z;\ (1-\eta)|z||p| \leq |p \cdot z| \leq 1/\gamma\}$$

and $\tilde{C}_\mu$ appears in (M).

(S) There exist some constants $R_0 > 0$, $\varepsilon_0 > 0$ and $\gamma_0 > 0$ s.t. for all $0 < R < R_0, \varepsilon < \varepsilon_0$ and $\gamma \geq \gamma_0$ the following condition holds for all $|x - \bar{x}| \leq R$ and $|t - t_0| \leq R$ and $R/2 \leq |p| \leq R$

$$F(x,t,\varepsilon p, \varepsilon(I - \gamma p \otimes p), \varepsilon l) \geq \varepsilon F(x,t,p,I - \gamma p \otimes p, l).$$

As we shall see in §3.4 the assumption (M) which states that the measure μ_x is bounded at infinity, uniformly with respect to x and the possible singularity at the origin is of order $|z|^2$ is not sufficient to ensure condition (N). The following assumption is in general needed, provided that the nonlinearity F is nondegenerate in the nonlocal term.

(M^c) For any $x \in \Omega$ there exist $1 < \beta < 2$, $0 \leq \eta < 1$ and a constant $C_\mu(\eta) > 0$ such that the

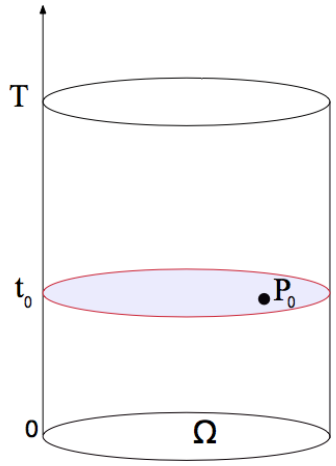

Figure 3.3: Horizontal propagation of maxima: if the maximum is attained at some point $P_0 = (x_0, t_0)$ then the function becomes constant in the connected component $C(P_0)$ of the domain $\Omega \times \{t_0\}$ which contains the point (x_0, t_0).

following holds with $\mathscr{C}_{\eta,\gamma}(p)$ as before

$$\int_{\mathscr{C}_{\eta,\gamma}(p)} |z|^2 \mu_x(dz) \geq C_\mu(\eta)\gamma^{\beta-2}, \forall \gamma \geq 1.$$

As pointed out in section §3.4, (M^c) holds for a wide class of Lévy measures as well as $(N)-(S)$ for a class of nonlinearities F.

Theorem 3.2.2. *Assume the family of measures $\{\mu_x\}_{x\in\Omega}$ satisfies assumptions (M). Let $u \in USC(\mathbb{R}^N \times [0,T])$ be a viscosity subsolution of (3.1) that attains a global maximum at $P_0 = (x_0, t_0) \in Q_T$. If F satisfies $(E), (N)$, and (S) then u is constant in $C(P_0)$.*

Proof. We proceed as for locally uniformly parabolic equations and argue by contradiction.

1. Suppose there exists a point $P_1 = (x_1, t_0)$ such that $u(P_1) < u(P_0)$. The solution u being upper semi-continuous, by classical arguments we can construct for fixed t_0 a ball $B(\bar{x}, R)$ where

$$u(x, t_0) < M = \max_{\mathbb{R}^N}(u(\cdot, t_0)), \forall x \in B(\bar{x}, R).$$

In addition there exists $x^* \in \partial B(\bar{x}, R)$ such that $u(x^*, t_0) = M$. Translating if necessary the center $\bar{x}$ in the direction $x^* - \bar{x}$, we can choose $R < R_0$, with R_0 given by condition (N).

Moreover we can extend the ball to an ellipsoid

$$\mathscr{E}_R(\bar{x}, t_0) := \{(x,t);\ |x-\bar{x}|^2 + \lambda|t-t_0|^2 < R^2\}$$

with λ large enough the function u satisfies

$$u(x,t) < M, \text{ for } (x,t) \in \overline{\mathscr{E}_R(\bar{x}, t_0)} \text{ s.t. } |x-\bar{x}| \leq R/2.$$

Remark that $(x^*, t_0) \in \partial\mathscr{E}_R(\bar{x}, t_0)$ with $u(x^*, t_0) = M$.

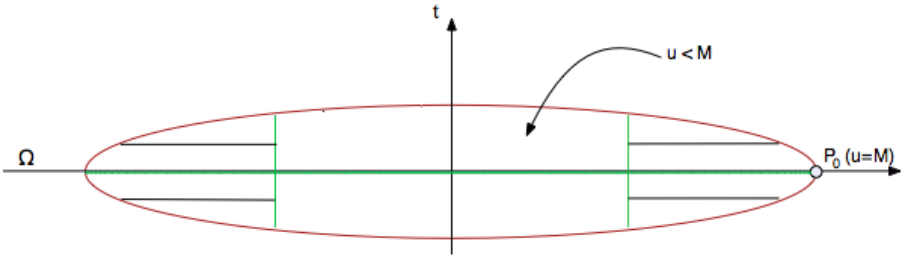

Figure 3.4: Construction of the ellipsoid $\mathscr{E}_R(\bar{x},t_0) := \{(x,t);\ |x-\bar{x}|^2+\lambda|t-t_0|^2 < R^2\}$ and of the corresponding auxiliary function v such that inside the dashed area, v is a strict supersolution of the integro-differential equation.

2. Introduce the auxiliary function

$$v(x,t) = e^{-\gamma R^2} - e^{-\gamma(|x-\bar{x}|^2+\lambda|t-t_0|^2)}$$

where $\gamma > 0$ is a large positive constant, yet to be determined. Note that $v = 0$ on $\partial\mathscr{E}_R(\bar{x},t_0)$ and $-1 < v < 0$, in $\mathscr{E}_R(\bar{x},t_0)$. Denote $d(x,t) = |x-\bar{x}|^2+\lambda|t-t_0|^2$. Direct computations give

$$\begin{aligned} v_t(x,t) &= 2\gamma e^{-\gamma d(x,t)}\lambda(t-t_0) \\ Dv(x,t) &= 2\gamma e^{-\gamma d(x,t)}(x-\bar{x}) \\ D^2v(x,t) &= 2\gamma e^{-\gamma d(x,t)}(I-2\gamma(x-\bar{x})\otimes(x-\bar{x})). \end{aligned}$$

In upcoming Proposition 3.2.1 we show there exist two positive constants $c = c(\eta,R)$ and $\gamma_0 > 0$ such that for $\gamma \geq \gamma_0$, the following estimate of the nonlocal term holds

$$\mathscr{I}[x,t,v] \leq 2\gamma e^{-\gamma d(x,t)}\Big\{\tilde{C}_\mu - c\gamma\int_{\mathscr{C}_{\eta,\gamma}(x-\bar{x})}|(x-\bar{x})\cdot z|^2\mu_x(dz)\Big\}$$

in the subdomain $\mathscr{D}_R(\bar{x},t_0) := \{(x,t)\in\mathscr{E}_R(\bar{x},t_0); |x-\bar{x}| > R/2\}$.

3. From the nondegeneracy condition (N) and scaling assumption (S) we get that v is a strict supersolution at points (x,t) in $\mathscr{D}_R(\bar{x},t_0)$. Indeed, for γ large enough

$$F\Big(x,t,x-\bar{x},I-2\gamma(x-\bar{x})\otimes(x-\bar{x}),\tilde{C}_\mu - c\gamma\int_{\mathscr{C}_{\eta,\gamma}(x-\bar{x})}|(x-\bar{x})\cdot z|^2\mu_x(dz)\Big) > 0$$

On the other hand

$$\begin{aligned} v_t(x,t) + F(x,t,Dv(x,t),D^2v(x,t),\mathscr{I}[x,t,v]) \\ = 2\gamma e^{-\gamma d(x,t)}\lambda(t-t_0) + F\Big(x,t,2\gamma e^{-\gamma d(x,t)}(x-\bar{x}), \\ \ldots, 2\gamma e^{-\gamma d(x,t)}(I-2\gamma(x-\bar{x})\otimes(x-\bar{x})\Big), \\ \ldots, 2\gamma e^{-\gamma d(x,t)}\Big\{\tilde{C}_\mu - c\gamma\int_{\mathscr{C}_{\eta,\gamma}(x-\bar{x})}|(x-\bar{x})\cdot z|^2\mu_x(dz)\Big\}\Big) \end{aligned}$$

This further implies that

$$\begin{aligned} v_t(x,t) + F(x,t,Dv(x,t),D^2v(x,t),\mathscr{I}[x,t,v]) \\ \geq 2\gamma e^{-\gamma d(x,t)}\big(\lambda(t-t_0) + F\big(x,t,x-\bar{x},I-2\gamma(x-\bar{x})\otimes(x-\bar{x}), \\ \ldots,\tilde{C}_\mu - c\gamma\int_{\mathscr{C}_{\eta,\gamma}(x-\bar{x})}|(x-\bar{x})\cdot z|^2\mu_x(dz)\big)\big) > 0. \end{aligned}$$

Furthermore, the scaling assumption (S) ensures the existence of a constant $\varepsilon_0 > 0$ such that for all $\varepsilon < \varepsilon_0$, εv is a strict supersolution of (3.1) in $\mathscr{D}_R(\bar{x},t_0)$. Indeed we have

$$\begin{aligned} \varepsilon v_t(x,t) + F(x,t,\varepsilon Dv(x,t),\varepsilon D^2v(x,t),\varepsilon\mathscr{I}[x,t,v]) \\ \geq \varepsilon\big(v_t(x,t) + F(x,t,Dv(x,t),D^2v(x,t),\mathscr{I}[x,t,v])\big) > 0. \end{aligned}$$

4. Remark that

$$\begin{aligned} v \geq 0 \quad &\text{in} \quad \mathscr{E}_R^c(\bar{x},t_0) \\ u < M \quad &\text{in} \quad \mathscr{E}_R(\bar{x},t_0)\setminus\mathscr{D}_R(\bar{x},t_0). \end{aligned}$$

Therefore, there exists some $\varepsilon_0 > 0$ such that for all $\varepsilon < \varepsilon_0$ outside the domain $\mathscr{D}_R(\bar{x},t_0)$

$$u(x,t) \leq u(x^*,t_0) + \varepsilon v(x,t).$$

Then we claim that the inequality holds inside $\mathscr{D}_R(\bar{x},t_0)$. Indeed, if $u \leq u(x^*,t_0) + \varepsilon v$ does not hold, then $\max_{\mathbb{R}^N}(u - M - \varepsilon v) > 0$ would be attained in $\mathscr{D}_R(\bar{x},t_0)$ at say, (x',t'). Since u is a viscosity subsolution the following would hold

$$\varepsilon v_t(x',t') + F(x',t',\varepsilon Dv(x',t'),\varepsilon D^2v(x',t'),\mathscr{I}[x',t',\varepsilon v]) \leq 0$$

arriving thus to a contradiction with the fact that $M + \varepsilon v$ is a strict supersolution of (3.1).

5. The function $u(x,t) - \varepsilon v(x,t)$ has therefore a global maximum at (x^*,t_0). Since u is a viscosity subsolution of (3.1), we have

$$\varepsilon v_t(x^*,t_0) + F(x^*,t_0,\varepsilon Dv(x^*,t_0),\varepsilon D^2v(x^*,t_0),\mathscr{I}[x^*,t_0,\varepsilon v]) \leq 0.$$

As before, we arrived at a contradiction because εv is a strict supersolution and thus the converse inequality holds at (x^*,t_0). Consequently, the assumption made is false and u is constant in the horizontal component of P_0. □

In the following we give the estimate for the nonlocal operator acting on the auxiliary function. We use the same notations as before.

Proposition 3.2.1. *Let $R > 0$, $\lambda > 0, \gamma > 0$ and consider the smooth function*

$$\begin{aligned} v(x,t) &= e^{-\gamma R^2} - e^{-\gamma d(x,t)} \\ d(x,t) &= |x-\bar{x}|^2 + \lambda|t-t_0|^2 \end{aligned}$$

Then there exist two constants $c = c(\eta,R)$ and $\gamma_0 > 0$ such that for $\gamma \geq \gamma_0$ the nonlocal operator

satisfies

$$\mathscr{I}[x,t,v] \le 2\gamma e^{-\gamma d(x,t)}\{\tilde{C}_\mu - c\gamma \int_{\{(1-\eta)|z||x-\bar{x}|\le|(x-\bar{x})\cdot z|\le 1/\gamma\}} |(x-\bar{x})\cdot z|^2 \mu_x(dz)\}$$

for all $R/2 < |x-\bar{x}| < R$.

Proof. In order to estimate the nonlocal term $\mathscr{I}[x,t,v]$, we split the domain of integration into three pieces and take the integrals on each of these domains. Namely we part the unit ball into the subset

$$\mathscr{C}_{\eta,\gamma}(x-\bar{x}) = \{z; (1-\eta)|z||x-\bar{x}| \le |(x-\bar{x})\cdot z| \le 1/\gamma\}$$

and its complementary. Indeed $\mathscr{C}_{\eta,\gamma}(x-\bar{x})$ lies inside the unit ball, as for $|x-\bar{x}| \ge R/2$ and for γ large enough

$$|z| \le \frac{1}{\gamma(1-\eta)|x-\bar{x}|} \le \frac{2}{\gamma(1-\eta)R} \le 1. \tag{3.10}$$

Thus we write the nonlocal term as the sum

$$\mathscr{I}[x,t,v] = \mathscr{T}^1[x,t,v] + \mathscr{T}^2[x,t,v] + \mathscr{T}^3[x,t,v]$$

with

$$\begin{aligned}
\mathscr{T}^1[x,t,v] &= \int_{|z|\ge 1} (v(x+z,t) - v(x,t))\mu_x(dz) \\
\mathscr{T}^2[x,t,v] &= \int_{B\setminus\mathscr{C}_{\eta,\gamma}(x-\bar{x})} (v(x+z,t) - v(x,t) - Dv(x,t)\cdot z)\mu_x(dz) \\
\mathscr{T}^3[x,t,v] &= \int_{\mathscr{C}_{\eta,\gamma}(x-\bar{x})} (v(x+z,t) - v(x,t) - Dv(x,t)\cdot z)\mu_x(dz).
\end{aligned}$$

In the sequel, we show that each integral term is controlled from above by an exponential term of the form $\gamma e^{-\gamma d(x,t)}$. In addition, the last integral is driven by a nonpositive quadratic nonlocal term.

Lemma 3.2.1. *We have*

$$\mathscr{T}^1[x,t,v] \le e^{-\gamma d(x,t)} \int_{|z|\ge 1} \mu_x(dz), \forall (x,t) \in \Omega \times [0,T].$$

Proof. The estimate is due to the uniform bound of the measures μ_x away from the origin. Namely

$$\begin{aligned}
\mathscr{T}^1[x,t,v] &= \int_{|z|\ge 1} (-e^{-\gamma d(x+z,t)} + e^{-\gamma d(x,t)})\mu_x(dz) \\
&\le \int_{|z|\ge 1} e^{-\gamma d(x,t)}\mu_x(dz) = e^{-\gamma d(x,t)} \int_{|z|\ge 1} \mu_x(dz) \le e^{-\gamma d(x,t)}\tilde{C}_\mu.
\end{aligned}$$

□

Lemma 3.2.2. *We have*

$$\mathscr{T}^2[x,t,v] \le \gamma e^{-\gamma d(x,t)} \int_B |z|^2 \mu_x(dz), \forall (x,t) \in \Omega \times [0,T].$$

Proof. Note that $\mathscr{T}^2[x,t,v] = -\mathscr{T}^2[x,t,e^{-\gamma d}]$. From Lemma 3.6.1 in Appendix

$$\mathscr{T}^2[x,t,e^{-\gamma d}] \ge e^{-\gamma d(x,t)} \mathscr{T}^2[x,t,-\gamma d] = -\gamma e^{-\gamma d(x,t)} \mathscr{T}^2[x,t,d].$$

Taking into account the expression for $d(x,t)$, we get that

$$\begin{aligned} \mathscr{T}^2[x,t,v] &\le \gamma e^{-\gamma d(x,t)} \int_{B\setminus \mathscr{C}_{\eta,\gamma}(x-\bar{x})} (d(x+z,t) - d(x,t) - Dd(x,t)\cdot z)\mu_x(dz) \\ &= \gamma e^{-\gamma d(x,t)} \int_{B\setminus \mathscr{C}_{\eta,\gamma}(x-\bar{x})} |z|^2 \mu_x(dz) \\ &\le \gamma e^{-\gamma d(x,t)} \int_B |z|^2 \mu_x(dz) \le \gamma e^{-\gamma d(x,t)} \tilde{C}_\mu. \end{aligned} \tag{3.11}$$

□

Lemma 3.2.3. *There exist two positive constants $c = c(\eta, R)$ and $\gamma_0 > 0$ such that for $\gamma \ge \gamma_0$*

$$\mathscr{T}^3[x,t,v] \le e^{-\gamma d(x,t)} \big(\gamma \int_B |z|^2 \mu_x(dz) - 2c\gamma^2 \int_{\mathscr{C}_{\eta,\gamma}(x-\bar{x})} |(x-\bar{x})\cdot z|^2 \mu_x(dz)\big).$$

for all $(x,t) \in \mathscr{D}_R$.

Proof. Rewrite equivalently the integral as

$$\mathscr{T}^3[x,t,v] = \mathscr{T}^3[x,t,v - e^{-\gamma R^2}] = -\mathscr{T}^3[x,t,e^{-\gamma d}].$$

We apply then Lemma 3.6.2 in Appendix to the function $e^{-\gamma d}$ and get that for all $\delta > 0$ there exists $c = c(\eta, R) > 0$ such that

$$\begin{aligned} \mathscr{T}^3[x,t,e^{-\gamma d}] &\ge e^{-\gamma d(x,t)} \big(\mathscr{T}^3[x,t,-\gamma d] + 2c\gamma^2 \int_{\mathscr{C}_{\eta,\gamma}(x-\bar{x})} \big(d(x+z,t) - d(x,t)\big)^2 \mu_x(dz)\big) \\ &= -\gamma e^{-\gamma d(x,t)} \big(\mathscr{T}^3[x,t,d] - 2c\gamma \int_{\mathscr{C}_{\eta,\gamma}(x-\bar{x})} \big(d(x+z,t) - d(x,t)\big)^2 \mu_x(dz)\big). \end{aligned}$$

Remark that $\mathscr{C}_{\eta,\gamma}(x-\bar{x}) \subseteq D_\delta$ for $\delta = 2 + \frac{2}{(1-\eta)R}$, with

$$\mathscr{D}_\delta = \{z;\ \gamma\big(d(x+z,t) - d(x,t)\big) \le \delta\} = \{z;\ \gamma(2(x-\bar{x})\cdot z + |z|^2) \le \delta\}.$$

We have thus

$$\mathscr{T}^3[x,t,v] \le \gamma e^{-\gamma d(x,t)} \big(\mathscr{T}^3[x,t,d] - 2c\gamma \int_{\mathscr{C}_{\eta,\gamma}(x-\bar{x})} \big(d(x+z,t) - d(x,t)\big)^2 \mu_x(dz)\big).$$

Taking into account the expression of $d(x,t)$, direct computations give

$$\begin{aligned}\mathscr{T}^3[x,t,d] &= \int_{\mathscr{C}_{\eta,\gamma}(x-\bar{x})}\big(d(x+z,t)-d(x,t)-Dd(x,t)\cdot z\big)\mu_x(dz)\\ &= \int_{\mathscr{C}_{\eta,\gamma}(x-\bar{x})}|z|^2\mu_x(dz)\le\int_B|z|^2\mu_x(dz),\end{aligned}$$

while the quadratic term is bounded from below by

$$\begin{aligned}\int_{\mathscr{C}_{\eta,\gamma}(x-\bar{x})}\big(d(x+z,t)-d(x,t)\big)^2\mu_x(dz) &= \int_{\mathscr{C}_{\eta,\gamma}(x-\bar{x})}|2(x-\bar{x})\cdot z+|z|^2|^2\mu_x(dz)\\ &\ge \int_{\mathscr{C}_{\eta,\gamma}(x-\bar{x})}|(x-\bar{x})\cdot z|^2\mu_x(dz).\end{aligned}$$

Indeed, recall that $|x-\bar{x}|\ge R/2$ and see that for all $z\in\mathscr{C}_{\eta,\gamma}(x-\bar{x})$

$$\begin{aligned}(1-\eta)|x-\bar{x}||z|\le 1/\gamma &\Rightarrow |z|\le\frac{2}{\gamma R(1-\eta)}\\ (1-\eta)|x-\bar{x}||z|\le|(x-\bar{x})\cdot z| &\Rightarrow |z|\le\frac{2|(x-\bar{x})\cdot z|}{R(1-\eta)}\end{aligned}$$

Then for $\gamma_0=4/R^2(1-\eta)^2$ and $\gamma\ge\gamma_0$ we have the estimate

$$\begin{aligned}|2(x-\bar{x})\cdot z+|z|^2| &\ge 2|(x-\bar{x})\cdot z|-|z|^2\ge 2|(x-\bar{x})\cdot z|-\frac{4|(x-\bar{x})\cdot z|}{\gamma R^2(1-\eta)^2}\\ &= |(x-\bar{x})\cdot z|\big(2-\frac{4}{\gamma R^2(1-\eta)^2}\big)\ge|(x-\bar{x})\cdot z|.\end{aligned}$$

Therefore, we obtain the upper bound for the integral term

$$\mathscr{T}^3[x,t,v]\le\gamma e^{-\gamma d(x,t)}\big(\int_{\mathscr{C}_{\eta,\gamma}(x-\bar{x})}|z|^2\mu_x(dz)-2c\gamma\int_{\mathscr{C}_{\eta,\gamma}(x-\bar{x})}|(x-\bar{x})\cdot z|^2\mu_x(dz)\big).$$

□

From the three lemmas estimating the integral terms we deduce that

$$\begin{aligned}\mathscr{I}[x,t,v] &\le e^{-\gamma d(x,t)}\Big\{\int_{|z|\ge1}\mu_x(dz)+2\gamma\int_B|z|^2\mu_x(dz)-2c\gamma^2\int_{\mathscr{C}_{\eta,\gamma}(x-\bar{x})}|(x-\bar{x})\cdot z|^2\mu_x(dz)\Big\}\\ &\le 2\gamma e^{-\gamma d(x,t)}\big\{\tilde{C}_\mu-c\gamma\int_{\mathscr{C}_{\eta,\gamma}(x-\bar{x})}|(x-\bar{x})\cdot z|^2\mu_x(dz)\big\}.\end{aligned}$$

□

3.2.3 Local Vertical Propagation of Maxima

We show that if $u\in USC(\mathbb{R}^N\times[0,T])$ is a viscosity subsolution of (3.1) which attains a maximum at $P_0=(x_0,t_0)\in Q_T$, then the maximum propagates locally in rectangles, say,

$$\mathscr{R}(x_0,t_0)=\{(x,t)||x^i-x_0^i|\le a^i,\,t_0-a_0\le t\le t_0\}$$

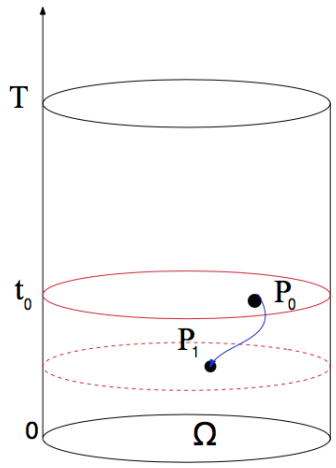

Figure 3.5: Vertical propagation of maxima: if the maximum is attained at some time t_0 then at any time $t < t_0$ one can find another point taking the maximum value.

where we have denoted $x = (x^1, x^2, ..., x^N)$. Denote by $\mathscr{R}_0(x_0, t_0)$ the rectangle $\mathscr{R}(x_0, t_0)$ less the top face $\{t = t_0\}$.

Local vertical propagation of maxima occurs under softer assumptions on the nondegeneracy and scaling conditions. More precisely, we suppose the following holds:

(N') For any $(x_0, t_0) \in Q_T$ there exists $\lambda > 0$ such that

$$\lambda + F(x_0, t_0, 0, I, \tilde{C}_\mu) > 0$$

where $\tilde{C}_\mu$ is given by assumption (M).

(S') There exist two constants $r_0 > 0$, $\varepsilon_0 > 0$ such that for all $\varepsilon < \varepsilon_0$ and $0 < r < r_0$ the following condition holds for all $(x, t) \in B((x_0, t_0), r)$, $|p| \le r$, $l \le \tilde{C}_\mu$

$$F(x, t, \varepsilon p, \varepsilon I, \varepsilon l) \ge \varepsilon F(x, t, p, I, l).$$

Theorem 3.2.3. *Let $u \in USC(\mathbb{R}^N \times [0, T])$ be a viscosity subsolution of (3.1) that attains a maximum at $P_0 = (x_0, t_0) \in Q_T$. If F satisfies $(E), (N')$ and (S') then for any rectangle $\mathscr{R}(x_0, t_0)$, $\mathscr{R}_0(x_0, t_0)$ contains a point $P \neq P_0$ such that $u(P) = u(P_0)$.*

Proof. Similarly to the horizontal propagation of maxima, we argue by contradiction.

1. Suppose there exists a rectangle $\mathscr{R}(x_0, t_0)$ on which $u(x, t) < M = u(x_0, t_0)$, with $\mathscr{R}_0(x_0, t_0) \subseteq \Omega \times [0, t_0)$. Denote $h(x, t) = \frac{1}{2}|x - x_0|^2 + \lambda(t - t_0)$ with $\lambda > 0$ a constant yet to be determined. Consider the auxiliary function

$$v(x, t) = 1 - e^{-h(x,t)}.$$

Direct calculations give

$$\begin{aligned}
&v_t(x,t) = \lambda e^{-h(x,t)}\\
&Dv(x,t) = e^{-h(x,t)}(x-x_0)\\
&D^2v(x,t) = e^{-h(x,t)}(I-(x-x_0)\otimes(x-x_0)),
\end{aligned}$$

Note that

$$\begin{aligned}
v(x_0,t_0) = 0 \qquad & v_t(x_0,t_0) = \lambda\\
Dv(x_0,t_0) = 0 \quad & D^2v(x_0,t_0) = I.
\end{aligned}$$

The nonlocal term is written as the sum of two integral operators:

$$\mathscr{I}[x,t,v] = \mathscr{T}^1[x,t,v] + \mathscr{T}^2[x,t,v],$$

where

$$\begin{aligned}
\mathscr{T}^1[x,t,v] &= \int_{|z|\geq 1}(v(x+z,t)-v(x,t))\mu_x(dz)\\
\mathscr{T}^2[x,t,v] &= \int_B (v(x+z,t)-v(x,t)-Dv(x,t)\cdot z)\mu_x(dz).
\end{aligned}$$

Similarly to Lemma 3.2.1 we obtain the estimate:

Lemma 3.2.4. *We have*

$$\mathscr{T}^1[x,t,v] \leq e^{-h(x,t)}\int_{|z|\geq 1}\mu_x(dz), \forall (x,t)\in\Omega\times[0,T].$$

On the other hand, the estimate obtained for the second integral term is softer than the estimate obtained in the case of the horizontal propagation of maxima.

Lemma 3.2.5. *We have*

$$\mathscr{T}^2[x,t,v] \leq e^{-h(x,t)}\int_B |z|^2\mu_x(dz), \forall (x,t)\in\Omega\times[0,T].$$

Proof. 1. From Lemma 3.6.1 we have

$$\mathscr{T}^2[x,t,v] = -\mathscr{T}^2[x,t,e^{-h}] \leq e^{-h(x,t)}\mathscr{T}^2[x,t,h].$$

We then use a second-order Taylor expansion for h and get

$$\begin{aligned}
\mathscr{T}^2[x,t,h] &= \frac{1}{2}\int_B \sup_{\theta\in(-1,1)}\left(D^2h(x+\theta z,t)z\cdot z\right)\mu_x(dz)\\
&= \frac{1}{2}\int_B |z|^2\mu_x(dz) \leq \frac{1}{2}\int_B |z|^2\mu_x(dz),
\end{aligned}$$

from where the conclusion. □

We now go back to the proof of the theorem and see that

$$\mathscr{I}[x,t,v] \le e^{-h(x,t)}\tilde{C}_\mu.$$

In particular $\mathscr{I}[x_0,t_0,v] \le \tilde{C}_\mu$.

2. From the nondegeneracy assumption (N') we have that there exists $\lambda > 0$ such that

$$\begin{aligned} v_t(x_0,t_0) + F(x_0,t_0,Dv(x_0,t_0),D^2v(x_0,t_0),\mathscr{I}[x_0,t_0,v]) \\ \ge v_t(x_0,t_0) + F(x_0,t_0,Dv(x_0,t_0),D^2v(x_0,t_0),\tilde{C}_\mu) \\ = \lambda + F(x_0,t_0,0,I,\tilde{C}_\mu) > 0. \end{aligned}$$

Hence v is a strict supersolution of (3.1) at (x_0,t_0). By the continuity of F, there exists $r < r_0$ such that $\forall (x,t) \in B((x_0,t_0),r) \subseteq Q_T$

$$v_t(x,t) + F(x,t,Dv(x,t),D^2v(x,t),\mathscr{I}[x,t,v]) \ge C > 0.$$

Consider then the set

$$S = B((x_0,t_0),r) \cap \{(x,t) | v(x,t) < 0\}.$$

By (S') there exists $\varepsilon_0 > 0$ such that $\forall \varepsilon < \varepsilon_0$, εv is a strict supersolution of (3.1) in S. Indeed

$$\begin{aligned} \varepsilon v_t(x,t) + F(x,t,\varepsilon Dv(x,t),\varepsilon D^2v(x,t),\varepsilon\mathscr{I}[x,t,v]) \ge \\ \varepsilon\big(v_t(x,t) + F(x,t,Dv(x,t),D^2v(x,t),\mathscr{I}[x,t,v])\big) > 0 \end{aligned}$$

3. Let ε_0 be sufficiently small such that

$$u(x,t) - u(x_0,t_0) \le \varepsilon v(x,t),\ \forall (x,t) \in \partial S.$$

Then, arguing as in the case of horizontal propagation of maxima we get

$$u(x,t) - u(x_0,t_0) \le \varepsilon v(x,t),\ \forall (x,t) \in S.$$

Thus (x_0,t_0) is a maximum of $u - \varepsilon v$ with $Dv(x_0,t_0) = \lambda > 0$. Since u is a subsolution, we have

$$\varepsilon v_t(x_0,t_0) + F(x_0,t_0,\varepsilon v(x_0,t_0),\varepsilon Dv(x_0,t_0),\varepsilon D^2v(x_0,t_0),\mathscr{I}[x_0,t_0,\varepsilon v]) \le 0.$$

We arrived at a contradiction with the fact that εv is a strict supersolution. Thus, the supposition is false and the rectangle contains a point $P \ne P_0$ such that $u(P) = u(P_0)$.

□

Example 3.2.1. *Non-local first order Hamilton Jacobi equations describing the dislocation dynamics*

$$u_t = (c(x) + M[u])|Du| \tag{3.12}$$

where M is a zero order nonlocal operator defined by

$$M[u](x,t) = \int_{\mathbb{R}^N} \big(u(x+z,t) - u(x,t)\big)\mu(dz)$$

with

$$\mu(dz) = g(\frac{z}{|z|})\frac{dz}{|z|^{N+1}}$$

have vertical propagation of maxima.

Indeed, they do not satisfy any of the sets of assumptions required by Theorems 3.2.1 and 3.2.2. Particularly nondegeneracy condition (N)

$$-\big(c(x)+\tilde{C}_\mu\big)|p| > 0$$

fails for example if $c(x) \geq 0$, and holds whenever $c(x) < -\tilde{C}_\mu$. Hence, one cannot conclude on horizontal propagation of maxima.

On the other hand we have local vertical propagation of maxima, since (N') is immediate and (S') is satisfied by $\tilde{F} = -c(x)|p|$, the linear approximation of the nonlinearity

$$-\big(c(x)+\varepsilon l)|\varepsilon p| = -\varepsilon c(x)|p| + o(\varepsilon^2).$$

3.2.4 Strong Maximum Principle

When both horizontal and local vertical propagation of maxima occur for a viscosity subsolution of (3.1) which attains a global maximum at an interior point, the function is constant in any rectangle contained in the domain $\overline{\Omega} \times [0, t_0]$ passing through the maximum point.

Proposition 3.2.2. *Let $u \in USC(\mathbb{R}^N \times [0,T])$ be a viscosity subsolution of (3.1) that attains a global maximum at $P_0 = (x_0, t_0) \in Q_T$. If F satisfies (E), $(N)-(N')$, and $(S)-(S')$, then u is constant in any rectangle $\mathscr{R}(x_0,t_0) \subseteq \overline{\Omega} \times [0,t_0]$.*

From the horizontal and local vertical propagation of maxima one can derive the Strong Maximum Principle. The proof is based on geometric arguments and is identical to that for fully nonlinear second order partial differential equations.

Theorem 3.2.4 (Strong Maximum Principle)**.** *Assume the family of measures $\{\mu_x\}_{x\in\Omega}$ satisfies assumption (M). Let $u \in USC(\mathbb{R}^N \times [0,T])$ be a viscosity subsolution of (3.1) that attains a global maximum at $P_0 = (x_0,t_0) \in Q_T$. If F satisfies (E), $(S)-(S')$, and $(N)-(N')$, then u is constant in $S(P_0)$.*

Proof. Suppose that $u \not\equiv u(P_0)$ in $S(P_0)$. Then there exists a point $Q \in S(P_0)$ such that $u(Q) < u(P_0)$. Then, we can connect Q to P_0 by a simple continuous curve γ lying in $S(P_0)$ such that the temporal coordinate t us nondecreasing from Q to P_0. On the curve γ there exists a point P_1 take takes the maximum value $u(P_1) = u(P_0)$ and at the same time, for all the points P on γ between Q and P_1 we have $u(P) < u(P_0)$. We construct a rectangle

$$x_i^1 - a \leq x_i \leq x_i^1 + a, i = 1,n,\ t^1 - a < t < t_1$$

where (x_i^1, t^1) are the coordinates of P_1 and a sufficiently small such that the rectangle does not exceed the domain Ω. Applying the vertical propagation of maxima we deduce that $u \equiv u(P_0)$

in this rectangle. Thus, the function is constant on the arc of the curve lying in this rectangle. But this contradicts the definition of P_1.

□

Similarly the following holds.

Theorem 3.2.5 (Strong Maximum Principle)**.** *Let $u \in USC(\mathbb{R}^N \times [0,T])$ be a viscosity subsolution of (3.1) in $\mathbb{R}^N \times (0,T)$ that attains a global maximum at $(x_0,t_0) \in \mathbb{R}^N \times (0,T]$. Assume the family of measures $\{\mu_x\}_{x\in\Omega}$ satisfies assumption (M) and F satisfies (E'), (S') and (N'). Then u is constant in $\overline{\bigcup_{n\geq 0} A_n} \times [0,t_0]$ with $\{A_n\}_n$ given by (3.8).*

3.3 Strong Maximum Principle for Lévy-Itô operators

The results established for general nonlocal operators remain true for Lévy-Itô operators. We translate herein the corresponding assumptions and theorems on the Strong Maximum Principle for second order integro-differential equations associated to Lévy-Itô operators

$$\mathcal{J}[x,t,u] = \int_{\mathbb{R}^N} (u(x+j(x,z),t) - u(x,t) - Du(x,t)\cdot j(x,z)1_B(z))\mu(dz),$$

where μ is a Lévy measure. In the sequel we assume that F respects the scaling assumption (S) and the nondegeneracy condition

(N_{LI}) For any $\bar{x} \in \Omega$ and $0 < t_0 < T$ there exist $R_0 > 0$ small enough and $0 < \eta < 1$ such that for any $0 < R < R_0$ and $c > 0$

$$F(x,t,p,I-\gamma p\otimes p, \tilde{C}_\mu - c\gamma \int_{\mathscr{C}_{\eta,\gamma}(p)} |p\cdot j(x,z)|^2 \mu(dz)) \to \infty \text{ as } \gamma \to \infty$$

uniformly for $|x-\bar{x}| \leq R$ and $|t-t_0| \leq R$, $R/2 \leq |p| \leq R$, where

$$\mathscr{C}_{\eta,\gamma}(p) = \{z;\ (1-\eta)|j(x,z)||p| \leq |p\cdot j(x,z)| \leq 1/\gamma\}.$$

and that the Lévy measure μ satisfies assumptions

(M_{LI}) there exists a constant $\tilde{C}_\mu > 0$ such that for any $x \in \Omega$,

$$\int_B |j(x,z)|^2 \mu(dz) + \int_{\mathbb{R}^N \setminus B} \mu(dz) \leq \tilde{C}_\mu;$$

(M^c_{LI}) For any $x \in \Omega$ there exist $1 < \beta < 2$, $0 \leq \eta < 1$ and a constant $C_\mu(\eta) > 0$ such that the following holds

$$\int_{\mathscr{C}_{\eta,\gamma}(p)} |j(x,z)|^2 \mu(dz) \geq C_\mu(\eta)\gamma^{\beta-2}, \forall \gamma \geq 1.$$

Theorem 3.2.1 holds for Lévy-Itô operators, since Lévy Itô measures can be written as push-forwards of some Lévy measure $\tilde{\mu}$

$$\mu_x = (j(x,\cdot)_*(\tilde{\mu}))$$

defined for measurable functions ϕ as

$$\int_{\mathbb{R}^N} \phi(x)\mu_x(dz) = \int_{\mathbb{R}^N} \phi(j(x,z))\tilde{\mu}(dz).$$

Hence it is sufficient to replace $\text{supp}(\mu_x) = j(x, \text{supp}(\tilde{\mu}))$ in order to get the result.

Theorem 3.3.1. *Assume the L'evy measure μ satisfies assumption (M_{LI}). Let $u \in USC(\mathbb{R}^N \times [0,T])$ be a viscosity subsolution of (3.1) that attains a maximum at $P_0 = (x_0, t_0) \in Q_T$. If F satisfies $(E), (S)$, and (N_{LI}) then u is constant in $C(P_0)$.*

Proof. Since the proof is technically the same, we just point out the main differences, namely the estimate of the nonlocal term. Consider as before the smooth function

$$v(x,t) = e^{-\gamma R^2} - e^{-\gamma d(x,t)}$$

where $d(x,t) = |x-\bar{x}|^2 + \lambda|t-t_0|^2$, for large $\gamma > \gamma_0$. Write similarly the nonlocal term as the sum

$$\mathcal{J}[x,t,v] = \mathcal{I}^1[x,t,v] + \mathcal{I}^2[x,t,v] + \mathcal{I}^3[x,t,v]$$

where

$$\begin{aligned}
\mathcal{I}^1[x,t,v] &= \int_{|z|\geq 1} (v(x+j(x,z),t) - v(x,t))\mu(dz) \\
\mathcal{I}^2[x,t,v] &= \int_{B\setminus \mathcal{C}_{\eta,\gamma}(x-\bar{x})} (v(x+j(x,z),t) - v(x,t) - Dv(x,t)\cdot j(x,z))\mu(dz) \\
\mathcal{I}^3[x,t,v] &= \int_{\mathcal{C}_{\eta,\gamma}(x-\bar{x})} (v(x+j(x,z),t) - v(x,t) - Dv(x,t)\cdot j(x,z))\mu(dz)
\end{aligned}$$

with

$$\mathcal{C}_{\eta,\gamma}(x-\bar{x}) = \{(1-\eta)|j(x,z)||x-\bar{x}| \leq |(x-\bar{x})\cdot j(x,z)| \leq 1/\gamma\}.$$

Then the nonlocal operator satisfies for all $(x,t) \in \mathcal{D}_R$

$$\begin{aligned}
\mathcal{I}^1[x,t,v] &\leq e^{-\gamma d(x,t)} \int_{|z|\geq 1} \mu(dz). \\
\mathcal{I}^2[x,t,v] &\leq \gamma e^{-\gamma d(x,t)} \int_B |j(x,z)|^2 \mu(dz). \\
\mathcal{I}^3[x,t,v] &\leq e^{-\gamma d(x,t)} \big[\gamma \int_B |j(x,z)|^2\mu(dz) - 2c\gamma^2 \int_{\mathcal{C}_{\eta,\gamma}(x-\bar{x})} |(x-\bar{x})\cdot j(x,z)|^2\mu(dz)\big].
\end{aligned}$$

from where we get the global estimation

$$\begin{aligned}
\mathcal{J}[x,t,v] &\leq e^{-\gamma d(x,t)}\big[\int_B \mu(dz) + 2\gamma \int_B |j(x,z)|^2\mu(dz) \\
&\qquad\qquad -2c\gamma^2 \int_{\mathcal{C}_{\eta,\gamma}(x-\bar{x})} |(x-\bar{x})\cdot j(x,z)|^2\mu(dz)\big] \\
&\leq 2\gamma e^{-\gamma d(x,t)}\big[\tilde{C}_\mu - c\gamma \int_{\mathcal{C}_{\eta,\gamma}(x-\bar{x})} |(x-\bar{x})\cdot j(x,z)|^2\mu(dz)\big].
\end{aligned}$$

□

Vertical propagation of maxima holds under the same conditions. Strong Maximum Principle can thus be formulated for Lévy-Itô operators.

Theorem 3.3.2 (Strong Maximum Principle - Lévy Itô)**.** *Assume the measure μ satisfies assumption (M_{LI}). Let $u \in USC(\mathbb{R}^N \times [0,T])$ be a viscosity subsolution of (3.1) that attains a global maximum at $P_0 = (x_0, t_0) \in Q_T$. If F satisfies (E), $(S)-(S')$, and $(N_{LI})-(N')$, then u is constant in $S(P_0)$.*

Theorem 3.3.3 (Strong Maximum Principle - Lévy Itô)**.** *Let $u \in USC(\mathbb{R}^N \times [0,T])$ be a viscosity subsolution of (3.1) in $\mathbb{R}^N \times (0,T)$ that attains a global maximum at $(x_0, t_0) \in \mathbb{R}^N \times (0,T]$. Assume the measure μ satisfies assumption (M_{LI}) and F satisfies (E_0), (S') and (N'). Then u is constant in $\overline{\bigcup_{n\geq 0} A_n} \times [0,t_0]$ with $\{A_n\}_n$ given by (3.8).*

3.4 Examples

In this section we discuss the validity of the Strong Maximum Principle on several representative examples.

3.4.1 Horizontal Propagation of Maxima by Translations of Measure Supports

As pointed out in section 3.2, translations of measure supports starting at any maximum point x_0 lead to horizontal propagation of maxima. In particular, Theorem 3.2.1 holds for nonlocal terms integrated against Lévy measures whose supports are the whole space.

Example 3.4.1. *Consider a pure nonlocal diffusion*

$$u_t - \mathscr{I}[x,t,u] = 0 \text{ in } \mathbb{R}^N \times (0,T) \tag{3.13}$$

where $\mathscr{I}$ is the Lévy operator integrated against the Lévy measure associated with the fractional Laplacian $(-\Delta)^{\beta/2}$:

$$\mu(dz) = \frac{dz}{|z|^{N+\beta}}.$$

Then the support of the measure is the whole space *and thus horizontal propagation of maxima holds for equation (3.13) by Theorem 3.2.1.*

Example 3.4.2. *Let $N = 2$ and consider equation (3.13) with $\{\mu_x\}_x$ a family of* Lévy measures charging two axis *meeting at the origin*

$$\mu_x(dz) = 1_{\{z_1 = \pm \alpha z_2\}} \nu_x(dz),$$

with $\alpha > 0$ and $supp(\nu_x) = \mathbb{R}^2$, for all $x \in \mathbb{R}^2$. Even though zero is not an interior point of the support, translations of measure supports starting at any point x_0 cover the whole space, propagating thus maxima all over $\mathbb{R}^2$.

Similarly, horizontal propagation of maxima holds if measures charge cones

$$\mu_x(dz) = 1_{\{|z_1|>\alpha|z_2|\}}\nu_x(dz),$$

with $\alpha > 0$ *and* $supp(\nu_x) = \mathbb{R}^2$.

3.4.2 Strong Maximum Principle driven by the Nonlocal Term under Nondegeneracy Conditions.

There are equations for which propagation of maxima does not propagate just by translating measure supports, but cases when it requires a different set of assumptions. Nondegeneracy and scaling conditions of the nonlinearity F need to be satisfied in order to have a Strong Maximum Principle. But to ensure condition (N), one has to assume (M^c).

Example 3.4.3. *Consider as before equation (3.13) and let* μ *be the* Lévy measure *associated to the fractional Laplacian* but restricted to half space

$$\mu(dz) = 1_{\{z_1\geq 0\}}(z)\frac{dz}{|z|^{N+\beta}}, \beta \in (1,2).$$

where $z = (z_1, z') \in \mathbb{R}\times\mathbb{R}^{N-1}$. *Then* $\mathbb{R}^N$ *can not be covered by translations of the measure support and therefore one cannot conclude the function* u *is constant on the whole domain, except for particular cases like the periodic case. However,* $C^{0,\alpha}$ *regularity results hold (cf. [BCI11]) and we expect to have Strong Maximum Principle.*

We show that the nondegeneracy and scaling assumptions are satisfied in the case of Example 3.4.3. Before proceeding to the computations, remark that

$$\begin{aligned} \mathscr{C}_{\eta,\gamma}(p) &= \{z; (1-\eta)|p||z| \leq |p\cdot z| \leq 1/\gamma\} && (3.14)\\ &= \{z; (1-\eta)|p||\gamma z| \leq |p\cdot \gamma z| \leq 1\} = \gamma^{-1}\mathscr{C}_{\eta,1}(p) && (3.15)\end{aligned}$$

$$\begin{aligned} \gamma\int_{\mathscr{C}_{\eta,\gamma}(p)\cap\{z_1\geq 0\}} |p\cdot z|^2\frac{dz}{|z|^{N+\beta}} &= \gamma^{-1}\int_{\mathscr{C}_{\eta,1}(p)\cap\{z_1\geq 0\}} \gamma^{\beta}|p\cdot z|^2\frac{dz}{|z|^{N+\beta}}\\ &\geq \gamma^{\beta-1}|p|^2(1-\eta)^2\int_{\mathscr{C}_{\eta,1}(p)\cap\{z_1\geq 0\}} |z|^2\frac{dz}{|z|^{N+\beta}}\\ &= C(\eta)\gamma^{\beta-1}|p|^2\end{aligned}$$

where $C(\eta) = (1-\eta)^2\int_{\mathscr{C}_{\eta,1}(p)\cap\{z_1\geq 0\}} |z|^2 dz/|z|^{N+\beta}$ is a positive constant.

This further implies nondegeneracy condition (N). Indeed, there exist $R_0 > 0$ small enough and $0 \leq \eta < 1$ such that for any $0 < R < R_0$ and for all $R/2 < |p| < R$

$$-\tilde{C}_\mu + c\gamma\int_{\mathscr{C}_{\eta,\gamma}(p)\cap\{z_1\geq 0\}} |p\cdot z|^2\frac{dz}{|z|^{N+\beta}} \geq -\tilde{C}_\mu + \tilde{C}(\eta)\gamma^{\beta-1}|p|^2 \to \infty \text{ as } \gamma\to\infty$$

as long as $\beta > 1$. The rest of assumptions follow immediately.

Similar results hold for the following PIDE arising in the context of growing interfaces [Woy01]:

$$u_t + \frac{1}{2}|Du|^2 - \mathscr{I}[x,t,u] = 0, \text{ in } \mathbb{R}^N \times (0,T) \tag{3.16}$$

with $\mathscr{I}$ is a general nonlocal operator of form (3.3).

Remark 3.4.1. *For integro-differential equations of the type*

$$u_t + b(x,t)|Du|^m - \mathscr{I}[x,t,u] = 0 \text{ in } \mathbb{R}^N \times (0,T) \tag{3.17}$$

with b a continuous function and μ as in Example 3.4.3. Strong Maximum Principle holds for $m \geq 1$, and for $m < 1$ if $b(\cdot) \geq 0$.

3.4.3 Strong Maximum Principle coming from Local Diffusion Terms

Theorem 3.2.4 applies to integro-differential equations uniformly elliptic with respect to the diffusion term and linear in the nonlocal operator.

Example 3.4.4. *Quasilinear parabolic integro-differential equations of the form*

$$u_t - tr(A(x,t)D^2u) - \mathscr{I}[x,t,u] = 0 \text{ in } \mathbb{R}^N \times (0,T) \tag{3.18}$$

with $A(x,t)$ such that

$$a_0(x,t)I \leq A(x,t) \leq a_1(x,t)I, \ a_1(x,t) \geq a_0(x,t) > 0$$

satisfy Strong Maximum Principle.

We check the nondegeneracy and scaling conditions for this equation.

$$\begin{aligned}
(N) \qquad & -\text{trace}(A(x,t)(I-\gamma p\otimes p)) - \tilde{C}_\mu + c\gamma\int_{\mathscr{C}_\gamma} |p\cdot z|^2\mu_x(dz) = \\
& -\text{trace}(A(x,t)) + \gamma\text{trace}(A(x,t)p\otimes p)) - \tilde{C}_\mu + c\gamma\int_{\mathscr{C}_\gamma} |p\cdot z|^2\mu_x(dz) \geq \\
& \underbrace{-a_1(x,t)N + a_0(x,t)\gamma|p|^2 - \tilde{C}_\mu}_{\gg 0, \text{ for } \gamma \text{ large}} + \underbrace{c\gamma\int_{\mathscr{C}_\gamma} |p\cdot z|^2\mu_x(dz)}_{\geq 0}. \\
(N') \qquad & \lambda - \text{trace}(A(x,t)) - \tilde{C}_\mu \geq \lambda - a_1(x,t)N - \tilde{C}_\mu > 0.
\end{aligned}$$

The scaling properties are immediate since the nonlinearity is 1-homogeneous.

Remark 3.4.2. *More generally, one can consider equations of the form*

$$u_t + F(x,t,Du,D^2u) - \mathscr{I}[x,t,u] = 0 \tag{3.19}$$

for which the corresponding differential operator F satisfies the nondegeneracy and scaling assumptions. The nonlocal term is driven by the second order derivatives and thus Strong Maximum Principle holds.

3.4.4 Strong Maximum Principle for Mixed Differential-Nonlocal terms

We consider mixed integro-differential equations, i.e. equations for which local diffusions occur only in certain directions and nonlocal diffusions on the orthogonal ones, and show they satisfy Strong Maximum Principle. This is quite interesting, as the equations might be degenerate in both local or nonlocal terms, but the overall behavior is driven by their interaction (the two diffusions cannot cancel simultaneously).

Example 3.4.5. *Consider the following equation where local and nonlocal diffusions are mixed up*

$$u_t - \mathscr{I}_{x_1}[u] - \Delta_{x_2} u = 0 \text{ in } \mathbb{R}^N \times (0,T) \tag{3.20}$$

for $x = (x_1, x_2) \in \mathbb{R}^d \times \mathbb{R}^{N-d}$. The diffusion term gives the ellipticity in the direction of x_2, while the nonlocal term gives it in the direction of x_1

$$\mathscr{I}_{x_1}[u] = \int_{\mathbb{R}^d} (u(x_1 + z_1, x_2) - u(x) - D_{x_1} u(x) \cdot z_1 1_B(z_1)) \mu_{x_1}(dz_1)$$

where μ_{x_1} is a Lévy measure satisfying (M) with $\tilde{C}^1_\mu$. The payoff for the Strong Maximum Principle to hold is assumption (M^c), with $\beta > 1$; then Theorem 3.2.4 applies.

Indeed the nondegeneracy conditions (N) and (N') hold, because when γ is large enough and $\beta > 1$ the following holds

$$\begin{aligned}
(N) \qquad & -I_{N-d} + \gamma p_2 \otimes p_2 - \tilde{C}^1_\mu + c\gamma \int_{\mathscr{C}^1_{\eta,\gamma}(p_1)} |p_1 \cdot z_1|^2 \mu_{x_1}(dz_1) \geq \\
& -(N-d) + \gamma |p_1|^2 - \tilde{C}^1_\mu + c\gamma(1-\eta)^2 |p_1|^2 \int_{\mathscr{C}^1_{\eta,\gamma}(p_1)} |z_1|^2 \mu_{x_1}(dz_1) \geq \\
& -(N-d+\tilde{C}^1_\mu) + \gamma |p_1|^2 + \tilde{C}^1(\eta) \gamma^{\beta-1} |p_1|^2 \geq -c_0 + c_1 \gamma^{\beta-1} \left(|p_1|^2 + |p_2|^2 \right)
\end{aligned}$$

where $\tilde{C}^1(\eta)$, c_0 and c_1 are positive constants and

$$\mathscr{C}^1_{\eta,\gamma}(p_1) = \{z_1 \in \mathbb{R}^d; (1-\eta)|p_1||z_1| \leq |p_1 \cdot z_1| \leq 1/\gamma\}.$$

As far as the scaling assumptions are concerned it is sufficient to see that the nonlinearity is 1-homogeneous.

Remark 3.4.3. *In general, linear integro-differential equations of the form*

$$u_t - a(x)\mathscr{I}_{x_1}[u] - c(x)\Delta_{x_2} u = 0 \text{ in } \mathbb{R}^N \times (0,T) \tag{3.21}$$

or

$$u_t - a(x)\mathscr{I}_{x_1}[u] - c(x)\mathscr{I}_{x_2}[u] = 0 \text{ in } \mathbb{R}^N \times (0,T) \tag{3.22}$$

satisfy Strong Maximum Principle if the corresponding Lévy measure(s) verify (M) and (M^c), with $\beta > 1$ and if $a, c \geq \zeta > 0$ in $\mathbb{R}^N$.

Indeed, F is 1-homogeneous and (N) holds:

$$c(x)\big(-I_{N-d}+\gamma p_2\otimes p_2\big)+a(x)\big(-\tilde{C}^1_\mu+c\gamma\int_{\mathscr{C}_{\eta,\gamma}(p_1)}|p_1\cdot z_1|^2\mu_{x_1}(dz_1)\big)\geq$$
$$\geq -c_0(a(x)+c(x))+c_1\gamma^{\beta-1}\big(a(x)|p_1|^2+c(x)|p_2|^2\big)$$

respectively

$$a(x)\big(-\tilde{C}^1_\mu+c\gamma\int_{\mathscr{C}_{\eta,\gamma}(p_1)}|p_1\cdot z_1|^2\mu_{x_1}(dz_1)\big)+$$
$$c(x)\big(-\tilde{C}^2_\mu+c\gamma\int_{\mathscr{C}_{\eta,\gamma}(p_2)}|p_2\cdot z_2|^2\mu_{x_2}(dz_2)\big)\geq$$
$$\geq -c_0(a(x)+c(x))+c_1\gamma^{\beta-1}\big(a(x)|p_1|^2+c(x)|p_2|^2\big).$$

where $\mathscr{C}_{\eta,\gamma}(p_i)=\{z_i;|p_i\cdot z_i|\leq 1/\gamma\}$, for $i=1,2$.

3.5 Strong Comparison Principle

Let $\Omega\subset\mathbb{R}^N$ be a bounded, *connected* domain. In this section, we use Strong Maximum Principle to prove a Strong Comparison Result of viscosity sub and supersolution for integro-differential equations of the form (3.1)

$$u_t+F(x,t,Du,D^2u,\mathscr{J}[x,t,u])=0,\text{ in }\Omega\times(0,T) \tag{3.23}$$

with the Dirichlet boundary condition

$$u=\varphi\text{ on }\Omega^c\times[0,T] \tag{3.24}$$

where φ is a continuous function.

Let μ be a Lévy measure satisfying (M_{LI}). Assume that the function j appearing in the definition of $\mathscr{J}$ has the following property: there exists $C_0>0$ such that for all $x,y\in\Omega$ and $|z|\leq\delta$

$$|j(x,z)|\leq C_0|z|$$
$$|j(x,z)-j(y,z)|\leq C_0|z||x-y|.$$

We will need some additional assumptions on the equation, that we state in the following. Suppose the nonlinearity F is Lipschitz continuous with respect to the variables p, X and l and for each $0<R<\infty$ there exist a function $\omega_R(r)\to 0$, as $r\to 0$, c_R a positive constant and $0\leq\lambda_R<\Lambda_R$ such that

$$(H)\qquad F(y,s,q,Y,l_2)-F(x,t,p,X,l_1)\leq$$
$$\omega_R(|(x,t)-(y,s)|)+c_R|p-q|+\mathscr{M}^+_R(X-Y)+c_R(l_1-l_2),$$

for all $x, y \in \Omega$, $t, s \in [0,T]$, $X, Y \in \mathbb{S}^N(\Omega)$ satisfying for some $\varepsilon > 0$

$$\begin{bmatrix} X & 0 \\ 0 & -Y \end{bmatrix} \leq \frac{1}{\varepsilon}\begin{bmatrix} I & -I \\ -I & I \end{bmatrix} + \begin{bmatrix} Z & 0 \\ 0 & 0 \end{bmatrix}, \text{ with } Z \in \mathbb{S}^N(\Omega).$$

and $|p|, |q| \leq R$ and $l_1, l_2 \in \mathbb{R}$, where $\mathscr{M}_R^+$ is Pucci's maximal operator:

$$\mathscr{M}_R^+(X) = \Lambda_R \sum_{\lambda_j > 0} \lambda_j + \lambda_R \sum_{\lambda_j < 0} \lambda_j$$

with λ_j being the eigenvalues of X.

Theorem 3.5.1 (Strong Comparison Principle)**.** *Assume the Lévy measure μ satisfies assumption (M_c) with $\beta > 1$. Let $u \in USC(\mathbb{R}^N \times [0,T])$ be a viscosity subsolution and $v \in LSC(\mathbb{R}^N \times [0,T])$ a viscosity supersolution of (3.1), with the Dirichlet boundary condition (3.24). Suppose one of the following conditions holds:*

(a) F satisfies (H) with w_R and c_R independent of R or
(b) $u(\cdot,t), v(\cdot,t) \in Lip(\Omega)$, $\forall\, t \in [0,T)$ and F satisfies (H).

If $u - v$ attains a maximum at $P_0 = (x_0, t_0) \in \Omega \times (0,T)$, then $u - v$ is constant in $C(P_0)$.

Proof. The proof relies on finding the equation for which $w = u - v \in USC(\mathbb{R}^N \times [0,T])$ is a viscosity subsolution and applying strong maximum principle results for the latter. However, the conclusion is not immediate as linearizion does not go hand in hand with the viscosity solution theory approach and difficulties imposed by the behavior of the measure near the singularity might appear.

1. Let $w = u - v$ and consider ϕ a smooth test-function such that $w - \phi$ has a strict global maximum at (x_0, t_0). We penalize the test function around the maximum point, by doubling the variables, i.e. we consider the auxiliary function

$$\Psi_{\varepsilon,\eta}(x,y,t,s) = u(x,t) - v(y,s) - \frac{|x-y|^2}{\varepsilon^2} - \frac{(t-s)^2}{\eta^2} - \phi(x,t).$$

Then there exist a sequence of global maximum points $(x_\varepsilon, y_\varepsilon, t_\eta, s_\eta)$ of function $\Psi_{\varepsilon,\eta}$ with the properties

$$\begin{aligned} &(x_\varepsilon, t_\eta), (y_\varepsilon, s_\eta) \to (x_0, t_0) \text{ as } \eta, \varepsilon \to 0 \\ &\frac{|x_\varepsilon - y_\varepsilon|^2}{\varepsilon^2} \to \varepsilon \text{ as } \varepsilon \to 0 \\ &\frac{(t_\eta - s_\eta)^2}{\eta^2} \to 0 \text{ as } \eta \to 0 \end{aligned}$$

and the test-function φ being continuous

$$\lim_{\eta,\varepsilon \to 0} (u(x_\varepsilon, t_\eta) - v(y_\varepsilon, s_\eta)) = u(x_0, t_0) - v(x_0, t_0). \tag{3.25}$$

In addition, there exist $X_\varepsilon, Y_\varepsilon \in \mathbb{S}^N$ such that

$$(a_\eta + \phi_t(x_\varepsilon, t_\eta), p_\varepsilon + D\phi(x_\varepsilon, t_\eta), X_\varepsilon + D^2\phi(x_\varepsilon, t_\eta)) \in \overline{\mathscr{D}}^{2,+} u(x_\varepsilon, t_\eta)$$
$$(a_\eta, p_\varepsilon, Y_\varepsilon) \in \overline{\mathscr{D}}^{2,-} v(y_\varepsilon, s_\eta)$$

$$\begin{bmatrix} X_\varepsilon + D\phi(x_\varepsilon, t_\eta) & 0 \\ 0 & -Y_\varepsilon \end{bmatrix} \leq \frac{4}{\varepsilon^2} \begin{bmatrix} I & -I \\ -I & I \end{bmatrix} + \begin{bmatrix} D\phi(x_\varepsilon, t_\eta) & 0 \\ 0 & 0 \end{bmatrix}$$

and p_ε, a_η are defined by

$$p_\varepsilon := 2\frac{x_\varepsilon - y_\varepsilon}{\varepsilon^2} \text{ and } a_\eta := 2\frac{t_\eta - s_\eta}{\eta^2}.$$

Consider the test function

$$\phi^1_{\varepsilon,\eta}(x,t) = v(y_\varepsilon, s_\eta) + \frac{|x - y_\varepsilon|^2}{\varepsilon^2} + \frac{(t - s_\eta)^2}{\eta^2} + \phi(x,t).$$

Then $u - \phi^1_{\varepsilon,\eta}$ has a global maximum at (x_ε, t_η). But u is a subsolution of (3.1) and thus for $\delta > 0$ the following holds

$$\begin{aligned} \phi_t(x_\varepsilon, t_\eta) + a_\eta + F\big(x_\varepsilon, t_\eta, D\phi(x_\varepsilon, t_\eta) + p_\varepsilon, D^2\phi(x_\varepsilon, t_\eta) + X_\varepsilon, \ldots \\ \ldots, \mathscr{J}^1_\delta[x_\varepsilon, t_\eta, \phi + \frac{|x - y_\varepsilon|^2}{\varepsilon^2}] + \mathscr{J}^2_\delta[x_\varepsilon, t_\eta, D\phi(x_\varepsilon, t_\eta) + p_\varepsilon, u]\big) \leq 0. \end{aligned}$$

Similarly, consider the test function

$$\phi^2_{\varepsilon,\eta}(y,s) = u(x_\varepsilon, t_\eta) - \frac{|x_\varepsilon - y|^2}{\varepsilon^2} - \frac{(t_\eta - s)^2}{\eta^2} - \phi(x_\varepsilon, t_\eta).$$

Then $v - \phi^2_{\varepsilon,\eta}$ has a global minimum at (y_ε, s_η). But v is a supersolution of (3.1) and thus:

$$a_\eta + F\big(y_\varepsilon, s_\eta, p_\varepsilon, Y_\varepsilon, \mathscr{J}^1_\delta[y_\varepsilon, s_\eta, \frac{|x_\varepsilon - y|^2}{\varepsilon^2}] + \mathscr{J}^2_\delta[y_\varepsilon, s_\eta, p_\varepsilon, v]\big) \geq 0.$$

Subtracting the two inequalities and taking into account (H) we get that for all $\delta > 0$

$$\begin{aligned} \phi_t(x_\varepsilon, t_\eta) \quad &- \quad \omega(|(x_\varepsilon, t_\eta) - (y_\varepsilon, s_\eta)|) - c|D\phi(x_\varepsilon, t_\eta)| - \mathscr{M}^+(D^2\phi(x_\varepsilon, t_\eta) + X_\varepsilon - Y_\varepsilon) \\ &- \quad c(\mathscr{J}^1_\delta[x_\varepsilon, t_\eta, \phi + \frac{|x - y_\varepsilon|^2}{\varepsilon^2}] + \mathscr{J}^2_\delta[x_\varepsilon, t_\eta, D\phi(x_\varepsilon, t_\eta) + p_\varepsilon, u]) \\ &- \quad c(\mathscr{J}^1_\delta[y_\varepsilon, s_\eta, -\frac{|x_\varepsilon - y|^2}{\varepsilon^2}] - \mathscr{J}^2_\delta[y_\varepsilon, s_\eta, p_\varepsilon, v]) \leq 0. \end{aligned}$$

Taking into account the matrix inequality and the sublinearity of Pucci's operator, we deduce that

$$\mathscr{M}^+(D^2\phi(x_\varepsilon, t_\eta) + X_\varepsilon - Y_\varepsilon) \leq \mathscr{M}^+(D^2\phi(x_\varepsilon, t_\eta)).$$

On the other hand, we seek to estimate the integral terms. For this purpose denote

$$\begin{aligned}
l_u(z) &:= u(x_\varepsilon + j(x_\varepsilon, z), t_\eta) - u(x_\varepsilon, t_\eta) - (p_\varepsilon + D\phi(x_\varepsilon, t_\eta)) \cdot j(x_\varepsilon, z) \\
l_v(z) &:= v(y_\varepsilon + j(y_\varepsilon, z), s_\eta) - v(y_\varepsilon, s_\eta) - p_\varepsilon \cdot j(y_\varepsilon, z) \\
l_\phi(z) &:= \phi(x_\varepsilon + j(x_\varepsilon, z), t_\eta) - \phi(x_\varepsilon, t_\eta) - D\phi(x_\varepsilon, t_\eta) \cdot j(x_\varepsilon, z).
\end{aligned}$$

Fix $\delta' \gg \delta$ and split the integrals into:

$$\begin{aligned}
\mathscr{J}^2_\delta[x_\varepsilon, t_\eta, p_\varepsilon + D\phi(x_\varepsilon, t_\eta), u] &= \mathscr{J}^2_{\delta'}[x_\varepsilon, t_\eta, p_\varepsilon + D\phi(x_\varepsilon, t_\eta), u] + \int_{\delta<|z|<\delta'} l_u(z)\mu(dz) \\
\mathscr{J}^2_\delta[y_\varepsilon, s_\eta, p_\varepsilon, v] &= \mathscr{J}^2_{\delta'}[y_\varepsilon, s_\eta, p_\varepsilon, v] + \int_{\delta<|z|<\delta'} l_v(z)\mu(dz).
\end{aligned}$$

Since $(x_\varepsilon, y_\varepsilon, t_\eta, s_\eta)$ is a maximum of $\Psi_{\varepsilon,\eta}$ we have

$$\begin{aligned}
u(x_\varepsilon + j(x_\varepsilon, z), t_\eta) - v(y_\varepsilon + j(y_\varepsilon, z), s_\eta) - \frac{|x_\varepsilon + j(x_\varepsilon, z) - y_\varepsilon - j(y_\varepsilon, z)|^2}{\varepsilon^2} - \\
-\phi(x_\varepsilon + j(x_\varepsilon, z), t_\eta) \le u(x_\varepsilon, t_\eta) - v(y_\varepsilon, s_\eta) - \frac{|x_\varepsilon - y_\varepsilon|^2}{\varepsilon^2} - \phi(x_\varepsilon, t_\eta)
\end{aligned}$$

from where we get

$$\begin{aligned}
l_u(z) - l_v(z) &\le l_\phi(z) + \frac{|j(x_\varepsilon, z) - j(y_\varepsilon, z)|^2}{\varepsilon^2} \\
&\le l_\phi(z) + C_0^2 \frac{|x_\varepsilon - y_\varepsilon|^2}{\varepsilon^2}|z|^2.
\end{aligned}$$

This leads us to

$$\int_{\delta<|z|<\delta'} l_u(z)\mu(dz) - \int_{\delta<|z|<\delta'} l_v(z)\mu(dz) \le \int_{\delta<|z|<\delta'} l_\phi(z)\mu(dz) + O(\frac{|x_\varepsilon - y_\varepsilon|^2}{\varepsilon^2}).$$

Letting first δ go to zero, we get

$$\begin{aligned}
\limsup_{\delta\to 0} \big(\mathscr{J}^2_\delta[x_\varepsilon, t_\eta, p_\varepsilon + D\phi(x_\varepsilon, t_\eta), u] - \mathscr{J}^2_\delta[y_\varepsilon, s_\eta, p_\varepsilon, v]\big) \le \\
\le \mathscr{J}^2_{\delta'}[x_\varepsilon, t_\eta, p_\varepsilon + D\phi(x_\varepsilon, t_\eta), u] - \mathscr{J}^2_{\delta'}[y_\varepsilon, s_\eta, p_\varepsilon, v] \\
+ \mathscr{J}^1_{\delta'}[x_\varepsilon, t_\eta, \phi] + O(\frac{|x_\varepsilon - y_\varepsilon|^2}{\varepsilon^2})
\end{aligned}$$

whereas close to the origin

$$\begin{aligned}
\mathscr{J}^1_\delta[x_\varepsilon, t_\eta, \frac{|x - y_\varepsilon|^2}{\varepsilon^2}] - \mathscr{J}^1_\delta[y_\varepsilon, s_\eta, -\frac{|x_\varepsilon - y|^2}{\varepsilon^2}] &= \frac{2}{\varepsilon^2}\int_{|z|\le\delta} |j(x_\varepsilon, z)|^2\mu(dz) \to 0 \\
\mathscr{J}^1_\delta[x_\varepsilon, t_\eta, \phi] \le \int_{|z|\le\delta} \big(\sup_{|\theta|<1} D^2\phi(x_\varepsilon + \theta j(x_\varepsilon, z), t_\eta) j(x_\varepsilon, z) \cdot j(x_\varepsilon, z)\big)\mu(dz) &\to 0.
\end{aligned}$$

Furthermore, employing (3.25) and the regularity of the test function ϕ, as well as the upper

semicontinuity of $u-v$ and the continuity of the jump function j, we have

$$\begin{aligned}
&\limsup_{\eta,\varepsilon\to 0}\big(\mathscr{J}^2_{\delta'}[x_\varepsilon,t_\eta,p_\varepsilon+D\phi(x_\varepsilon,t_\eta),u]-\mathscr{J}^2_{\delta'}[y_\varepsilon,s_\eta,p_\varepsilon,v]\big)\\
&\quad\le\int_{|z|\ge\delta'}\limsup_{\eta,\varepsilon\to 0}\big((u(x_\varepsilon+j(x_\varepsilon,z),t_\eta)-v(y_\varepsilon+j(y_\varepsilon,z),s_\eta))\\
&\qquad\qquad-(u(x_\varepsilon,t_\eta)-v(y_\varepsilon,s_\eta))\\
&\qquad\qquad-(D\phi(x_\varepsilon,t_\eta)\cdot j(x_\varepsilon,z)+p_\varepsilon\cdot(j(x_\varepsilon,z)-j(y_\varepsilon,z)))1_B(z)\big)\mu(dz)\\
&\quad\le\int_{|z|\ge\delta'}\big(\limsup_{\eta,\varepsilon\to 0}(u(x_\varepsilon+j(x_\varepsilon,z),t_\eta)-v(y_\varepsilon+j(y_\varepsilon,z),s_\eta))\\
&\qquad\qquad-\lim_{\eta,\varepsilon\to 0}(u(x_\varepsilon,t_\eta)-v(y_\varepsilon,s_\eta))\\
&\qquad\qquad-\lim_{\eta,\varepsilon\to 0}D\phi(x_\varepsilon,t_\eta)\cdot j(x_\varepsilon,z)1_B(z)\big)\mu(dz)\\
&\quad\le\int_{|z|\ge\delta'}\big((u(x_0+j(x_0,z),t_\eta)-v(x_0+j(x_0,z),t_0))\\
&\qquad\qquad-(u(x_0,t_0)-v(x_0,t_0))\\
&\qquad\qquad-D\phi(x_0,t_0)\cdot j(x_0,z)\big)\mu(dz)=\mathscr{J}^2_{\delta'}[x_0,t_0,D\varphi(x_0,t_0),w].
\end{aligned}$$

Passing to the limits in the viscosity inequality we get, for all $\delta'>0$ that

$$\begin{aligned}
&\phi_t(x_0,t_0)-c|D\phi(x_0,t_0)|-\mathscr{M}^+(D^2\phi(x_0,t_0))-\\
&\qquad c(\mathscr{J}^1_{\delta'}[x_0,t_0,\phi]+\mathscr{J}^2_{\delta'}[x_0,t_0,D\varphi(x_0,t_0),w])\le 0.
\end{aligned}$$

Hence, w is a viscosity subsolution of the equation

$$w_t-c|Dw|-\mathscr{M}^+(D^2w)-c\mathscr{J}[x,t,w]=0 \text{ in } \Omega\times(0,T).$$

In case the sub and super-solutions are Lipschitz we take $R^*=\max\{||Du||_\infty,||Dv||_\infty\}$ and denote by $c=c_{R^*}$ and $w=w_{R^*}$.

2. The equation satisfies the strong maximum principle since the nonlinearity is positively 1-homogeneous and the nondegeneracy conditions (N) and (N') are satisfied.

$$\begin{aligned}
(N)\qquad &-c|p|-\mathscr{M}^+(I-\gamma p\otimes p)-c\tilde{C}_\mu+c\gamma\int_{\mathscr{C}_{\eta,\gamma}}|p\cdot j(x,z)|^2\mu(dz)\ge\\
&-c|p|-\mathscr{M}^+(I)+\gamma\mathscr{M}^-(p\otimes p)-c\tilde{C}_\mu+c\gamma\int_{\mathscr{C}_{\eta,\gamma}}|p\cdot j(x,z)|^2\mu(dz)\ge\\
&-c|p|-\Lambda N+\lambda\gamma|p|^2-c\tilde{C}_\mu+C(\eta)\gamma^{\beta-1}|p|^2>0, \text{ for } \gamma \text{ large}.
\end{aligned}$$

Therefore, SMaxP applies and we conclude that if $u-v$ attains a maximum inside the domain $\Omega\times(0,T)$ at some point (x_0,t_0) then $u-v$ is constant in $\Omega\times[0,t_0]$. □

Remark 3.5.1. *If Pucci's operator $\mathscr{M}^+$ appearing in hypothesis (H) is nondegenerate, i.e. $\lambda_R>0$, then one can consider any Lévy measure μ, not necessarily satisfying (M_c).*

Example 3.5.1. *The linear PIDE*

$$u_t - a(x)\Delta u - \mathscr{I}[x,t,u] = f(x) \text{ in } \Omega$$

with $a(x) \geq 0$, satisfies Strong Comparison, as (H) holds for the corresponding nonlinearity.

Example 3.5.2. *On the other hand, for the equation*

$$u_t + |Du|^m - \mathscr{I}[u] = f(x) \text{ in } \Omega$$

with $m \geq 2$ condition (H) holds if the sub and super-solutions are Lipschitz continuous in space.

Indeed, for u subsolution and v supersolution

$$\begin{aligned}(u-v)_t + |Du|^m - |Dv|^m - \mathscr{I}[u-v] \\ \geq (u-v)_t + m|Dv|^{m-2}(Du-Dv) - \mathscr{I}[u-v] \\ \geq (u-v)_t - cD(u-v) - \mathscr{I}[u-v].\end{aligned}$$

3.6 Appendix

We present in the following some useful properties of the nonlocal terms. For a given function v defined on $\mathbb{R}^N \times [0,T]$, consider the integral operators

$$\mathscr{I}[x,t,v] = \int_{\mathscr{D}} (v(x+z,t) - v(x,t) - Dv(x,t)\cdot z 1_B(z))\mu_x(dz),$$

and

$$\mathscr{J}[x,t,v] = \int_{\mathscr{D}} (v(x+j(x,z),t) - v(x,t) - Dv(x,t)\cdot j(x,z) 1_B(z))\mu(dz),$$

where the integral is taken over a domain $\mathscr{D} \subseteq \mathbb{R}^N$.

Lemma 3.6.1. *Any smooth function*

$$v(x,t) = e^{\varphi(x,t)}$$

satisfies the integral inequality

$$\mathscr{I}[x,t,v] \geq v \cdot \mathscr{I}[x,t,\varphi], \forall (x,t) \in \mathbb{R}^N \times [0,T]$$

Proof. The inequality is immediate from $e^y - 1 \geq y$, $\forall y \in \mathbb{R}$. More precisely

$$\begin{aligned}\mathscr{I}[x,t,v] &= \int_{\mathscr{D}} \left(e^{\varphi(x+z,t)} - e^{\varphi(x,t)} - e^{\varphi(x,t)} D\varphi(x,t)\cdot z 1_B(z)\right)\mu_x(dz) \\ &= e^{\varphi(x,t)} \int_{\mathscr{D}} \left(e^{\varphi(x+z,t)-\varphi(x,t)} - 1 - D\varphi(x,t)\cdot z 1_B(z)\right)\mu_x(dz) \\ &\geq e^{\varphi(x,t)} \int_{\mathscr{D}} \left(\varphi(x+z,t) - \varphi(x,t) - D\varphi(x,t)\cdot z 1_B(z)\right)\mu_x(dz).\end{aligned}$$

□

We straighten the convex inequality to the following:

Lemma 3.6.2. *Let v be a smooth function of the form*

$$v(x,t) = e^{\varphi(x,t)}.$$

Then for any $\delta \geq 0$ there exists a constant $c = \frac{1}{2}e^{-\delta}$ such that v satisfies

$$\mathscr{I}[x,t,v] \geq e^{\varphi(x,t)} \cdot [\mathscr{I}[x,t,\varphi] + c\int_{\mathscr{D}} (\varphi(x+z,t) - \varphi(x,t))^2 \mu_x(dz)],$$

for all $(x,t) \in \mathbb{R}^N \times [0,T]$, where the integral is taken over the domain $\mathscr{D} = \{\varphi(x+z) - \varphi(x) \geq -\delta\}$.

Proof. The proof is direct application of the exponential inequality

$$e^y - 1 \geq y + cy^2, \forall\, y \geq -\delta.$$

We now insert the previous inequality with $y = \varphi(x+z,t) - \varphi(x,t)$ in the nonlocal term and obtain

$$\begin{aligned}
\mathscr{I}[x,t,e^{\varphi}] &= e^{\varphi(x,t)} \int_{\mathscr{D}} \left(e^{\varphi(x+z,t)-\varphi(x,t)} - 1 - D\varphi(x,t)\cdot z 1_B(z)\right)\mu_x(dz) \\
&\geq e^{\varphi(x,t)} [\int_{\mathscr{D}} \left(\varphi(x+z,t) - \varphi(x,t) - D\varphi(x,t)\cdot z 1_B(z)\right)\mu_x(dz) \\
&\quad + c\int_{\mathscr{D}} \left((\varphi(x+z,t) - \varphi(x,t)\right)^2 \mu_x(dz)].
\end{aligned}$$

□

Similar results hold for Lévy-Itô operators.

Lemma 3.6.3. *The function $v(x,t) = e^{\varphi(x,t)}$, satisfies the integral inequality*

$$\mathscr{J}[x,t,v] \geq v \cdot \mathscr{J}[x,t,\varphi], \forall (x,t) \in \mathbb{R}^N \times [0,T].$$

Lemma 3.6.4. *For any $\delta \geq 0$ there exists a constant $c = \frac{1}{2}e^{-\delta}$ such that $v = e^{\varphi}$ satisfies*

$$\mathscr{J}[x,t,v] \geq e^{\varphi(x,t)} \cdot [\mathscr{J}[x,t,\varphi] + c\int_{\mathscr{D}} (\varphi(x+j(x,z),t) - \varphi(x,t))^2 \mu(dz)],$$

for all $(x,t) \in \mathbb{R}^N \times [0,T]$, where the integral is taken over $\mathscr{D} = \{\varphi(x+j(x,z)) - \varphi(x) \geq -\delta\}$.

3.7 Conclusion

We established in this chaper Strong Maximum Principle results for Nonlinear Integro-Differential Equations. The 'strong' principle states that a solution attaining a maximum at an interior point becomes constant. This comes separately from horizontal and vertical propagation of maxima. In particular, horizontal propagation of maxima can happen either by

translations of measure supports or it can come from the ellipticity of the equation with respect to the nonlocal term.

Furthermore, we introduced a new class of equations, termed *mixed integro-differential equations*, that are degenerate both in the local and nonlocal term, but nondegenerate in the local-nonlocal interaction.

We address in the following chapter regularity questions for this type of equations. In near future, we would like to investigate possible extensions of the Strong Maximum Principle for convex and concave Hamilton-Jacobi equations, and to Bellman-Isaacs equations.

CHAPTER 4

Lipschitz Regularity of Solutions for Mixed Integro-Differential Equations

On ne comprend jamais les maths, on s'y habitue.
Pierre Louis Lions, Collège de France, Paris
6 Novembre, 2009

Abstract: We establish *new Hölder and Lipschitz* estimates for viscosity solutions of a large class of nonlinear integro-differential equations, by the classical Ishii-Lions's method. We thus extend the Hölder regularity results recently obtained by Barles, Chasseigne and Imbert. In addition, we deal with a new class of nonlocal equations that we term *mixed integro-differential equations*. These equations are particularly interesting, as they are degenerate both in the local and nonlocal term, but their overall behavior is driven by the local-nonlocal interaction, e.g. the fractional diffusion may give the ellipticity in one direction and the classical diffusion in the complementary one.[1]

Résumé: Nous établissons de nouvelles estimations *Hölderiennes et Lipschitziennes* pour les solutions de viscosité d'une large classe d'équations intégro-différentielles non-linéaires, par la méthode classique de Ishii-Lions. Nous étendons ainsi les résultats de régularité récemment obtenus par Barles, Chasseigne et Imbert. De plus, nos résultats s'appliquent à une nouvelle classe d'équations non-locales que nous appelons *équations intégro-différentielles mixtes*. Ces équations sont particulièrement intéressantes, car elles sont dégénérées à la fois dans le terme local et nonlocal, mais leur comportement global est conduit par l'interaction locale-nonlocale, par example la diffusion fractionnaire peut donner l'ellipticité dans une direction et la diffusion classique dans la direction complémentaire.

Keywords: nonlinear integro-differential equations, Lipschitz regularity, viscosity solutions, Lévy processes

[1] This work represents the article *Lipschitz Regularity of Viscosity Solutions for Mixed Integro-Differential Equations*, in preparation.

Contents

4.1 Introduction

Ishii and Lions introduced in [IL90] a simple method to prove $C^{0,\alpha}$ regularity of viscosity solutions of fully nonlinear, possibly degenerate, elliptic partial differential equations, which in addition has the great advantage of providing *explicit* $C^{0,\alpha}$ *estimates*.

This simple method, closely related to classical viscosity solutions theory, was recently explored by Barles, Chasseigne and Imbert in [BCI11] for *second order, fully nonlinear elliptic partial integro-differential equations*, dealing with a large class of integro-differential operators, whose singular measures depend on x. The authors prove that the solution is α-Hölder continuous for any $\alpha < \min(\beta, 1)$, where β characterizes the singularity of the measure associated with the integral operator. However, in the case $\beta \geq 1$ the respective ad-literam estimates do not yield Lipschitz regularity. Using slightly different techniques and within a more general

framework that we make clear in the following, we *extend their Hölder regularity results to Lipschitz regularity*. In addition, we *establish both Hölder and Lipschitz estimates for a new class, of mixed integro-differential equations*, which we introduce in the sequel.

In order to treat a large class of nonlinear equations, they assume the nonlinearity satisfies a suitable ellipticity growth assumption. Roughly speaking, this assumption gives a suitable meaning to a generalized ellipticity of the equation in the sense that at each point of the domain, the ellipticity comes either from the second order term (the equation is strictly elliptic in the classical fully nonlinear sense), or from the nonlocal term (the equation is strictly elliptic in a nonlocal nonlinear sense).

In a recent study of the strong maximum principle for integro-differential equation [Cio], one can see that another type of *mixed ellipticity* might arise: at each point, the nonlinearity is *degenerate in the second-order term, and in the nonlocal term*, but *the combination of the local and the nonlocal diffusions renders the nonlinearity uniformly elliptic*. We term this type of equations *mixed integro-differential equations* since the diffusion term might give the ellipticity in one direction, whereas the nonlocal term in the complementary direction. For this type of nondegenerate equations, the assumptions in [BCI11] are not satisfied and we provide new Hölder and Lipschitz regularity results in this framework.

The simplest example of mixed integro-differential equations is given by

$$-\Delta_{x_1} u + (-\Delta_{x_2} u)^{\beta/2} = f(x_1, x_2)$$

where $(-\Delta_{x_2} u)^{\beta/2}$ denotes the fractional Laplacian with respect to x_2-variable

$$(-\Delta_{x_2} u)^{\beta/2} = -\int_{\mathbb{R}^{d_2}} \big(u(x_1, x_2 + z_2) - u(x_1, x_2) - D_{x_2} u(x_1, x_2) \cdot z_2 1_B(z_2)\big) \frac{dz_2}{|z_2|^{d_2+\beta}}.$$

In this case local diffusions occur only in x_1-direction and fractional diffusions in x_2-direction.

Using Ishii-Lions's viscosity method, we give both *Hölder and Lipschitz regularity results* of viscosity solutions for a *general class of mixed elliptic integro-differential equations* of the type

$$\begin{aligned} &F_0(u(x), Du, D^2u, \mathscr{I}[x,u]) + \\ &\quad F_1(x_1, D_{x_1}u, D^2_{x_1x_1}u, \mathscr{I}_{x_1}[x,u]) + F_2(x_2, D_{x_2}u, D^2_{x_2x_2}u, \mathscr{I}_{x_2}[x,u]) = f(x) \end{aligned} \tag{4.1}$$

as well as evolution equations

$$\begin{aligned} &u_t + F_0(u(x), Du, D^2u, \mathscr{I}[x,u]) + \\ &\quad F_1(x_1, D_{x_1}u, D^2_{x_1x_1}u, \mathscr{I}_{x_1}[x,u]) + F_2(x_2, D_{x_2}u, D^2_{x_2x_2}u, \mathscr{I}_{x_2}[x,u]) = 0. \end{aligned} \tag{4.2}$$

A point in $x \in \mathbb{R}^d$ is written as $x = (x_1, x_2) \in \mathbb{R}^{d_1} \times \mathbb{R}^{d_2}$, with $d = d_1 + d_2$. The symbols u_t, Du, D^2u stand for the derivative with respect to time, respectively the gradient and the Hessian matrix with respect to x. Subsequently, we write the gradient on components as $Du = (D_{x_1}u, D_{x_2}u)$ and the Hessian matrix $D^2u \in \mathbb{S}^d$ (with $\mathbb{S}^d$ the set of real symmetric $d \times d$

matrices) as a block matrix of the form

$$D^2 u = \begin{bmatrix} D^2_{x_1 x_1} u & D^2_{x_1 x_2} u \\ D^2_{x_2 x_1} u & D^2_{x_2 x_2} u \end{bmatrix}.$$

$\mathscr{I}[x,u]$ is an integro-differential operator, taken on the whole space $\mathbb{R}^d$, associated to Lévy processes

$$\mathscr{I}[x,u] = \int_{\mathbb{R}^d} (u(x+z) - u(x) - Du(x)\cdot z 1_B(z))\mu_x(dz)$$

where $1_B(z)$ denotes the indicator function of the unit ball B and $\left(\mu_x\right)_{x\in\mathbb{R}^d}$ is a family of Lévy measures, i.e. nonnegative, possibly singular, Borel measures on $\mathbb{R}^d$ such that

$$\sup_{x\in\mathbb{R}^d} \int_{\mathbb{R}^d} \min(|z|^2, 1)\mu_x(dz) < \infty.$$

Accordingly, one has the directional integro-differential operators

$$\mathscr{I}_{x_1}[x,u] = \int_{\mathbb{R}^{d_1}} (u(x_1+z, x_2) - u(x_1,x_2) - D_{x_1}u(x)\cdot z 1_B(z))\mu^1_{x_1}(dz)$$
$$\mathscr{I}_{x_2}[x,u] = \int_{\mathbb{R}^{d_2}} (u(x_1, x_2+z) - u(x_1,x_2) - D_{x_2}u(x)\cdot z 1_B(z))\mu^2_{x_2}(dz).$$

We consider as well the special class of Lévy-Itô operators, defined as follows

$$\mathscr{J}[x,u] = \int_{\mathbb{R}^d} (u(x+j(x,z)) - u(x) - Du(x)\cdot j(x,z) 1_B(z))\mu(dz)$$

where μ is a Lévy measure and $j(x,z)$ is the size of the jumps at x satisfying

$$\sup_{x\in\mathbb{R}^d} \int_{\mathbb{R}^d} \min(|j(x,z)|^2, 1)\mu(dz) < \infty.$$

Similarly, we deal with directional Lévy-Itô integro-differential operators

$$\mathscr{J}_{x_1}[x,u] = \int_{\mathbb{R}^{d_1}} (u(x_1+j(x_1,z), x_2) - u(x_1,x_2) - D_{x_1}u(x)\cdot j(x_1,z) 1_B(z))\mu^1(dz)$$
$$\mathscr{J}_{x_2}[x,u] = \int_{\mathbb{R}^{d_2}} (u(x_1, x_2+j(x_2,z)) - u(x_1,x_2) - D_{x_2}u(x)\cdot j(x_2,z) 1_B(z))\mu^2(dz).$$

We assume the nonlinearities are continuous and *degenerate elliptic*, i.e.

$$F_i(...,X,l) \le F_i(...,Y,l') \text{ if } X \ge Y,\ l \ge l',$$

for all $X, Y \in \mathbb{S}^{d_i}$ and $l, l' \in \mathbb{R}$, $i = 0,1,2$.

In addition, we suppose that the three nonlinearities satisfy suitable strict ellipticity and growth conditions, that we omit here for the sake of simplicity, but will be made precise in the following section. These structural growth conditions can be illustrated on the following

example:

$$-a_1(x_1)\Delta_{x_1}u - a_2(x_2)\mathscr{I}_{x_2}[x,u] - \mathscr{I}[x,u] + b_1(x_1)|D_{x_1}u_1|^{k_1} + b_2(x_2)|D_{x_2}u|^{k_2} + |Du|^n + cu = f(x)$$

where the nonlocal term $\mathscr{I}_{x_2}[x,u]$ has fractional exponent $\beta \in (0,2)$ and $a_i(x_i) > 0$, for $i = 1,2$.

When $\beta > 1$, we show that the solution is Lipschitz continuous for mixed equations with gradient terms $b_i(x_i)|D_{x_i}u|^{k_i}$ having a natural growth $k_i \le \beta$ if b_i bounded. If in addition b_i are τ-Hölder continuous, then the solution remains Lipschitz for gradient terms up to growth $k_i \le \tau + \beta$. When $\beta \le 1$, the solution is α-Hölder continuous for any $\alpha < \beta$. The critical case $\beta = 1$ is left open.

Recently there have been many papers dealing with $C^{0,\alpha}$ estimates and regularity of solutions (not necessarily in the viscosity setting) for fully nonlinear PIDEs and the literature has been considerably enriched.

As far as the *viscosity solutions* are concerned, there are essentially two approaches for proving Hölder or Lipschitz regularity: Ishii-Lions's method mentioned above, and by ABP estimates and Krylov - Safonov type Harnack inequalities (see Silvestre [Sil06], Caffarelli and Silvestre [CS09] and the references therein). The two above methods do not cover the same class of equations and each of it has its own advantages. The powerful Harnack approach applies for *uniformly elliptic fully nonlinear equations*, with *rough coefficients* and leads in general to further regularity such as $C^{1,\alpha}$, but requires some integrability condition of the measure at infinity. On the other hand, viscosity methods apply under weaker ellipticity assumptions and therefore deal with a *large* class of *degenerate, fully nonlinear equations*, in particular with *super-linear gradient growth*, allow measures which are only bounded at infinity, but require Hölder continuous coefficients and do not seem to yield further regularity.

Regularity theory for *nonlocal evolution equations of variational type* with measurable kernels can be developed using the original ideas of De Giorgi [DG57] and Nash [Nas58] from the calculus of variations. In this setting, Caffarelli, Chan and Vaseur [CCV] show that solutions with initial data in L^2 become instantaneously bounded and Hölder continuous. Their arguments are closely related to the work of Kassmann [Kas09], Kassmann and Bass [BK05a], where the Moser approach for the stationary case is fully developed. Within the variational framework, Caffarelli, Roquejoffre an Savin [CRS10] establish geometric properties, existence and regularity of nonlocal minimal surfaces.

This chapter is organized as follows. In Section §4.2 we give the appropriate definition of viscosity solution, make precise the ellipticity growth conditions to be satisfied by the nonlinearities and list the assumptions on the nonlocal terms. Section §4.3 is devoted to the main results, which for the sake of clarity are given in the periodic setting. We state partial regularity results, provide the complete proof, and then present the global regularity result. In the next Section §4.4 we consider several significant examples and discuss the main assumptions required by the regularity results and their implications. Extensions to the nonperiodic setting, parabolic versions of the equations, Bellman-Isaacs equations and multiple nonlinearities are recounted in Section §4.5. At last we detail in Section §4.6 the technical Lipschitz and Hölder estimates for the general nonlocal operators and Lévy-Itô operators, which are essentially the backbone of the main results.

4.2 Notations and Assumptions

4.2.1 Viscosity Solutions for Integro-Differential Equations

To overcome the difficulties imposed by behavior at infinity of the measures $(\mu_x)_x$, as well as the singularity at the origin, we often need to split the nonlocal terms into

$$\begin{aligned}\mathscr{I}_\delta^1[x,u] &= \int_{|z|\le\delta}\big(u(x+z)-u(x)-Du(x)\cdot z1_B(z)\big)\mu_x(dz)\\ \mathscr{I}_\delta^2[x,p,u] &= \int_{|z|>\delta}\big(u(x+z)-u(x)-p\cdot z1_B(z)\big)\mu_x(dz)\end{aligned}$$

respectively

$$\begin{aligned}\mathscr{J}_\delta^1[x,u] &= \int_{|z|\le\delta}\big(u(x+j(x,z))-u(x)-Du(x)\cdot j(x,z)1_B(z)\big)\mu(dz)\\ \mathscr{J}_\delta^2[x,p,u] &= \int_{|z|>\delta}\big(u(x+j(x,z))-u(x)-p\cdot j(x,z)1_B(z)\big)\mu(dz)\end{aligned}$$

with $0<\delta<1$ and $p\in\mathbb{R}^{\tilde{d}}$.

There are several equivalent definitions of viscosity solutions [BI08], but we will mainly refer to the following one.

Definition 4.2.1 (Viscosity solutions)**.** *An upper semi-continuous (in short usc) function $u:\mathbb{R}^d\to\mathbb{R}$ is a* subsolution *of (4.1) if for any $\phi\in C^2(\mathbb{R}^d)$ such that $u-\phi$ attains a global maximum at $x\in\mathbb{R}^d$*

$$\begin{aligned}&F_0(u(x),D\phi(x),D^2\phi(x),\mathscr{I}_\delta^1[x,t,\phi]+\mathscr{I}_\delta^2[x,t,D\phi(x,t),u])+\\ &F_1(x_1,D_{x_1}\phi(x),D^2_{x_1x_1}\phi(x),\mathscr{I}^1_{x_1,\delta}[x,t,\phi]+\mathscr{I}^2_{x_1,\delta}[x,t,D\phi(x,t),u])+\\ &F_2(x_2,D_{x_2}\phi(x),D^2_{x_2x_2}\phi(x),\mathscr{I}^1_{x_2,\delta}[x,t,\phi]+\mathscr{I}^2_{x_1,\delta}[x,t,D\phi(x,t),u])\le f(x).\end{aligned}$$

A lower semi-continuous (in short lsc) function $u:\mathbb{R}^d\to\mathbb{R}$ is a subsolution *of (4.1) if for any $\phi\in C^2(\mathbb{R}^d)$ such that $u-\phi$ attains a global minimum at $x\in\mathbb{R}^d$*

$$\begin{aligned}&F_0(u(x),D\phi(x),D^2\phi(x),\mathscr{I}_\delta^1[x,t,\phi]+\mathscr{I}_\delta^2[x,t,D\phi(x,t),u])+\\ &F_1(x_1,D_{x_1}\phi(x),D^2_{x_1x_1}\phi(x),\mathscr{I}^1_{x_1,\delta}[x,t,\phi]+\mathscr{I}^2_{x_1,\delta}[x,t,D\phi(x,t),u])+\\ &F_2(x_2,D_{x_2}\phi(x),D^2_{x_2x_2}\phi(x),\mathscr{I}^1_{x_2,\delta}[x,t,\phi]+\mathscr{I}^2_{x_1,\delta}[x,t,D\phi(x,t),u])\ge f(x).\end{aligned}$$

4.2.2 Ellipticity Growth Conditions

We assume that the nonlinearities F_i, with $i=0,1,2$ satisfy (one or more of) the next assumptions. The precise selection for each of the nonlinearities shall be given later on, when the regularity result is stated. Further examples and comments upon the restrictions of these nonlinearities are provided in section §4.4.

$(H0)$ There exists $\tilde{\gamma}\in\mathbb{R}$ such that for any $u,v\in\mathbb{R}$, $p\in\mathbb{R}^{\tilde{d}}$, $X\in\mathbb{S}^{\tilde{d}}$ and $l\in\mathbb{R}$

$$F(u,p,X,l)-F(v,p,X,l)\ge\tilde{\gamma}(u-v)\text{ when }u\ge v.$$

($H1$) There exist two functions $\Lambda^1, \Lambda^2 : \mathbb{R}^{\tilde{d}} \to [0,\infty)$ such that $\Lambda^1(x) + \Lambda^1(x) \geq \Lambda^0 > 0$ and for each $0 < R < \infty$ there exist some constants $k \geq 0$, $\tau \in (0,1]$ $\theta, \tilde{\theta} \in (0,1]$ such that for any $x, y \in \mathbb{R}^{\tilde{d}}$, $p \in \mathbb{R}^{\tilde{d}}$, $l \leq l'$ and any $\varepsilon > 0$

$$\begin{aligned} F(y,p,Y,l') - F(x,p,X,l) \leq \\ \Lambda^1(x)\big((l-l') + \frac{|x-y|^{2\theta}}{\varepsilon} + |x-y|^{\tau}|p|^{k+\tau} + C^1|p|^k\big) + \\ \Lambda^2(x)\big(\mathrm{tr}(X-Y) + \frac{|x-y|^{2\tilde{\theta}}}{\varepsilon} + |x-y|^{\tau}|p|^{2+\tau} + C^2|p|^2\big) \end{aligned}$$

if $X, Y \in \mathbb{S}^{\tilde{d}}$ satisfy, the inequality

$$-\frac{1}{\varepsilon}\begin{bmatrix} I & 0 \\ 0 & I \end{bmatrix} \leq \begin{bmatrix} X & 0 \\ 0 & -Y \end{bmatrix} \leq \frac{1}{\varepsilon}\begin{bmatrix} Z & -Z \\ -Z & Z \end{bmatrix}, \tag{4.3}$$

with $Z = I - \bar{\omega}\hat{a} \otimes \hat{a}$, for some $\hat{a} \in \mathbb{R}^{\tilde{d}}$ unit vector, and $\bar{\omega} \geq 1$.

($H2$) $F(\cdot, l)$ is Lipschitz continuous, uniformly with respect to all the other variables.

($H3$) For any $R > 0$ there exists a modulus of continuity ω_F such that for any $\varepsilon > 0$

$$F(y, \frac{x-y}{\varepsilon}, Y, l) - F(x, \frac{x-y}{\varepsilon}, X, l) \leq \omega_F\left(\frac{|x-y|^2}{\varepsilon} + |x-y|\right)$$

for all $x, y \in \mathbb{R}^{\tilde{d}}$, $X, Y \in \mathbb{S}^{\tilde{d}}$, with $|X|, |Y| \leq R$, satisfying the matrix inequality (4.3) with $Z = I$ and $l \in \mathbb{R}$.

4.2.3 Lévy Measures for General Nonlocal Operators

We recall that in this case, the nonlocal term $\mathscr{I}[x,u]$ is an integro differential operator defined by

$$\mathscr{I}[x,u] = \int_{\mathbb{R}^{\tilde{d}}} \big(u(x+z) - u(x) - Du(x)\cdot z 1_B(z)\big)\mu_x(dz) \tag{4.4}$$

where 1_B denotes the indicator function of the unit ball and $(\mu_x)_x$ is a family of Lévy measures. We need to make a series of assumptions for family of Lévy measures that we state below.

($M1$) There exists a constant $\tilde{C}_\mu > 0$ such that

$$\sup_{x \in \mathbb{R}^{\tilde{d}}} \big(\int_B |z|^2 \mu_x(dz) + \int_{\mathbb{R}^{\tilde{d}} \setminus B} \mu_x(dz)\big) \leq \tilde{C}_\mu.$$

($M2$) There exists $\beta \in (0,2)$ such that for every $a \in \mathbb{R}^{\tilde{d}}$ there exist $0 < \eta < 1$ and a constant $C_\mu > 0$ such that the following holds for any $x \in \mathbb{R}^{\tilde{d}}$

$$\int_{\mathscr{C}_{\eta,\delta}} |z|^2 \mu_x(dz) \geq C_\mu \, \eta^{\frac{\tilde{d}-1}{2}} \, \delta^{2-\beta}, \forall \delta > 0$$

with $\mathscr{C}_{\eta,\delta} := \{z \in B_\delta; (1-\eta)|z||a| \leq |a \cdot z|\}$.

($M3$) There exist $\beta \in (0,2)$, $\gamma \in (0,1)$ and a constant $C_\mu > 0$ such that for any $x, y \in \mathbb{R}^{\tilde{d}}$

$$\int_{B_\delta} |z|^2 |\mu_x - \mu_y|(dz) \leq C_\mu |x-y|^\gamma \, \delta^{2-\beta}$$

and

$$\int_{B\setminus B_\delta} |z||\mu_x - \mu_y|(dz) \leq \begin{cases} C_\mu |x-y|^\gamma \, \delta^{1-\beta} & \text{if } \beta \neq 1 \\ C_\mu |x-y|^\gamma \, |\ln(\delta)| & \text{if } \beta = 1. \end{cases}$$

At the same time, we assume that the directional Lévy measures satisfy similar assumptions.

Remark 4.2.1. To make precise the form of ($M2$) we consider the fractional Laplacian with exponent β and compute in $\mathbb{R}^2$

$$\begin{aligned} \int_{\mathscr{C}_{\eta,\delta}} |z|^2 \mu(dz) &= \frac{\text{vol}(\mathscr{C}_{\eta,\delta})}{\text{vol}(B_\delta)} \int_{B_\delta} |z|^2 \mu(dz) = \frac{\text{vol}(\mathscr{C}_{\eta,1})}{\text{vol}(B_1)} \int_{B_\delta} |z|^2 \mu(dz) \\ &= \delta^{2-\beta} \frac{\text{vol}(\mathscr{C}_{\eta,1})}{\text{vol}(B_1)} \int_{B_1} |z|^2 \mu(dz) = \delta^{2-\beta} \frac{\theta}{\pi} \int_{B_1} |z|^2 \mu(dz), \end{aligned}$$

where θ denotes the angle giving the aperture of the cone. Taking into account the definition of $\mathscr{C}_{\eta,1}$ we have for small angles θ

$$\eta = 1 - \cos(\theta) = -\frac{\theta^2}{2} + o(\theta^2)$$

and hence $\theta \simeq \sqrt{\eta}$, from where we deduce ($M2$).

In higher dimension $d \geq 3$, the volume of the cone is given in spherical coordinates, with normal direction $a = (0,0,...,1)$ and polar angle ϕ_1, by the formula

$$\text{vol}(\mathscr{C}_{\eta,1}) = \int_0^\theta \sin^{d-2}(\phi_1) d\phi_1 ... \int_0^\pi \sin(\phi_{d-2}) d\phi_{d-2} \int_0^{2\pi} d\phi_{d-1} \int_0^1 r^{d-1} dr.$$

For small angles θ the volume can be approximated by

$$\text{vol}(\mathscr{C}_{\eta,1}) \approx \frac{\theta^{d-1}}{d-1} \int_0^\pi \sin^{d-3}(\phi_2) d\phi_2 ... \int_0^\pi \sin(\phi_{d-2}) d\phi_{d-2} \int_0^{2\pi} d\phi_{d-1} \int_0^1 r^{d-1} dr.$$

Therefore there exists a positive constant $C > 0$ such that

$$\frac{\text{vol}(\mathscr{C}_{\eta,1})}{\text{vol}(B_1)} \geq C\theta^{d-1} = C\eta^{\frac{d-1}{2}}$$

and hence, denoting by $C_\mu = C \int_{B_1} |z|^2 \mu(dz)$, we have ($M_2$)

$$\int_{\mathscr{C}_{\eta,\delta}} |z|^2 \mu(dz) \geq C\eta^{\frac{d-1}{2}} \delta^{2-\beta} \int_{B_1} |z|^2 \mu(dz) = C_\mu \eta^{\frac{d-1}{2}} \delta^{2-\beta}.$$

4.2.4 Lévy Measures for Lévy-Itô Operators

Lévy-Itô operators are defined by

$$\mathscr{J}[x,u] = \int_{\mathbb{R}^{\tilde{d}}_*} \big(u(x+j(x,z)) - u(x) - Du(x)\cdot j(x,z)1_B(z)\big)\mu(dz). \tag{4.5}$$

In the sequel, we assume that the jump function satisfies the following conditions.

($J1$) There exists a constant $\tilde{C}_\mu > 0$ such that

$$\sup_{x\in\mathbb{R}^{\tilde{d}}} \int_B |j(x,z)|^2\mu(dz) + \int_{\mathbb{R}^{\tilde{d}}\setminus B} \mu(dz) \le \tilde{C}_\mu.$$

($J2$) There exists $\beta\in(0,2)$ such that for every $a\in\mathbb{R}^{\tilde{d}}$ there exist $0<\eta<1$ and a constant $C_\mu>0$ such that the following holds for any $x\in\mathbb{R}^{\tilde{d}}$

$$\int_{\mathscr{C}_{\eta,\delta}} |j(x,z)|^2\mu(dz) \ge C_\mu\, \eta^{\frac{d-1}{2}}\, \delta^{2-\beta}, \forall \delta>0$$

with $\mathscr{C}_{\eta,\delta} := \{z; |j(x,z)|\le\delta,\ (1-\eta)|j(x,z)||a| \le |a\cdot z|\}$.

($J3$) There exist $\gamma\in(0,1]$ and two constants $c_0, C_0 > 0$ such that for any $x\in\mathbb{R}^{\tilde{d}}$ and $z\in\mathbb{R}^{\tilde{d}}$

$$c_0|z| \le |j(x,z)| \le C_0|z|$$

and for all $z\in B$ and $x,y\in\mathbb{R}^{\tilde{d}}$

$$|j(x,z)-j(y,z)| \le C_0|z||x-y|^\gamma.$$

($J4$) There exists $\beta\in(0,2)$ such that for $\delta>0$ small enough

$$\int_{B\setminus B_\delta} |z|\mu(dz) \le \begin{cases} \tilde{C}_\mu\delta^{1-\beta}, & \text{if } \beta\neq 1 \\ \tilde{C}_\mu|\ln(\delta)| & \text{if } \beta = 1. \end{cases}$$

($J5$) There exists a constant $\tilde{C}_\mu > 0$ such that

$$\int_{\mathbb{R}^{\tilde{d}}\setminus B} |z|\mu(dz) \le \tilde{C}_\mu.$$

In case several assumptions hold simultaneously, the constants denoted similarly are considered to be the same (e.g. β, C_μ, $\tilde{C}_\mu$).

4.3 Lipschitz Continuity of Viscosity Solutions

In order to establish Lipschitz or Hölder regularity results for the solution u, we shift the function and show that the corresponding difference can be uniformly controlled by

$$\phi(t) = Lt^{\alpha}, \text{ for all } \alpha \in (0,1].$$

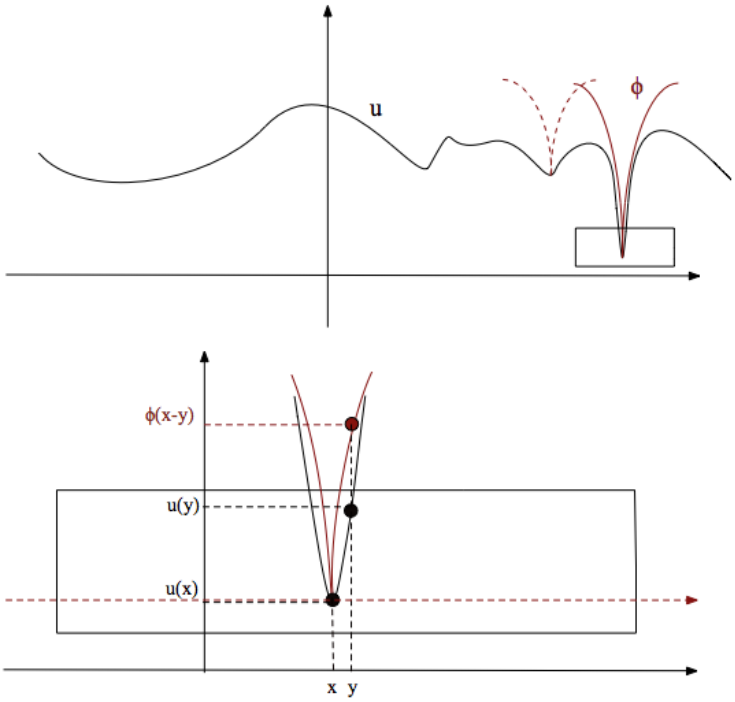

Figure 4.1: Uniformly controlling the shift of u by $\phi(|x-y|) = L|x-y|^{\alpha}$, for all $\alpha \in (0,1]$.

Remark 4.3.1. *Roughly speaking, one has to look at the maximum of the function*

$$(x,y) \mapsto u(x) - u(y) - \phi(|x-y|)$$

and, in the case of elliptic PDEs, *follow the uniqueness proof with a careful analysis of the matrix inequality given by Jensen-Ishii's lemma. Precise computations show that we just need ellipticity of the equation in the gradient direction. In the case of nonlocal diffusions, one has to translate in a proper way the ellipticity in the gradient direction. And this is reflected in the nondegeneracy conditions* $(M2)$*, respectively* $(J2)$ *required by the family of Lévy measures.*

For the sake of simplicity, we give the proof in the periodic setting. This yields $C^{0,\alpha}$ regularity instead of local regularity. At the same time it allows us to avoid the localization terms, meant to overcome the behavior at infinity of the solutions, which is related to the integrability of the singular measure away from the origin.

4.3.1 Partial Regularity Results

Theorem 4.3.1 (**Partial regularity for periodic, mixed PIDEs - general nonlocal operators**). *Let f be a continuous, periodic function. Assume the nonlinearities F_i, $i = 0,1,2$ are degenerate elliptic and that they satisfy the following:*

- *F_0 is $\mathbb{Z}^d$-periodic and satisfies assumptions $(H0)$, $(H2)$ with $\tilde{d} = d$ and some constant $\tilde{\gamma}$;*
- *F_1 is $\mathbb{Z}^{d_1}$-periodic and satisfies $(H1)$ with $\tilde{d} = d_1$, for some functions Λ^1 , Λ^2 and some parameters Λ^0, $k \geq 0$, $\tau, \theta, \tilde{\theta} \in (0,1]$;*
- *F_2 is $\mathbb{Z}^{d_2}$-periodic and satisfies $(H2)$, $(H3)$ with $\tilde{d} = d_2$.*

Let μ^0, $\left(\mu^1_{x_1}\right)_{x_1}$ and μ^2 be Lévy measures on $\mathbb{R}^d$, $\mathbb{R}^{d_1}$, $\mathbb{R}^{d_2}$ respectively associated to the integro-differential operators $\mathscr{I}[x,u]$, $\mathscr{I}_{x_1}[x,u]$ and $\mathscr{J}_{x_2}[x,u]$. Suppose

- *$\left(\mu^1_{x_1}\right)_{x_1}$ satisfies $(M1)-(M3)$ for some C_{μ^1}, $\tilde{C}_{\mu^1}$, β and γ, with $\begin{cases} k \leq \beta, & \beta > 1 \\ k < \beta, & \beta \leq 1; \end{cases}$*
- *the jump function $j(x_2,z)$ satisfies $(J1)$, $(J3)$ and $(J5)$ for some C_{μ^2}, $\tilde{C}_{\mu^2}$, and $\gamma = 1$.*

Then any periodic continuous viscosity solution u of

$$\begin{aligned} &F_0(u(x), Du, D^2u, \mathscr{I}[x,u]) + \\ &\quad F_1(x_1, D_{x_1}u, D^2_{x_1x_1}u, \mathscr{I}_{x_1}[x,u]) + F_2(x_2, D_{x_2}u, D^2_{x_2x_2}u, \mathscr{J}_{x_2}[x,u]) = f(x) \end{aligned} \tag{4.6}$$

(a) is locally Lipschitz continuous in the x_1 variable if $\beta > 1$;

(b) is $C^{0,\alpha}$ continuous in the x_1 variable with $\alpha < \frac{\beta-k}{1-k}$, if $\beta \leq 1$.

The Lipschitz/ Hölder constant L depends on $||u||_\infty$, the dimension of the space d, the constants associated to the Lévy measures as well as the constants required by the growth condition $(H1)$.

Remark 4.3.2. *In particular, when $d_1 = d$ and $F_0 \equiv 0, F_2 \equiv 0$ we extend to Lipschitz the Hölder regularity result, recently obtained by Barles, Chasseigne and Imbert in [BCI11].*

Proof. The proof of the regularity of u consists of two steps: we first show that the solution u is $C^{0,\alpha}$ continuous for all $\alpha \in (0,1)$, then we check that in the subcritical case $\beta > 1$ this implies the Lipschitz continuity. We use the viscosity method introduced by Ishii and Lions in [IL90].

STEP 1. We introduce the auxiliary function

$$\psi(x_1, y_1, x_2) = u(x_1, x_2) - u(y_1, x_2) - \phi(x_1 - y_1)$$

where ϕ is a radial function of the form

$$\phi(z) = \varphi(|z|)$$

with a suitable choice of a smooth increasing concave function $\varphi : \mathbb{R}_+ \to \mathbb{R}_+$ satisfying $\varphi(0) = 0$ and $\varphi(t_0) \geq 2||u||_\infty$ for some $t_0 > 0$. Our aim is to show that

$$\psi(x_1, y_1, x_2) \leq 0, \text{ if } |x_1 - y_1| < t_0, \forall x_2 \in \mathbb{R}^{d_2}.$$

This yields the desired regularity result, for a proper choice of φ. Namely, $\varphi = Lt^{\alpha}$ will give the Hölder partial regularity of the solution

$$|u(x_1,x_2)-u(y_1,x_2)| \leq L|x_1-y_1|^{\alpha}, \text{ if } |x_1-y_1|<t_0$$

and $\varphi = L(t-\rho t^{1+\alpha})$ the Lipschitz partial regularity

$$|u(x_1,x_2)-u(y_1,x_2)| \leq L|x_1-y_1|, \text{ if } |x_1-y_1|<t_0.$$

STEP 2. To this end, we argue by contradiction and assume that $\psi(x_1,y_1,x_2)$ has a positive strict maximum at some point $(\bar{x}_1,\bar{y}_1,\bar{x}_2)$

$$M=\psi(\bar{x}_1,\bar{y}_1,\bar{x}_2)=\max_{x_1,y_2\in\mathbb{R}^{d_1},x_2\in\mathbb{R}^{d_2}}\psi(x_1,y_1,x_2)>0.$$

Denote by $\bar{x}=(\bar{x}_1,\bar{x}_2)$ and by $\bar{y}=(\bar{y}_1,\bar{x}_2)$. Then

$$\varphi(|\bar{x}-\bar{y}|)\leq u(\bar{x})-u(\bar{y}) \quad \leq \quad \omega_u(|\bar{x}-\bar{y}|) \tag{4.7}$$

$$\varphi(|\bar{x}-\bar{y}|)\leq u(\bar{x})-u(\bar{y}) \quad \leq \quad 2||u||_{\infty}. \tag{4.8}$$

To be able to extract some valuable information hereafter, we need to construct test functions defined on the whole space $\mathbb{R}^d$. For this reason, we penalize ψ around the maximum by doubling the variables, staying at the same time as close as possible to the maximum point. Therefore, we consider the auxiliary function

$$\psi_{\varepsilon}(x,y)=u(x_1,x_2)-u(y_1,y_2)-\phi(x_1-y_1)-\frac{|x_2-y_2|^2}{\varepsilon^2}$$

whose maximum is attained, say at $(x^{\varepsilon},y^{\varepsilon})$. Denote its maximum value by

$$M^{\varepsilon}=\psi_{\varepsilon}(x^{\varepsilon},y^{\varepsilon})=\max_{x,y\in\mathbb{R}^d}\psi_{\varepsilon}(x,y).$$

Then the following holds.

Lemma 4.3.1. *Up to a subsequence, the sequences of maximum points* $\left((x^{\varepsilon},y^{\varepsilon})\right)_{\varepsilon}$ *and of maximum values* $(M^{\varepsilon})_{\varepsilon}$ *satisfy as* $\varepsilon\to 0$

$$M^{\varepsilon}\to M, \qquad \frac{|x_2^{\varepsilon}-y_2^{\varepsilon}|^2}{\varepsilon^2}\to 0, \qquad (x^{\varepsilon},y^{\varepsilon})\to(\bar{x},\bar{y}).$$

STEP 3. Let $\bar{a}=(\bar{a}_1,\bar{a}_2)=\bar{x}-\bar{y}$, $p=(p_1,p_2)=(D\phi(\bar{a}_1),0)$ and denote by

$$a^{\varepsilon}=(a_1^{\varepsilon},a_2^{\varepsilon})=x^{\varepsilon}-y^{\varepsilon}, \qquad \hat{a}^{\varepsilon}=\frac{a^{\varepsilon}}{|a^{\varepsilon}|}, \qquad p^{\varepsilon}=(p_1^{\varepsilon},p_2^{\varepsilon})=(D\phi(a_1^{\varepsilon}),2\frac{x_2^{\varepsilon}-y_2^{\varepsilon}}{\varepsilon^2}).$$

Since $x_1^{\varepsilon}\neq y_1^{\varepsilon}$, for ε small enough the function ϕ is smooth and we can apply the Jensen-Ishii's lemma for integro-differential equations [BI08]. This yields the existence, for each $\varepsilon>0$ of two

sequences of matrices $(X^{\varepsilon,\zeta})_\zeta, (Y^{\varepsilon,\zeta})_\zeta \subset \mathbb{S}^d$ of the form

$$X^{\varepsilon,\zeta} = \begin{bmatrix} X_1^{\varepsilon,\zeta} & 0 \\ 0 & X_2^{\varepsilon,\zeta} \end{bmatrix} \text{ and } Y^{\varepsilon,\zeta} = \begin{bmatrix} Y_1^{\varepsilon,\zeta} & 0 \\ 0 & Y_2^{\varepsilon,\zeta} \end{bmatrix}, \tag{4.9}$$

which correspond to the sub and superjets of u at the points x^ε and y^ε. In addition the block diagonal matrix satisfies

$$-\frac{1}{\zeta}\begin{bmatrix} I_d & 0 \\ 0 & I_d \end{bmatrix} \leq \begin{bmatrix} X^{\varepsilon,\zeta} & 0 \\ 0 & -Y^{\varepsilon,\zeta} \end{bmatrix} \leq \begin{bmatrix} Z & -Z \\ -Z & Z \end{bmatrix} + o_\zeta(1), \tag{4.10}$$

with Z a block matrix of the form (4.9), with blocks

$$\begin{aligned} Z_1 &= D^2\phi(a_1^\varepsilon) = \frac{\varphi'(|a_1^\varepsilon|)}{|a_1^\varepsilon|} I_{d_1} + \left(\varphi''(|a_1^\varepsilon|) - \frac{\varphi'(|a_1^\varepsilon|)}{|a_1^\varepsilon|}\right) \hat{a}_1^\varepsilon \otimes \hat{a}_1^\varepsilon \\ Z_2 &= \frac{2}{\varepsilon^2} I_{d_2}. \end{aligned}$$

By Lemma 4.7.1 the triplets of block matrices $(X_i^{\varepsilon,\zeta}, Y_i^{\varepsilon,\zeta}, Z_i)$ for $i = 1,2$ satisfy bound (4.10). Then, by sup and inf matrix convolution (see Lemmas 4.7.2 and 4.7.3 in Appendix) we build matrices, that we still denote by $X^{\varepsilon,\zeta}$ and $Y^{\varepsilon,\zeta}$, for which the corresponding blocks $X_i^{\varepsilon,\zeta}$ and $Y_i^{\varepsilon,\zeta}$ for $i = 1,2$ satisfy double bounds

$$-\frac{4}{\bar{\varepsilon}}\begin{bmatrix} I_{d_1} & 0 \\ 0 & I_{d_1} \end{bmatrix} \leq \begin{bmatrix} X_1^{\varepsilon,\zeta} & 0 \\ 0 & -Y_1^{\varepsilon,\zeta} \end{bmatrix} \leq \begin{bmatrix} \tilde{Z}_1 & -\tilde{Z}_1 \\ -\tilde{Z}_1 & \tilde{Z}_1 \end{bmatrix} + o_\zeta(1) \tag{4.11}$$

$$-\frac{4}{\varepsilon^2}\begin{bmatrix} I_{d_2} & 0 \\ 0 & I_{d_2} \end{bmatrix} \leq \begin{bmatrix} X_2^{\varepsilon,\zeta} & 0 \\ 0 & -Y_2^{\varepsilon,\zeta} \end{bmatrix} \leq \frac{4}{\varepsilon^2}\begin{bmatrix} I_{d_2} & 0 \\ 0 & I_{d_2} \end{bmatrix} + o_\zeta(1) \tag{4.12}$$

with $\tilde{Z}_1 = Z_1^{\frac{\bar{\varepsilon}}{2}}$, where

$$\bar{\varepsilon} = \frac{|a_1^\varepsilon|}{\varphi'(|a_1^\varepsilon|)}.$$

In addition, from the monotonicity of the sup and inf convolution (4.31) the new block matrices $X^{\varepsilon,\zeta}$ and $Y^{\varepsilon,\zeta}$ are still sub and superjets of u at x^ε, respectively y^ε

$$\begin{aligned} (p^\varepsilon, X^{\varepsilon,\zeta}) &\in \mathscr{J}^{2,+}(u(x^\varepsilon)) \\ (p^\varepsilon, Y^{\varepsilon,\zeta}) &\in \mathscr{J}^{2,-}(u(y^\varepsilon)). \end{aligned}$$

Since the bounds in (4.11) and (4.12) are uniform with respect to ζ, we can let $\zeta \to 0$ and obtain two matrices X^ε and Y^ε satisfying the double inequality required by the ellipticity growth condition (H1), which are still sub and superjets of u at x^ε, respectively y^ε. Hence, they satisfy

the viscosity inequalities

$$F_0(u(x^\varepsilon),p^\varepsilon,X^\varepsilon,\mathscr{I}[x^\varepsilon,p^\varepsilon,u])+\sum_{i=1,2}F_i(\bar{x}_i^\varepsilon,p_i^\varepsilon,X_i^\varepsilon,\mathscr{I}_{x_i}[x^\varepsilon,p_i^\varepsilon,u])\le f(x^\varepsilon)$$
$$F_0(u(y^\varepsilon),p^\varepsilon,Y^\varepsilon,\mathscr{I}[y^\varepsilon,p^\varepsilon,u])+\sum_{i=1,2}F_i(\bar{y}_i^\varepsilon,p_i^\varepsilon,Y_i^\varepsilon,\mathscr{I}_{y_i}[y^\varepsilon,p_i^\varepsilon,u])\ge f(y^\varepsilon).$$

Subtracting the above inequalities and denoting

$$\begin{aligned}E_0(x^\varepsilon,y^\varepsilon,u) &= F_0\left(u(y^\varepsilon),p^\varepsilon,Y^\varepsilon,\mathscr{I}[y^\varepsilon,p^\varepsilon,u]\right)-F_0\left(u(x^\varepsilon),p^\varepsilon,X^\varepsilon,\mathscr{I}[x^\varepsilon,p^\varepsilon,u]\right)+f(x^\varepsilon)-f(y^\varepsilon)\\ E_i(\bar{x}_i^\varepsilon,\bar{y}_i^\varepsilon,u) &= F_i\left(\bar{y}_i^\varepsilon,p_i^\varepsilon,Y_i^\varepsilon,\mathscr{I}_{y_i}[y^\varepsilon,p_i^\varepsilon,u]\right)-F_i\left(\bar{x}_i^\varepsilon,p_i^\varepsilon,X_i^\varepsilon,\mathscr{I}_{x_i}[x^\varepsilon,p_i^\varepsilon,u]\right),\ i=1,2,\end{aligned}$$

we get that

$$0\le E_0(x^\varepsilon,y^\varepsilon,u)+E_1(x_1^\varepsilon,y_1^\varepsilon,u)+E_2(x_2^\varepsilon,y_2^\varepsilon,u). \tag{4.13}$$

STEP 4. In the following we estimate each of these terms as $\varepsilon\to 0$, bringing into play the ellipticity growth assumptions satisfied by each nonlinearity.

Since $u(y^\varepsilon)\le u(x^\varepsilon)$, $X^\varepsilon\le Y^\varepsilon$, the monotonicity assumption (H_0), the ellipticity (E) with respect to the second order term and the nonlocal term and the Lipschitz continuity $(H2)$ of F_0 with respect to the nonlocal term yield

$$E_0(x^\varepsilon,y^\varepsilon,u)\le\tilde{\gamma}\big(u(y^\varepsilon)-u(x^\varepsilon)\big)+L_{F_0}\big(\mathscr{I}[x^\varepsilon,p^\varepsilon,u]-\mathscr{I}[y^\varepsilon,p^\varepsilon,u]\big)_+ +f(x^\varepsilon)-f(y^\varepsilon).$$

When the Lévy-Itô measures corresponding to the nonlinearity F_0 do not depend on x, we immediately deduce from the maximum condition that

$$u(x^\varepsilon+z)-v(y^\varepsilon+z)\le u(x^\varepsilon)-v(y^\varepsilon)$$

which renders nonpositive the difference of the nonlocal terms

$$\mathscr{I}[x^\varepsilon,p^\varepsilon,u]-\mathscr{I}[y^\varepsilon,p^\varepsilon,u]\le 0.$$

Therefore, passing to the limits as $\varepsilon\to 0$ and employing Lemma 4.3.1 we have

$$\limsup_{\varepsilon\to 0}E_0(x^\varepsilon,y^\varepsilon,u)\le-\tilde{\gamma}M. \tag{4.14}$$

The estimate of E_2 does not depend on the choice of φ and is given by the growth condition $(H3)$ and the Lipschitz continuity of $F_2(\cdot,l)$, uniformly with respect to all the other variables

$$E_2(x_2^\varepsilon,y_2^\varepsilon,u)\ \le\ \omega_{F_2}\Big(\frac{|a_2^\varepsilon|^2}{\varepsilon^2}+|a_2^\varepsilon|\Big)+L_{F_2}\left(\mathscr{I}_{x_2}[x^\varepsilon,p_2^\varepsilon,u]-\mathscr{I}_{y_2}[y^\varepsilon,p_2^\varepsilon,u]\right)_+$$

where L_{F_2} is the Lipschitz constant of $F_2(\cdot,l)$. From Proposition 4.6.3 the quadratic estimates for Lévy-Itô operators hold

$$\begin{aligned}&\mathscr{I}_{x_2}[x^\varepsilon,p_2^\varepsilon,u]-\mathscr{I}_{y_2}[y^\varepsilon,p_2^\varepsilon,u]\le\\ &\quad C\frac{1}{\varepsilon^2}\int_{|z_2|\le\delta}|z_2|^2\mu^2(dz_2)+C\frac{|a_2^\varepsilon|^2}{\varepsilon^2}\int_{|z_2|\ge\delta}|z_2|^2\mu^2(dz_2)+C\frac{|a_2^\varepsilon|^2}{\varepsilon^2}\int_{|z_2|\ge 1}|z_2|\mu^2(dz_2)\end{aligned}$$

for some positive constant C. As $\delta \to 0$, the estimate reads

$$\mathscr{I}_{x_2}[x^\varepsilon, p_2^\varepsilon, u] - \mathscr{I}_{y_2}[y^\varepsilon, p_2^\varepsilon, u] \leq C\tilde{C}_{\mu^2}\frac{|a_2^\varepsilon|^2}{\varepsilon^2}.$$

Letting now $\varepsilon \to 0$ and using Lemma 4.3.1 which ensures that $\frac{|a_2^\varepsilon|^2}{\varepsilon^2} \to 0$ we are finally lead to

$$\limsup_{\varepsilon\to 0} E_2(x_2^\varepsilon, y_2^\varepsilon, u) \leq 0. \tag{4.15}$$

For the estimate of E_1, we use the ellipticity growth condition $(H1)$

$$\begin{aligned} E_1(x_1^\varepsilon, y_1^\varepsilon, u) \quad \leq \quad & \Lambda^1(x_1^\varepsilon)\Big(\big(\mathscr{I}_{x_1}[x^\varepsilon, p_1^\varepsilon, u] - \mathscr{I}_{y_1}[y^\varepsilon, p_1^\varepsilon, u]\big) + \frac{|a_1^\varepsilon|^{2\theta}}{\bar{\varepsilon}} + |a_1^\varepsilon|^\tau |p_1^\varepsilon|^{k+\tau} + C_1^1|p_1^\varepsilon|^k\Big) \\ & \Lambda^2(x_1^\varepsilon)\Big(\mathrm{tr}(X_1^\varepsilon - Y_1^\varepsilon) + \frac{\omega_{F_1}(|a_1^\varepsilon|)}{\bar{\varepsilon}} + |a_1^\varepsilon|^\tau |p_1^\varepsilon|^{2+\tau} + C_1^2|p_1^\varepsilon|^2\Big) \end{aligned}$$

where we recall that $p_1^\varepsilon = D\phi(a_1^\varepsilon) = L\varphi'(|a_1^\varepsilon|)\hat{a}_1^\varepsilon$. The goal is show that, for each choice of φ (measuring either the Hölder or the Lipschitz continuity), the right hand side quantity is negative, arriving thus to a contradiction.

STEP 5.1. **Hölder continuity.** In order to establish the Hölder regularity of solutions, we consider the auxiliary function

$$\varphi = Lt^\alpha, \text{ with } \alpha < \min(1, \beta).$$

In this case, we apply Corollary 4.6.2, to the functions $u(\cdot, x_2)$ and $u(\cdot, y_2)$, which yields the following Hölder estimate for the difference of the nonlocal terms

$$\mathscr{I}_{x_1}[x^\varepsilon, p_1^\varepsilon, u] - \mathscr{I}_{y_1}[y^\varepsilon, p_1^\varepsilon, u] \leq -L|a_1^\varepsilon|^{\alpha-\beta}\Big\{C(\alpha, \mu^1) - o_{|a_1^\varepsilon|}(1)\Big\} + O(1).$$

Lemma 4.7.4 applies with $\tilde{Z}_1 = Z_1^{\frac{\bar{\varepsilon}}{2}}$, $\bar{\varepsilon} = \big(L\alpha|a_1^\varepsilon|^{\alpha-2}\big)^{-1}$, $\omega = 2-\alpha$ and hence the trace is bounded by

$$\mathrm{trace}(X_1^\varepsilon - Y_1^\varepsilon) \leq -8\bar{\omega}\big(L\alpha|a_1^\varepsilon|^{\alpha-2}\big) \tag{4.16}$$

where $\bar{\omega} = \frac{\omega-1}{\omega+1}$ is a constant in $(0, \frac{1}{3})$. We plug these estimates into the inequality for E_1. Letting ε go to zero and employing Lemma 4.3.1 we obtain the following bound

$$\limsup_{\varepsilon\to 0} E_1(x_1^\varepsilon, y_1^\varepsilon, u) \leq \Lambda^0\, \mathscr{E}^1(|\bar{a}|) + \Lambda^0\, \mathscr{E}^2(|\bar{a}|) + O(1)$$

where for $C(\alpha, \mu^1) = \alpha C_0$ and $2\theta + \beta > 2$

$$\begin{aligned} \mathscr{E}^1(|\bar{a}|) \quad &= \quad -L|\bar{a}|^{\alpha-\beta}\big(\alpha C_0 - o_{|\bar{a}|}(1)\big) + |\bar{a}|^{2\theta}\big(L\alpha|\bar{a}|^{\alpha-2}\big) + |\bar{a}|^\tau\big(L\alpha|\bar{a}|^{\alpha-1}\big)^{k+\tau} + C_1^1\big(L\alpha|\bar{a}|^{\alpha-1}\big)^k \\ &= \quad -L|\bar{a}|^{\alpha-\beta}\Big\{\alpha C_0 - o_{|\bar{a}|}(1) - \alpha^{k+\tau}|\bar{a}|^{\beta-k}\big(L|\bar{a}|^\alpha\big)^{k+\tau-1} - C_1^1\alpha^k|\bar{a}|^{\beta-k}\big(L|\bar{a}|^\alpha\big)^{k-1}\Big\} \end{aligned}$$

and

$$\begin{aligned}\mathscr{E}^2(|\bar{a}|) &= -8\bar{\omega}\big(L\alpha|\bar{a}|^{\alpha-2}\big)+|\bar{a}|^{2\tilde{\theta}}\big(L\alpha|\bar{a}|^{\alpha-2}\big)+|\bar{a}|^{\tau}\left(L\alpha|\bar{a}|^{\alpha-1}\right)^{2+\tau}+C_1^2\left(L\alpha|\bar{a}|^{\alpha-1}\right)^2\\ &= -L|\bar{a}|^{\alpha-2}\Big\{\alpha\big(8\bar{\omega}-|\bar{a}|^{2\tilde{\theta}}\big)-\alpha^{2+\tau}\left(L|\bar{a}|^{\alpha}\right)^{1+\tau}-C_1^2\alpha^2L|\bar{a}|^{\alpha}\Big\}.\end{aligned}$$

Using the fact that $L|\bar{a}|^{\alpha}\leq 2||u||_{\infty}$ we have

$$\mathscr{E}^2(|\bar{a}|) \leq -L|\bar{a}|^{\alpha-2}\Big\{\alpha\big(8\bar{\omega}-|\bar{a}|^{2\tilde{\theta}}\big)-\alpha^{2+\tau}\left(2||u||_{\infty}\right)^{1+\tau}-C_1^2\alpha^2\left(2||u||_{\infty}\right)\Big\}.$$

As far as $\mathscr{E}^1$ is concerned, we further argue differently for the subcritical and supercritical case, with respect to the Lévy exponent β, and accordingly with respect to k and τ. Namely

(a) if $1<k\leq\beta$, in which case $k+\tau-1>0$, $k-1>0$, we have

$$\begin{aligned}\mathscr{E}^1(|\bar{a}|) \leq -L|\bar{a}|^{\alpha-\beta}\Big\{&\alpha C_0-o_{|\bar{a}|}(1)-\alpha^{k+\tau}|\bar{a}|^{\beta-k}\left(2||u||_{\infty}\right)^{k+\tau-1}\\ &-C_1^1\alpha^k|\bar{a}|^{\beta-k}\left(2||u||_{\infty}\right)^{k-1}\Big\}.\end{aligned}$$

(b) if $k<\min(1,\beta)$, then

(b.1) for $0<k<1-\tau$ and $\beta-k+\alpha(k+\tau-1)>0$

$$\begin{aligned}\mathscr{E}^1(|\bar{a}|) &\leq -L|\bar{a}|^{\alpha-\beta}\Big\{\alpha C_0-o_{|\bar{a}|}(1)-\alpha^{k+\tau}|\bar{a}|^{\beta-k+\alpha(k+\tau-1)}L^{k+\tau-1}\\ &\qquad -C_1^1\alpha^k|\bar{a}|^{\beta-k+\alpha(k-1)}L^{k-1}\Big\}\\ &= -L|\bar{a}|^{\alpha-\beta}\Big(\alpha C_0-o_{|\bar{a}|}(1)\Big).\end{aligned}$$

(b.2) for $1-\tau<k\leq 1$ and $\beta-k+\alpha(k+\tau-1)>0$

$$\begin{aligned}\mathscr{E}^1(|\bar{a}|) &\leq -L|\bar{a}|^{\alpha-\beta}\Big\{\alpha C_0-o_{|\bar{a}|}(1)-\alpha^{k+\tau}\left(2||u||_{\infty}\right)^{k+\tau-1}\\ &\qquad -C_1^1\alpha^k|\bar{a}|^{\beta-k+\alpha(k-1)}L^{k-1}\Big\}\\ &= -L|\bar{a}|^{\alpha-\beta}\Big\{\alpha C_0-o_{|\bar{a}|}(1)-\alpha^{k+\tau}\left(2||u||_{\infty}\right)^{k+\tau-1}\Big\}.\end{aligned}$$

This implies that for α small enough the two terms become (large) negative

$$\lim_{L\to\infty}\mathscr{E}^1(|\bar{a}|)=-\infty \text{ and } \lim_{L\to\infty}\mathscr{E}^2(|\bar{a}|)=-\infty.$$

Hence

$$\lim_{L\to\infty}\limsup_{\varepsilon\to 0}E_1(x_1^{\varepsilon},y_1^{\varepsilon},u)=-\infty. \tag{4.17}$$

We now turn back to inequality (4.13), let first $\varepsilon\to 0$ and then $L\to\infty$. Plugging in the estimates (4.14) - (4.17) we arrive to a contradiction. Therefore, we have proved up to this point the $C^{0,\alpha}$ regularity of the solution, for α small enough. Note that the exponent α only depends on $||u||_{\infty}$, k and τ.

We further use this first step to provide the $C^{0,\alpha}$ regularity for all $\alpha\in(0,1)$. To this end, we

estimate $L|\bar{a}|^\alpha$ with the modulus of continuity of u and get

$$\mathscr{E}^2(|\bar{a}|) \leq -L|\bar{a}|^{\alpha-2}\Big\{\alpha\big(8\bar{\omega}-|\bar{a}|^{2\tilde{\theta}}\big)-\alpha^{2+\tau}\left(\omega_u(|\bar{a}|)\right)^{1+\tau}-C_1^2\alpha^2\omega_u(|\bar{a}|)\Big\}.$$

Taking into account that $\omega_u(|\bar{a}|)\leq \bar{L}|\bar{a}|^{\bar{\alpha}}$ for some $\bar{\alpha}$ small, we come back to the original estimates in case $k>1$ and to the estimates given in $(b.1)$ when $k\in(0,1-\tau)$, respectively $(b.2)$ when $k\in(1-\tau,1)$, where α is everywhere replaced with $\bar{\alpha}$. By similar arguments we obtain

$$\begin{aligned}\mathscr{E}^1(|\bar{a}|) &\leq -L|\bar{a}|^{\alpha-\beta}\Big(\alpha C_0-o_{|\bar{a}|}(1)\Big)\\ \mathscr{E}^2(|\bar{a}|) &\leq -L|\bar{a}|^{\alpha-2}\Big(\alpha C_0-o_{|\bar{a}|}(1)\Big).\end{aligned}$$

This yields (4.17) for L sufficiently large, and therefore completes the $C^{0,\alpha}$ regularity result.

STEP 5.2. **Lipschitz continuity.** In the case $\beta>1$, we establish the Lipschitz regularity of solutions. Therefore, we consider the auxiliary function

$$\varphi(t)=\begin{cases} L\big(t-\varrho t^{1+\alpha}\big), & t\in[0,t_0]\\ \varphi(t_0), & t>t_0\end{cases}$$

where $\alpha\in(0,1)$ will be chosen small enough and $t_0=\sqrt[\alpha]{\frac{1}{\rho(1+\alpha)}}$. We remind that α is connected to the aperture of the cone corresponding to $\eta\sim|\bar{a}|^{2\alpha}$. In order to estimate the difference of the nonlocal terms, we apply Corollary 4.6.1, to the same choice of functions $u(\cdot,x_2)$ and $u(\cdot,y_2)$:

$$\mathscr{I}_{x_1}[x^\varepsilon,p_1^\varepsilon,u]-\mathscr{I}_{y_1}[y^\varepsilon,p_1^\varepsilon,u]\leq -L|a_1^\varepsilon|^{(1-\beta)+\alpha(d_1+2-\beta)}\Big\{\Theta(\varrho,\alpha,\mu^1)-o_{|a_1^\varepsilon|}(1)\Big\}+O(1).$$

At this point, we fix ρ such that the constant $\Theta(\varrho,\alpha,\mu)$ is positive. We then apply Lemma 4.7.4 with $\tilde{Z}_1=Z_1^{\frac{\bar{\varepsilon}}{2}}$, where this time

$$\bar{\varepsilon}=|a_1^\varepsilon|\varphi'(|a_1^\varepsilon|)=\big(L|a_1^\varepsilon|^{-1}-L\rho(1+\alpha)|a_1^\varepsilon|^{\alpha-1}\big)^{-1}.$$

Indeed, for t small enough, the function $L(t-\rho t^{1+\alpha})$ is concave and subsequently $\omega=1-\varphi''(|a_1^\varepsilon|)\bar{\varepsilon}>1$. Thus

$$\operatorname{trace}(X_1^\varepsilon-Y_1^\varepsilon) \leq -\frac{8}{\bar{\varepsilon}}\frac{\omega-1}{\omega+1}=\frac{8\varphi''(|a_1^\varepsilon|)}{2-\varphi''(|a_1^\varepsilon|)\bar{\varepsilon}}.$$

Note that in this case $\frac{\omega-1}{\omega+1}$ depends on $|a_1^\varepsilon|$. However there exists a positive constant $\bar{\omega}$ such that for $|\bar{a}|$ small

$$\frac{8\varphi''(|a_1^\varepsilon|)}{2-\varphi''(|a_1^\varepsilon|)\bar{\varepsilon}} \leq 8\bar{\omega}\varphi''(|a_1^\varepsilon|).$$

Thus, denoting by $c_0=\rho(1+\alpha)$, second order terms are bounded by

$$\operatorname{trace}(X_1^\varepsilon-Y_1^\varepsilon) \leq -8c_0\bar{\omega}\big(L\alpha|a_1^\varepsilon|^{\alpha-1}\big).$$

We plug these estimates into the inequality for E_1. Letting ε go to zero and employing Lemma 4.3.1 we arrive as before to

$$\limsup_{\varepsilon\to 0} E_1(x_1^\varepsilon, y_1^\varepsilon, u) \le \Lambda^0\, \mathscr{E}^1(|\bar a|) + \Lambda^0\, \mathscr{E}^2(|\bar a|) + O(1),$$

where denoting by $C_0 = \Theta(\varrho, \alpha, \mu^1)$ the terms $\mathscr{E}^1, \mathscr{E}^2$ are given by

$$\begin{aligned}
\mathscr{E}^1(|\bar a|) &= -L|\bar a|^{(1-\beta)+\alpha(d_1+2-\beta)}\big(C_0 - o_{|\bar a|}(1)\big) + |\bar a|^{2\theta}\Big(L|\bar a|^{-1}\big(1-c_0|\bar a|^\alpha\big)\Big) \\
&\quad + |\bar a|^\tau\Big(L\big(1-c_0|\bar a|^\alpha\big)\Big)^{\beta+\tau} + C_1^1\Big(L\big(1-c_0|\bar a|^\alpha\big)\Big)^{\beta} \\
\mathscr{E}^2(|\bar a|) &= -8\, c_0\, \bar\omega\Big(L\alpha|\bar a|^{\alpha-1}\Big) + |\bar a|^{2\tilde\theta}\Big(L|\bar a|^{-1}\big(1-c_0|\bar a|^\alpha\big)\Big) \\
&\quad + |\bar a|^\tau\Big(L\big(1-c_0|\bar a|^\alpha\big)\Big)^{2+\tau} + C^2\Big(L\big(1-c_0|\bar a|^\alpha\big)\Big)^{2}.
\end{aligned}$$

Whenever $\alpha(d_1+3-\beta) < 2\theta - 2 - \beta$ the second term in $\mathscr{E}^1$ behaves like $o\big(|\bar a|^{(1-\beta)+\alpha(d_1+2-\beta)}\big)$. Taking $L|\bar a|^{(1-\beta)+\alpha(d_1+2-\beta)}$ as a commune multiplier and using that $1 - c_0|\bar a|^\alpha \le 1$ we have

$$\begin{aligned}
\mathscr{E}^1(|\bar a|) &\le -L|\bar a|^{(1-\beta)+\alpha(d_1+2-\beta)}\Big\{C_0 - o_{|\bar a|}(1) \\
&\qquad - |\bar a|^{-\alpha(d_1+2-\beta)}\Big(L|\bar a| - c_0 L|\bar a|^{\alpha+1}\Big)^{\beta+\tau-1} \\
&\qquad - C_1^1|\bar a|^{-\alpha(d_1+2-\beta)}\Big(L|\bar a| - c_0 L|\bar a|^{\alpha+1}\Big)^{\beta-1}\Big\} \\
&\le -L|\bar a|^{(1-\beta)+\alpha(d_1+2-\beta)}\Big\{C_0 - o_{|\bar a|}(1) \\
&\qquad - 2|\bar a|^{-\alpha(d_1+2-\beta)}\Big(\varphi(|\bar a|)\Big)^{\beta+\tau-1} \\
&\qquad - 2C_1^1|\bar a|^{-\alpha(d_1+2-\beta)}\Big(\varphi(|\bar a|)\Big)^{\beta-1}\Big\}.
\end{aligned}$$

On the other hand, similar techniques give us an estimate for $\mathscr{E}^2$:

$$\begin{aligned}
\mathscr{E}^2(|\bar a|) &\le -L|\bar a|^{\alpha-1}\Big\{8c_0\alpha\bar\omega - |\bar a|^{2\tilde\theta}|\bar a|^{-\alpha} \\
&\qquad - |\bar a|^{-\alpha}\Big(L|\bar a| - c_0 L|\bar a|^{\alpha+1}\Big)^{1+\tau} \\
&\qquad - C_1^2|\bar a|^{-\alpha}\Big(L|\bar a| - c_0 L|\bar a|^{\alpha+1}\Big)\Big\} \\
&\le -L|\bar a|^{\alpha-1}\Big\{8c_0\alpha\bar\omega - |\bar a|^{2\tilde\theta}|\bar a|^{-\alpha} \\
&\qquad - 2|\bar a|^{-\alpha}\Big(\varphi(|\bar a|)\Big)^{1+\tau} \\
&\qquad - 2C_1^2|\bar a|^{-\alpha}\Big(\varphi(|\bar a|)\Big)\Big\}.
\end{aligned}$$

When α is small enough we have $|\bar a|^{2\tilde\theta}|\bar a|^{-\alpha} = o_{|\bar a|}(1)$. Then

$$\mathscr{E}^2(|\bar a|) \le -L|\bar a|^{\alpha-1}\Big\{C_1 - o_{|\bar a|}(1) - 2|\bar a|^{-\alpha}\Big(\varphi(|\bar a|)\Big)^{1+\tau} - 2C_1^2|\bar a|^{-\alpha}\Big(\varphi(|\bar a|)\Big)\Big\}.$$

Since we have just seen that u is Hölder continuous for any $\tilde{\alpha} \in (0,1)$, we have

$$\varphi(|\bar{a}|)|\bar{a}|^{-\tilde{\alpha}} \to 0, \text{ as } L \to \infty.$$

Using this relation in the previous inequalities estimating $\mathscr{E}^1$ and $\mathscr{E}^2$ we get that, for L large enough

$$\begin{aligned} \mathscr{E}^1(|\bar{a}|) &\leq -L|\bar{a}|^{(1-\beta)+\alpha(d_1+2-\beta)}\Big(C_0 - o_{|\bar{a}|}(1)\Big) \\ \mathscr{E}^2(|\bar{a}|) &\leq -L|\bar{a}|^{\alpha-1}\Big(C_0 - o_{|\bar{a}|}(1)\Big). \end{aligned}$$

Hence (4.17) holds and this further yields the desired contradiction. □

Remark 4.3.3. *When $k = \beta = 1$, the solution is α-Hölder continuous, with α small enough. Unfortunately in this case we cannot characterize the Hölder exponent α.*

Remark 4.3.4. *When $\beta < 1$, if $C_1^1 = 0$ in $(H1)$ and $\beta(k+\tau) > k$, then the solution is exactly $C^{0,\beta}$.*

Since the concave estimates for Lévy-Itô operators are of the same order as those for general nonlocal operators, similar regularity results hold. Namely, we have the following.

Theorem 4.3.2 (**Partial regularity for periodic, mixed PIDEs - Lévy-Itô operators**)**.** *Let f be continuous and periodic. Assume the nonlinearities F_i, $i = 0,1,2$ are degenerate elliptic and that*

- *F_0 is $\mathbb{Z}^d$-periodic and satisfies assumptions $(H0)$, $(H2)$ with $\tilde{d} = d$ and some constant $\tilde{\gamma}$;*
- *F_1 is $\mathbb{Z}^{d_1}$-periodic and satisfies $(H1)$ with $\tilde{d} = d_1$, for some functions Λ^1 , Λ^2 and some parameters Λ^0, $k \geq 0$, $\tau, \theta, \tilde{\theta} \in (0,1]$;*
- *F_2 is $\mathbb{Z}^{d_2}$-periodic and satisfies $(H2)$, $(H3)$ with $\tilde{d} = d_2$.*

Let μ^0, μ^1 and μ^2 be Lévy measures on $\mathbb{R}^d$, $\mathbb{R}^{d_1}$ and $\mathbb{R}^{d_2}$, respectively associated to the integro-differential operators $\mathscr{I}[x,u]$, $\mathscr{J}_{x_1}[x,u]$ and $\mathscr{J}_{x_2}[x,u]$. Suppose

- *the jump function $j^1(x_1,z)$ satisfies assumptions $(J1)$ - $(J4)$, for some parameters β, C_{μ^1}, $\tilde{C}_{\mu^1}$, and $\gamma \in (1-\beta/2, 1]$, and in addition $\begin{cases} k \leq \beta, & \beta > 1 \\ k < \beta, & \beta \leq 1; \end{cases}$*
- *the jump function $j^2(x_2,z)$ satisfies assumptions $(J1)$, $(J3)$ with $\gamma = 1$, and $(J5)$, for some parameters C_{μ^2}, $\tilde{C}_{\mu^2}$.*

Then any bounded, continuous viscosity solution u of

$$\begin{aligned} &F_0(u(x), Du, D^2u, \mathscr{I}[x,u]) + \\ &\quad F_1(x_1, D_{x_1}u, D^2_{x_1x_1}u, \mathscr{J}_{x_1}[x,u]) + F_2(x_2, D_{x_2}u, D^2_{x_2x_2}u, \mathscr{J}_{x_2}[x,u]) = f(x) \end{aligned} \tag{4.18}$$

(a) is Lipschitz continuous in the x_1 variable, if $\beta > 1$;

(b) is $C^{0,\alpha}$ continuous in the x_1 variable with $\alpha < \frac{\beta-k}{1-k}$, if $\beta \leq 1$.

The Lipschitz/ Hölder constant L depends on $||u||_\infty$, the dimension of the space d, the constants associated to the Lévy measures as well as the constants required by the growth condition $(H1)$.

4.3.2 Global Regularity

It follows immediately from the previous results that as long as both nonlinearities F_1 and F_2 satisfy assumptions $(H1)-(H3)$, the solution is global Lipschitz or Hölder continuous.

Corollary 4.3.1 (**Global regularity for periodic, mixed PIDEs**). *Let the nonlinearities F_i, $i = 0,1,2$ be degenerate elliptic, continuous and periodic, f continuous and periodic. Assume the following:*

- *F_0 satisfies assumptions $(H0)$, $(H2)$ with $\tilde{d} = d$ and some constant $\tilde{\gamma} > 0$;*
- *F_i with $i = 1,2$ satisfy assumptions $(H1)-(H3)$ with $\tilde{d} = d_i$, for some functions Λ_i^1, Λ_i^2 and some constants $k_i \geq 0$, $\tau_i \in [0,1], \theta_i, \tilde{\theta}_i \in (0,1]$.*

Let μ^0, μ^i, with $i = 1,2$ be Lévy measures on $\mathbb{R}^d$, $\mathbb{R}^{d_i}$ respectively associated to the integro-differential operators $\mathscr{I}[x,u]$, $\mathscr{J}_{x_i}[x,u]$ and suppose the corresponding jump functions $j^i(x_i,z_i)$ satisfy assumptions $(J1)-(J5)$ for some constants β_i, C_{μ^i}, $\tilde{C}_{\mu^i}$, with $\gamma = 1$ in $(J3)$. Then any periodic continuous viscosity solution u of

$$\begin{aligned} &F_0(u(x), Du, D^2u, \mathscr{I}[x,u]) + \\ &\quad F_1(x_1, D_{x_1}u, D^2_{x_1x_1}u, \mathscr{J}_{x_1}[x,u]) + F_2(x_2, D_{x_2}u, D^2_{x_2x_2}u, \mathscr{J}_{x_2}[x,u]) = f(x) \end{aligned} \tag{4.19}$$

(a) is Lipschitz continuous, if $\beta_i > 1$ and $k_i \leq \beta_i$ for $i = 1,2$;

(b) is $C^{0,\alpha}$ continuous with $\alpha < \min(\frac{\beta_1 - k_1}{1-k_1}, \frac{\beta_2 - k_2}{1-k_2})$, if $\beta \leq 1$ and $k_i < \beta_i$ for $i = 1,2$.

The Lipschitz/Hölder constant depends on $||u||_\infty$, on the dimension of the space d and only on the constants associated to the Lévy measures and on the constants required by the growth condition $(H1)$.

At first glance, the fact that $(H1)$ and $(H3)$ must hold simultaneously seems to exclude a large class of nonlinear equations dealing with directional gradient or drift terms such as $|D_{x_i}u|^r$ or $|b(x_i)|D_{x_i}u|^{k+\tau}$, $r,k > 0$. Indeed, taking in the ellipticity growth condition $(H1)$ $l = l'$, $p = \frac{x-y}{\varepsilon}$ and $\tilde{\theta} = \theta$ we get

$$F(y, \frac{x-y}{\varepsilon}, Y, l) - F(x, \frac{x-y}{\varepsilon}, X, l) \leq \Lambda(x)\Big(\mathrm{tr}(X-Y) + \frac{|x-y|^{2\theta}}{\varepsilon} + \frac{|x-y|^{k+2\tau}}{\varepsilon^{k+\tau}} + \frac{|x-y|^r}{\varepsilon^r}\Big).$$

Hence $(H3)$ would hold whenever $k = r = 0$, $\theta = 1$. In this case $(H1)$ and $(H3)$ could be joined together in assumption

(H) There exist two functions $\Lambda^1, \Lambda^2 : \mathbb{R}^{\tilde{d}} \to [0,\infty)$ such that $\Lambda^1(x) + \Lambda^1(x) \geq \Lambda_0 > 0$ and for each $0 < R < \infty$ there exists a modulus of continuity $\omega_F(r) \to 0$, as $r \to 0$ such that for any $x, y \in \mathbb{R}^{\tilde{d}}$, $p \in \mathbb{R}^{\tilde{d}}$, $l \leq l'$ and any $\varepsilon > 0$

$$\begin{aligned} &F(y,p,Y,l') - F(x,p,X,l) \leq \\ &\qquad \Lambda^1(x)(l-l') + \Lambda^2(x)\mathrm{tr}(X-Y) + \omega_F(|x-y|(1+|p|) + \frac{|x-y|^2}{\varepsilon}) \end{aligned}$$

if $X, Y \in \mathbb{S}^{\tilde{d}}$ satisfy inequality (4.3) with $Z = I - \bar{\omega}\hat{z} \otimes \hat{z}$, for $z \in \mathbb{R}^{\tilde{d}}$ and $\bar{\omega} \geq 1$.

Nevertheless, one can argue under weaker growth assumptions, by a *cut-off gradients* argument for equations of the type:

$$F_0(u(x), Du, D^2u, \mathscr{I}[x,u]) + \\ F_1(x_1, D_{x_1}u, D^2_{x_1x_1}u, \mathscr{J}_{x_1}[x,u]) + F_2(x_2, D_{x_2}u, D^2_{x_2x_2}u, \mathscr{J}_{x_2}[x,u]) = f(x) \tag{4.20}$$

where F_i, for $i = 1,2$ satisfy assumptions $(H1)-(H2)$ and F_0 satisfies $(H2)$ and $(H0)$ with $\tilde{\gamma} > 0$.

Roughly speaking, one should look at the approximated equation with $|Du|$ replaced by $|Du| \wedge R$, for $R > 0$ and remark that its solutions are Lipschitz continuous, with the Lipschitz norm independent of R, thus the solution of the original problem is also Lipschitz continuous. This is made precise by defining, for each $i = 0,1,2$ the following functions

$$F_i^R(\cdot, p, X, l) = \begin{cases} F_i(\cdot, p, X, l), & \text{if } |p| \le R \\ F_i(\cdot, R\frac{p}{|p|}, X, l), & \text{if } |p| \ge R. \end{cases}$$

Consider then the approximated problem

$$F_0^R(u^R(x), Du^R, D^2u^R, \mathscr{I}[x,u^R]) + \\ F_1^R(x_1, D_{x_1}u^R, D^2_{x_1x_1}u^R, \mathscr{J}_{x_1}[x,u^R]) + F_2^R(x_2, D_{x_2}u^R, D^2_{x_2x_2}u^R, \mathscr{J}_{x_2}[x,u^R]) = f(x) \tag{4.21}$$

and remark that $(H3)$ holds. Thus the approximated problem (4.21) has a Lipschitz/Hölder viscosity solution, whose continuity constant depends on $||u^R||_\infty$ the constants required by the Lévy measures and those appearing in the ellipticity growth assumption $(H1)$.

Let

$$M := |F_1(0,0,0,0)| + ||F_1(x_1,0,0,0)||_\infty + ||F_2(x_2,0,0,0)||_\infty + ||f||_\infty.$$

Since $M(\tilde{\gamma})^{-1}$ and $-M(\tilde{\gamma})^{-1}$ are respectively a supersolution and a subsolution of the approximated problem (4.21), by a comparison result between sub and super-solutions we have due to $(H0)$

$$||u^R||_\infty \le \frac{M}{\tilde{\gamma}}.$$

Therefore, the Lipschitz constant of u^R is independent of R. Observing that for R large enough the solution u^R of the approximated problem is as well a solution of the original, we conclude.

4.4 Examples and Discussion on Assumptions

4.4.1 Classical Nonlinearities

By Theorem 4.3.1 we extend the Hölder regularity result in [BCI11] to Lipschitz regularity when the nonlocal exponent $\beta > 1$. As already presented in the introduction, this result applies for equations that are strictly elliptic in a generalized sense: at each point, the nonlinearity is *either non degenerate in the second-order term,* or is *nondegenerate in the nonlocal term.*

4.4.1.1 Model Equation

A model equation for such nondegenerate equations is

$$-\operatorname{tr}(A(x)D^2u) - c(x)\mathscr{I}[x,u] + b(x)|Du|^k + |Du|^r = 0 \quad \text{in } \mathbb{R}^d\,, \tag{4.22}$$

where A and c are continuous functions, $b \in C^{0,\tau}(\mathbb{R}^d)$, with $0 \le \tau \le 1$, $k, r, \in (0, 2+\tau)$. $\mathscr{I}[x,u]$ is a non-local term of type (4.4) or (4.5) of exponent $\beta \in (0,2)$. We comment in the following the ellipticity growth assumption $(H1)$ and make precise the role of each term.

- One has to assume that equation (4.22) is strictly elliptic in the sense that

$$A(x) \ge \Lambda^1(x) I \quad \text{and} \quad c(x) \ge \Lambda^2(x) \quad \text{in } \mathbb{R}^d \tag{4.23}$$

  with

$$\Lambda^1(x) + \Lambda^2(x) \ge \Lambda^0 > 0.$$

  Thus the equation may be degenerate in the local or the nonlocal term as for all $x \in \mathbb{R}^d$, $A(x) \ge 0$ and $c(x) \ge 0$. However, at each point either $A(x)$ is a positive definite matrix and the equation is strictly elliptic in the classical sense, or $c(x) > 0$ and $\mathscr{I}[x,u]$ satisfies suitable nondegeneracy assumptions (that we discuss below) and the equation is strictly elliptic with respect to the integro-differential term.

- $A = \sigma^T\sigma$ *with* σ *a bounded, uniformly continuous function* which maps $\mathbb{R}^d$ into the space of $N \times p$-matrices for some $p \le N$. It can be checked that

$$-\big(\operatorname{tr}(A(x)X) - \operatorname{tr}(A(y)Y)\big) \le d\,\frac{\omega_\sigma^2(|x-y|)}{\varepsilon}$$

  for any $X, Y \in \mathbb{S}^d$ satisfying inequality (4.3).

- The nonlocal term can be writen as a general nonlocal operator

$$\begin{aligned} c(x)\mathscr{I}[x,u] &= c(x)\int_{\mathbb{R}^d}\big(u(x+z) - u(x) - Du(x)\cdot z1_B(z)\big)\mu_x(dz) \\ &= \int_{\mathbb{R}^d}\big(u(x+z) - u(x) - Du(x)\cdot z1_B(z)\big)c(x)\mu_x(dz) \end{aligned}$$

  where $\big(\mu_x\big)_x$ is a family of Lévy measures, satisfying assumptions $(M1)-(M3)$. When $c : \mathbb{R}^d \to \mathbb{R}$ *is* γ*-Hölder continuous* the results for general nonlocal operators literally apply for the new family of operators associated to the Lévy measures $\tilde{\mu}_x = c(x)\mu_x$.

  For a Lévy-Itô type operator, the nonlocal term can be writen as

$$\begin{aligned} c(x)\mathscr{I}[x,u] &= c(x)\int_{\mathbb{R}^d}\big(u(x+j(x,z)) - u(x) - Du(x)\cdot j(x,z)1_B(z)\big)\mu(dz) \\ &= \int_{\mathbb{R}^d}\big(u(x+j(x,z)) - u(x) - Du(x)\cdot j(x,z)1_B(z)\big)c(x)\mu(dz) \end{aligned}$$

  where the jump function $j(x,z)$ satisfies assumptions $(J1)-(J5)$. In this case, the results for general nonlocal operators do not apply ad-literam! Otherwise we could have con-

sidered Lévy-Itô operators as a particular case of general integro-differential operators. However, when *c is γ-Hölder continuous*, combining estimates arguments (see Section §4.6) used for Lévy-Itô operators with those for general nonlocal operators, we arrive to the same conclusion.

- *$b:\mathbb{R}^d \to \mathbb{R}$ is a τ-Hölder continuous function, or just a bounded continuous function.* The growth conditions k, r on the gradient are related to the regularity of coefficients of b.

  When $\beta > 1$, the solution is Lipschitz continuous for gradient terms $b(x)|Du|^k$ with natural growth $k \le \beta$ and b bounded. If in addition b is τ-Hölder continuous, then the solution remains Lipschitz for gradient terms with growth $k \le \tau + \beta$. Similarly, the solution is Lipschitz for any term gradient term $|Du|^r$ with $r \le \beta$.

4.4.1.2 Advection Fractional Diffusion Equation

Several recent papers deal with the regularity of solutions for the advection fractional diffusion equation

$$u_t + (-\Delta_{x_2} u)^{\beta/2} + b(x) \cdot Du = f.$$

One distinguishes three cases, according to the order of fractional diffusion. The case $\beta < 1$ is known as the supercritical case, since the fractional diffusion is of lower order than the advection; conversely, $\beta > 1$ is the subcritical case. In between we have the critical value $\beta = 1$, when the drift and the diffusion are of the same order.

As we shall see in the following section §4.5, the regularity results apply as well for parabolic PIDEs and in the non-periodic setting. We obtain that the solution is Lipschitz continuous in the subcritical case $\beta > 1$ with b bounded; hence the fractional diffusion is stronger than the advection and prescribes the regularity of the solution. In the supercritical case $\beta \le 1$, the solution is β Hölder continuous whenever b is $C^{1-\beta+\tau}$, where $\tau > 0$.

Recently, Silvestre obtained similar results by Harnack techniques [Sila]. In addition to our results, he showed [Silb] that when $\beta \ge 1$ and the vector field b is $C^{1-\beta+\tau}$ the solution becomes $C^{1,\tau}$. Hölder regularity results were shown by Caffarelli and Vasseur [CV10] using De Giorgi's approach, for divergence free vector fields b belonging to the class BMO. A similar approach is given by Kiselev and Nazarov in [KN10].

4.4.2 A Toy-Model for the Mixed Case

As discussed before, there is another interesting type of *mixed ellipticity*: at each point, the nonlinearity is *degenerate both in the second-order term, and in the nonlocal term*, but *the combination of the local and the nonlocal diffusions renders the nonlinearity uniformly elliptic.* The simplest example of this kind of equations is given by

$$-\Delta_{x_1} u + (-\Delta_{x_2} u)^{\beta/2} = f(x_1, x_2)$$

where $(-\Delta_{x_2} u)^{\beta/2}$ denotes the fractional Laplacian with respect to the x_2-variable

$$(-\Delta_{x_2} u)^{\beta/2} = -\int_{\mathbb{R}^{d_2}} \big(u(x_1, x_2 + z_2) - u(x_1, x_2) - D_{x_2} u(x_1, x_2) \cdot z_2 1_B(z_2)\big) \frac{dz_2}{|z_2|^{d_2+\beta}}.$$

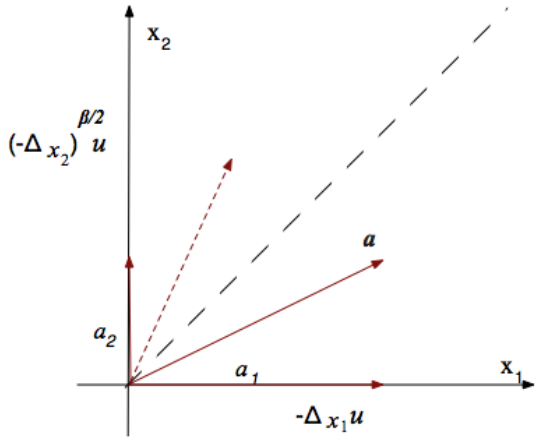

Figure 4.2: Local diffusions occur only in x_1-directions and fractional diffusions in x_2-directions.

It is clear that the equation is degenerate both with respect to the local and the nonlocal term, as both the Laplacian and the fractional Laplacian are incomplete. Indeed, the directional classical Laplacian has all the eigenvalues corresponding to the x_2 variable zero and therefore the nonlinearity F is degenerate with respect to the second order term D^2u. On the other hand, the degeneracy with respect to the nonlocal term comes from the fact that

$$\mu(dz_2) = \frac{dz_2}{|z_2|^{d_2+\beta}}$$

could be viewed as the restriction of the fractional Laplacian to the subspace $\{z_1 = 0\}$

$$\nu(dz) = 1_{\{z_1=0\}}(dz_1)\mu(dz_2).$$

Therefore, for a cone in the direction a orthogonal to x_2 we have

$$\int_{\mathscr{C}^d_{\eta,\delta}} |z|^2\nu(dz) = \int_{\mathscr{C}^{d_2}_{\eta,\delta}} |z_2|^2\mu(dz_2) = 0$$

where $\mathscr{C}^{d_2}_{\eta,\delta} = \{z_2 \in B^{d_2}_\delta; (1-\eta)|z_2||a| \le |a_2 \cdot z_2|\}$. Thus, $(M2)$ and $(J2)$ fail.

Remark 4.4.1. *If we try to argue directly in $\mathbb{R}^d$ and apply the regularity result as if we had only one nonlinearity defined on the whole space, then the best result we can get is Hölder regularity of the solution, except for the diagonal direction, i.e. for all $\varepsilon \in (0,1]$ the following holds for all $\alpha \in (0,\varepsilon)$*

$$u(x) - u(y) \le C|x-y|^\alpha, \forall x, y, \in \mathbb{R}^d \text{ s.t. } \max_{i=1,2} \frac{|x_i - y_i|}{|x-y|} \ge \sqrt{\frac{1}{2-\varepsilon}}.$$

In addition, the further we go from the diagonal, the better the regularity of the solution is.

Let us check that when the gradient direction is the diagonal between x_1 and x_2 there is not possible to retrieve Hölder continuity directly. For this purpose, consider X, Y matrices satisfy-

ing inequality (4.3), with $Z = D\phi(a)$, where $\phi(z) = L|z|^\alpha$. Let $a = (a_1, a_2) = \bar{x} - \bar{y}$ be the gradient direction. The matrix inequality can be rewritten as follows

$$Xz \cdot z - Yz' \cdot z' \leq D^2\phi(a)(z - z') \cdot (z - z'). \tag{4.24}$$

Estimate of the diffusion terms. Applying (4.24) to $z = -z' = e_1 = \frac{1}{|a_1|}(a_1, 0)$ and to $z = z' = (e, 0)$ for any unit vector e orthogonal to e_1 we obtain

$$\mathrm{tr}\big(X_1 - Y_1\big) \leq 4D^2\phi(a)e_1 \cdot e_1.$$

Therefore taking into account the expression for $D^2\phi(a) = \varphi'(|a|)\frac{1}{|a|}(I - \hat{a} \otimes \hat{a}) + \varphi''(|a|)\hat{a} \otimes \hat{a}$,

$$\mathrm{tr}\big(X_1 - Y_1\big) \leq 4\frac{\varphi'(|a|)}{|a|}(1 - \frac{|a_1|^2}{|a|^2}) + 4\varphi''(|a|)\frac{|a_1|^2}{|a|^2}.$$

Using that $\phi(z) = L|z|^\alpha$ with $\alpha \in (0, \varepsilon)$ and $L > 0$ the previous inequality reads

$$\mathrm{tr}\big(X_1 - Y_1\big) \leq 4L\alpha|a|^{\alpha-2}(1 + (\alpha - 2)\frac{|a_1|^2}{|a|^2}). \tag{4.25}$$

This expression is negative only if

$$\frac{|a_1|^2}{|a|^2} > \frac{1}{2 - \varepsilon}.$$

Hence, when the gradient direction is "closer“ to the x_1-axis, the classical diffusion gains and the regularity is driven by the classical Laplacian.

Estimate of the nonlocal terms. As already made precise, the ellipticity of the equation comes in this case from the nondegeneracy assumption $(M2)$ with respect to the Lévy measures. Accordingly, the estimate that renders the nonlocal difference negative comes from the evaluation on the cone in the gradient direction. In view of $(M2)$ we have by rough approximations, for $e_2 = \frac{1}{|a_2|}(0, a_2)$

$$\begin{aligned}
\mathscr{I}_{x_2}[\bar{x}, u] - \mathscr{I}_{x_2}[\bar{y}, u] &\leq \int_{\mathscr{C}_{\eta,\delta}} \sup_{|s|<1} \big(D^2_{a_2 a_2}\phi(a + s(0, z_2))z_2 \cdot z_2\big)\mu(dz_2) \\
&= \int_{\mathscr{C}_{\eta,\delta}} \sup_{|s|<1} \big((1 - \tilde{\eta}^2)\frac{\varphi'(|a + s(0, z_2)|)}{|a + s(0, z_2)|} + \tilde{\eta}^2\varphi''(|a + s(0, z_2)|)\big)|z_2|^2\mu(dz) \\
&\lesssim c\Big((1 - \tilde{\eta}^2)\frac{\varphi'(|a|)}{|a|}(1 - \frac{|a_2|^2}{|a|^2}) + \tilde{\eta}^2\varphi''(|a|)\frac{|a_2|^2}{|a|^2}\Big) \\
&= cL\alpha|a|^{\alpha-2}\left(1 + \tilde{\eta}^2(\alpha - 2)\frac{|a_2|^2}{|a|^2}\right).
\end{aligned}$$

This expression is negative only if

$$\frac{|a_1|^2}{|a|^2} > \frac{1}{\tilde{\eta}^2(2 - \varepsilon)}.$$

Similarly, when the gradient direction is "closer“ to the x_2-axis, the fractional diffusion gains and the regularity is driven by the (directional) fractional Laplacian.

4.4.3 Mixed Integro-Differential Equations with First-Order Terms

Partial and global, Hölder and Lipschitz regularity results apply for a general class of mixed integro-differential equations. As pointed out in the previous theorems, the three nonlinearities must satisfy suitable strict ellipticity and growth conditions. The typical examples one can solve under those assumptions can be summed up by the following equation

$$-a_1(x_1)\Delta_{x_1}u - a_2(x_2)\mathscr{I}_{x_2}[x,u] - \mathscr{I}[x,u] + b_1(x_1)|D_{x_1}u_1|^{k_1} + b_2(x_2)|D_{x_2}u|^{k_2} + |Du|^n + cu = f(x)$$

where for $i = 1,2$ $a_i(x_i) \geq 0$ and $a_i \in C^{0,\gamma}(\mathbb{R}^{d_i})$, $b_i \in C^{0,\tau}(\mathbb{R}^{d_i})$ with $0 \leq \tau \leq 1$, $k_i \in (0, 2+\tau)$, $n \geq 0$ and $c > 0$. We have thus considered

$$\begin{aligned} F_0(u(x), Du, D^2u, \mathscr{I}[x,u]) &= -\mathscr{I}[x,u] + |Du|^n + cu \\ F_1(x_1, D_{x_1}u, D^2_{x_1x_1}u, \mathscr{J}_{x_1}[x,u]) &= -a_1(x_1)\Delta_{x_1}u + b_1(x_1)|D_{x_1}u_1|^{k_1} \\ F_2(x_2, D_{x_2}u, D^2_{x_2x_2}u, \mathscr{J}_{x_2}[x,u]) &= -a_2(x_2)\mathscr{I}_{x_2}[x,u] + b_2(x_2)|D_{x_2}u|^{k_2}. \end{aligned}$$

Let us examine each of these terms and see the requirements they have to satisfy, in order to ensure partial or global regularity of solutions. To fix ideas, suppose the nonlocal term $\mathscr{I}_{x_2}[x,u]$ is an integro-differential operator of fractional exponent $\beta \in (0,2)$.

In both situations, the nonlocal term $\mathscr{I}[x,u]$ can either be a general nonlocal operator associated to some Lévy measure μ^0, or a Lévy-Itô operator. We emphasize on the fact that the associated Lévy measure has no x-dependency. This explains as well the lack of any coefficient $a_0(x)$ in front of the nonlocal term $\mathscr{I}[x,u]$. The gradient term $|Du|^n$ is allowed to have any possible growth $n \geq 0$.

As far as we are interested in partial regularity results, the constant c may be any real number, since we just need cu to be bounded. Yet, when combining the partial regularity results to obtain global regularity, F_1 and F_2 are submitted to rather restrictive assumptions, due to the uniqueness requirements. Thus, when b_1 and b_2 depend explicitly on x_1, respectively x_2 the corresponding gradient terms are restrained to sublinear growth. To turn around this difficulty and obtain regularity of solutions in superlinear cases, one can argue by approximation, truncating the gradient terms and using Corollary 4.3.1 for obtaining uniform gradient bounds. To perform this program, c must be positive: $c > 0$.

We first discuss the *partial regularity* of the solution with respect to each of its variables. To this end, we need classical regularity assumptions in one set of variables, and uniqueness type assumptions in the other variables.

- *Partial regularity in x_2-variable* requires ellipticity of the equation in x_2 direction:

$$a_1(x_1) \geq 0 \text{ and } a_2(x_2) > 0,\ \forall x_1 \in \mathbb{R}^{d_1}, x_2 \in \mathbb{R}^{d_2}.$$

  To ensure the uniqueness argument in x_1-variable, we must take $a_1(x) = \sigma_1(x)^2$ with σ_1 a Lipschitz continuous function.

  The nonlocal term $\mathscr{I}_{x_2}[x,u]$ is either a general integro-differential operator or a Lévy-Itô operator. To ensure nondegeneracy, $(M1)-(M3)$, respectively $(J1)-(J4)$ must hold.

When $\beta > 1$, the solution is Lipschitz continuous in the x_2 variable for directional gradient terms $b_2(x_2)|D_{x_2}u|^{k_2}$ having a natural growth $k_2 \leq \beta$ if b_2 is bounded *and* directional gradient terms $b_1(x_1)|D_{x_1}u|^{k_1}$ with linear growth $k_1 = 1$ if b_1 is Lipschitz (or sublinear growth $k_1 < 1$ if $b_1 \in C^{0,k_1}(\mathbb{R}^{d_1})$). If in addition b_2 is τ-Hölder continuous, then the solution remains Lipschitz for gradient terms up to growth $k_2 \leq \tau + \beta$.

When $\beta \leq 1$, the solution is α-Hölder continuous for any $\alpha < \frac{\beta - k_2}{1-k_2}$.

- *Partial regularity in x_1-variable* requires nondegeneracy of the equation in x_1 direction

$$a_1(x_1) > 0, \ \forall x_1 \in \mathbb{R}^{d_1}.$$

In this case, in the x_2 variable, we can only deal with nonlocal operators of Lévy-Itô type $\mathscr{I}_{x_2}[x,u] = \mathscr{J}_{x_2}[x,u]$, for which the jump function is Lipschitz continuous and satisfies the structural conditions $(J1)$, $(J3)$ and $(J5)$. The uniqueness constraint with respect to x_2 does not allow any x_2-dependence of the Lévy-measure associated to the nonlocal term, and hence $a_2(x_2)$ should be a constant function. Then the solution is Lipschitz in the x_1 variable, for directional gradient terms $b_1(x_1)|D_{x_1}u|^{k_1}$ having a natural growth $k_1 \leq 2 + \tau$ with $b_1 \in C^{0,\tau}(\mathbb{R}^{d_1})$, $0 \leq \tau \leq 1$.

Once again, the uniqueness hypothesis forces directional gradient terms $b_2(x_2)|D_{x_2}u|^{k_2}$ to have growth $k_2 = 1$ and b_2 is Lipschitz continuous.

Global regularity holds under slightly weaker assumptions than the partial regularity. It follows by interchanging the roles of x_1 and x_2.

Accordingly, the equation must be strongly elliptic both in the local and nonlocal term

$$a_1(x_1) > 0 \ \text{ and } \ a_2(x_2) > 0 \ \forall x_1 \in \mathbb{R}^{d_1}, x_2 \in \mathbb{R}^{d_2}.$$

The nonlocal term $\mathscr{I}_{x_2}[x,u]$ is necessarily a Lévy-Itô operator, satisfying the nondegeneracy assumption $(J2)$, as well as the rest of structural conditions $(J1) - (J5)$.

$a_1(x_1) = \sigma_1(x_1)^2 > 0$, with σ_1 Lipschitz continuous and $a_2(x) \equiv a_2 > 0$ constant function.

Joining the partial Lipschitz regularity results, we get Lipschitz continuity of the solution whenever b_1 and b_2 are Lipschitz continuous for linear, directional gradient terms $b_1(x_1)|D_{x_1}u|$ and $b_2(x_2)|D_{x_2}u|$. The linear growth is constraint by the uniqueness argument.

However, looking at the approximated equations with $|Du|$ replaced by $|Du| \wedge R$, for $R > 0$ and noting that the solutions are Lipschitz continuous, with the Lipschitz norm independent of R when $c > 0$, we obtain Lipschitz continuous viscosity solutions for general equations, dealing with gradient terms of growth $k_1 \leq 2$, $k_2 \leq \tau + \beta$, when $b_2 \in C^{0,\tau}(\mathbb{R}^{d_2})$.

Similarly, we get α-Hölder continuous solutions, for any $\alpha < \frac{\beta - k_2}{1-k_2} \leq 1$.

4.5 Some Extensions of the Regularity Results

4.5.1 Non-periodic Setting

Theorem 4.5.1. *Let f be continuous and periodic, the nonlinearities F_i, $i = 0,1,2$ be degenerate elliptic, continuous and periodic, such that F_0 satisfies $(H0)$ and $(H2)$ and that both F_i, for $i = 1,2$ satisfy assumptions $(H2)$ and $(H1')$, with $\tilde{d} = d_i$, for some functions Λ_i^1, Λ_i^2 and some constants $k_i \geq 0$, $\tau_i, \theta_i, \tilde{\theta}_i \in (0,1]$, where*

$(H1')$ *There exist two functions $\Lambda^1, \Lambda^2 : \mathbb{R}^{\tilde{d}} \to [0,\infty)$ such that $\Lambda^1(x) + \Lambda^1(x) \geq \Lambda^0 > 0$ and for each $0 < R < \infty$ there exist some constants $k \geq 0$, $\tau, \theta, \tilde{\theta} \in (0,1]$ such that for any $x, y \in \mathbb{R}^{\tilde{d}}$, $p, q \in \mathbb{R}^{\tilde{d}}$, $|q| < R$, $l \leq l'$ and any $\varepsilon > 0$*

$$
\begin{aligned}
F(y,p,Y,l') - F(x,p+q,X,l) \leq \\
&\Lambda^1(x)\big((l-l') + \frac{|x-y|^{2\theta}}{\varepsilon} + |x-y|^{\tau}|p|^{k+\tau} + C^1|p|^k\big) + \\
&\Lambda^2(x)\big(tr(X-Y) + \frac{|x-y|^{2\tilde{\theta}}}{\varepsilon} + |x-y|^{\tau}|p|^{2+\tau} + C^2|p|^2\big) + O(K,R)
\end{aligned}
$$

if $X, Y \in \mathbb{S}^{\tilde{d}}$ satisfy, inequality

$$
-\frac{1}{\varepsilon}\begin{bmatrix} I & 0 \\ 0 & I \end{bmatrix} \leq \begin{bmatrix} X & 0 \\ 0 & -Y \end{bmatrix} \leq \frac{1}{\varepsilon}\begin{bmatrix} Z & -Z \\ -Z & Z \end{bmatrix} + K\begin{bmatrix} I & 0 \\ -0 & 0 \end{bmatrix},
$$

for some $Z = I - \bar{\omega}\hat{a} \otimes \hat{a}$, with $\hat{a} \in \mathbb{R}^d$ a unit vector;

Let μ^0, μ^i, with $i = 1,2$ and $j^i(x_i, z_i)$ satisfy assumptions $(J1) - (J5)$ for some constants β_i, C_{μ^i}, $\tilde{C}_{\mu^i}$, with $\gamma = 1$ in $(J3)$. Then any bounded continuous viscosity solution u of (4.20) is

(a) locally Lipschitz continuous, if $\beta_i > 1$ and $k_i \leq \beta_i$ for $i = 1,2$, and

(b) locally $C^{0,\alpha}$ continuous with $\alpha < \min(\frac{\beta_1 - k_1}{1-k_1}, \frac{\beta_2 - k_2}{1-k_2})$, if $\beta \leq 1$ and $k_i < \beta_i$ for $i = 1,2$.

The Lipschitz/Hölder constant depends on $||u||_\infty$, on the dimension of the space d and only on the constants associated to the Lévy measures and on the constants required by the growth condition $(H1)$.

Proof. The fact that the solution is not periodic anymore, requires a localization term when measuring the shift of the solution. Thus, in order to prove the local continuity of the solution, either if it refers to Hölder or Lipschitz, we need to show that for each x^0 in the domain, there exists a constant K, depending on x^0, such that for a proper choice of α (both in the Hölder in the Lipschitz case) there exists a constant L, depending on x^0, large enough such that the auxiliary function

$$
\psi(x_1, y_1, x_2) = u(x_1, x_2) - u(y_1, x_2) - L\varphi(|x_1 - y_1|) - \frac{K}{2}|(x_1, x_2) - (x_1^0, x_2^0)|^2
$$

attains a nonpositive maximum. The proof is technically the same, except that here there will be an additional contribution in the estimate of the nonlocal terms, coming from the localization term. The point is to show that this contribution is of order $O(K)$.

□

4.5.2 Parabolic Integro-Differential Equations

The techniques developed herein apply literally to parabolic integro-differential equations.

Corollary 4.5.1. *Let f, the nonlinearities F_i and the jump functions $j^i(x_i, z_i)$ satisfy the assumptions of Corollary 4.3.1. Then any x-periodic continuous viscosity solution u of*

$$u_t + F_0(u(x), Du, D^2u, \mathscr{I}[x,u]) + F_1(x_1, D_{x_1}u, D^2_{x_1x_1}u, \mathscr{I}_{x_1}[x,u]) + F_2(x_2, D_{x_2}u, D^2_{x_2x_2}u, \mathscr{I}_{x_2}[x,u]) = f(x). \tag{4.26}$$

(a) is Lipschitz continuous on $[0,T]$, if $\beta_i > 1$ and $k_i \le \beta_i$ for $i = 1,2$;

(b) is $C^{0,\alpha}$ continuous on $[0,T]$, with $\alpha < \min(\frac{\beta_1 - k_1}{1-k_1}, \frac{\beta_2 - k_2}{1-k_2})$, if $\beta \le 1$ and $k_i < \beta_i$ for $i = 1,2$.

The Lipschitz/Hölder constant depends on $||u||_\infty$, on the dimension of the space d and only on the constants associated to the Lévy measures and on the constants required by the growth condition $(H1)$.

Proof. The key difference with the previous proof consists in considering the space-time auxiliary function

$$\psi(t, x_1, y_1, x_2) = u(t, x_1, x_2) - u(t, y_1, x_2) - \phi(x_1 - y_1)$$

and show that $\max_{t,x_1,x_2,y_2} \psi(t, x_1, y_1, x_2) < 0$. By small space-time perturbations

$$\psi_{\varepsilon,\varsigma}(x, y, s, t) = u(t, x_1, x_2) - u(s, y_1, y_2) - \phi(x_1 - y_1) - \frac{|x_2 - y_2|^2}{\varepsilon^2} - \frac{(t-s)^2}{\varsigma^2},$$

this leads to considering in the nonlocal Jensen-Ishii's lemma the parabolic sub and superjets

$$(r^{\varepsilon,\varsigma}, p^{\varepsilon,\varsigma}, X^{\varepsilon,\varsigma}) \in \mathscr{J}^{2,+}_p(u(x^{\varepsilon,\varsigma}))$$
$$(r^{\varepsilon,\varsigma}, p^{\varepsilon,\varsigma}, Y^{\varepsilon,\varsigma}) \in \mathscr{J}^{2,-}_p(u(y^{\varepsilon,\varsigma}))$$

with $r^{\varepsilon,\varsigma} = 2\frac{t-s}{\varsigma^2}$. Writing down the viscosity inequalities, note that the $r^{\varepsilon,\varsigma}$ is the commune term corresponding to the first order time-derivative, and hence it vanishes by subtraction. Therefore, when passing to the limits in inequality (4.13), we can first let ς go to zero. The rest of the proof is literally the same. □

4.5.3 Bellman-Isaacs Equations

These results can be extended to fully nonlinear equations, that arise naturally in stochastic control problems for jump-diffusion processes. The following Bellman-Isaacs type equation

arises

$$\sup_{\gamma\in\Gamma}\inf_{\delta\in\Delta}\left(F_0^{\gamma,\delta}(...,\mathscr{J}^{\gamma,\delta}[x,u])+F_1^{\gamma,\delta}(...,\mathscr{J}_{x_1}^{\gamma,\delta}[x,u])+F_2^{\gamma,\delta}(...,\mathscr{J}_{x_2}^{\gamma,\delta}[x,u])-f^{\gamma,\delta}(x)\right)=0$$

where $\mathscr{J}^{\gamma,\delta}[x,u]$ is a family of Lévy-Itô operators associated with a common Lévy measure μ^0 and a family of jump functions $j_0^{\gamma,\delta}(x,z)$, respectively $\mathscr{J}_{x_i}^{\gamma,\delta}[x,u]$ are families of Lévy-Itô operators associated with the Lévy measures μ^i and the families of jump functions $j_i^{\gamma,\delta}(x_i,z)$, for $i=1,2$.

A typical (and practical) example is

$$\begin{aligned}F_0^{\gamma,\delta} &= cu-\frac{1}{2}\mathrm{tr}(A^{\gamma,\delta}(x)D^2u)-\mathscr{J}^{\gamma,\delta}[x,u]-b^{\gamma,\delta}(x)\cdot Du\\ F_i^{\gamma,\delta} &= -\frac{1}{2}\mathrm{tr}(a_i^{\gamma,\delta}(x_i)D^2_{x_ix_i}u)-\mathscr{J}_{x_i}^{\gamma,\delta}[x,u]-b_i^{\gamma,\delta}(x)\cdot D_{x_i}u.\end{aligned}$$

Similar techniques to the previous yield the Hölder and Lipschitz continuity of solutions of Bellman-Isaacs equations, provided that the structure condition $(H1)$ is uniformly satisfied by $F_i^{\gamma,\delta}$, for $i=1,2$, as well as the assumptions $(J1)-(J5)$ by the family of jump functions $j_i^{\gamma,\delta}(x_i,z)$. In occurrence, the constants and functions appearing therein must be independent of γ and δ. For the above example, it is sufficient that $A^{\gamma,\delta}(x), a_i^{\gamma,\delta}(x), b_i^{\gamma,\delta}(x), f^{\gamma,\delta}(x)$ are bounded in $W^{1,\infty}$, uniformly in γ and δ.

The proof is based on the classical inequality

$$\sup_{\gamma}\inf_{\delta}(\cdots)-\sup_{\gamma}\inf_{\delta}(\cdots)\leq\sup_{\gamma,\delta}(\cdots-\cdots).$$

4.5.4 Multiple Nonlinearities

The problem can be easily generalized to multiple nonlinearities

$$F_0(u(x),Du,D^2u,\mathscr{I}[x,u])+\sum_{i\in I}F_i(x_i,D_{x_i}u,D^2_{x_ix_i}u,\mathscr{J}_{x_i}[x,u])=f(x). \tag{4.27}$$

The proof can be resumed to the previous one, by grouping all the variables for which we employ uniqueness type arguments.

4.6 Estimates for Integro - Differential Operators

All these results are based on a series of estimates for the nonlocal terms, that me make precise in the following. The reader not interested in technical details may skip this section.

4.6.1 General Nonlocal Operators

Proposition 4.6.1 (**Concave estimates - general nonlocal operators).** *Assume condition* $(M1)$ *holds. Let* u,v *be two bounded functions and* $\varphi:[0,\infty)\to\mathbb{R}$ *be a smooth increasing concave*

function. Define

$$\psi(x,y) = u(x) - v(y) - \varphi(|x-y|)$$

and assume the maximum of ψ is positive and attained at $(\bar{x},\bar{y})$, with $\bar{x} \neq \bar{y}$. Let $a = \bar{x} - \bar{y}$, $\hat{a} = a/|a|$, $p = \varphi'(|a|)\hat{a}$. Then the following holds

$$\begin{aligned}\mathscr{I}[\bar{x},p,u] - \mathscr{I}[\bar{y},p,v] \leq 2\tilde{C}_\mu \max(||u||_\infty, ||v||_\infty) + \\ \int_{\mathscr{C}_{\eta,\delta}} \sup_{|s|<1} \big((1-\tilde{\eta}^2)\frac{\varphi'(|a+sz|)}{|a+sz|} + \tilde{\eta}^2\varphi''(|a+sz|)\big)|z|^2 \frac{\mu_{\bar{x}}+\mu_{\bar{y}}}{2}(dz) + \\ 2\varphi'(|a|)\int_{B\setminus B_\delta} |z||\mu_{\bar{x}} - \mu_{\bar{y}}|(dz) + \int_{B_\delta\setminus\mathscr{C}_{\eta,\delta}} \sup_{|s|<1} \frac{\varphi'(|a+sz|)}{|a+sz|}|z|^2|\mu_{\bar{x}} - \mu_{\bar{y}}|(dz),\end{aligned}$$

where

$$\mathscr{C}_{\eta,\delta} = \{z \in B_\delta; (1-\eta)|z||a| \leq |a\cdot z|\}$$

and $\delta = |a|\delta_0 > 0$, $\tilde{\eta} = \frac{1-\eta-\delta_0}{1+\delta_0} > 0$ with $\delta_0 \in (0,1)$, $\eta \in (0,1)$ small enough.

Remark 4.6.1. *The aperture of the cone is given by η and changes accordingly to $|a|$. In order to ensure Lipschitz continuity of solutions, η must be chosen to behave like a power of $|a|$, i.e. $\eta \sim |a|^\alpha$, and thus is diminishing as the modulus of the gradient approaches zero:* $\lim_{|a|\to 0}\eta(|a|) = 0$. *Remark that as $|a| \to 0$, $\mathscr{C}_{\eta,\delta}$ degenerates to the line whose direction is given by the gradient.*

Proof. We split the domain of integration into three pieces and take the integrals on each of these domains. Namely we part the ball of radius δ into the subset $\mathscr{C}_{\eta,\delta}$ and its complementary, with $\eta = \eta(|a|)$ and $\delta = \delta(|a|)$. Let

$$\phi(z) = \varphi(|z|).$$

Then $p = D\phi(a)$. We write thus the difference of the nonlocal terms, evaluated at the maximum point $(\bar{x},\bar{y})$, as the sum

$$\mathscr{I}[\bar{x},p,u] - \mathscr{I}[\bar{y},p,v] = \mathscr{T}^1(\bar{x},\bar{y}) + \mathscr{T}^2(\bar{x},\bar{y}) + \mathscr{T}^3(\bar{x},\bar{y})$$

where

$$\begin{aligned}\mathscr{T}^1(\bar{x},\bar{y}) &= \int_{|z|\geq 1}\big(u(\bar{x}+z) - u(\bar{x})\big)\mu_{\bar{x}}(dz) - \int_{|z|\geq 1}\big(v(\bar{y}+z) - v(\bar{y})\big)\mu_{\bar{y}}(dz) \\ \mathscr{T}^2(\bar{x},\bar{y}) &= \int_{\mathscr{C}_{\eta,\delta}}\big(u(\bar{x}+z) - u(\bar{x}) - p\cdot z\big)\mu_{\bar{x}}(dz) \\ &\qquad - \int_{\mathscr{C}_{\eta,\delta}}\big(v(\bar{y}+z) - v(\bar{y}) - p\cdot z\big)\mu_{\bar{y}}(dz) \\ \mathscr{T}^3(\bar{x},\bar{y}) &= \int_{B\setminus\mathscr{C}_{\eta,\delta}}\big(u(\bar{x}+z) - u(\bar{x}) - p\cdot z\big)\mu_{\bar{x}}(dz) \\ &\qquad - \int_{B\setminus\mathscr{C}_{\eta,\delta}}\big(v(\bar{y}+z) - v(\bar{y}) - p\cdot z\big)\mu_{\bar{y}}(dz).\end{aligned}$$

In the following, we give estimates for each of these integral terms, that are based on the con-

sequence of the maximum condition:

$$u(\bar{x}+z)-u(\bar{x})-p\cdot z\leq v(\bar{y}+z')-v(\bar{y})-p\cdot z+\\ \phi(\bar{x}-\bar{y}+z-z')-\phi(\bar{x}-\bar{y})-D\phi(a)\cdot(z-z'). \tag{4.28}$$

Lemma 4.6.1. *$\mathcal{T}^1(\bar{x},\bar{y})$ is uniformly bounded with respect to all the parameters. More precisely*

$$\mathcal{T}^1(\bar{x},\bar{y})\leq 2\max(||u||_\infty,||v||_\infty)\sup_{x\in\mathbb{R}^d}\mu_x(\mathbb{R}^d\setminus B).$$

Proof. Since the functions u and v are bounded, we immediately deduce that

$$\mathcal{T}^1(\bar{x},\bar{y}) \quad\leq\quad 2||u||_\infty\int_{|z|\geq 1}\mu_{\bar{x}}(dz)+2||v||_\infty\int_{|z|\geq 1}\mu_{\bar{y}}(dz).$$

We conclude by recalling that the measures μ_x are uniformly bounded away from the origin, by assumption $(M1)$.

□

Lemma 4.6.2. *Let $\delta=|a|\delta_0$ with $\delta_0\in(0,1)$ small, η be small enough such that $1-\eta-\delta_0>0$ and*

$$\tilde{\eta}=\frac{1-\eta-\delta_0}{1+\delta_0}.$$

Then the nonlocal term $\mathcal{T}^2$ satisfies

$$\mathcal{T}^2(\bar{x},\bar{y}) \quad\leq\quad \frac{1}{2}\int_{\mathscr{C}_{\eta,\delta}}\sup_{|s|<1}\big((1-\tilde{\eta}^2)\frac{\varphi'(|a+sz|)}{|a+sz|}+\tilde{\eta}^2\varphi''(|a+sz|)\big)|z|^2(\mu_{\bar{x}}+\mu_{\bar{y}})(dz).$$

Remark 4.6.2. *The previous notations have been introduced to simplify the form of the estimates. It is important to note however that the coefficients appearing in the convex combination of the derivatives of φ depend explicitly on $\tilde{\eta}$ and not on the aperture of the cone, given in terms of η. We eventually set $\eta\sim|a|^{2\alpha}$ and $\delta_0\sim|a|^\alpha$, thus we expect to have $\tilde{\eta}\simeq 1$. Consequently, the second derivative of φ would dominate the nonlocal difference and would render $\mathcal{T}^2(\bar{x},\bar{y})$ as negative as possible.*

Proof. Taking $z'=0$, respectively $z=0$ in inequality (4.28) we have

$$\begin{aligned} u(\bar{x}+z)-u(\bar{x})-p\cdot z \quad&\leq\quad \phi(a+z)-\phi(a)-D\phi(a)\cdot z\\ -\big(v(\bar{y}+z')-v(\bar{y})-p\cdot z'\big) \quad&\leq\quad \phi(a-z')-\phi(a)+D\phi(a)\cdot z'. \end{aligned}$$

Therefore

$$\begin{aligned} \mathcal{T}^2(\bar{x},\bar{y}) \quad\leq\quad &\int_{\mathscr{C}_{\eta,\delta}}\big(\phi(a+z)-\phi(a)-D\phi(a)\cdot z\big)\mu_{\bar{x}}(dz)\\ &+\int_{\mathscr{C}_{\eta,\delta}}\big(\phi(a-z')-\phi(a)+D\phi(a)\cdot z'\big)\mu_{\bar{y}}(dz). \end{aligned}$$

The integral terms corresponding to ϕ can be rewritten as

$$\int_0^1 (1-s)ds \int_{\mathscr{C}_{\eta,\delta}} \big(D^2\phi(a+sz)z\cdot z\big)\mu_{\bar{x}}(dz) + \int_{-1}^0 (1+s)ds \int_{\mathscr{C}_{\eta,\delta}} \big(D^2\phi(a-sz)z\cdot z\big)\mu_{\bar{y}}(dz).$$

Remark that the first and second derivatives of $\phi(z)=\varphi(|z|)$ are given by the formulas

$$\begin{aligned} D\phi(z) &= \varphi'(|z|)\hat{z} \\ D^2\phi(z) &= \varphi'(|z|)\frac{1}{|z|}(I-\hat{z}\otimes\hat{z}) + \varphi''(|z|)\hat{z}\otimes\hat{z}, \end{aligned}$$

and in particular

$$D^2\phi(a+sz)z\cdot z = \frac{\varphi'(|a+sz|)}{|a+sz|}\big(|z|^2 - |\widehat{(a+sz)}\cdot z|^2\big) + \varphi''(|a+sz|)|\widehat{(a+sz)}\cdot z|^2.$$

On the set $\mathscr{C}_{\eta,\delta}$ we have the following upper and lower bounds

$$\begin{aligned} &|(a+sz)| \geq |a| - |s||z| \geq |a| - \delta = |a|(1-\delta_0) \\ &|(a+sz)| \leq |a| + |s||z| \leq |a| + \delta = |a|(1+\delta_0) \\ &|(a+sz)\cdot z| \geq |a\cdot z| - s|z|^2 \geq |a\cdot z| - \delta|z| \geq (1-\eta-\delta_0)|z||a|. \end{aligned} \tag{4.29}$$

Hence we deduce that for all $s\in(-1,1)$

$$|\widehat{(a+sz)}\cdot z| \geq \tilde{\eta}|z|, \text{ with } \tilde{\eta} = \frac{1-\eta-\delta_0}{1+\delta_0}.$$

Recalling that φ is increasing and concave, we get

$$D^2\phi(a+sz)z\cdot z \leq (1-\tilde{\eta}^2)\varphi'(|a+sz|)\frac{1}{|a+sz|}|z|^2 + \tilde{\eta}^2\varphi''(|a+sz|)|z|^2.$$

This implies that the integral terms corresponding to ϕ are bounded by

$$\frac{1}{2}\int_{\mathscr{C}_{\eta,\delta}} \sup_{|s|<1}\Big((1-\tilde{\eta}^2)\frac{\varphi'(|a+sz|)}{|a+sz|} + \tilde{\eta}^2\varphi''(|a+sz|)\Big)|z|^2(\mu_{\bar{x}}+\mu_{\bar{y}})(dz).$$

□

Lemma 4.6.3. *The following estimate holds*

$$\mathscr{T}^3(\bar{x},\bar{y}) \leq \int_{B_\delta\setminus\mathscr{C}_{\eta,\delta}} \sup_{|s|<1}\frac{\varphi'(|a+sz|)}{|a+sz|}|z|^2|\mu_{\bar{x}}-\mu_{\bar{y}}|(dz) + 2\varphi'(|a|)\int_{B\setminus B_\delta}|z||\mu_{\bar{x}}-\mu_{\bar{y}}|(dz).$$

Proof. When estimating the nonlocal term outside the cone, one has to keep it as small as possible, though it remains positive. Therefore we consider, as for proving Hölder continuity of solutions, the signed measure $\mu=\mu_{\bar{x}}-\mu_{\bar{y}}$. Consider its Jordan decomposition $\mu=\mu^+-\mu^-$

and denote by $|\mu|$ the corresponding total variation measure. Then, if K is the support of the positive variation μ^+, one can define the minimum of the two measures as

$$\mu_* = \mathbf{1}_K \mu_{\bar{y}} + (1 - \mathbf{1}_K)\mu_{\bar{x}}.$$

But then, the measures $\mu_{\bar{x}}$ and $\mu_{\bar{y}}$ can be rewritten as the

$$\mu_{\bar{x}} = \mu_* + \mu^+ \text{ and } \mu_{\bar{y}} = \mu_* + \mu^-.$$

With these notations in mind, we rewrite the nonlocal term $\mathscr{T}^3$ as

$$\begin{aligned}\mathscr{T}^3(\bar{x},\bar{y}) &= \int_{B\setminus\mathscr{C}_{\eta,\delta}} (u(\bar{x}+z)-u(\bar{x})-p\cdot z-(v(\bar{y}+z)-v(\bar{y})-p\cdot z))\mu_*(dz)+\\ &\quad \int_{B\setminus\mathscr{C}_{\eta,\delta}} (u(\bar{x}+z)-u(\bar{x})-p\cdot z)\mu^+(dz)-\\ &\quad \int_{B\setminus\mathscr{C}_{\eta,\delta}} (v(\bar{y}+z)-v(\bar{y})-p\cdot z)\mu^-(dz).\end{aligned}$$

Choosing successively $z' = z$, $z' = 0$ and $z = 0$ in (4.28) and noting that

$$u(\bar{x}+z)-u(\bar{x})-p\cdot z \le v(\bar{y}+z')-v(\bar{y})-p\cdot z$$

we deduce that

$$\begin{aligned}\mathscr{T}^3(\bar{x},\bar{y}) &\le \int_{B\setminus\mathscr{C}_{\eta,\delta}} \big(\phi(a+z)-\phi(a)-D\phi(a)\cdot z\big)\mu^+(dz)\\ &\qquad + \int_{B\setminus\mathscr{C}_{\eta,\delta}} \big(\phi(a-z)-\phi(a)+D\phi(a)\cdot z\big)\mu^-(dz).\end{aligned}$$

For estimating the integral terms corresponding to ϕ, we split the domain of integration into $B\setminus B_\delta$ and $B_\delta\setminus\mathscr{C}_{\eta,\delta}$. On the first set, from the concavity and monotonicity of φ we have

$$\phi(a+z)-\phi(a)-D\phi(a)\cdot z \le \varphi(|a|+|z|)-\varphi(|a|)-\varphi'(|a|)\hat{a}\cdot z \le 2\varphi'(|a|)|z|$$

whereas on $B_\delta\setminus\mathscr{C}_{\eta,\delta}$ we use a second order Taylor expansion and we take into account that φ is smooth, $\varphi'\ge 0$ and $\varphi''\le 0$ to obtain the upper bound

$$\sup_{|s|<1}\big(\phi(|a+sz|)-\phi(|a|)-D\phi(a)\cdot z\big) \le \sup_{|s|<1} D^2\phi(a+sz)z\cdot z \le \sup_{|s|<1}\frac{\varphi'(|a+sz|)}{|a+sz|}|z|^2.$$

Therefore we get the estimate

$$\mathscr{T}^3(\bar{x},\bar{y}) \le 2\varphi'(|a|)\int_{B\setminus B_\delta}|z||\mu_{\bar{x}}-\mu_{\bar{y}}|(dz)+\int_{B_\delta\setminus\mathscr{C}_{\eta,\delta}}\sup_{|s|<1}\frac{\varphi'(|a+sz|)}{|a+sz|}|z|^2|\mu_{\bar{x}}-\mu_{\bar{y}}|(dz).$$

□

Form the three above lemmas, we obtain the final estimate for the nonlocal term. □

Corollary 4.6.1 (Lipschitz estimates)**.** *Let* $(M1)-(M3)$ *hold, with* $\beta>1$. *Under the assumptions of Proposition 4.6.1 with*

$$\varphi(t)=\begin{cases} L\big(t-\varrho t^{1+\alpha}\big), & t\in[0,\theta] \\ \varphi(\theta), & t>\theta \end{cases}$$

where $\alpha\in\Big(0,\min(\frac{\gamma}{d+1},\frac{\beta-1}{d+2-\beta})\Big)$, ϱ *is a positive large constant such that* $\varrho\alpha 2^{\alpha-1}>1$,

$$\theta=\max_t(t-\varrho t^{1+\alpha})=\sqrt[\alpha]{\frac{1}{\rho(1+\alpha)}}\ \text{and}\ L>\frac{||u||_\infty+||v||_\infty}{\varphi(\theta)}$$

the following holds: there exists a positive constant $C=C(\mu)$ *such that for* $\Theta(\varrho,\alpha,\mu)=C\big(\rho\alpha 2^{\alpha-1}-1\big)$ *we have*

$$\mathscr{I}[\bar{x},p,u]-\mathscr{I}[\bar{y},p,v]\le -L|a|^{(1-\beta)+\alpha(d+2-\beta)}\big\{\Theta(\varrho,\alpha,\mu)-o_{|a|}(1)\big\}+O(\tilde{C}_\mu).$$

Proof. Remark that $|a|<\theta$. Indeed, since the maximum of ψ is positive we have, due to the lower bound on L that

$$\varphi(|a|)<\frac{||u||_\infty+||v||_\infty}{L}\le\varphi(\theta)$$

which by the strict monotonicity of φ implies the desired inequality. We first evaluate the estimate that renders the integral difference negative, namely:

$$\begin{aligned}
&\sup_{|s|<1}\big((1-\tilde{\eta}^2)\varphi'(|a+sz|)\frac{1}{|a+sz|}+\tilde{\eta}^2\varphi''(|a+sz|)\big)\\
&\qquad=L\sup_{|s|<1}\big((1-\tilde{\eta}^2)\frac{1-\varrho(1+\alpha)|a+sz|^\alpha}{|a+sz|}-\tilde{\eta}^2\varrho\alpha(1+\alpha)|a+sz|^{\alpha-1}\big)\\
&\qquad\le\sup_{|s|<1}\big(\frac{1-\tilde{\eta}^2}{|a+sz|}-\varrho(1+\alpha)(1-\tilde{\eta}^2+\alpha\tilde{\eta}^2)|a+sz|^{\alpha-1}\big)\\
&\qquad\le L\sup_{|s|<1}\big(\frac{1-\tilde{\eta}^2}{|a+sz|}-\varrho\alpha|a+sz|^{\alpha-1}\big).
\end{aligned}$$

But this quantity has to be integrated over the cone $\mathscr{C}_{\eta,\delta}$, in which case $|a+sz|$ satisfies

$$|a|(1-\delta_0)\le|a+sz|\le|a|(1+\delta_0).$$

Thus, observing that $1-\tilde{\eta}^2\le 2(1-\tilde{\eta})$, the previous inequality takes the form

$$\begin{aligned}
&\sup_{|s|<1}\big((1-\tilde{\eta}^2)\varphi'(|a+sz|)\frac{1}{|a+sz|}+\tilde{\eta}^2\varphi''(|a+sz|)\big)\\
&\qquad\le L\big(\frac{2(1-\tilde{\eta})}{|a|(1-\delta_0)}-\varrho\alpha(1+\delta_0)^{\alpha-1}|a|^{\alpha-1}\big).
\end{aligned}$$

Let $\tilde{\eta}$ be of the form

$$1-\tilde{\eta}=|a|^\alpha\tilde{\eta}_0$$

with small $\tilde{\eta}_0 < \frac{1}{4}$. Choose accordingly δ_0 and η of the form

$$\delta_0 = c_1|a|^{\alpha_1} \qquad \eta = c_2|a|^{\alpha_2}.$$

Recalling that $\tilde{\eta} = \frac{1-\delta_0-\eta}{1+\delta_0}$ and plugging in the previous, we get that c_1, c_2, α_1 and α_2 must satisfy

$$2c_1|a|^{\alpha_1} - |a|^{\alpha}\tilde{\eta}_0 = c_1\tilde{\eta}_0|a|^{\alpha+\alpha_1} - c_2|a|_2^{\alpha}.$$

Identifying the coefficients we obtain

$$\delta_0 = \frac{1}{2}|a|^{\alpha}\tilde{\eta}_0, \text{ and } \eta = \frac{1}{2}|a|^{2\alpha}\tilde{\eta}_0^2.$$

Subsequently, this choice of parameters gives us

$$\sup_{|s|<1}\big((1-\tilde{\eta}^2)\varphi'(|a+sz|)\frac{1}{|a+sz|} + \tilde{\eta}^2\varphi''(|a+sz|)\big) \le -L\big(\varrho\alpha 2^{\alpha-1} - 4\tilde{\eta}_0\big)|a|^{\alpha-1}$$

which leads to a negative upper bound of the integral term taken over the cone $\mathscr{C}_{\eta,\delta}$

$$\begin{aligned}\int_{\mathscr{C}_{\eta,\delta}} \sup_{|s|<1}\big((1-\tilde{\eta}^2)\varphi'(|a+sz|)\frac{1}{|a+sz|} + \tilde{\eta}^2\varphi''(|a+sz|)\big)|z|^2\mu_{\tilde{x}}(dz)& \\ \le -L\big(\varrho\alpha 2^{\alpha-1} - 1\big)|a|^{\alpha-1}\int_{\mathscr{C}_{\eta,\delta}}|z|^2\mu_{\tilde{x}}(dz).&\end{aligned}$$

Let $\Theta_\varrho = \varrho\alpha 2^{\alpha-1} - 1 > 0$ and employ $(M2)$ and the fact that $\delta = |a|\delta_0$ to finally get

$$\begin{aligned}\int_{\mathscr{C}_{\eta,\delta}} \sup_{|s|<1}\big((1-\tilde{\eta}^2)\varphi'(|a+sz|)\frac{1}{|a+sz|} + \tilde{\eta}^2\varphi''(|a+sz|)\big)|z|^2\mu_{\tilde{x}}(dz)& \\ \le -L\Theta_\varrho|a|^{\alpha-1}C_\mu\eta^{\frac{d-1}{2}}\delta^{2-\beta}& \\ = -L\Theta_\varrho C_\mu^1|a|^{\alpha-1}|a|^{\alpha(d-1)}|a|^{(1+\alpha)(2-\beta)}.&\end{aligned}$$

Less technical estimates give similar upper bounds for the other two integrals. More precisely, we have in view of assumption $(M3)$

$$\begin{aligned}\varphi'(|a|)\int_{B\setminus B_\delta}|z||\mu_{\tilde{x}} - \mu_{\tilde{y}}|(dz) &\le LC_\mu|a|^\gamma\delta^{1-\beta} \\ &= LC_\mu^2|a|^\gamma|a|^{(1+\alpha)(1-\beta)}\end{aligned}$$

and

$$\begin{aligned}\int_{B_\delta\setminus\mathscr{C}_{\eta,\delta}}\sup_{|s|<1}\frac{\varphi'(|a+sz|)}{|a+sz|}|z|^2|\mu_{\tilde{x}} - \mu_{\tilde{y}}|(dz) &\le L\frac{C_\mu|a|^\gamma\delta^{2-\beta}}{|a|(1-\delta_0)} \\ &\le LC_\mu^3|a|^{\gamma-1}|a|^{(1+\alpha)(2-\beta)}.\end{aligned}$$

For $\beta > 1$ and $\alpha > 0$ such that $\gamma > \alpha(d+1)$ the difference of the nonlocal term becomes negative

$$\begin{aligned}\mathscr{I}[\bar{x},p,u]-\mathscr{I}[\bar{y},p,v] \leq \\ &\leq -L|a|^{1-\beta}\left\{C_\mu^1\Theta_\varrho|a|^{\alpha(d+2-\beta)}-C_\mu^2|a|^{\gamma+\alpha(1-\beta)}-C_\mu^3|a|^{\gamma+\alpha(2-\beta)}\right\}+O(\tilde{C}_\mu)\\ &= -L|a|^{(1-\beta)+\alpha(d+2-\beta)}\left\{C_\mu^1\Theta_\varrho-o_{|a|}(1)\right\}+O(\tilde{C}_\mu).\end{aligned}$$

□

Corollary 4.6.2 (Hölder estimates)**.** *Let* $(M1)-(M3)$ *hold, with* $\beta\in(0,2)$*. Under the assumptions of Proposition 4.6.1 with*

$$\varphi(t)=Lt^\alpha,$$

where $\alpha\in(0,\min(\beta,1))$ *and* L *is a large positive constant, the following holds: there exists a positive constant* $C(\alpha,\mu)=\alpha C(\mu)$ *such that*

$$\mathscr{I}[\bar{x},p,u]-\mathscr{I}[\bar{y},p,v]\leq -L|a|^{\alpha-\beta}\left\{C(\alpha,\mu)-o_{|a|}(1)\right\}+O(\tilde{C}_\mu).$$

Proof. Estimating the integrand of the nonlocal difference $\mathscr{T}^2$ we get

$$\begin{aligned}\sup_{|s|<1}&\left((1-\tilde{\eta}^2)\varphi'(|a+sz|)\frac{1}{|a+sz|}+\tilde{\eta}^2\varphi''(|a+sz|)\right)\\ &= L\alpha\left(1-(2-\alpha)\tilde{\eta}^2\right)\sup_{|s|<1}\left(|a+sz|^{\alpha-2}\right)\\ &\leq -L\alpha\left((2-\alpha)\tilde{\eta}^2-1\right)(1+\delta_0)^{\alpha-2}|a|^{\alpha-2}.\end{aligned}$$

Choosing η and δ_0 sufficiently small such that

$$(2-\alpha)\tilde{\eta}^2=(2-\alpha)\left(\frac{1-\eta-\delta_0}{1+\delta_0}\right)^2>1+\frac{1-\alpha}{2}$$

we obtain a negative bound of the integral term over the cone $\mathscr{C}_{\eta,\delta}$, for $\delta=|a|\delta_0$

$$\begin{aligned}\int_{\mathscr{C}_{\eta,\delta}}&\sup_{|s|<1}\left((1-\tilde{\eta}^2)\varphi'(|a+sz|)\frac{1}{|a+sz|}+\tilde{\eta}^2\varphi''(|a+sz|)\right)|z|^2\mu_{\bar{x}}(dz)\\ &\leq -L\alpha\frac{1-\alpha}{2}(1+\delta_0)^{\alpha-2}|a|^{\alpha-2}\int_{\mathscr{C}_{\eta,\delta}}|z|^2\mu_{\bar{x}}(dz)\\ &\leq -LC(\alpha,\mu)|a|^{\alpha-\beta},\end{aligned}$$

with $C(\alpha,\mu)=\alpha C_\mu^1=\alpha\left(C_\mu 2^{-3}\eta^{\frac{d-1}{2}}\delta_0^{2-\beta}\right)$. In addition, we have the estimates of the other two integral terms, when $\beta\neq 1$

$$\varphi'(|a|)\int_{B\setminus B_\delta}|z||\mu_{\bar{x}}-\mu_{\bar{y}}|(dz)\leq L\alpha|a|^{\alpha-1}C_\mu|a|^\gamma\delta^{1-\beta}=L\alpha C_\mu^2|a|^\gamma|a|^{\alpha-\beta}$$

with $C_\mu^2 = C_\mu \delta_0^{1-\beta}$, and for $\beta = 1$

$$\varphi'(|a|)\int_{B\setminus B_\delta} |z||\mu_{\bar{x}} - \mu_{\bar{y}}|(dz) \le L\alpha C_\mu^2 |a|^\gamma |\ln(|a|\delta_0)||a|^{\alpha-\beta}.$$

Similarly

$$\int_{B_\delta\setminus\mathscr{C}_{\eta,\delta}} \sup_{|s|<1} \frac{\varphi'(|a+sz|)}{|a+sz|}|z|^2|\mu_{\bar{x}} - \mu_{\bar{y}}|(dz)$$
$$\le L\alpha(|a|(1-\delta_0))^{\alpha-2}\int_{B_\delta\setminus\mathscr{C}_{\eta,\delta}} |z|^2|\mu_{\bar{x}} - \mu_{\bar{y}}|(dz) \le L\alpha C_\mu^3 |a|^\gamma |a|^{\alpha-\beta}$$

with $C_\mu^3 = C_\mu \delta_0^{2-\beta}$. Therefore the difference of the nonlocal term becomes negative, as bounded from above by

$$\mathscr{I}[\bar{x},p,u] - \mathscr{I}[\bar{y},p,v] \le -L|a|^{\alpha-\beta}\big(C(\alpha,\mu) - o_{|a|}(1)\big).$$

□

4.6.2 Lévy-Itô Operators

Proposition 4.6.2 (Concave estimates - Lévy-Itô operators). *Assume conditions* $(J1)$ *and* $(J3)$ *hold. Let* u, v *be two bounded functions,* $\varphi : [0,\infty) \to \mathbb{R}$ *be a smooth increasing concave function and define*

$$\psi(x,y) = u(x) - v(y) - \varphi(|x-y|).$$

Assume that ψ *attains a positive maximum at* $(\bar{x},\bar{y})$*, with* $\bar{x} \neq \bar{y}$*. Let* $a = \bar{x} - \bar{y}$*,* $\hat{a} = a/|a|$ *and* $p = \varphi'(|a|)\hat{a}$*. Then the following holds*

$$\mathscr{J}[\bar{x},p,u] - \mathscr{J}[\bar{y},p,v] \le 2\tilde{C}_\mu \max(||u||_\infty, ||v||_\infty) +$$
$$\int_{\substack{\mathscr{C}\\ x=\bar{x},\bar{y}}} \sup_{|s|<1} \left(\big((1-\tilde{\eta}^2)\frac{\varphi'(|a+sj(x,z)|)}{|a+sj(x,z)|} + \tilde{\eta}^2\varphi''(|a+sj(x,z)|)\big)|j(x,z)|^2\right)\mu(dz)$$
$$2\varphi'(|a|)\int_{\substack{B\setminus\mathscr{C}\\ |\Delta(z)|\ge\delta}} |\Delta(z)|\mu(dz) + \int_{\substack{B\setminus\mathscr{C}\\ |\Delta(z)|\le\delta}} \sup_{|s|<1} \frac{\varphi'(|a+s(\Delta(z))|)}{|a+s(\Delta(z))|}|\Delta(z)|^2\mu(dz)$$

where $\Delta(z) = j(\bar{x},z) - j(\bar{y},z)$*,*

$$\mathscr{C} = \{z; |j(\frac{\bar{x}+\bar{y}}{2},z)| \le \frac{\delta}{2} \quad \textit{and} \quad |j(\frac{\bar{x}+\bar{y}}{2},z)\cdot\hat{a}| \ge (1-\frac{\eta}{2})|j(\frac{\bar{x}+\bar{y}}{2},z)|)\}$$

$$\big(\frac{|a|}{2}\big)^\gamma \le \frac{c_0}{C_0}\frac{\eta}{4-\eta}, \qquad \delta = |a|\delta_0 > 0, \qquad \tilde{\eta} = \frac{1-\eta-\delta_0}{1+\delta_0} > 0$$

with $\delta_0 \in (0,1)$ *and* $\eta \in (0,1)$ *both sufficiently small.*

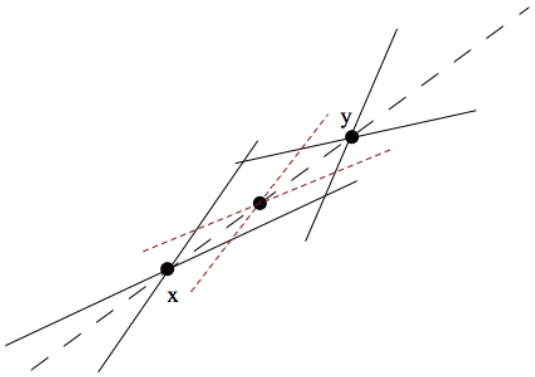

Figure 4.3: The middle cone $\mathscr{C}_{\delta/2,\eta/2}\big(\frac{\bar{x}+\bar{y}}{2}\big) \subset \mathscr{C}_{\delta,\eta}(\bar{x}) \cap \mathscr{C}_{\delta,\eta}(\bar{y})$.

Proof. In this case, the difference of the nonlocal terms reads

$$\begin{aligned}\mathscr{J}[\bar{x},p,u]-\mathscr{J}[\bar{y},p,v] &= \int_{\mathbb{R}^d_*}\big(u(\bar{x}+j(\bar{x},z)-u(\bar{x})-p\cdot j(\bar{x},z)1_B(z))\big)\mu(dz)- \\ &\quad \int_{\mathbb{R}^d_*}\big(v(\bar{y}+j(\bar{y},z)-v(\bar{y})-p\cdot j(\bar{y},z)1_B(z))\big)\mu(dz).\end{aligned}$$

Similarly to general nonlocal operators we split the domain of integration into a cone $\mathscr{C}$, its complementary in the unit ball $B\setminus\mathscr{C}$ and the region away from the origin $\mathbb{R}^d\setminus B$. Remark that the cone has the property

$$\mathscr{C}_{\delta/2,\eta/2}\big(\frac{\bar{x}+\bar{y}}{2}\big) \subset \mathscr{C}_{\delta,\eta}(\bar{x}) \cap \mathscr{C}_{\delta,\eta}(\bar{y}).$$

Indeed, for $|a|$ sufficiently small, such that $\big(\frac{|a|}{2}\big)^\gamma \le \frac{c_0}{C_0}$, we have

$$\begin{aligned}|j(\bar{x},z)| &\le |j(\frac{\bar{x}+\bar{y}}{2},z)-j(\bar{x},z)|+|j(\frac{\bar{x}+\bar{y}}{2},z)| \\ &\le C_0|z|\big(\frac{|a|}{2}\big)^\gamma+\frac{\delta}{2}\le\frac{\delta}{2}\frac{C_0}{c_0}\big(\frac{|a|}{2}\big)^\gamma+\frac{\delta}{2}\le\delta.\end{aligned}$$

At the same time, due to $\big(\frac{|a|}{2}\big)^\gamma \le \frac{c_0}{C_0}\frac{\eta}{4-\eta}$, we have

$$\begin{aligned}|j(\bar{x},z)\cdot\hat{a}| &\ge |j(\frac{\bar{x}+\bar{y}}{2},z)\cdot\hat{a}|-|j(\frac{\bar{x}+\bar{y}}{2},z)-j(\bar{x},z)| \\ &\ge (1-\frac{\eta}{2})|j(\frac{\bar{x}+\bar{y}}{2},z)|-|j(\frac{\bar{x}+\bar{y}}{2},z)-j(\bar{x},z)| \\ &\ge (1-\frac{\eta}{2})|j(\bar{x},z)|-(2-\frac{\eta}{2})|j(\frac{\bar{x}+\bar{y}}{2},z)-j(\bar{x},z)|) \\ &\ge (1-\frac{\eta}{2})|j(\bar{x},z)|-(2-\frac{\eta}{2})C_0|z|\big(\frac{|a|}{2}\big)^\gamma \\ &\ge (1-\frac{\eta}{2})|j(\bar{x},z)|-(2-\frac{\eta}{2})\frac{C_0}{c_0}|j(\bar{x},z)|\big(\frac{|a|}{2}\big)^\gamma \ge (1-\eta)|j(\bar{x},z)|.\end{aligned}$$

Let $\phi(z) = \varphi(|z|)$. Then $p = D\phi(a)$. Accordingly, we write the previous difference as the sum

$$\mathscr{J}[\bar{x}, p, u] - \mathscr{J}[\bar{y}, p, v] = \mathscr{T}^1(\bar{x}, \bar{y}) + \mathscr{T}^2(\bar{x}, \bar{y}) + \mathscr{T}^3(\bar{x}, \bar{y}),$$

where

$$\begin{aligned}
\mathscr{T}^1(\bar{x}, \bar{y}) &= \int_{|z|\geq 1} \big(u(\bar{x} + j(\bar{x}, z)) - u(\bar{x})\big)\mu(dz) \\
&\qquad - \int_{|z|\geq 1} \big(v(\bar{y} + j(\bar{y}, z)) - v(\bar{y})\big)\mu(dz) \\
\mathscr{T}^2(\bar{x}, \bar{y}) &= \int_{\mathscr{C}} \big(u(\bar{x} + j(\bar{x}, z)) - u(\bar{x}) - p \cdot j(\bar{x}, z)\big)\mu(dz) \\
&\qquad - \int_{\mathscr{C}} \big(v(\bar{y} + j(\bar{y}, z)) - v(\bar{y}) - p \cdot j(\bar{y}, z)\big)\mu(dz) \\
\mathscr{T}^3(\bar{x}, \bar{y}) &= \int_{B\setminus\mathscr{C}} \big(u(\bar{x} + j(\bar{x}, z)) - u(\bar{x}) - p \cdot j(\bar{x}, z)\big)\mu(dz) \\
&\qquad - \int_{B\setminus\mathscr{C}} \big(v(\bar{y} + j(\bar{y}, z)) - v(\bar{y}) - p \cdot j(\bar{y}, z)\big)\mu(dz).
\end{aligned}$$

As before, we seek to estimate each of these integral terms. □

Lemma 4.6.4. *$\mathscr{T}^1(\bar{x}, \bar{y})$ is uniformly bounded with respect to all the parameters, namely*

$$\mathscr{T}^1(\bar{x}, \bar{y}) \leq 2\max(||u||_\infty, ||v||_\infty) \sup_{x\in\mathbb{R}^d} \mu_x(\mathbb{R}^d \setminus B).$$

Lemma 4.6.5. *Let $\delta = |a|\delta_0$ and η small such that $1 - \eta - \delta_0 \geq 0$. We have*

$$\mathscr{T}^2(\bar{x}, \bar{y}) \leq \int_{\mathscr{C}} \sup_{\substack{|s|<1,\\ x=\bar{x},\bar{y}}} \big((1-\tilde{\eta}^2)\frac{\varphi'(|a + sj(x,z)|)}{|a + sj(x,z)|} + \tilde{\eta}^2\varphi''(|a + sj(x,z)|)|j(x,z)|^2\big)(dz)$$

where $\tilde{\eta} = (1 - \eta - \delta_0)(1 + \delta_0)^{-1}$.

Proof. Writing the maximum inequality at points $\bar{x}, \bar{y}$ for $z' = 0$ and $z = j(\bar{x}, z)$, respectively $z = 0, z' = j(\bar{y}, z)$ we have

$$\begin{aligned}
u(\bar{x} + j(\bar{x}, z)) - u(\bar{x}) - p \cdot j(\bar{x}, z) &\leq \phi(a + j(\bar{x}, z)) - \phi(a) - D\phi(a) \cdot j(\bar{x}, z) \\
-\big(v(\bar{y} + j(\bar{y}, z)) - v(\bar{y}) - p \cdot j(\bar{y}, z)\big) &\leq \phi(a - j(\bar{y}, z)) - \phi(a) + D\phi(a) \cdot j(\bar{y}, z).
\end{aligned}$$

Therefore

$$\begin{aligned}
\mathscr{T}^2(\bar{x}, \bar{y}) &\leq \int_{\mathscr{C}} \big(\phi(a + j(\bar{x}, z)) - \phi(a) - D\phi(a) \cdot j(\bar{x}, z)\big)\mu(dz) \\
&\qquad + \int_{\mathscr{C}} \big(\phi(a - j(\bar{y}, z)) - \phi(a) + D\phi(a) \cdot j(\bar{y}, z)\big)\mu(dz).
\end{aligned}$$

Taking into account that the set $\mathscr{C}$ is included in both $\mathscr{C}_{\eta,\delta}(\bar{x})$ and $\mathscr{C}_{\eta,\delta}(\bar{y})$ we have the following

upper and lower bounds for the jumps,

$$\begin{aligned} |a|(1+\delta_0) \geq |(a+sj(\bar{x},z))| &\geq |a|(1-\delta_0) \\ \widehat{|(a+sj(\bar{x},z))\cdot z|} &\geq \tilde{\eta}|j(\bar{x},z)| \end{aligned}$$

and we obtain the conclusion in a similar manner as we did for general nonlocal operators. □

Lemma 4.6.6. *Denote by* $\Delta(z) = j(\bar{x},z) - j(\bar{y},z)$. *Then*

$$\begin{aligned} \mathscr{T}^3(\bar{x},\bar{y}) \leq\ & 2\varphi'(|a|)\int_{B\setminus\mathscr{C};\ |\Delta(z)|\geq\delta} |\Delta(z)|\mu(dz) + \\ & \int_{B\setminus\mathscr{C};\ |\Delta(z)|\leq\delta} \sup_{|s|<1} \frac{\varphi'(|a+s\Delta(z)|)}{|a+s\Delta(z)|}|\Delta(z)|^2\mu(dz). \end{aligned}$$

Proof. We use again the maximum conditions to obtain the bound

$$\begin{aligned} \big(u(\bar{x}+j(\bar{x},z)) - u(\bar{x}) - p\cdot j(\bar{x},z)\big) - \big(v(\bar{y}+j(\bar{y},z)) - v(\bar{y}) - p\cdot j(\bar{y},z)\big) \leq \\ \phi(a+j(\bar{x},z)-j(\bar{y},z)) - \phi(a) - D\phi(a)\cdot(j(\bar{x},z)-j(\bar{y},z) \end{aligned}$$

which in particular implies

$$\mathscr{T}^3(\bar{x},\bar{y}) \leq \int_{B\setminus\mathscr{C}} \big(\phi(a+j(\bar{x},z)-j(\bar{y},z)) - \phi(a) - D\phi(a)\cdot(j(\bar{x},z)-j(\bar{y},z))\big)\mu(dz).$$

In order to estimate the integral terms corresponding to ϕ, we split the integral in two parts, as follows

$$\begin{aligned} &\int_{B\setminus\mathscr{C};\ |\Delta(z)|\geq\delta} \big(\phi(a+\Delta(z)) - \phi(a) - D\phi(a)\cdot\Delta(z)\big)\mu(dz) + \\ &\int_{B\setminus\mathscr{C};\ |\Delta(z)|\leq\delta} \big(\phi(a+\Delta(z)) - \phi(a) - D\phi(a)\cdot\Delta(z)\big)\mu(dz). \end{aligned}$$

On the first set we use the concavity and monotonicity of φ and deduce that

$$\phi(a+\Delta(z)) - \phi(a) - D\phi(a)\cdot\Delta(z) \leq 2\varphi'(|a|)|\Delta(z)|.$$

On $B\setminus\mathscr{C};\ |\Delta(z)|\leq\delta$ we use a second order Taylor expansion and we take into account that φ is a smooth increasing function with $\varphi''\leq 0$ to obtain the upper bound

$$\begin{aligned} \sup_{|s|<1}\big(\phi(|a+s\Delta(z)|) - \phi(|a|) - D\phi(a)\cdot\Delta(z)\big) &\leq \sup_{|s|<1} D^2\phi(a+s\Delta(z))\Delta(z)\cdot\Delta(z) \\ &\leq \sup_{|s|<1}\frac{\varphi'(|a+s\Delta(z)|)}{|a+s\Delta(z)|}|\Delta(z)|^2. \end{aligned}$$

Therefore we get the desired estimate. □

Corollary 4.6.3 (Lipschitz estimates)**.** *Let $\beta > 2(1-\gamma)$ and assume conditions $(J1)-(J4)$ hold. Under the assumptions of Proposition 4.6.2 with*

$$\varphi(t) = \begin{cases} L\big(t - \varrho t^{1+\alpha}\big), & t \in [0,\theta] \\ \varphi(\theta), & t > \theta \end{cases}$$

where $\alpha \in \Big(0, \min\Big(\frac{\gamma\beta}{d+1}, \frac{2\gamma-2+\beta}{d+2-\beta}\Big)\Big)$, ϱ is a large positive constant such that $\varrho\alpha 2^{\alpha-1} > 1$,

$$\theta = \sqrt[\alpha]{\frac{1}{\rho(1+\alpha)}} \text{ and } L > \frac{||u||_\infty + ||v||_\infty}{\varphi(\theta)}$$

the following holds: there exists a positive constant $C = C(\mu)$ such that for $\Theta(\varrho,\alpha,\mu) = C\big(\rho\alpha 2^{\alpha-1} - 1\big)$ we have

$$\mathscr{J}[\bar{x},p,u] - \mathscr{J}[\bar{y},p,v] \le -L|a|^{(1-\beta)+\alpha(d+2-\beta)}\big\{\Theta(\varrho,\alpha,\mu) - o_{|a|}(1)\big\} + O(\tilde{C}_\mu).$$

Remark 4.6.3. *The condition $\beta > 2(1-\gamma)$ connects the singularity of the measure with the regularity of the jumps. It basically states that the more singular the measure is, the less regular the jumps can be.*

Proof. We first evaluate, as for general nonlocal operators, the expression

$$\begin{aligned} &\sup_{|s|\le 1}\big((1-\tilde{\eta}^2)\varphi'(|a+sj(x,z)|)\frac{1}{|a+sj(x,z)|} + \tilde{\eta}^2\varphi''(|a+sj(x,z)|)\big) \\ &\qquad \le L\Big(\frac{2(1-\tilde{\eta})}{|a|(1-\delta_0)} - \varrho\alpha(1+\delta_0)^{\alpha-1}|a|^{\alpha-1}\Big). \end{aligned}$$

For $\tilde{\eta} = 1 - |a|^\alpha\tilde{\eta}_0$ with sufficiently small $\tilde{\eta}_0 < \frac{1}{4}$, consider as before the constant $\Theta_\varrho = \varrho\alpha 2^{\alpha-1} - 4\tilde{\eta}_0 > 0$. Then, using assumption $(J2)$ we have

$$\begin{aligned} &\int_{\mathscr{C}} \sup_{|s|<1}\big((1-\tilde{\eta}^2)\varphi'(|a+sz|)\frac{1}{|a+sz|} + \tilde{\eta}^2\varphi''(|a+sz|)\big)|j(\bar{x},z)|^2\mu(dz) \\ &\qquad \le -L\Theta_\varrho|a|^{\alpha-1}\int_{\mathscr{C}}|j(\bar{x},z)|^2\mu(dz) \\ &\qquad \le -L\Theta(\varrho,\mu)|a|^{(1-\beta)+\alpha(d+2-\beta)}. \end{aligned}$$

Similarly, taking into account assumptions $(J3)-(J4)$ and that $\delta = |a|\delta_0 \sim |a|^{\alpha+1}$ we obtain

$$\begin{aligned} \varphi'(|a|)\int_{B\setminus\mathscr{C};\,|\Delta(z)|\ge\delta}|\Delta(z)|\mu(dz) &\le LC_0|a|^\gamma\int_{B\setminus\mathscr{C};\,|z|\ge\delta|a|^{-\gamma}}|z|\mu(dz) \\ &\le LC_\mu^2|a|^\gamma|a|^{(1+\alpha-\gamma)(1-\beta)} \end{aligned}$$

and

$$\begin{aligned} \int_{B\setminus\mathscr{C};\,|\Delta(z)|\le\delta}\sup_{|s|<1}\frac{\varphi'(|a+s\Delta(z)|)}{|a+s\Delta(z)|}|\Delta(z)|^2\mu(dz) &\le \frac{L}{|a|(1-\delta_0)}\int_{B\setminus\mathscr{C};\,|\Delta(z)|\le\delta}|\Delta(z)|^2\mu(dz) \\ &\le LC_\mu^3|a|^{2\gamma-1}. \end{aligned}$$

Since $\beta > 2(1-\gamma)$, $\gamma\beta > \alpha(d+1)$ and $2\gamma-2+\beta > \alpha(d+2-\beta)$ the difference of the nonlocal term is negative, being bounded by

$$\begin{aligned}
&\mathscr{J}[\bar{x},p,u]-\mathscr{J}[\bar{y},p,v]\\
&\quad\le -L|a|^{1-\beta}\left\{\Theta(\varrho,\mu)|a|^{\alpha(d+2-\beta)}-C_\mu^2|a|^{\gamma+(\alpha-\gamma)(1-\beta)}-C_\mu^3|a|^{2\gamma-2+\beta}\right\}+O(\tilde{C}_\mu)\\
&\quad= -L|a|^{(1-\beta)+\alpha(d+2-\beta)}\left\{\Theta(\varrho,\mu)-o_{|a|}(1)\right\}+O(\tilde{C}_\mu).
\end{aligned}$$

□

Corollary 4.6.4 (Hölder estimates)**.** *Let $\beta > 2(1-\gamma)$ and assume conditions $(J1)-(J4)$ hold. Under the assumptions of Proposition 4.6.1 with*

$$\varphi(t) = Lt^\alpha,$$

where $\alpha \in (0,\min(1,\beta))$ and L is a positive large constant, the following holds: there exists a positive constant $C(\alpha,\mu) = \alpha C(\mu)$ such that

$$\mathscr{J}[\bar{x},p,u]-\mathscr{J}[\bar{y},p,v] \le -L|a|^{\alpha-\beta}\left\{C(\alpha,\mu)-o_{|a|}(1)\right\}+O(\tilde{C}_\mu).$$

Proof. Similarly to general nonlocal operators, taking into account $(J2)$ we have

$$\begin{aligned}
\int_{\mathscr{C}}\sup_{|s|\le 1}\Big((1-\tilde{\eta}^2)\varphi'(|a+sj(x,z)|)\frac{1}{|a+sj(x,z)|}+\tilde{\eta}^2\varphi''(|a+sj(x,z)|)\Big)|j(\bar{x},z)|^2\mu(dz)&\\
\le -L\alpha(1-\alpha)2^{\alpha-3}|a|^{\alpha-2}\int_{\mathscr{C}}|z|^2\mu(dz)&\\
\le -LC(\alpha,\mu)|a|^{\alpha-\beta},&
\end{aligned}$$

with $C(\alpha,\mu) = \alpha 2^{-3}C_0\eta^{\frac{d-1}{2}}\delta_0^{2-\beta}$. In addition, we have the estimates

$$\begin{aligned}
\varphi'(|a|)\int_{B\setminus\mathscr{C};\ |\Delta(z)|\ge\delta}|\Delta(z)|\mu(dz) &\le L\alpha|a|^{\alpha-1}C_0|a|^\gamma\int_{B\setminus\mathscr{C};\ |z|\ge\delta|a|^{-\gamma}}|z|\mu(dz)\\
&\le L\alpha C_\mu^2|a|^{\alpha-\beta+\gamma\beta}
\end{aligned}$$

with $C^2(\mu,\delta_0) = C_0\delta_0^{1-\beta}$ if $\beta\neq 1$, respectively

$$\varphi'(|a|)\int_{B\setminus\mathscr{C};\ |\Delta(z)|\ge\delta}|\Delta(z)|\mu(dz) \le L\alpha C_\mu^2|a|^{\alpha-\beta}|a|^\gamma\ln(|a|\delta_0)$$

for $\beta = 1$. Finally,

$$\begin{aligned}
\int_{B\setminus\mathscr{C};\ |\Delta(z)|\le\delta}\sup_{|s|<1}\frac{\varphi'(|a+s\Delta(z)|)}{|a+s\Delta(z)|}|\Delta(z)|^2\mu(dz)&\\
\le L\alpha(|a|(1-\delta_0))^{\alpha-2}\int_{B\setminus\mathscr{C};\ |\Delta(z)|\le\delta}|\Delta(z)|^2\mu(dz)&\\
\le L\alpha C_\mu^3|a|^{2\gamma-2+\beta}|a|^{\alpha-\beta}&
\end{aligned}$$

with $C_\mu^3 = (1-\delta_0)^{\alpha-2}C_0^2 C_\mu$. For α sufficiently small we have

$$\mathscr{J}[\bar{x},p,u] - \mathscr{J}[\bar{y},p,v] \leq -L|a|^{\alpha-\beta}\big(C(\alpha,\mu) - o_{|a|}(1)\big).$$

□

Proposition 4.6.3 (Quadratic estimates - Lévy-Itô operators). *Let (J1) (J3) and (J4) hold. Let u, v be two bounded functions and assume the auxiliary function*

$$\psi_\varepsilon(x,y) = u(x) - v(y) - \frac{|x-y|^2}{\varepsilon^2}$$

attains a positive maximum at $(\bar{x},\bar{y})$, with $\bar{x} \neq \bar{y}$. Denote by $a = \bar{x} - \bar{y}$ and by $p = 2\frac{\bar{x}-\bar{y}}{\varepsilon^2}$. Then the following holds

$$\begin{aligned}\mathscr{J}[\bar{x},p,u] - \mathscr{J}[\bar{y},p,u] \leq \\ 2C_0^2\frac{1}{\varepsilon^2}\int_{B_\delta}|z|^2\mu(dz) + C_0^2\frac{|a|^{2\gamma}}{\varepsilon^2}\int_{|z|\geq\delta}|z|^2\mu(dz) + 2C_0\frac{|a|^{1+\gamma}}{\varepsilon^2}\int_{|z|\geq 1}|z|\mu(dz).\end{aligned}$$

Proof. By definition, we have

$$u(\bar{x}+j(\bar{x},z)) - v(\bar{y}+j(\bar{y},z')) - \frac{|\bar{x}+j(\bar{x},z)-\bar{y}-j(\bar{y},z')|^2}{\varepsilon^2} \leq u(\bar{x}) - v(\bar{y}) - \frac{|\bar{x}-\bar{y}|^2}{\varepsilon^2}.$$

We split the difference of the integral terms into

$$\mathscr{J}[\bar{x},p,u] - \mathscr{J}[\bar{y},p,u] = \mathscr{T}_q^1(\bar{x},\bar{y}) + \mathscr{T}_q^2(\bar{x},\bar{y}) + \mathscr{T}_q^3(\bar{x},\bar{y})$$

where this time the integrals are taken over the ball $B_\delta = B(0,\delta)$, the circular crown $B\setminus B_\delta$ and the exterior of the unit ball $\mathbb{R}^d \setminus B$:

$$\begin{aligned}\mathscr{T}_q^1(\bar{x},\bar{y}) &= \int_{B_\delta}\big(u(\bar{x}+j(\bar{x},z)) - u(\bar{x}) - p\cdot j(\bar{x},z)\big)\mu(dz) \\ &\qquad - \int_{B_\delta}\big(v(\bar{y}+j(\bar{y},z)) - v(\bar{y}) - p\cdot j(\bar{y},z)\big)\mu(dz) \\ \mathscr{T}_q^2(\bar{x},\bar{y}) &= \int_{B\setminus B_\delta}\big(u(\bar{x}+j(\bar{x},z)) - u(\bar{x}) - p\cdot j(\bar{x},z)\big)\mu(dz) \\ &\qquad - \int_{B\setminus B_\delta}\big(v(\bar{y}+j(\bar{y},z)) - v(\bar{y}) - p\cdot j(\bar{y},z)\big)\mu(dz) \\ \mathscr{T}_q^3(\bar{x},\bar{y}) &= \int_{|z|\geq 1}\big(u(\bar{x}+j(\bar{x},z)) - u(\bar{x})\big)\mu(dz) \\ &\qquad - \int_{|z|\geq 1}\big(v(\bar{y}+j(\bar{y},z)) - v(\bar{y})\big)\mu(dz).\end{aligned}$$

Lemma 4.6.7. *The following estimate holds*

$$\mathscr{T}_q^1(\bar{x},\bar{y}) \leq \frac{2}{\varepsilon^2}\int_{B_\delta}|j(\bar{x},z)|^2\mu(dz).$$

Proof. Taking in (4.6.2) $z' = 0$ and $z = 0$, we have respectively $j(\bar{y}, z') = 0$, $j(\bar{x}, z) = 0$. Hence

$$\begin{aligned} &u(\bar{x} + j(\bar{x}, z)) - u(\bar{x}) - p \cdot j(\bar{x}, z) \leq \\ &\qquad \frac{|\bar{x} + j(\bar{x}, z) - \bar{y}|^2}{\varepsilon^2} - \frac{|\bar{x} - \bar{y}|^2}{\varepsilon^2} - p \cdot j(\bar{x}, z) = \frac{|j(\bar{x}, z)|^2}{\varepsilon^2} \\ &-\big(v(\bar{y} + j(\bar{y}, z')) - v(\bar{y}) - p \cdot j(\bar{y}, z')\big) \leq \\ &\qquad \frac{|\bar{x} - \bar{y} - j(\bar{y}, z')|^2}{\varepsilon^2} - \frac{|\bar{x} - \bar{y}|^2}{\varepsilon^2} + p \cdot j(\bar{y}, z') = \frac{|j(\bar{y}, z)|^2}{\varepsilon^2}. \end{aligned}$$

Integrating on B_δ we have

$$\mathcal{T}_q^1(\bar{x}, \bar{y}) \quad \leq \quad 2 \int_{B_\delta} \frac{|j(\bar{x}, z)|^2}{\varepsilon^2} \mu(dz).$$

□

Lemma 4.6.8. *The following estimate holds*

$$\mathcal{T}_q^2(\bar{x}, \bar{y}) \quad \leq \quad \frac{1}{\varepsilon^2} \int_{B \setminus B_\delta} |j(\bar{x}, z) - j(\bar{y}, z)|^2 \mu(dz).$$

Proof. Taking $z = z'$ in inequality (4.6.2) and subtracting the corresponding gradients we obtain the inequality

$$\begin{aligned} &\big(u(\bar{x} + j(\bar{x}, z)) - u(\bar{x}) - p \cdot j(\bar{x}, z)\big) - \big(v(\bar{y} + j(\bar{y}, z)) - v(\bar{y}) - p \cdot j(\bar{y}, z)\big) \leq \\ &\qquad \frac{|\bar{x} + j(\bar{x}, z) - \bar{y} - j(\bar{y}, z)|^2}{\varepsilon^2} - \frac{|\bar{x} - \bar{y}|^2}{\varepsilon^2} - p \cdot (j(\bar{x}, z) - j(\bar{y}, z)). \end{aligned}$$

Integrating on the circular crown $B \setminus B_\delta$ and computing the quadratic form on the right hand side, we get the estimate

$$\mathcal{T}_q^2(\bar{x}, \bar{y}) \leq \int_{B \setminus B_\delta} \frac{|j(\bar{x}, z) - j(\bar{y}, z)|^2}{\varepsilon^2} \mu(dz).$$

□

Lemma 4.6.9. *The following estimate holds*

$$\mathcal{T}_q^3(\bar{x}, \bar{y}) \quad \leq \quad \frac{1}{\varepsilon^2} \int_{|z| \geq 1} |j(\bar{x}, z) - j(\bar{y}, z)|^2 \mu(dz) + |p| \int_{|z| \geq 1} |j(\bar{x}, z) - j(\bar{y}, z)| \mu(dz).$$

Proof. Once again, for $z = z'$ in inequality (4.6.2) we obtain the inequality

$$\begin{aligned} &\big(u(\bar{x} + j(\bar{x}, z)) - u(\bar{x})\big) - \big(v(\bar{y} + j(\bar{y}, z)) - v(\bar{y})\big) \leq \\ &\qquad \frac{|\bar{x} + j(\bar{x}, z) - \bar{y} - j(\bar{y}, z)|^2}{\varepsilon^2} - \frac{|\bar{x} - \bar{y}|^2}{\varepsilon^2}. \end{aligned}$$

Integrating on $\mathbb{R}^d \setminus B$ and computing the right hand side we get

$$\mathcal{T}_q^3(\bar{x},\bar{y}) \leq \int_{|z|\geq 1}\big(p\cdot(j(\bar{x},z)-j(\bar{y},z))+\frac{|j(\bar{x},z)-j(\bar{y},z)|^2}{\varepsilon^2}\big)\mu(dz).$$

□

From the three above lemmas we deduce that

$$\begin{aligned}\mathcal{J}[\bar{x},p,u]-\mathcal{J}[\bar{y},p,u] \leq\ & \frac{2}{\varepsilon^2}\int_{B_\delta}|j(\bar{x},z)|^2\mu(dz)+\\ & \frac{1}{\varepsilon^2}\int_{|z|\geq\delta}|j(\bar{x},z)-j(\bar{y},z)|^2\mu(dz)+\\ & 2\frac{|a|}{\varepsilon^2}\int_{|z|\geq 1}|j(\bar{x},z)-j(\bar{y},z)|\mu(dz).\end{aligned}$$

Taking into account $(J3)$ we further arrive to the estimate

$$\begin{aligned}&\mathcal{J}[\bar{x},p,u]-\mathcal{J}[\bar{y},p,u]\leq\\ &\quad 2C_0^2\frac{1}{\varepsilon^2}\int_{B_\delta}|z|^2\mu(dz)+C_0^2\frac{|a|^{2\gamma}}{\varepsilon^2}\int_{|z|\geq\delta}|z|^2\mu(dz)+2C_0\frac{|a|^{1+\gamma}}{\varepsilon^2}\int_{|z|\geq 1}|z|\mu(dz).\end{aligned}$$

□

4.7 Appendix

Lemma 4.7.1. *Let X, Y and Z be block matrices of the form*

$$X=\begin{bmatrix}X_1 & 0\\ 0 & X_2\end{bmatrix}$$

such that they satisfy the inequality

$$\begin{bmatrix}X & 0\\ 0 & -Y\end{bmatrix}\leq\begin{bmatrix}Z & -Z\\ -Z & Z\end{bmatrix} \tag{4.30}$$

Then the block matrices X_i, Y_i satisfy inequality (4.30) with Z_i, for $i=1,2$.

Proof. The previous matrix inequality can be rewritten in the form

$$Xz\cdot z-Yz'\cdot z'\leq Z(z-z')\cdot(z-z').$$

Due to the form of the block matrices, namely the secondary diagonal null, we can write the inequality on components, for $z=(z_1,z_2)$, $z'=(z_1',z_2')$

$$\sum_{i=1,2}\big(X_iz_i\cdot z_i-Y_iz_i'\cdot z_i'\big)\leq\sum_{i=1,2}\big(Z_i(z_i-z_i')\cdot(z_i-z_i')\big).$$

Thus, taking $z=(z_1,0)$ and $z'=(z_1',0)$, respectively $z=(0,z_2)$ and $z'=(0,z_2')$ we get the corresponding inequality for the block matrices X_i, Y_i, Z_i.

□

Lemma 4.7.2. *Let X, Y and Z be symmetric matrices satisfying inequality (4.30). Consider the sup and inf convolutions, defined by*

$$X^\varepsilon z\cdot z=\sup_{\xi\in\mathbb{R}^d}\left\{X\xi\cdot\xi-\frac{|z-\xi|^2}{\varepsilon}\right\} \text{ and } Y_\varepsilon z\cdot z=\inf_{\xi\in\mathbb{R}^d}\left\{Y\xi\cdot\xi+\frac{|z-\xi|^2}{\varepsilon}\right\}.$$

Then X^ε, Y_ε and Z^ε satisfy aswell inequality (4.30). In addition we have

$$-\frac{1}{\varepsilon}I, X\le X^\varepsilon \text{ and } Y_\varepsilon\le Y,\frac{1}{\varepsilon}I. \tag{4.31}$$

Proof. Evaluating (4.30) at $(\xi,-\xi)$ and using the triangular inequality we have

$$\left(X\xi\cdot\xi-\frac{|z-\xi|^2}{\varepsilon}\right)-\left(Y\xi\cdot\xi+\frac{|z'+\xi|^2}{\varepsilon}\right)\le 4Z\xi\cdot\xi-\frac{|z-z'-2\xi|^2}{\varepsilon}.$$

Taking the supremum over all ξ we get that

$$\sup_\xi\left(X\xi\cdot\xi-\frac{|z-\xi|^2}{\varepsilon}\right)-\inf_\xi\left(Y\xi\cdot\xi+\frac{|z'-\xi|^2}{\varepsilon}\right)\le\sup_\xi\left(Z\xi\cdot\xi-\frac{|z-z'-\xi|^2}{\varepsilon}\right)$$

that is exactly

$$X^\varepsilon z\cdot z-Y_\varepsilon z'\cdot z'\le Z^\varepsilon(z-z')\cdot(z-z').$$

Moreover, considering the particular values $\xi=0$, respectively $\xi=z$ we have from the definition of sup and inf matrix convolutions the desired inequalities. □

Lemma 4.7.3. *Let $Z=\frac{1}{\alpha}(I-\omega\hat{a}\otimes\hat{a})$, where $\hat{a}\in\mathbb{S}^{d-1}$, $\alpha>0$ and $\omega\ge 0$. Then the following holds*

$$Z^{\frac{\alpha}{2}}=\frac{2}{\alpha}\left(I-\frac{2\omega}{1+\omega}\hat{a}\otimes\hat{a}\right). \tag{4.32}$$

Proof. By definition

$$Z^{\frac{\alpha}{2}}z\cdot z=\sup_\xi\left\{Z\xi\cdot\xi-2\frac{|z-\xi|^2}{\alpha}\right\}$$

and the supremum is attained at points $\bar{\xi}$ satisfying $Z\bar{\xi}=\frac{2}{\alpha}(\bar{\xi}-z)$, or equivalently

$$(I-\omega\hat{a}\otimes\hat{a})\bar{\xi}=2(\bar{\xi}-z).$$

Taking the inner product with $\hat{a}$ in this identity, we have

$$\bar{\xi}\cdot\hat{a}=\frac{2}{1+\omega}z\cdot\hat{a}.$$

Taking now the inner product with z in the same identity, we have

$$\bar{\xi}\cdot z = 2|z|^2 - \omega(z\cdot\hat{a})(\bar{\xi}\cdot\hat{a}) = 2|z|^2 - \frac{2\omega}{1+\omega}(z\cdot\hat{a})^2.$$

Therefore

$$\begin{aligned} Z^{\frac{\alpha}{2}} z\cdot z &= \frac{2}{\alpha}\left((\bar{\xi}-z)\cdot\bar{\xi} - |z-\bar{\xi}|^2\right) \\ &= \frac{2}{\alpha}\left((\bar{\xi}-z)\cdot z\right) \\ &= \frac{2}{\alpha}\left(|z|^2 - \frac{2\omega}{1+\omega}(z\cdot\hat{a})^2\right). \end{aligned}$$

□

Lemma 4.7.4. *Let X, Y, Z satisfy the block inequality (4.30), with $Z^{\frac{\alpha}{2}}$ given by equation (4.32), for some $\omega \geq 1$. Then the following holds:*

$$tr(X-Y) \leq -\frac{8(\omega-1)}{\alpha(1+\omega)}.$$

Proof. Rewrite the matrix inequality in the form

$$Xz\cdot z - Yz'\cdot z' \leq Z^{\frac{\alpha}{2}}(z-z')\cdot(z-z').$$

Taking $z = -z' = \hat{a}$ we have

$$X\hat{a}\cdot\hat{a} - Y\hat{a}\cdot\hat{a} \leq 4Z^{\frac{\alpha}{2}}\hat{a}\cdot\hat{a}$$

whereas for any vector z orthogonal to $\hat{a}$

$$Xz\cdot z - Yz\cdot z \leq 0.$$

Therefore

$$\text{trace}(X-Y) \leq \frac{8}{\alpha}\left(|a|^2 - \frac{2\omega}{1+\omega}|a|^2\right) = -\frac{8(\omega-1)}{\alpha(\omega+1)}.$$

□

4.8 Conclusion

We established in this chapter Lipschitz and Hölder regularity results for viscosity solutions of integro-differential equations within a new framework, of mixed integro-differential equations. In particular, for directional Lévy-Itô operators of fractional exponent β, we showed that the solution is Lipschitz continuous in the subcritical case $\beta > 1$ and Hölder continuous in the critical and supercritical case $\beta \leq 1$. The Lipschitz continuity for the critical case $\beta = 1$ is left open and we would like to investigate it in near future.

At the same time, we would like to consider the Harnack ABP approach for mixed integro-differential equations and inquire regularity of solutions for equations with bounded, measurable coefficients.

Last but not least, this work was motivated by the study of long time behavior of periodic viscosity solutions for integro-differential equations, that we are considering for the moment in a companion paper.

Part II

Image Restoration and Visualization by Curvature Motions

CHAPTER 5

Curves and Curvatures. State of the art

A youth who had begun to read geometry with Euclid, when he had learnt the first proposition, inquired, "What do I get by learning these things?" So Euclid called a slave and said "Give him three pence, since he must make a gain out of what he learns."

Euclid of Alexandria (325-265 B.C.E)

Abstract: This chapter presents a review, analysis and comparison of numerical methods implementing the curvature motion and the affine curvature motion for 2D images, shapes, and curves. These *curvature scale spaces* lead, in principle, to a multiscale curvature estimator in digital images. [1]

Résumé : Ce chapitre présente une analyse et comparaison de méthodes numériques associés à l'équation par courbure moyenne et sa variante affine, à la fois pour les images, pour les ensembles et pour les courbes. Ces *espaces échelles* permettent a priori de faire des estimations des courbures dans les images.

Keywords: curvature scale space, mean curvature motion, affine curvature motion, curve shortening, affine shortening, level lines, topographic maps, finite difference scheme, stack filter

[1] This chapter is a brief State of the Art on Curvature Motions and corresponding Algorithms.

Contents

5.1 Introduction

Attneave's founding 1954 paper [Att54] on image perception anticipated the numerical analysis of digital pictures. He argued on neurological grounds that the human brain could not possible use *all* the information provided by states of simulation. But actually, the brain registers *regions where color changes abruptly (contours), and furthermore angles and peaks of curvature*.

As mentioned in the introduction, our final goal is to implement this idea and show that computers can register the same information as the human brain, with the hope that further post-processing algorithms can take advantage of it. We show in Chapter 7 how curvatures can be accurately estimated by a direct computation on level lines, after their independent smoothing (as illustrated in Fig. 5.1).

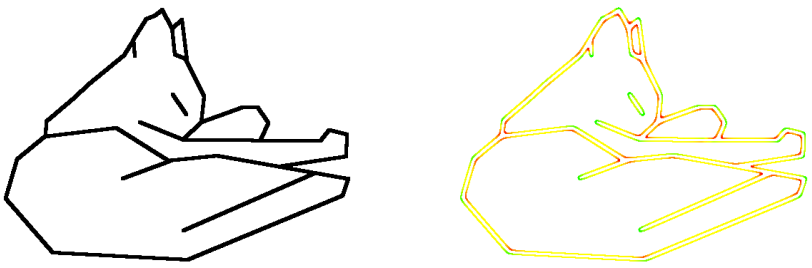

Figure 5.1: Attneave's figure illustrating the prominent role of curvature peaks in image perception and its curvature map computed by level lines shortening.

At present, because of noise and aliasing artifacts (as illustrated in Fig. 7.27), the direct computation of curvatures on a raw image is impossible This explains why, in one of the first

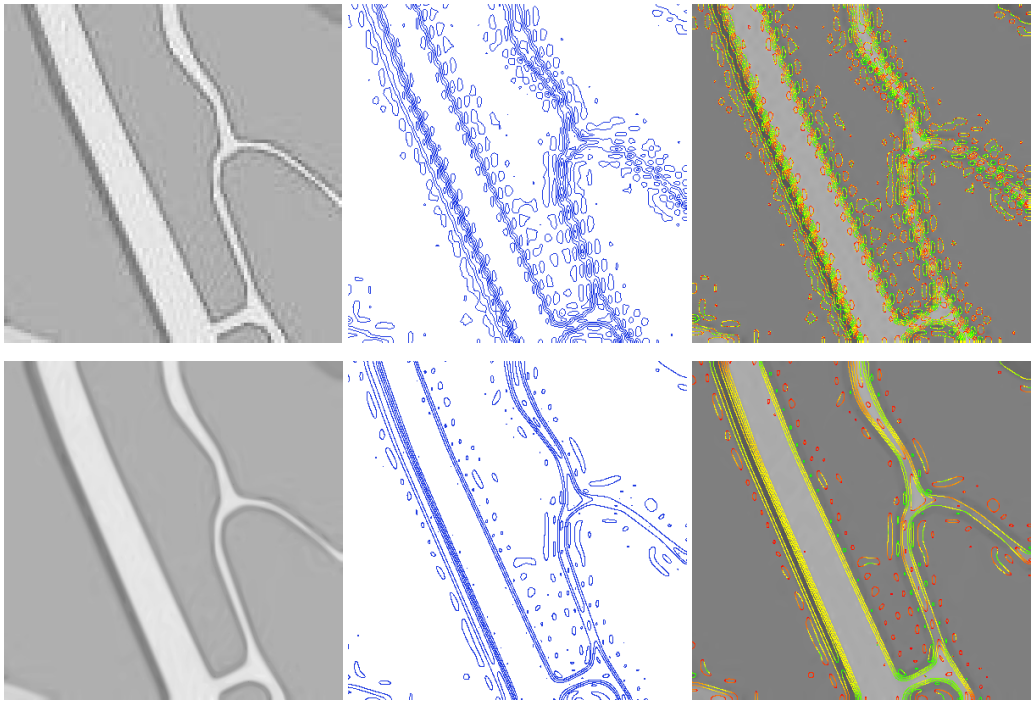

Figure 5.2: Top: Piece of map with roads, its corresponding level lines and non-filtered curvature map. Bottom: smoothed image, by affine curvature, smoothed level lines and curvature map after filtering.

serious attempts to cope with this numerical challenge, Asada and Brady [AB86] introduced the concept of *multiscale curvature*. They suggested to approximate contours by splines and to smooth them by a 1D heat equation. Their explicit goal was to implement Attneave's idea that shapes must be represented by curvature extrema. This paper led to increasingly sophisticated attempts to analyze planar shapes by their curvatures. A first difficulty is that, at fine scale, contours have high curvatures everywhere. Another problematic issue is the extraction of the contours on which the curvature could be computed. Contours obtained by "edge detection" are broken and plagued with spurious branches, which hinder the computation of any reliable curvature.

Clarifying the subject has required a fairly elaborate series of mathematical contributions. Grayson [Gra87] proved that the intrinsic heat equation smooths Jordan curves and preserves their topology. The Osher-Sethian level set method [OS88] implements the motion by mean curvature of an embedded manifold by applying the mean curvature PDE to its signed distance function. Chen-Giga-Goto [CGG91] and Evans-Spruck [ES91] elaborated a viscosity solution theory for the scalar mean curvature motion. A mathematical link between the median filter and the motion by mean curvature was conjectured by Merriman, Bence and Osher [MBO92] and later proved by several authors [BG95], [Eva93], [Ish95].

In parallel, Mackworth and Moktharian [MM86] proposed a fast numerical scheme to smooth a curve by the intrinsic heat equation. But their shape extraction algorithm was unconvincing. Caselles et al. realized the potential of using directly the image level lines instead of its edges. They proposed to perform contrast invariant image analysis directly on the set

of level lines, or *topographic map* [CCM96]. A fast algorithm computing the topographic map was developed by Monasse and Guichard in [MG98].

Sapiro and Tannenbaum [ST93a] discovered the affine curve shortening and Alvarez et al. [AGLM93] the affine invariant and contrast invariant image smoothing. A remarkably fast and simple geometric algorithm for affine shortening was given by Moisan in [Moi98].

The work developed in the following chapters builds on the above mentioned contributions and describes a complete image processing numerical chain starting from a digital image and ending with an accurate computation and visualization tool of its curvatures and curvature evolutions. It, hopefully, advances Attneave's program and yields what we shall term an *image curvature microscope*.

The present chapter starts with a review of the main classes of curvature algorithms, focusing on isotropic curvature equations and on the two curvature powers that are relevant for image analysis, namely 1 and 1/3. There are several definitions of curvature and of multiscale curvature, and we shall detail them before entering into the discussion of how to compute them. The next two sections review and compare the various types of numerical analysis for curvature motion, and clarify the links between them.

5.2 Curvature Scale Spaces

5.2.1 Curvatures

Digital images are given in discrete sampled forms on a rectangle Ω but the underlying continuous substratum is assumed to be C^∞ and interpolated as such on Ω. By Sard's theorem and by the implicit function theorem for almost every level λ, the iso-level set $u^{(-1)}(\lambda)$ is a finite union of disjoint smooth Jordan curves. These Jordan curves are called the level lines of u and coincide with the topological boundaries of upper and lower level sets.

Assume in the following that u is at least C^2 in a neighborhood of a point $\mathbf{x_0} \in \Omega$ and that its gradient is not null, $Du(\mathbf{x_0}) \neq 0$. Then the scalar curvature of u at $\mathbf{x_0}$, denoted by $\mathrm{curv}(u)(\mathbf{x_0})$, is the real number defined by

$$\mathrm{curv}(u)(\mathbf{x_0}) = \frac{u_{xx}u_y^2 - 2u_{xy}u_xu_y + u_{yy}u_x^2}{(u_x^2+u_y^2)^{3/2}}(\mathbf{x_0}). \tag{5.1}$$

This scalar curvature at $\mathbf{x_0}$ is linked to the vectorial curvature of the level line passing by $\mathbf{x_0}$. The vectorial curvature of a C^2 curve $\mathbf{x}(\mathbf{s})$ parameterized by a length parameter s (so that $|\mathbf{x}'(s)| = 1$) is defined by

$$\kappa(\mathbf{x}) := \mathbf{x}''(s).$$

The link between the vectorial curvature of an image level line $\kappa(\mathbf{x})$ and the scalar curvature $\mathrm{curv}(u)(\mathbf{x})$ at nonsingular points is given by the next formula. Denote by $\mathbf{x} = \mathbf{x}(s)$ the level line of u passing by $\mathbf{x}_0$. Then

$$\kappa(\mathbf{x_0}) = -\mathrm{curv}(u)(\mathbf{x_0}).\frac{Du}{|Du|}(\mathbf{x_0}). \tag{5.2}$$

This relation already suggests that the curvature can be computed in two quite different ways: either as the curvature of a level line extracted from the image and parameterized by

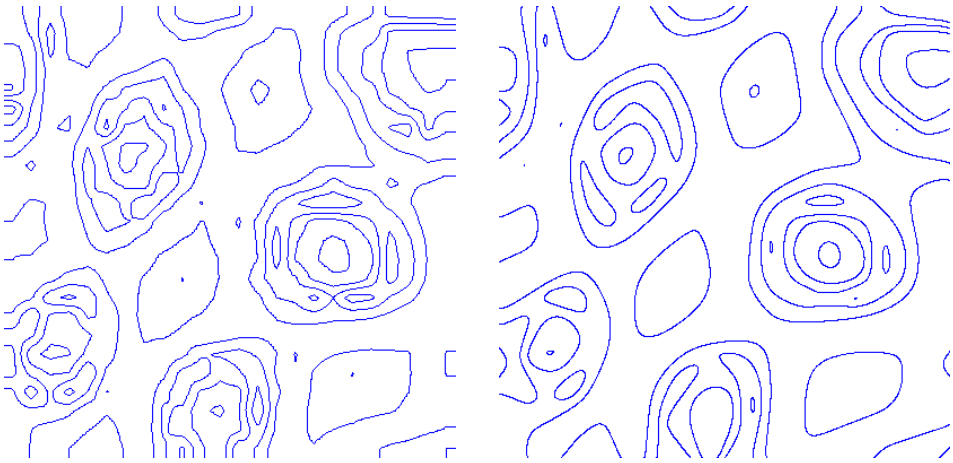

Figure 5.3: Curve evolution by Curve Shortening, or the intrinsic heat equation. By this (nonlinear) evolution a curve instantly becomes smooth and shrinks asymptotically to a circle.

length, or as a 2D differential operator. In both cases, a previous smoothing (of the level line, of the level sets) is necessary, which introduces a new parameter, the smoothing *scale*. Hence the notion of *curvature scale space* which will be associated with curve or image evolutions.

5.2.2 Curve Evolutions

5.2.2.1 Curve Shortening

Curve smoothing by the *heat equation* was one of the first versions of curve analysis proposed by Mackworth and Mokhtarian in [MM86]. Smoothing a curve by separately smoothing the coordinate functions seems reasonable, yet the evolved curve may develop self-crossings and singularities. This model error was corrected in [MM92] by the same authors. Instead of applying the heat equation for relatively long times, they proposed an evolution by *Curve Shortening* (also called *intrinsic heat equation*)

$$\frac{\partial \mathbf{x}}{\partial t} = \kappa(\mathbf{x}). \tag{CS}$$

By this (nonlinear) evolution a curve instantly becomes smooth, shrinks asymptotically to a circle and develops no singularities or self-crossings. The proofs of these properties were given by Gage and Hamilton for convex Jordan curves [GH86] and later extended to embedded curves by Grayson [Gra87].

Theorem 5.2.1 (Grayson, '87)**.** *Let $\mathbf{x}_0$ be a C^2 Jordan curve. By using the intrinsic heat equation, it is possible to evolve $\mathbf{x}_0$ into a family of Jordan curves $\mathbf{x}(t,s)$ such that $\mathbf{x}(0,s) = \mathbf{x}_0(s)$ and such that for every $t > 0$, $\mathbf{x}(t,s)$ is C^∞ (actually analytical) and satisfies the equation (CS). Furthermore, for every $t > 0$, $\mathbf{x}(t,s)$ has only a finite number of inflection points and curvature extrema, and the number of these points does not increase with t. For every initial curve, there is a scale t_0 such that the curve $\mathbf{x}(t,s)$ is convex for $t \geq t_0$ and there is a scale t_1 such that the curve $\mathbf{x}(t,s)$ is a single point for $t \geq t_1$.*

5.2.2.2 Affine Shortening.

The Affine Shortening equation (AS)

$$\frac{\partial \mathbf{x}}{\partial t} = |\kappa|^{-\frac{2}{3}}\kappa(\mathbf{x})$$

is a surprising variant of curve shortening introduced by Sapiro and Tannenbaum in [ST93a], [ST93b]. Angenent, Sapiro and Tannenbaum [ST94] gave the existence and uniqueness proofs for affine shortening and showed a result similar to Grayson's theorem.

Theorem 5.2.2 (Angenent, Sapiro, Tannenbaum, '94)**.** *Let $\mathbf{x}_0$ be a C^2 Jordan curve. Then there is a unique classical solution $\mathbf{x}(t)$ of (AS). The curve eventually becomes convex and thereafter evolves towards an ellipse before collapsing.*

In computer vision the above equations are referred to as *curve scale spaces* or *shape scale spaces*. The term designates any process that smooths a Jordan curve and depends on a real parameter t, the scale. A shape scale space associates with an initial Jordan curve $\mathbf{x}(0,s) = \mathbf{x_0}(s)$ a family of smooth curves $\mathbf{x}(t,s)$. Curve shortening and affine shortening eliminate spurious details of the initial shape and retain simpler, more reliable versions of the shape. These smoothed shapes have finite codes in the sense of Attneave, since they have finitely many curvature extrema. A scale space is *causal* in the terminology of vision theory if it does not introduce new features. (New feature here means: a new extremum for some image differential operator). Thus, curve shortening and affine curve shortening define causal scale spaces. Indeed, the number of curvature extrema and inflexion points decreases by their application.

5.2.3 Image Evolutions

Alvarez *et al.* [AGLM93] characterized axiomatically all image multiscale theories, and gave explicit formulae for the partial differential equations generated by scale spaces. They showed that *causal, local scale spaces* are governed by PDEs and that under sound stability conditions for the scale space, the PDE's have unique viscosity solutions. In particular all causal, local, isometric and contrast invariant scale spaces are given by curvature evolution equations:

$$\frac{\partial u}{\partial t} = |Du|G(\text{curv}(u), t).$$

5.2.3.1 Mean Curvature Motion

The simplest equation in this class for which existence and uniqueness of viscosity solutions can be proved [CGG91],[ES91] is the mean curvature equation

$$\frac{\partial u}{\partial t} = |Du|\text{curv}(u) \qquad \text{(MCM)}$$

We refer to the 'user's guide' of Crandall, Ishii and Lions [CIL92] for further details about viscosity solutions. In this setting, the initial curve Σ_0 is considered as the zero level set of some function u_0 and its evolution is defined as the zero level set of the evolved function

$$\Sigma_t = \{x; u(x,t) = 0\},$$

Figure 5.4: From left to right we display the original image and its evolution by mean curvature motion. In this case, MCM restorates homogeneous parts, acting as a grain filter: small damaged areas vanish by short time smoothing.

shown to be purely geometrical.

Theorem 5.2.3 (Chen-Giga-Goto '91, Evans-Spruck '91)**.** *Let $u_0 \in BUC(\Omega)$. Then there exists a unique viscosity solution in $BUC(\Omega \times [0,\infty))$ of the mean curvature equation with initial data u_0. In addition, the iso-level set Σ_t does not depend upon the particular choice of the initial function u_0.*

5.2.3.2 Affine Curvature Motion

Planar shape recognition algorithms should ideally be projective invariant, namely invariant to all planar homographies. The affine curvature evolution

$$\frac{\partial u}{\partial t} = |Du|\text{curv}(u)^{1/3} \qquad \text{(ACM)}$$

has a more restrictive form of projective invariance: it commutes with all planar affine maps with determinant 1. It is therefore preferable to the scalar curvature motion, and is definitely the most invariant image smoothing algorithm ever. Like the curvature motion, it is invariant to any continuous increasing contrast change $u \to g(u)$.

5.2.4 Connection

A consequence of the contrast invariance for both mentioned equations is that, at least formally, *an image evolves by scalar mean curvature motion (resp. affine curvature motion) if and only if its level lines evolve by curvature shortening (resp. affine shortening).* This fact can be checked by elementary differential calculus under the assumption that the scalar solution $u(t,\mathbf{x})$ is smooth. Yet, precisely, the curvature evolution does not yield a C^2 function in time and space. Thus, the above equivalence is a bit trickier and is proved in Chapter 6.

5.3 Curvature algorithms

All sound shape smoothing algorithms in the computer vision literature perform curve shortening or affine curve shortening. But the numerical variety of the underlying numerical algorithms is worth noticing. This section discusses their history, implementation, advantages and drawbacks. There are three kinds of initial data for the algorithm: digital curves, digital sets, or digital images. We shall examine each in turn.

5.3.1 Algorithms on Curves

5.3.1.1 Discrete Curve Shortening or Dynamic Curve Evolution

As mentioned before, Mackworth and Mokhtarian proposed [MM92] an algorithm consistent with curve shortening (CS). Instead of applying the linear heat equation for relatively long times, it applies to a plane curve the non-linear heat equation, by successively convolving the arc length parameterization $\mathbf{x}(\cdot,t)$ at time n with a Gaussian kernel G_h of standard deviation proportional to $h^{\frac{1}{2}}$. The consistency of Algorithm 1 with (CS) is given by Theorem 5.3.1.

Algorithm 1: Discrete Curve Shortening (CS)

Input: Polygon Σ_0, gaussian signal G
Output: Evolved polygon Σ_n, after n iterations
1 **for** *all* $i = \overline{0,n}$ **do**
2 sample uniformly curve Σ_i ;
3 convolve curve Σ_i with G.

Theorem 5.3.1. *Let* $\mathbf{x}$ *be a* C^2 *curve parameterized by its length parameter* $s \in [0,L]$. *Then*

$$G_h * \mathbf{x}(s) - \mathbf{x}(s) = ch\kappa(\mathbf{x}(s)) + o(h). \tag{5.3}$$

where c *is a positive constant.*

5.3.1.2 Affine Plane Curve Evolution

Several attempts to define an affine-invariant analysis for polygons are described by Sapiro, Cohen and Bruckstein in [SCB97]. The 1/3 power law of planar motion perception and generation was related to affine invariance by Pollick and Sapiro in [PS97].

Moisan [Moi98] discovered an extremely fast and fully affine invariant geometric curve evolution consistent with affine shortening, which we summarize below. In the mathematical morphology terminology, this algorithm is an alternate filter, alternating an affine erosion and an affine dilation.
The consistency of Algorithm 3 with affine shortening (AS) is given in Theorem 5.3.2.

Theorem 5.3.2. *Let* $\mathbf{x}$ *be a* C^2 *curve parameterized by its length parameter* $s \in [0,L]$ *and* $\sigma > 0$. *To each point of* $\mathbf{x}(s)$, *we associate* $\mathbf{x}_\sigma(s)$, *defined as the middle point of the chord* $(\mathbf{x}(s-\delta),\mathbf{x}(s+\delta))$,

Algorithm 2: Discrete Affine Shortening (AS)

Input: Polygon Σ_0,
Output: Evolved polygon Σ_σ, at scale $\sigma^{2/3}$
1 break the curve into convex and concave parts ;
2 **for** *every convex/concave component* **do**
3 replace each component by the sequence of the middle points of each σ-chord such that one endpoint is a vertex of the polygonal curve;
4 concatenate the pieces of curves previously obtained.

where $\delta > 0$ is chosen in order that the area of the region enclosed by this chord and the piece of curve $\mathbf{x}|_{(s-\delta,s+\delta)}$ be equal to δ. Then

$$\mathbf{x}_\sigma(s) - \mathbf{x}(s) = c\sigma^{2/3}|\kappa(\mathbf{x})|^{-2/3}\kappa(\mathbf{x}) + o(\sigma^{2/3}) \text{ as } \sigma \to 0$$

where c is a positive constant.

Lisani and al. [LMMM00] and later Musé and al. [MSC+06] have used the affine curve evolution scheme for shape recognition and image comparison algorithms. We have limited ourselves to numerical schemes that are extremely fast, being linear or, in the case of Moisan's scheme, super-linear in time and unconditionally stable.

5.3.1.3 Backward Euler Method for Nonlinear Diffusions

There is, however, a rich literature on numerical schemes for anisotropic curvature motions occurring (e.g.) in crystalline formation. These motions can depend on other powers of the curvature than the relevant ones for image processing (1 and 1/3) and have a spatial anisotropy.

Mikula and Ševčovič have given theoretical and numerical methods for such more general curvature motions [MŠ99], [MŠ01]. They use implicit methods for curve evolution, which are very accurate but too slow to be performed on all image level lines. Their schemes are able to cope with almost arbitrarily high or low powers of the curvature, and they display an accurate asymptotic behavior.

Algorithm 3: Backward Euler Method for nonlinear diffusions

Input: Polygon Σ_0,
Output: Evolved polygon Σ_σ, parametrized by x_i at time $t_i = i\tau$
1 **for** *each* $i = 0,n$ **do**
2 find x_{i+1} by a semi-implicit finite difference scheme of the type

$$\frac{x_{i+1} - x_i}{\tau} = f_i(k_i, x_{i+1})$$

with f_i a nonlinearity depending on the curvature k_i of the curve x_i and the natural parameterization of the curve itself.

Cao and Moisan [CM02] have also proposed "morphological" schemes for the motion of curves by arbitrary powers of the curvature. They are described in detail in the book by Frédéric Cao [Cao03], which also contains a thorough numerical and mathematical analysis. For more general image PDE's performing nonlinear diffusion, finite volume methods have been proposed with remarkable results in [KM02].

5.3.2 Algorithms on Sets

Koenderink and van Doorn defined a *shape* in $\mathbb{R}^N$ as any closed subset X of $\mathbb{R}^N$ [KvD86]. They proposed to simulate the shape multiscale perception by applying the heat equation to the characteristic function of the shape, or, in other terms, to convolve it with Gaussians with increasing variance. Of course, the solution $G_t * \mathbf{1}_X$ is not a characteristic function and therefore the authors defined the evolved shape at scale t to be

$$X_t = \{\mathbf{x} \mid u(t,\mathbf{x}) \geq 1/2\}.$$

Similar to the heat equation for curve evolution, the method presents two inconveniences: the possible fusion of shapes which are too close, and the development of new singularities, which occur precisely at the times where two disjoint shapes coalesce.

The improvement of *dynamic shape* analysis is due to Merriman, Bence, and Osher who discovered and heuristically argued in [MBO92] that the convolution of the indicator function of a shape with a Gaussian followed by a threshold at $1/2$ simulated the mean-curvature motion.

Algorithm 4: Merriman-Bence-Osher Algorithm (threshold dynamic shape)

Input: initial shape X_0
Output: Evolved shape X_n at scale nh
for *i=0,n-1* **do**
    convolve the characteristic function of the shape X_i with G_h, where h is small;
    define $X_{i+1} = \{\mathbf{x} \mid G_h * \mathbf{1}_{X_i} \geq 1/2\}$.

The consistency of their arguments was checked by Barles and Georgelin [BG95] and Evans [Eva93]. In addition they showed that iterated median filters converge asymptotically to the *Mean Curvature Motion*

$$u_t = |Du|\text{curv}(u). \tag{MCM}$$

An extension of this result to all iterated weighted median filters was given by Ishii in [Ish95].

Algorithm 4 of Merriman, Bence and Osher is nothing but an *iterated median filter* applied to a binary image. The main problem of discrete median filters is their grid dependence which make them blind to small curvatures. For instance a black disk with radius 9 does not move if the discrete gaussian has a 2 pixels standard deviation. It is observed that the iterated process stops after a few iterations, making it an inaccurate scheme for MCM.

5.3.3 Algorithms on Images

5.3.3.1 Median Filters and Threshold Dynamics

Weighted median filters are defined by

$$\mathrm{Med}_k u(\mathbf{x}) = \inf_{B\in\mathscr{B}} \sup_{\mathbf{y}\in\mathbf{x}+B} u(\mathbf{y}). \tag{5.4}$$

where k is a radial density distribution and $\mathscr{B} = \{B \mid \int_B k(\mathbf{x})d\mathbf{x} = 1/2 \int k(\mathbf{x})d\mathbf{x}\}$, $\mathscr{B}$ being formed of measurable sets. The discrete implementation of the median filter is almost trivial.

Algorithm 5: Iterated Median Filter Algorithm

Input: initial image $u(\mathbf{x})$
Output: evolved image $\mathrm{Med}_k u(\mathbf{x})$

```
for every point x do
    consider the points y in a discrete neighborhood of x;
    compute the weight of y as the integral of k over the pixel of center y;
    take the weighted median value of the discrete neighborhood.
```

Algorithm 5 is fast but, like the dynamic shape, it is blind to small curvatures. Indeed, this algorithm applied on binary images is nothing but the dynamic shape, with the kernel k instead of a Gaussian [GM00]. The link with the curvature motion is obtained by scaling the convolution, exactly as in the Merriman-Bence-Osher dynamic shape algorithm. The result was shown by Guichard and Morel in [GM00]. Define the scaled median by $(\mathrm{Med}_k)_h = \mathrm{Med}_{k_h}$, where $k_h(\mathbf{x}) := \frac{1}{h^2}k(\frac{\mathbf{x}}{h})$. Then:

Theorem 5.3.3 (Guichard, Morel)**.** *If $u : \mathbb{R}^2 \to \mathbb{R}$ is C^2, then there is a constant c_k depending only on the kernel k such that*

1. *on every compact set $K \subset \{\mathbf{x} \mid Du(\mathbf{x}) \neq 0\}$,*

$$\mathrm{Med}_{k_h} u(\mathbf{x}) - u(\mathbf{x}) = c_k |Du(\mathbf{x})| \mathrm{curv}(u)(\mathbf{x}) h^2 + O(\mathbf{x}, h^3),$$

   where $|O(\mathbf{x}, h^3)| \leq C_K h^3$ for some constant C_K that depends only on u, k and K;

2. *on every compact set K in $\mathbb{R}^2$,*

$$|\mathrm{Med}_{k_h} u(\mathbf{x}) - u(\mathbf{x})| \leq C_K h^2$$

   where the constant C_K depends only on u, k and K.

In short, by the above theorem the iterated median filter is in theory an implementation of the mean curvature motion but, when applied on a digital image, it stops prematurely because of the blindness of the grid to small curvatures.

Adam Oberman's work [Obe06] is intimately related to median filters and to the threshold dynamics. The novelty of his paper consists in the radial lattice displacement of the neighborhood points, as well as its 3D variant. Accordingly, he gives a clever consistency proof. The

scheme is obviously monotone and therefore the convergence is guaranteed by the general approximation results for viscosity solutions given by Barles and Souganidis in [BS91].

5.3.3.2 Finite Difference Schemes

There are antecedent papers proposing robust schemes for the mean curvature motion or (more rarely) for the affine curvature motion. But, to the best of our knowledge, these papers do not attempt to compute the curvatures of the image. The present work defends the thesis that the curvature is a 1D operator, computable only on the level lines themselves, and only after the adequate smoothing has been applied to each level line.

FDSs either create oscillations or, if they are adequately regularized to avoid oscillations, cause a strong and spurious diffusion. As illustrated later on, even the tiniest diffusion or oscillation created by an FDS brings up spurious curvatures with erratic value and sign. To emphasize this diffusion-sharpness dilemma, we shall make a comparison between Guichard's scheme, which attempts to be the least diffusive and the most isotropic, the Crandall-Lions scheme [CL96], which is monotone but diffusive, and subsequently the standard finite difference scheme that discretizes formula (1).

Alvarez-Guichard-Morel's Finite Difference Scheme

An efficient finite difference scheme (FDS) implementation of the scalar curvature motions was proposed by Alvarez and Guichard and is described in [GM97] and [AM99]. Together with Marco Mondelli, we give in [MC10] a thorough analysis of this finite difference scheme for the mean curvature motions and its affine variant, also called the affine morphological scale space, in the image processing framework. This analysis brings in a series of parameters that allow us to compute an *accurate discrete* evolution of curvature motions. The choice of these parameters is based on intrinsic geometric properties of the evolution equations for *linear*, *radial* and *elliptical* functions. A detailed explanatory report, the ANSI C implementations and an on-line demo can be found in [CM10b].

The numerical scheme takes advantage of the diffusive interpretation of the equation, which can be expressed as the second derivative of u in the direction orthogonal to the gradient

$$|Du|\text{curv}(u) = u_{\xi\xi},$$

where $\xi = Du^{\perp}/|Du|$. The derivative is evaluated on a 3×3 stencil, as a linear combination of the corresponding values.

Denote the discrete samples of a continuous image u on a grid by $u_{i,j} = u(i\Delta x, j\Delta y)$. When $Du \neq 0$ the second derivative in the ξ direction can be expressed as

$$\begin{aligned}(u_{\xi\xi})_{i,j} \quad = \quad & \frac{1}{\Delta x^2}\big(-4\lambda_0 u_{i,j} + \lambda_1(u_{i+1,j} + u_{i-1,j}) + \lambda_2(u_{i,j+1} + u_{i,j-1}) + \\ & + \lambda_3(u_{i+1,j+1} + u_{i-1,j-1}) + \lambda_4(u_{i+1,j-1} + u_{i-1,j+1})\big)\end{aligned}$$

and thus the iterative sequence is defined by

$$u_{i,j}^{n+1} = u_{i,j}^{n} + \Delta t \cdot (u_{\xi\xi}^{n})_{i,j}. \tag{5.5}$$

Instead, if $|Du| = 0$, MCM is not well defined. Moreover when the gradient is small, its direction becomes substantially random, as it is driven by rounding and approximation errors, inevitable when dealing with a discrete scheme. Thus, when $|Du| < T_g$, we diffuse by half Laplacian, which is the expectation of $u_{\xi\xi}$ for a uniformly distributed ξ,

$$u_{i,j}^{n+1} = u_{i,j}^{n} + \frac{1}{2}\Delta t \cdot (\Delta u^n)_{i,j}, \tag{5.6}$$

with $(\Delta u)_{i,j} = u_{i+1,j} + u_{i-1,j} + u_{i,j+1} + u_{i,j-1} - 4u_{i,j}$.

A straightforward variant of the FDS applies to the affine curvature motion. The FDS is optimized to be as isotropic as possible and as close as possible to satisfy the maximum principle. It improves on the dynamic shape by computing correctly small curvatures, but it cannot properly handle the contrast invariance of the curvature equation. As shown in Fig. 5.5, the FDS creates new grey levels and blurs edges, spurious diffusions occur around image extrema and curves with thin boundary break and eventually collapse.

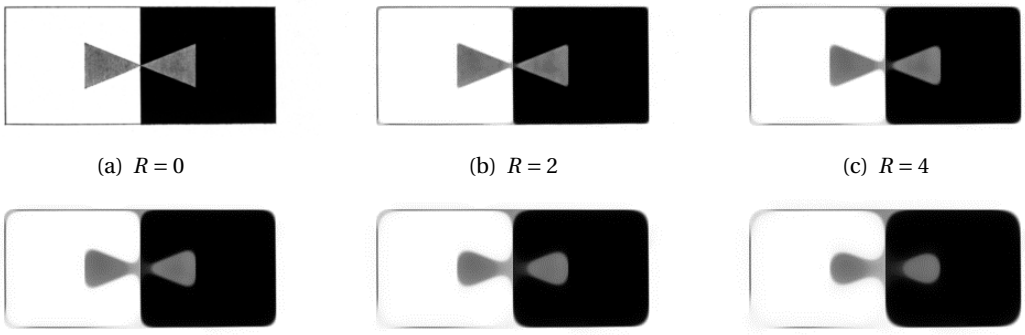

(a) $R = 0$ (b) $R = 2$ (c) $R = 4$

(d) $R = 6$ (e) $R = 8$ (f) $R = 10$

Figure 5.5: Mean curvature evolution of an image by a finite difference scheme. Each R represents the renormalized scale, i.e. a circle with radius R will disappear.

Crandall-Lions's Finite Difference Scheme

The finite difference scheme described by Crandall and Lions in [CL96] is monotone, consistent and stable; therefore its convergence is guaranteed by general approximation results (Barles and Souganidis [BS91]). Denote by u^n the discrete approximation of the solution at iteration n. Then the Crandall-Lions discrete curvature flow V is defined by

$$\begin{aligned} Vu^{n+1}(\rho z) &= u^n(x) + \\ & dt \sum_{i=1}^{N} \frac{u^n(\rho z + ha(Du^n(\rho z))e_i) + u^n(\rho z - ha(Du^n(\rho z))e_i) - 2u^n(\rho z)}{h^2} \end{aligned}$$

for all $z \in \mathbb{Z}^N$, where $\{e^i\}_{i=1,N}$ is the standard basis of $\mathbb{R}^N$ and

$$a(p) = I - \frac{p \otimes p}{|p|^2}.$$

There are for this scheme three delicate issues.

1. *The above formula does not fully discretize on a fixed grid* $\mathcal{G}_\rho$ because $a((Du^n)(\rho z))e_i$ is not a displacement on the grid. Thus, this is an adaptive stencil. One must involve for every grid function u^n its continuous piecewise linear interpolation $\tilde{u}^n$. Hence, the previous formula must be updated as

$$Vu^{n+1}(\rho z) = \tilde{u}^n(x) + \\ dt\sum_{i=1}^{N}\frac{\tilde{u}^n(\rho z + ha(Du^n(\rho z))e_i) + \tilde{u}^n(\rho z - ha(Du^n(\rho z))e_i) - 2u^n(\rho z)}{h^2}$$

   Note that in a second part of the paper the authors show that *the comparison principle cannot be guaranteed for finite difference schemes with a fixed stencil,* even for the linear case, when the matrix a has constant coefficients. This means that *a centered differences approximation dealing with fixed stencils* can create spurious oscillations and therefore parasitic curvatures. The scheme introduced by Guichard is a sort of intermediate solution: it *estimates the gradient direction* ξ *by evaluating numerically* $u_{\xi\xi} = curv(u)|Du|$ *with a quasi-linear scheme, based on a* 3×3 *stencil.* The scheme is quasi-linear because the coefficients of the linear combination are functions of the angle θ that the gradient direction makes with the horizontal axis.

2. The (updated) discretization scheme is not monotone. *To ensure monotonicity one has to add a diffusion term.* Thus the discretization scheme becomes

$$Tu^n = Vu^n + \alpha\Delta u^n,$$

   where

$$\Delta u^n = dt\sum_{i=1}^{N}\frac{u^n(\rho z + \rho e_i) + u^n(\rho z + \rho e_i) - 2u^n(\rho z)}{\rho^2}$$

   Even though asymptotically we still have consistency of this monotone scheme, numerically *this scheme introduces a 2D diffusion.*

3. The projection $a(p)$ has two unpleasant features: it is degenerate (in the sense that aa^T has zero eigenvalues) and has a singularity at $p = 0$. The first drawback can be easily handled by the choice of parameters such that the approximation scheme produces bounds on the perimeter. For the second one, one should replace $a(p)$ by

$$a_\varepsilon(p) = I - \frac{p\otimes p}{|p|^2+\varepsilon}.$$

   However, when the gradient is small, its direction becomes substantially random, being driven by rounding errors and noise. This is why Guichard et al. suggest to replace in this case the mean curvature diffusion by a half Laplacian, instead of using $a_\varepsilon(p)$.

Accordingly, several relations must be satisfied among the parameters to ensure convergence of the scheme to the continuous solution when $dt \to 0$. There is no convergence result for Guichard's scheme. Again, a small perturbation with a linear diffusion term should handle the problem, but would also render the scheme very diffusive in practice.

One can devise an FDS for the curvature motion which is monotone and consistent. However, all such schemes cause, even after few iterations, a non asked diffusion that creates new levels and spurious curvatures. As illustrated by Figure 5.6 and their comments, computing a curvature by FDS is simply disastrous, even on an image smoothed by LLS.

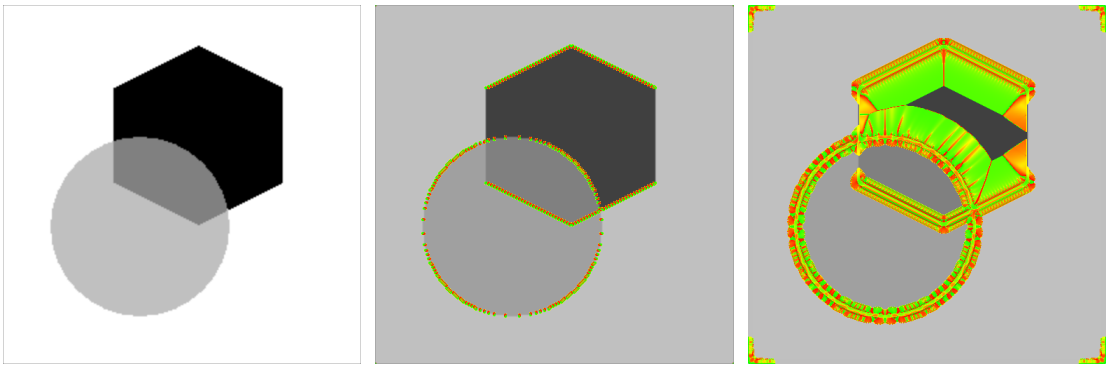

Figure 5.6: From left to right we display: original image sampled on a thin grid (using a bilinear zoom), curvatures computed with a finite difference scheme on the original image, curvatures computed with a finite difference scheme on the affine curvature evolution of the image.

Semi-Implicit Finite Difference Schemes

A different approach was given by Peter Smereka in [Sme03], where he uses semi-implicit methods to derive fast implementation of the level set evolution PDEs for curvature motions. The semi-implicit algorithm for the mean curvature flow is based on the formula

$$\text{curv}(u)|Du| = \Delta u - N(u)$$

where u is parameterized so that it remains close to the distance function (thus $N(u)$ is small and $|Du| \approx 1$). The discretization takes one step of forward Euler on the nonlinear term followed by one step of backward Euler on the linear term.

5.3.3.3 Level Set Extension, Superposition Principle, Stack Filters

FDSs for image curvature motions do not commute with increasing contrast changes. Yet, a full contrast invariance can be restored on any numerical scheme by coupling two techniques: the *superposition principle*, and the Osher-Sethian *level set extension*. The idea of the level set extension [OS88] is to treat a given curve as the zero level line of a signed distance to the curve. More generally a set, understood as a shape, is identified with its characteristic function. After applying the FDS to this function the evolved set can be obtained as the $1/2$ upper level set of the evolved function. Thus, the level set extension is a generalization of the threshold dynamic.

By the level set extension, a curve evolution is made in two steps: a) apply the FDS to the characteristic function of the shape bounded by the curve; b) take the $1/2$ level line of the result.

Since the image level lines are boundaries of the image upper level sets, it is natural to apply directly the level set extension to all upper level sets. This processes implicitly all level lines

of each level. After evolution of all upper level sets, an image is reconstructed by *superposition principle*. The superposition principle and its link to the contrast invariance property come from mathematical morphology [Ser82], [MS87]. If all upper level sets of a given image have been processed independently by an inclusion preserving scheme, then there is a single image having for level sets the evolved level sets. Any process that decomposes the image into the *stack* of its level sets and then reconstructs the processed image from the stack of its processed level sets is called a *stack filter*. The only requirement to make a stack filter with any numerical scheme is its monotonicity. Indeed, the inclusion of upper level sets in each other must be preserved. *Every stack filter is contrast invariant.* Indeed, the image upper (resp. lower) level sets $\mathscr{X}_\lambda u_0 := \{\mathbf{x}, u_0(\mathbf{x}) \geq \lambda\}$ (resp. $\leq \lambda$) of an image u_0 are invariant to increasing contrast changes.

In short a stack filter consists of:

a. extracting all image upper level sets,
b. processing each of them by a (monotonic) set operator (e.g. the FDS) and
c. reconstructing the evolved image by "superposition".

Thus Algorithm 6 is a contrast invariant curvature evolution. For example (see [GM97]) the image median filter is the stack filter of the threshold dynamics. It makes sense to apply the superposition principle strategy to FDSs because they are not contrast invariant, being diffusive and creating spurious level lines.

Algorithm 6: Stack Filter

Input: initial image $u(\mathbf{x})$
Output: evolved image $u(t,\mathbf{x})$
for *each* $\lambda \in [0,255]$, *in increasing order* **do**
  let $v_\lambda(\mathbf{x})$ be the characteristic function of $\mathscr{X}_\lambda u_0 := \{\mathbf{x}, u_0(\mathbf{x}) \geq \lambda\}$;
  apply to v_λ an FDS-scheme until scale t; this yields the images $w_\lambda(t,.)$;
  set $u(t,\mathbf{x}) = \max\{\lambda \mid w_\lambda(t,\mathbf{x}) \geq 1/2\}$ at each point $(t,\mathbf{x})$.

5.4 Discussion

One can devise an FDS for the curvature motion which is monotone and consistent. The not excessive complexity of our Finite Difference Schemes makes them an *easy to implement* and *fast to run* alternative for the operations of preprocessing common to almost all kinds of further numerical image analysis. On the other hand, FDSs lack some of the structural properties that characterize curvature motions, namely:

- *monotonicity*, since the FDSs always lead to slightly oscillatory solutions;
- *contrast invariance*, since they create new gray levels and blur edges;
- *Euclidean or affine invariance*, since they are grid dependent.

The first two problems could be overcomed by level set methods and *stack filters*. This means to apply the previous FDSs not directly to the input image, but to the characteristic

functions of its level sets and eventually to reconstruct the output image by superposition principle. However, stack filters are much slower than FDSs. In addition, they are still *pixel-based* and thus by evolving sets sampled on a fixed grid boundaries either jump by a positive integer number of pixels or do not move at all. It follows that these numerical motions are quantized and therefore blind to small curvatures. As we shall see in the experiments, they fall short of matching the human perception precision.

A more accurate procedure should sample all image level lines at a sub-pixel fine resolution and smooth them separately. A continuous, grid independent evolution of a digital image by curvature motion, that can jump over the hurdles listed above, is described in the following chapters. The *Level Lines Shortening* (*LLS*) algorithm extracts a sufficient number of level lines from the input image u_0, applies to each of them the geometric curvature motions and uses these evolved level lines to reconstruct the output evolved image.

CHAPTER 6

From Level Lines Shortening to Image Curvature Motion

It is through science that we prove, but through intuition that we discover.
Henri Poincare (1854 - 1912)

Abstract: In this chapter we define the continuous *Level Lines Shortening (LLS)* evolution of a two-dimensional image as the *Curve Shortening* operator acting simultaneously and independently on all the level lines of the initial data, and show that it computes a viscosity solution for the mean curvature motion. This provides an exact analytical framework for its numerical implementation, which runs online on any image at http://www.ipol.im/. Analogous results hold for its affine variant version, the Level Lines Affine Shortening. [1]

Résumé : Nous définissons dans ce chapitre l'évolution continue d'une image par *Level Lines Shortening (LLS)* comme l' opérateur de *Curve Shortening* qui agit simultanément et indépendamment sur chaque ligne de niveau de l'image de départ. On démontre que LLS donne de manière explicite une solution de viscosité pour le mouvement par courbure moyenne. Ceci correspond précisément à l'implémentation numérique, qui peut être testé en ligne sur tout image sur http://www.ipol.im/. Des résultats similaires sont montrés pour le mouvement par courbure affine.

Keywords: mean curvature motion, affine curvature motion, curve shortening, affine shortening, level lines, topographic maps

[1] This represents the article *A proof of equivalence between level lines shortening and curvature motion in image processing*, submitted to SIAM Journal on Mathematical Analysis, joint work with J.M. Morel. [CM]

Contents

6.1 Introduction

Geometric evolution equations, like the Curve Shortening problem

$$\frac{\partial x}{\partial t} = \mathbf{k}(x). \tag{CS}$$

have been studied in great detail using parametric methods from differential geometry. Many interesting results have been obtained in the past twenty five years. It is impossible to present them all, but we will focus on some results which our work is based on. It all goes back to '83, when Michael Gage proved an isoperimetric inequality for convex curves [Gag83]. This turned out to have an important application to curve shortening: namely a curve deformed along its normal vector field at a rate proportional to its curvature will have a decreasing ratio of L^2/A. One year later, Gage showed [Gag84] that the isoperimetric ratio L^2/A of the convex curve approaches 4π as the enclosed area approaches zero. Furthermore, if the one parameter family of curves $x(\cdot,t)$ is normalized by homotetic expansion such that each curve encloses area π, then the normalized flow converges to the unit circle. In a subsequent paper, Gage and Hamilton [GH86] showed that the evolving convex curves will not develop singularities and the evolution continues until the area inside the curve is zero. Grayson added in [Gra87] the fact that embedded curves become convex without developing singularities, closing thus the conjecture that curve shortening shrinks embedded plane curves smoothly (with convergence in the C^∞ topology) to points, with round limiting shape.

These results were extended to smooth curves embedded in a smooth Riemannian surface which is convex at infinity by Grayson [Gra89] and to arbitrary closed immersed curves on complete surfaces of bounded curvature by Gage [Gag90].

Motivated by finding affine invariant flows in computer vision and image processing [ST93a], [ST93b] Sapiro and Tannenbaum defined an affine invariant curve evolution in [ST94]

$$\frac{\partial x}{\partial t} = |\mathbf{k}|^{-2/3}\mathbf{k}(x). \tag{AS}$$

They proved an affine version of the classical isoperimetric inequality. Similarly to curve shortening, this inequality is used to show that in the case of convex plane curves, the affine isoperimetric ratio is a non-decreasing function of time. The authors showed that this affine isoperimetric ratio converges to the value for the ellipse $8\pi^2$ and that the evolving curve converges, in the Hausdorff metric, to an ellipse. In a subsequent paper they extended the affine shortening flow to non-convex curves [AST98] and showed that any simple closed curve shrinks to a point under (AS) flow.

However, if the curves are immersed in the plane but not embedded they will surely develop singularities, though they stay smooth until the curvature blows up. If one considers for example the Limaçon of Pascal (given in polar coordinates by $r = 1 + 2cos(\theta)$), then the little loop will shrink faster than the big loop and eventually turns into a cusp. In the higher dimensional case, G. Huisken has shown [Hui84] that a convex hypersurface shrinks to a point. Nevertheless, embedded surfaces in space can develop singularities if they are not convex. For example, a dumbbell will pinch off and pop, changing the topological type of surface.

It is thus difficult to track the evolution of the curve (or the hypersurface) across singularities, by parametric methods. To overcome the problems generated in the classical geometric approach, some alternative descriptions were given. There have been two different undertakings: in the setting of varifold theory from geometric measure theory [Bra78], and in the setting of level set methods [OS88] and accordingly, of viscosity solutions as in Crandall and Lions [CL83], Crandall, Evans and Lions [CEL84], Jensen, Lions and Souganidis [JLS88], Ishii [Ish89] and C randall, Ishii and Lions [CIL92]. In the following we make precise the latter.

The curve, or more generally the hypersurface, is given as the zero level set of some continuous function u_0

$$\Sigma_0 = \{x; u_0(x) = 0\}.$$

One considers then the Cauchy problem for the parabolic PDE

$$\frac{\partial u}{\partial t} = |Du|\text{curv}(u), \tag{MCM}$$

with initial data u_0, and defines the evolution of Σ_0 at time t as the zero level set of $u(\cdot, t)$

$$\Sigma_t = \{x; u(x, t) = 0\}$$

Osher and Sethian [OS88] and Sethian [Set99] used various techniques to study the (MCM) flow and related PDEs numerically, whereas the theoretical justification was given by Chen-Giga-Goto in [CGG91] and Evans and Spruck in [ES91]. They showed there exists a unique bounded, uniformly continuous viscosity solution of (MCM) and that the definition of the generalized motion by mean curvature does not depend on the choice of the initial function. The work of Chen, Giga and Goto [CGG91], Giga and Goto [GG92] included as well generalizations

to a large class of geometric problems, covering in particular the affine curvature motion

$$\frac{\partial u}{\partial t} = |Du|\big(\mathrm{curv}(u)\big)^{1/3}. \tag{ACM}$$

However, for semi-continuous initial data, there is in general, *more than one solution* of the initial value problem as pointed out by Soner in [Son93]. In fact, this is the case whenever the level set develops a nonempty interior or becomes 'fat'. This difficulty was explained by Barles, Soner and Souganidis in [BSS93].

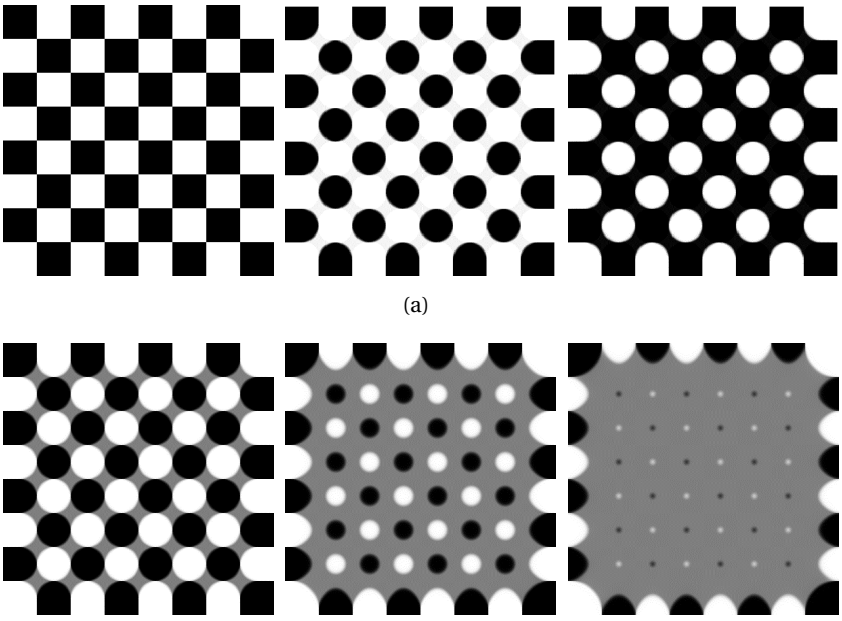

(a)

(b)

Figure 6.1: Checkerboard image evolving by mean curvature motion. (a) The fattening phenomena discards uniqueness of solutions for semi-continuous functions. (b) For bounded uniformly continuous initial data, the level set is uniquely defined.

The *Level Lines Shortening (LLS)* builds on the previous mentioned contributions and connects explicitly the geometric approach for curve shortening evolutions and the viscosity framework for curvature motions. More precisely, LLS is an operator that first extracts all the level lines of an image, then independently and simultaneously smooths all of its level lines by curve shortening (CS) (respectively affine shortening (AS)) and eventually reconstructs, at each step, a new image from the evolved level lines. The chain is based on a topological structure, the inclusion tree of level lines as a full and non-redundant representation of an image [CM10a], and on a topological property, the monotonicity of curve shortening with respect to inclusion. Therefore, the hierarchy of the level lines is maintained while performing the smoothing.

The aim of this chapter is to rigorously justify that the Level Lines Shortening computes explicitly a viscosity solution for the *Mean Curvature Motion* respectively that the Level Lines Affine Shortening provides a viscosity solution for the *Affine Curvature Motion*. Evans and Spruck checked in [ES91] the consistency of the level set approach with the classical motion

by mean curvature. More precisely, they showed that the mean curvature motion agrees with the classical motion, if and as long as the latter exists. The results applies for a smooth hypersurface, given as the connected boundary of a bounded open set. Their arguments are based on comparison techniques with lower barriers for the approximated mean curvature motion and strongly use the fact that the hypersurface is the zero level set of its (signed) distance function. However, the result does not describe the complete behavior of *all* the level lines of a Lipschitz function. Namely, if we are given a Lipschitz function u_0 which evolves by mean curvature in the viscosity sense, are all of its level lines evolving independently by curve shortening? For dimension $n \geq 3$ the result is not true, since hypersurfaces can develop singularities and can change topology. Thanks to Grayson's theorem, the 2D case has a very peculiar structure which we will take advantage of. We will show that evolving independently and simultaneously by curve shortening *all* the level lines of a function is equivalent to applying directly a mean curvature motion to the functions itself.

The initial image will be considered as an element of a particular space of functions $\mathcal{VS}(\Omega)$ that we term space of very simple functions and is related to fattening phenomena for Lipschitz continuous functions. This class corresponds to bilinearly interpolated images defined on a rectangle Ω whose topographic maps contain only Jordan curves. The set of very simple functions arises naturally in image processing, since level lines corresponding to noncritical levels are sufficient to grant an exact reconstruction of the digital image (see Chapter 7).

In this way, the described chain corresponds exactly to its numerical implementation [CMMM] and has the advantage of satisfying both numerically and analytically all the invariance properties required by the scale space in question. The discrete LLS overcomes all the hurdles arising with numerical methods based on pixel approximation. In addition, this scheme leads to an accurate curvature estimate, based on a direct computation on all its level lines.

The chapter is organized as follows. In section §6.2 we define the class of very simple functions as approximations for Lipschitz functions. Section §6.3 is devoted to the definition of the Level Lines Shortening evolution, as an operator acting both on crowns of Jordan curves and flat areas, and on very simple functions. In the last section §6.4 we give the equivalence result.

6.2 Modeling Level Lines Shortening

6.2.1 Crowns of Jordan Curves

A Jordan curve is a one to one continuous map from the unit circle S^1 into $\mathbb{R}^2$. A Jordan curve Σ splits the plane in two connected components. We denote by $Int(\Sigma)$ the open bounded component and by $Ext(\Sigma)$ the open unbounded component.

Definition 6.2.1. *Let Σ^1 and Σ^2 be two Jordan curves. We say that Σ^1 **surrounds** (strictly) Σ^2 and we write $\Sigma^1 \preceq \Sigma^2$ ($\Sigma^1 \prec \Sigma^2$) if $Int(\Sigma^1) \subseteq Int(\Sigma^2)$ (respectively $\overline{Int(\Sigma^1)} \subset Int(\Sigma^2)$).*

This defines a partial order on the set of planar Jordan curves.

[1] http://www.ipol.im/pub/algo/cmmm_image_curvature_microscope/

Definition 6.2.2. *We say that a Jordan Σ curve is **piecewise** C^1, or in $C_p^{0,1}(S^1)$ if it has finite length $l(\Sigma) \geq 0$, any length parametrization is piecewise C^1 and if at each discontinuity point for the tangent there are left and right tangent vectors, which are not collinear.*

Definition 6.2.3. *We say that a sequence of curves Σ^n **converges** in $C_p^{0,1}(S^1)$ to a curve Σ if, denoting by $s \in [0, l(\Sigma)] \to x(s)$ a length parameterization of Σ, there are Lipschitz parameterizations $s \in [0, l(\Sigma)] \to x^n(s)$ for Σ^n such that $x^n(s)$ tends uniformly to $x(s)$, and the left and right unit tangent vectors of $x^n(s)$ tend uniformly to the left and right tangent vectors of $x(s)$.*

Remark 6.2.1. When $l(\Sigma) = 0$, these conditions are reduced to the uniform convergence of $x^n(s)$ toward $x(s)$. This convergence can be defined by a family of neighborhoods around each element of $C_p^{0,1}(S^1)$, which therefore is a topological space.

Definition 6.2.4. *A **crown** $\Sigma : (\lambda, \mu) \to C_p^{0,1}(S^1)$ is a continuous and monotone map Σ from the interval (λ, μ) into $C_p^{0,1}(S^1)$. If the map is defined on the closed/open interval we talk about **closed/open crown**.*

Definition 6.2.5. *When the crown is closed and increasing, $\Sigma(\lambda) = \Sigma^\lambda$ is called the **interior curve of the crown** and $\Sigma(\mu) = \Sigma^\mu$ its **exterior curve of the crown**. If the crown is decreasing, these names exchange. The range of the open/closed crown is denoted by $\Sigma(]\lambda, \mu[)$, $\Sigma([\lambda, \mu])$, respectively. The crown itself as an ordered family of curves will also be denoted by $\Sigma^{[\lambda,\mu]}$ or $(\Sigma^\nu)_{\nu\in(\lambda,\mu)}$.*

Remark 6.2.2. It is known [Bou66] that given two linearly ordered sets X and Y endowed with the topologies $\tau(X)$ and $\tau(Y)$ respectively, then ϕ is a homeomorphism of X onto $\phi(X)$ if and only if ϕ is continuous and strictly monotone. Therefore, a crown Σ as defined above is a homeomorphism from (λ, μ) onto $\Sigma^{(\lambda,\mu)}$.

Definition 6.2.6. *Let $A \subset \Omega$ be a bounded, connected set, whose boundary consists of a finite number of disjoint Jordan curves. We call **exterior curve of** A the unique Jordan curve Σ^e whose interior contains A and **interior curve(s)** the other Jordan curves Σ^i, $i \in I$.*

6.2.2 The Class of Very Simple Functions

A digital image is usually known by its samples $\{u(i, j)\}_{0\leq i\leq M, 0\leq j\leq N}$. on a rectangular grid of $\Omega = [0, M] \times [0, N]$, We assume that the underlying image $0 \leq u(x) \leq 1$ whose samples are the $u(i, j)$ is a Lipschitz function defined on Ω, the continuous image domain. We shall always assume that $u(x) = 0$ on the boundary of the domain $\partial\Omega$ and that $u(x) > 0$ in the interior of Ω.

The bilinear interpolation in Ω is the simplest continuous interpolation from the discrete samples $u(i, j)$. This interpolate, still denoted u, is defined as the unique function coinciding with the digital image u on the samples which is bilinear in each dual pixel. This means that u has the form

$$u(x_1, x_2) = \alpha x_1 + \beta x_2 + \gamma x_1 x_2 + \delta$$

on each square with vertices (i, j), $(i + 1, j)$, $(i, j + 1)$, $(i + 1, j + 1)$. This bilinear interpolation is therefore positive on the interior of the domain and zero on $\partial\Omega$. The set of bilinear interpolates of digital images on Ω will be denoted by $\mathscr{BL}(\Omega)$. The next result is a sane consistency property of the bilinear interpolation.

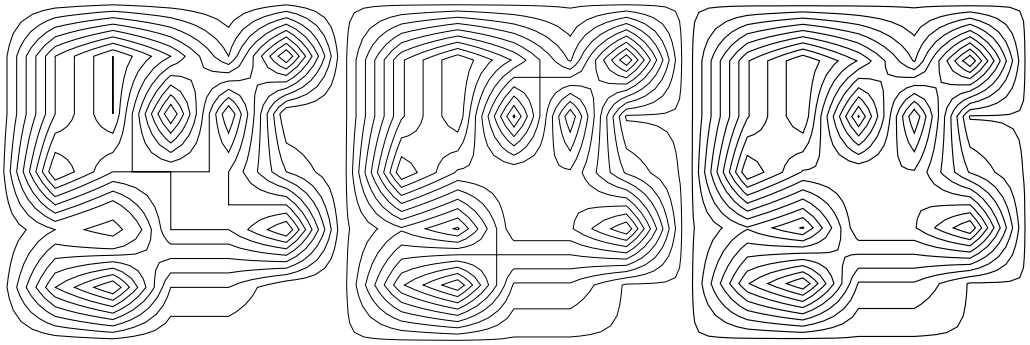

(a) (b) (c)

Figure 6.2: Topological structure of the family of level lines, for a bilinear interpolated image. For every level $0 \leq \lambda \leq 1$, except for a finite set, the iso-level sets $\{u = \lambda\}$ are made of a finite set of piecewise C^1 Jordan curves. At critical levels λ_k, they can have a rather complicated form: they can have T-junctions or reduce to segments (a), contain square pixels (thus being flat areas) or have self-crossings at saddle points (b). However, by fattening the iso-level sets corresponding to the critical levels, the topology of level sets becomes very simple: only Jordan curves or flat sets (c).

Proposition 6.2.1. *If u defined on Ω is Lipschitz and only known by its samples, its bilinear interpolate converges uniformly to u when the grid mesh tends to zero.*

The references [LMR01], [LMMM00], [CM10a] show that the bilinear interpolation brings a long list of numerically useful topological properties.

Proposition 6.2.2. (Properties of level lines of bilinear interpolates)

*(L1) For every level $0 \leq \lambda \leq 1$ except for a finite set of levels $\lambda_1, \ldots, \lambda_n$ called **critical**, the iso-level set $\{u = \lambda\}$ is the disjoint union of a finite set of piecewise-C^1 Jordan curves, denoted by $(\Sigma^{\lambda,i})_{i \in I_\lambda}$ where I_λ is a finite set of indices;*

(L2) The open set $\Omega \setminus u^{-1}(\{\lambda_1, \ldots, \lambda_n\})$ has a finite number of connected components. Each connected component is the range of an open crown $\Sigma^{]\mu,\nu[}$ where $\mu, \nu \in \{\lambda_1, \ldots, \lambda_n\}$. As a consequence, Ω is partitioned in open crowns and in the closed iso-level sets $\{u = \lambda_i\}$ corresponding to the critical levels.

Sketch of proof. A dual pixel will contain a critical level either if it is flat, or if it contains a saddle point. In both cases there is only one critical level in the pixel. Since there is a finite number of pixels, there is a finite number of critical levels. At any other level, the restriction of an iso-level set to a given pixel is either empty, or is a single piece of hyperbola. since the bilinear interpolate is continuous, these pieces of hyperbolae concatenate at each pixel boundary to form one or several disjoint Jordan curves. □

The above structure is quite simple, but it does not describe the structure of level lines at the critical levels λ_k, which can take a rather complicated form as illustrated in Figure 7.2. To define a curvature evolution for these sets would be cumbersome. We shall overcome this drawback, both numerically and analytically, by building a still simpler approximation. This approximation of the image is obtained by fattening all critical iso-level sets into open sets whose boundary is a finite set of Jordan level curves. Their curvature evolution will simply be

defined by the curvature evolution of their boundary. Thus, we define a still simpler approximation for Lipschitz functions, deduced from the bilinear interpolation.

Definition 6.2.7. *We say that a Lipschitz function u on Ω is* ***very simple*** *and we denote by $u \in \mathcal{VS}(\Omega)$ if it satisfies properties $(L1)$, $(L2)$ and*

(L3) Each crown $\Sigma^{]\mu,\nu[}$ can be completed into a closed crown by adding its interior and exterior curves Σ^{μ} and Σ^{ν}, which are limits in the $C_p^{0,1}(S^1)$ topology of the level lines of the crown.

Remark 6.2.3. As a consequence, for very simple functions, Ω is the disjoint union of the ranges of a finite number of compact crowns, and of a finite number of flat open connected components, each belonging to some critical level λ_k,

$$\Omega = \left(\bigcup_{k \in K} \Sigma^{[\mu_k,\nu_k],k} \right) \cup \left(\bigcup_{\substack{j \in \{1,\cdots,n\}, \\ l \in J_j}} F^{\lambda_j,l} \right) \tag{6.1}$$

where K is the finite set of all crown indexes, $\mu_k, \nu_k \in \{\lambda_1, \cdots, \lambda_n\}$ are critical levels, and J_j is the finite set of indexes of open connected components of the iso-level set of u at λ_j.

Definition 6.2.8. *We call* ***flat regions*** *of $u_0 \in \mathcal{VS}(\Omega)$ the open sets $F^{\lambda_j,l}$, whose boundaries are unions of a finite number of piecewise-C^1 Jordan level curves, and on which the function is constant:*

$$u(x) = \lambda_j, \ \forall x \in F^{\lambda_j,l}, \ l \in J_j.$$

Lemma 6.2.1. *Every Lipschitz function can be approximated uniformly by a sequence of very simple functions.*

Proof. For all $u \in Lip(\Omega)$ and $\varepsilon > 0$ we build a function $v \in \mathcal{VS}(\Omega)$ such that

$$\sup_{x \in \Omega} |u(x) - v(x)| < \varepsilon.$$

By Proposition 6.2.1, we can assume that $u \in \mathcal{BL}(\Omega)$. We can order the set of its critical levels $\lambda_1 < \lambda_2 < ... < \lambda_n$. Then define, for $0 < \varepsilon < \frac{1}{2} \min_j |\lambda_{j+1} - \lambda_j|$, the function $v(x) = f_\varepsilon(u(x))$, where f is the 1-Lipschitz nondecreasing function

$$f_\varepsilon(t) = \begin{cases} t, & t \leq \lambda_1 - \varepsilon \\ \lambda_k - k\varepsilon & \lambda_k - \varepsilon \leq t \leq \lambda_k + \varepsilon, \quad k = \overline{1,n} \\ t - k\varepsilon & \lambda_k + \varepsilon \leq t \leq \lambda_{k'} - \varepsilon, \quad k = \overline{1,n-1} \\ t - n\varepsilon, & t \geq \lambda_n + \varepsilon \end{cases} \tag{6.2}$$

We have $|f(t) - t| \leq n\varepsilon$, thus $\max_\Omega |u - v| \leq n\varepsilon$ which proves the convergence claim.

It remains to check that the function $v \in \mathcal{VS}(\Omega)$. The critical levels of v are inherited from u and consist of $\{\lambda_k - k\varepsilon\}_{k=1,\ldots,n}$. By construction, all the level lines of v at noncritical levels are level lines of u at noncritical levels and hence Jordan level curves, grouped in crowns. Consider now the flat regions of v, which are the open connected components of the sets

$$\{\lambda_k - \varepsilon < u < \lambda_k + \varepsilon\}, \ k = \overline{1,n}.$$

Since $\varepsilon < \frac{1}{2}\min_k(\lambda_{k+1} - \lambda_k)$, the boundary of each one of these flat regions is contained in the union of the level sets $\{u = \lambda_k - \varepsilon\}$ and $u = \{\lambda_k + \varepsilon\}$ which are a finite number of Jordan curves. Each one of these Jordan curves belongs to a crown $\Sigma^{]\lambda_k,\lambda_{k'}[}$ of u which is truncated into a crown $\Sigma^{]\lambda_k - k\varepsilon, \lambda_{k'} - k'\varepsilon[}$ of v. □

6.3 Level Lines Shortening Operator

6.3.1 LLS Semigroup Operator

Given a very simple function $u_0 \in \mathcal{VS}(\Omega)$, its Level Lines Shortening evolution consists in evolving independently and simultaneously by Curve Shortening each of its level lines, denoted by $\Sigma_0^{\lambda,i}$, and eventually reconstructing, for each time $t > 0$, a new function $u(\cdot, t)$ whose level lines are the evolutions $\Sigma_t^{\lambda,i}$, where the subscript t denotes the time t. This definition, will have to be proven consistent. Our goal is therefore to prove the commutative diagram:

$$\begin{array}{ccc} u_0(\cdot) & \xrightarrow{\quad level\ lines\ extraction \quad} & \{\Sigma_0^{\lambda,i}\}_{\lambda,i} \\ MCM/LLS \Big\downarrow & & \Big\downarrow CS \\ u(\cdot,t) & \xleftarrow{\quad reconstruction \quad} & \{\Sigma_t^{\lambda,i}\}_{\lambda,i}. \end{array}$$

To this end, we shall use several fine properties of curve shortening evolution [Gra87], [GH86], which is given in terms of a nonlinear geometric partial differential equation

$$\frac{\partial x}{\partial t}(s,t) = \mathbf{k}(s,t) \tag{6.3}$$

where $x(s,t)$ is a family of smooth Jordan curves parameterized for each t by a length parameter. The vector $\mathbf{k}$ is the acceleration which is normal to the curve, points towards its concavity, and whose norm is the radius of the osculatory circle.

Theorem 6.3.1. *The curve shortening evolution has the following properties:*

(P1) For any Jordan $C^{0,1}(S^1)$ curve Σ_0, there exists a collapsing time $T(\Sigma_0) > 0$ such that the Cauchy problem (6.3) has a unique solution Σ_t in

$$C^{0,1}\left(S^1 \times [0, T(\Sigma_0))\right) \cap C^{\infty}\left(S^1 \times (0, T(\Sigma_0))\right)$$

which still is a Jordan curve. We set $\Sigma_t = \emptyset$ for $t > T(\Sigma_0)$.

(P2) The map $\Sigma_0 \mapsto \Sigma_t$ is continuous for the $C_p^{0,1}(S^1)$ topology of Definition 6.2.2. For $t = T(\Sigma_0)$ the curve collapses to a point $x(\Sigma_0)$.

(P3) Before collapsing at time $T(\Sigma_0)$, the curve Σ_t - rescaled at constant area equal to π - converges in the $C_p^{0,1}(S^1)$ topology to the unit circle centered at the collapsing point $x(\Sigma_0)$.

(P4) Inclusion Principle:

- *if* $\Sigma^1 \preceq \Sigma^2$, *then* $\Sigma^1_t \preceq \Sigma^2_t$ *for all* $t > 0$.
- *if* $\Sigma^1 \prec \Sigma^2$, *then* $\Sigma^1_t \prec \Sigma^2_t$ *for all* $t > 0$.

(P5) The min-distance of any two disjoint curves increases with time until one of the curve collapses

$$dist(\Sigma^1_s, \Sigma^2_s) < dist(\Sigma^1_t, \Sigma^2_t), \forall s \leq t.$$

(P6) Convex curves remain convex and shrink in time: $\Sigma_t \preceq \Sigma_0$.

Theorem 6.3.2. *Properties* $(P1) - (P6)$ *hold for affine shortening:*

$$\frac{\partial x}{\partial t}(s,t) = |\mathbf{k}|^{-2/3}\mathbf{k}(s,t) \tag{6.4}$$

except for $(P3)$ *which is replaced by*

$(P3)'$ *Before collapsing at time* $T(\Sigma_0)$, *the curve* Σ_t *converges in the* $C^{0,1}_p(S^1)$ *topology to an ellipse centered at the collapsing point* $x(\Sigma_0)$.

Let $u_0 \in \mathcal{VS}(\Omega)$ be a very simple function and $\{\Sigma^{\lambda,i}_0\}_{\lambda, i\in I_\lambda}$ its level lines. Denote by $\Sigma^{\lambda,i}_t$ the evolution of $\Sigma^{\lambda,i}_0$ at time t

$$\Sigma^{\lambda,i}_0 \xrightarrow{CS} \Sigma^{\lambda,i}_t.$$

Our first purpose is to show that the family of smooth Jordan curves $\{\Sigma^{\lambda,i}_t\}_{\lambda,i\in I_\lambda}$ is actually the set of level lines of a very simple image $u(\cdot,t)$.

Definition 6.3.1. *Let* $\Sigma^{[\zeta,\mu]}_0 = \left(\Sigma^\lambda_0\right)_{\lambda\in[\zeta,\mu]}$ *be a closed crown. We call* ***level lines shortening of the crown*** $\Sigma^{[\zeta,\mu]}_0$ *the family of curves*

$$LLS(t)\left(\Sigma^{[\zeta,\mu]}_0\right) := (\Sigma^\lambda_t)_{\lambda\in[\zeta,\mu]}.$$

where Σ^λ_t *are the curve (affine) shortening evolutions of* Σ^λ_0 *for all* $\lambda \in [\zeta,\mu]$.

To fix ideas we refer in the following to increasing crowns. Analogous results hold for decreasing crowns.

Proposition 6.3.1. *Consider a closed increasing crown* $\Sigma^{[\zeta,\mu]}$. *Then the collapsing time* $T(\lambda) = T(\Sigma^\lambda)$ *of the curves of the crown is a continuous increasing function of* $\lambda \in [\zeta,\mu]$. *The level lines shortening at time* $t < T(\Sigma^\mu)$ *transforms* $\Sigma^{[\zeta,\mu]}$ *into a closed crown*

$$LLS(t)\left(\Sigma^{[\zeta,\mu]}_0\right) = \Sigma^{[\max(\zeta, T^{-1}(t)),\mu]}_t.$$

Proof. Since the composition of two continuous maps is continuous, and the composition of two strictly monotone maps is strictly monotone, this is an immediate consequence of Theorem 6.3.1 and of the definition of crowns. By property $(P1)$ level lines shortening preserves space-time continuity, whereas by $(P4)$ it preserves strict monotonicity. □

In short, a crown remains a crown by level lines shortening, and is made of all curves of the initial crown which have not collapsed yet. It is convenient to also define the evolution of a flat region.

Definition 6.3.2. *Let $F_0^{\lambda_j,l}$, $l \in J_j$ be a flat region of $u_0 \in \mathcal{VS}(\Omega)$ at level λ_j, of exterior curve Σ_0^e and interior curves Σ_0^m, $m \in M$. We call the* ***level lines shortening of the flat region*** *$F_0^{\lambda_j,l}$, $l \in J_j$ the set defined by*

$$LLS(t)(F_0^{\lambda_j,l}) = F_t^{\lambda_j,l} := Int(\Sigma_t^e) \cap \left(\bigcap_m Ext(\Sigma_t^m) \right), \ \forall t < T(\Sigma^e)$$

where Σ_t^e and Σ_t^m, $m \in M$ are the curve shortening evolutions of Σ_0^e and Σ_0^m, $m \in M$.

The initial flat region remains a region whose boundary is made of all Jordan curves of its initial boundary which have not collapsed. By the inclusion principle the last curve to disappear is the external boundary. When it collapses, the region disappears.

Theorem 6.3.3 (Definition of LLS for very simple functions)**.** *Let u_0 be a very simple Lipschitz function, with critical levels $\{\lambda_k\}_{k=1,\cdots,n}$, Jordan curves $\Sigma_0^{\lambda,i}$ indexed by their level λ and $i \in I_\lambda$, and of flat regions $F_0^{\lambda_j,l}$ at critical levels λ_j, indexed by $l \in J_j$. The* ***level lines shortening evolution of the function*** *u_0 is the function $LLS(t)(u_0) = u(\cdot,t)$ defined by*

$$u(x,t) = \begin{cases} \lambda, & \text{if } x \in \Sigma_t^{\lambda,i} \\ \lambda_j, & \text{if } x \in F_t^{\lambda_j,l} \\ 0, & \text{if } x \in \Omega \setminus \Omega_t \end{cases} \tag{6.5}$$

where Ω_t is the domain surrounded by the curve shortening evolution $(\partial\Omega)_t$ of the domain boundary $\partial\Omega_0$ (which is the only zero-level curve of u_0). Then this definition is complete, consistent, the evolved function is a very simple function $u(\cdot,t) \in \mathcal{VS}(\Omega)$ whose Lipschitz constant is smaller than or equal to the initial one.

Proof. The initial domain Ω is partitioned in crowns and flat regions whose boundaries are either interior or exterior curves of crowns, or $\partial\Omega$. By the min-distance property ($P5$) in Theorem 6.3.1, when time increases the evolved level curves of u_0 fall apart from each other and so do the boundary curves of the flat regions. Thus, by Proposition 6.3.1 and Definition 6.3.2 the crowns never meet and the flat regions are at all times the connected components of the complementary in Ω_t of the union of crowns. In other terms the evolved crowns and evolved flat regions form a partition of Ω_t given by

$$\Omega_t = \left(\bigcup_{k \in K} \Sigma_t^{[\mu_k,\nu_k],k} \right) \cup \left(\bigcup_{\substack{j \in \{1,\cdots,n\}, \\ l \in J_j}} F_t^{\lambda_j,l} \right) \tag{6.6}$$

On the other hand, the boundary of Ω is convex and remains convex by curve shortening (property ($P6$) in Theorem 6.3.1). Hence if points x initially belonging to Ω have been crossed by the evolving boundary, we have $u(x,t) = 0$. This renders the definition complete and consistent.

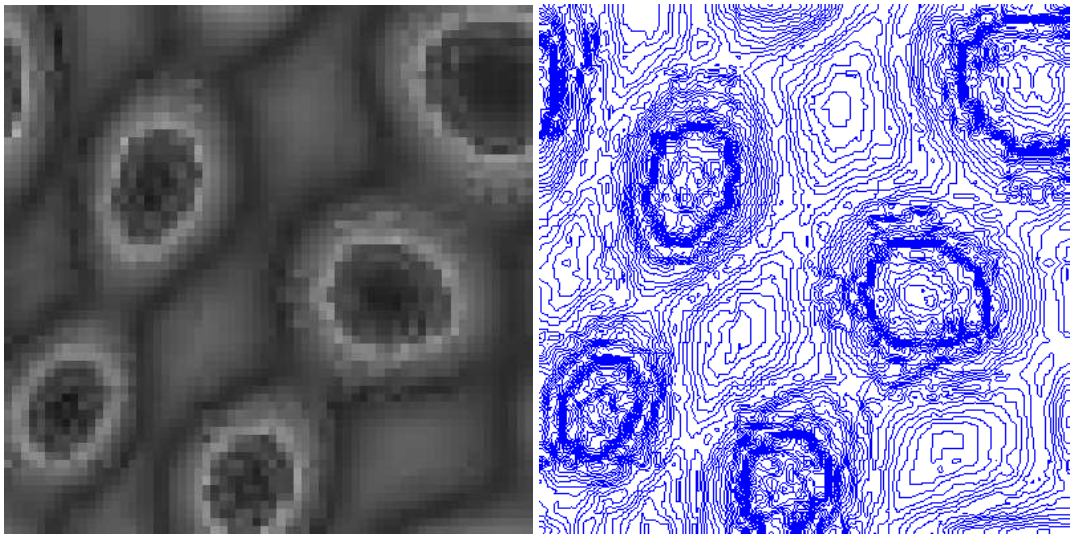

(a) Image associated to a very simple function and its corresponding level lines.

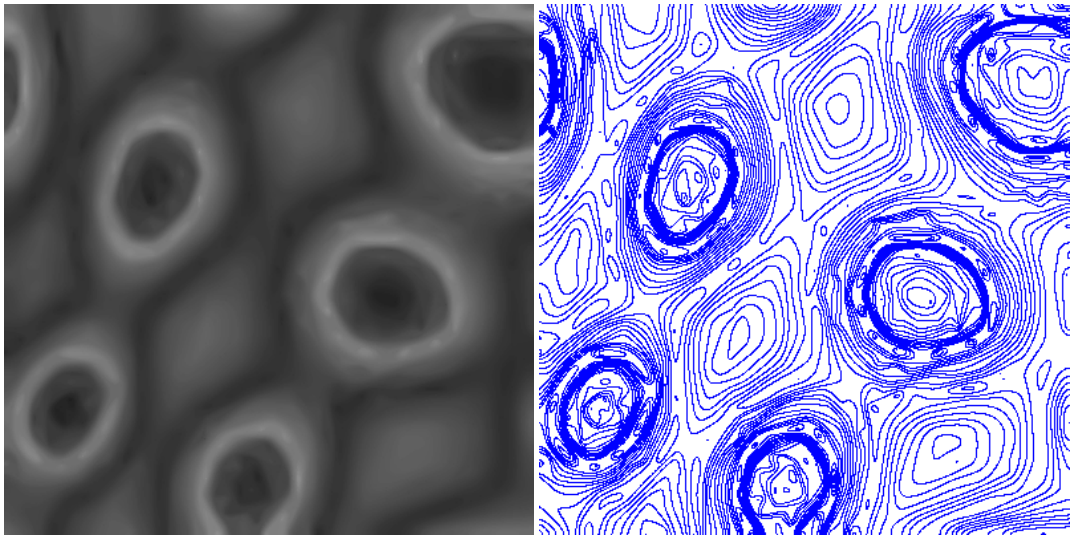

(b) The LLS operator maps very simple functions onto very simple functions.

Figure 6.3: The Level Lines Shortening (LLS) numerical chain: from the original image (top-left), the family of all its simple level lines is extracted at quantized non-degenerate levels (top-right). Simultaneously and independently, each level line is evolved (bottom-right) and the evolved image having these level lines is reconstructed (bottom-left). Both the images and their families of level lines satisfy the topological properties $(L1)$, $(L2)$, $(L3)$. Performing the LLS evolution, digitization artifacts due to noise, compression and under-sampling are attenuated.

Let us show that $u(\cdot,t)$ is Lipschitz. A function is L-Lipschitz if and only if the min-distance between any two of its level sets with levels λ and μ is larger than $\frac{|\lambda-\mu|}{L}$. More precisely, since the min distance between a flat region and another, or between a flat region and a level line, is always attained on the level lines which bound the flat regions, we have

$$Lip(u_0) = \max\{\frac{|\zeta-\mu|}{\text{dist}(\Sigma_0^\zeta, \Sigma_0^\mu)}\}.$$

Since all min-distances between level lines increase (property ($P5$), Theorem 6.3.1), we have

$$\frac{|\zeta-\mu|}{\text{dist}(\Sigma_0^\zeta, \Sigma_0^\mu)} \geq \frac{|\zeta-\mu|}{\text{dist}(\Sigma_t^\zeta, \Sigma_t^\mu)}.$$

Thus the Lipschitz constant of $u(\cdot,t)$ is smaller than or equal to the Lipschitz constant of u_0. □

Definition 6.3.3. *We call **Level Lines Shortening operator**, shortly LLS, the above operator acting on the class of very simple functions,*

$$\begin{aligned} LLS(t) : \mathcal{VS}(\Omega) &\mapsto \mathcal{VS}(\Omega) \\ u_0 &\mapsto u(\cdot,t). \end{aligned}$$

Since the curve shortening itself is a semigroup, $LLS(t)$ also is a semigroup, namely

$$LLS(t+s)u_0 = LLS(t)(LLS(s)u_0).$$

Corollary 6.3.1. *The **level lines affine shortening evolution** of a very simple function*

$$LLAS(t)(u_0)(x) := \begin{cases} \lambda, & \text{if } x \in \Sigma_t^{\lambda,i} \\ \lambda_j, & \text{if } x \in F_t^{\lambda_j,l} \\ 0, & \text{if } x \in \Omega \setminus \Omega_t \end{cases} \tag{6.7}$$

where $\Sigma_t^{\lambda,i}$ and $F_t^{\lambda_j,l}$ are the affine shortening evolutions of the initial level lines, respectively flat areas, is well defined and maps $\mathcal{VS}(\Omega)$ onto itself, preserving the semigroup property.

Proof. This comes immediately from Theorem 6.3.2, which ensures that all the topological properties of curve shortening hold as well for affine shortening. □

6.3.2 Properties of Level Lines Shortening

Lemma 6.3.1. *Let ϕ_0 a radial increasing function centered at x_0, i.e. $\phi_0(x) = \varphi(|x|)$ with φ increasing. Then its level lines shortening evolution is given by*

$$\phi(x,t) = \varphi\left(\sqrt{|x|^2 + 2(t-t_0)}\right)$$

and its affine shortening evolution is given by

$$\phi(x,t) = \varphi\left(\sqrt[\frac{4}{3}]{|x|^{\frac{4}{3}} + \frac{4}{3}(t-t_0)}\right).$$

Lemma 6.3.2 (Local comparison)**.** *Let u_0 be a very simple function, ϕ_0 a radial increasing function centered at x_0, and denote by $u(\cdot,t)$ and $\phi(\cdot,t)$ their LLS/LLAS evolutions. If in a local neighborhood $\mathcal{N}(x_0)$ of x_0 the following holds*

$$u_0(x) \leq \phi_0(x), \forall\, x \in \mathcal{N}(x_0)$$

then there exists a short time $t_0 > 0$ such that

$$u(x_0,t) \leq \varphi(x_0,t), \forall 0 < t < t_0.$$

Proof. We argue for LLS, the case LLAS being analogue. The level set $\{\phi_0 < \lambda\}$ is the open disk with radius $\phi_0^{-1}(\lambda)$ and satisfies the inclusion

$$\{x \in \mathcal{N}(x_0); \phi_0(x) < \lambda\} \subset \{x \in \mathcal{N}(x_0); u_0(x) < \lambda\}$$

Then every level line Σ^{λ,ϕ_0} of ϕ_0 surrounds no point belonging to a level set of the same level of u_0. By the inclusion principle and the topological structure of the level lines for a very simple image, this property is preserved for all $t \leq t_0$ where t_0 is the vanishing time for the largest level line of ϕ in the neighborhood $\mathcal{N}(x_0)$. Indeed if the level set of $u(x,t)$ is a flat part bounded by Jordan curves, by the min-distance property $(P5)$ these Jordan curves never cross in their evolution the circles corresponding to the level set for $\phi(x,t)$. If the level set of $u(x,t_0)$ is a finite set of level lines, in the same way the evolved level lines of $u(x,t)$ never cross the circular level line of $\phi(x,t)$.

On the other hand x_0 belongs to all the level lines of $\phi(\cdot,t)$, for all times $t < t_0$. Hence the value of $u(\cdot,t)$ at x_0 must necessarily be less than the minimum level of $\phi(\cdot,t)$, which is attained exactly at x_0. Consequently

$$u(x_0,t) \leq \phi(x_0,t), \forall\, t < t_0.$$

□

Proposition 6.3.2 (Space-Time Continuity)**.** *Let $u_0 \in \mathcal{VS}(\Omega)$ be L-Lipschitz continuous and consider its level lines (affine) shortening evolution $u(\cdot,t) = LL(A)S(t)(u_0)$, for all $t \in (0,\infty)$. Then $u \in C^0(\Omega \times [0,\infty))$.*

Proof. We want to find a Lipschitz type estimate for the function u and we argue separately in space and time:

$$|u(x,t) - u(x_0,t_0)| \leq |u(x,t) - u(x_0,t)| + |u(x_0,t) - u(x_0,t_0)|.$$

By Theorem 6.3.3 the LLS evolution $u(\cdot,t)$ at any time $t > 0$ of the initial function u_0 remains $L - Lipschitz$ continuous and hence

$$|u(x,t) - u(x_0,t)| \leq L|x - x_0|.$$

The time-continuity follows from comparisons with shrinking cones. More precisely, the Lipschitz continuity at time t_0 tells us there exists $\phi(\cdot, t_0)$ a L-Lipschitz radial upper barrier $u(x, t_0) \le \phi(x, t_0)$, touching u at point x_0,given by

$$\phi(x, t_0) = u(x_0, t_0) + L|x - x_0|.$$

By Lemma 6.3.1, its LLS evolution is

$$\phi(x, t) = u(x_0, t_0) + L\sqrt{|x - x_0|^2 + 2(t - t_0)}.$$

It follows from the local comparison with radial functions given in Lemma 6.3.2 that

$$u(x_0, t) \le \phi(x_0, t) = u(x_0, t_0) + L\sqrt{2(t - t_0)}.$$

Consequently

$$|u(x, t) - u(x_0, t_0)| \le L\left(|x - x_0| + \sqrt{2(t - t_0)}\right).$$

This proves that $u(x, t)$ is uniformly continuous in t and x. Similar results hold for LLAS. □

The structure of very simple functions implies that there is only a finite number of possible **collapsing times**, namely times $t_*^k > 0$ where some crown collapses to a point. At these times $t_*^1 < t_*^2 \cdots < t_*^m$ there is one (or several) collapse pairs $(t_*^k, \Sigma^{\lambda_k, i_k})$. The next lemma gives a stability property for flat regions.

Lemma 6.3.3 (Flatness)**.** *Let u_0 be a very simple functions and $u(\cdot, t)$ its LL(A)S evolution at time t. Let x_0 be a point in a flat region of $u(\cdot, t_0)$ and suppose that it is not a collapsing point. Then there exists $\delta_0 > 0$ such that x_0 stays in a flat region of $u(\cdot, t)$, for all $|t - t_0| < \delta_0$.*

Proof. Since x_0 belongs to a flat area of $u(\cdot, t_0)$ there exists a small ball $B(x_0, r_0)$ centered at x_0 meeting no other level line of $u(\cdot, t_0)$:

$$\Sigma_{t_0}^{\lambda, i} \cap B(x_0, r_0) = \emptyset. \tag{6.8}$$

The number of collapsing points being finite, we can also choose r_0 small enough, so that $B(x_0, r_0)$ contains no collapsing point of the evolution of u. Let $\partial B(x_0, r(t))$ be the circle centered at x_0 and evolving by Curve Shortening such that $r(t_0) = r_0$.

1. Fix $\delta_1 = r_0^2/4$ such that $\partial B(x_0, r(t))$ has not collapsed at time $t = t_0 + \delta_1$. Then it follows from (6.8) and from the inclusion principle that for all $t < t_0 + \delta_1$ no level line of $u(\cdot, t)$ meets the ball $B(x_0, r(t))$

$$\Sigma_t^{\lambda, i} \cap B(x_0, r(t)) = \emptyset,$$

where $r(t) = \sqrt{r_0^2 - 2(t - t_0)}$.

2. We now prove that there exists a time δ_2 and a radius $\rho > 0$ such that for all $t \in (t_0 - \delta_2, t_0)$ no level curve of $u(\cdot, t)$ meets $B(x_0, \rho)$. Assume by contradiction that there exist t_j, x_j and curves $\Sigma_{t_j}^{\lambda_j}$ of *LLS* evolution of u such that

$$t_j \to t_0,\ x_j \to x_0 \text{ with } x_j \in \Sigma_{t_j}^{\lambda_j}. \tag{6.9}$$

Consider the corresponding initial curves $\Sigma_0^{\lambda_j}$. Since the ball $B(x_0, r_0)$ contains no collapsing points of u, the evolutions $\Sigma_t^{\lambda_j}$ will have uniformly bounded curvature, and thus stay uniformly bounded in the $C_p^{0,1}(S^1)$ topology. It is then possible to extract a converging subsequence to Σ_0^{λ}. By the continuity property $(P2)$ in Theorem 6.3.1, it follows that $\Sigma_{t_0}^{\lambda_0}$ contains x_0, which contradicts our initial assumption.

□

6.4 Equivalence with the Curvature Motions

We start with a formal derivation of this equivalence. For this purpose, assume that u is a smooth function, whose gradient does not vanish in the neighborhood $\mathcal{N}(x_0)$ of some point x_0, where $x_0 \in \Sigma_t := \{x; u(x,t) = 0\}$. Let $\nu(\cdot, t)$ be a smooth unit vector field to Σ_t and $x(t) \in \Sigma_t \cap \mathcal{N}(x_0)$. Differentiating the relation $u(t, x(t)) = 0$ with respect to t we get

$$u_t + Du\frac{\partial x}{\partial t} = 0. \tag{6.10}$$

Choose in the neighborhood $\mathcal{N}(x_0)$, $\nu = \frac{Du}{|Du|}$. Then the scalar curvature with respect to this choice of the normal satisfies $k = -\text{curv}(u)$. Multiplying equation (6.10) by the vector Du we see that (MCM) is satisfied at point (x_0, t_0) if and only if $\frac{\partial x}{\partial t}$ is collinear with Du and (CS) holds.

6.4.1 Mean Curvature Motion

We rewrite the geometric curve shortening in the form

$$\frac{\partial x}{\partial t} = k\nu, \tag{CS}$$

where k denotes the scalar curvature and ν the unit normal to the curve, with ν continuous and the sign of k guaranteeing that $k\nu$ points towards the interior of the domain surrounded by the curve at convex points and towards the exterior at concave points. We are interested in its equivalence with

$$\begin{cases} u_t = |Du|\text{curv}(u), & \text{in } \mathbb{R}^2 \times [0,\infty) \\ u(\cdot,0) = u_0, & \text{on } \mathbb{R}^2. \end{cases} \tag{MCM}$$

where

$$|Du|\text{curv}(u) = |Du|div(\frac{Du}{|Du|}) = \sum_{i,j=1}^{2}(\delta_{ij} - \frac{u_{x_i}u_{x_j}}{|Du|^2})u_{x_ix_j}.$$

We refer to a viscosity solution for the parabolic PDE, which is defined in terms of point-wise behavior with respect to a smooth test function. We use herein the definition presented by Morel and Guichard in [GM00], which was proven by Barles and Georgelin [BG95] to be equivalent with the viscosity solutions given by Evans and Spruck in [ES91] and Chen, Giga and Goto in [CGG91].

Definition 6.4.1. *A function $u \in C(\mathbb{R}^2 \times [0,\infty)) \cap L^\infty(\mathbb{R}^2 \times [0,\infty))$ is a **viscosity sub-solution** of (MCM) iff for each $\phi \in C^\infty(\mathbb{R}^2 \times [0,\infty))$ such that $u-\phi$ has a local maximum at (x_0,t_0) we have*

$$\begin{aligned} \phi_t(x_0,t_0) &\le |D\phi| curv(\phi)(x_0,t_0) && \text{if } D\phi(x_0,t_0) \neq 0 \\ \phi_t(x_0,t_0) &\le 0 && \text{if } D\phi(x_0,t_0) = 0 \text{ and } D^2\phi(x_0,t_0) = 0. \end{aligned}$$

*A function $u \in C(\mathbb{R}^2 \times [0,\infty)) \cap L^\infty(\mathbb{R}^2 \times [0,\infty))$ is a **viscosity super-solution** of (MCM) iff for each $\phi \in C^\infty(\mathbb{R}^2 \times [0,\infty))$ such that $u-\phi$ has a local minimum at (x_0,t_0) we have*

$$\begin{aligned} \phi_t(x_0,t_0) &\le |D\phi| curv(\phi)(x_0,t_0) && \text{if } D\phi(x_0,t_0) \neq 0 \\ \phi_t(x_0,t_0) &\le 0 && \text{if } D\phi(x_0,t_0) = 0 \text{ and } D^2\phi(x_0,t_0) = 0. \end{aligned}$$

Remark 6.4.1. *The above definition can be further simplified [GM00]: replacing "local maximum (minimum)" with "strict local maximum (minimum)" one obtains an equivalent definition of viscosity solutions. Furthermore, it is enough to consider test functions of the form $\phi(x,t) = f(x) + g(t)$.*

Theorem 6.4.1. *Let $u_0 \in \mathscr{F}(\Omega)$. Then the Level Lines Shortening evolution of the function u_0,*

$$u(x,t) = LLS(t)u_0(x), \forall x \in \mathbb{R}^2, \forall t \in [0,\infty)$$

is a viscosity solution for (MCM) with initial data u_0,

Proof. It is sufficient to check that $u(x,t)$ is a viscosity sub-solution. Analogous assertions hold for viscosity super-solutions. Let $\phi \in C^\infty(\mathbb{R}^2 \times [0,\infty))$ such that $u-\phi$ has a strict local maximum at (x_0,t_0). Adding if necessary a constant, suppose that

$$\begin{cases} u(x_0,t_0) = \phi(x_0,t_0) = \lambda \\ u(x,t) < \phi(x,t), \forall (x,t) \in V \end{cases} \tag{6.11}$$

where V is a small neighborhood of (x_0,t_0). The proof is completed by the next three lemmas, where we distinguish two situations: either the point x_0 is inside a flat region of $u(\cdot,t_0)$ (lemma 6.4.1), or it belongs to some level line, singular or not of this function (lemma 6.4.3 in the case where $D\phi(t_0,x_0) = 0$, and lemma 6.4.2 when the gradient is not zero). □

Lemma 6.4.1. *Let x_0 be a point in a flat area of $u(\cdot,t_0)$. Then*

$$D\phi(x_0,t_0) = 0 \text{ and } \phi_t(x_0,t_0) = 0.$$

Proof. By Lemma 6.3.3, the function u is constant in a small neighborhood $\mathscr{N}(x_0,t_0)$. From the local maximum condition we deduce that the point (x_0,t_0) is a local minimum for the test function $\phi \in C^\infty$, which yields the conclusion.

□

We consider now the case when x_0 belongs to a level line $\Sigma_{t_0}^{\lambda,u}$ of the function $u(\cdot,t_0)$. By the construction of $LLS(t)u_0$ this level line is following the classical curve shortening.

Lemma 6.4.2. *Let x_0 belong to a level line $\Sigma_{t_0}^{\lambda,u}$ of the function $u(\cdot,t_0)$. Let ϕ be a smooth test function such that at the maximum point (x_0,t_0) of $u-\phi$*

$$D\phi(x_0,t_0)\neq 0.$$

Then ϕ satisfies

$$\phi_t \leq |D\phi| div(\frac{D\phi}{|D\phi|}) \text{ at } (x_0,t_0).$$

Proof. 1. The non-degeneracy condition $D\phi(x_0,t_0)\neq 0$ and the regularity of the test function ϕ imply by the implicit function theorem that the iso-level set

$$\Sigma_{t_0}^{\lambda,\phi}=\{x\in\Omega;\phi(x,t_0)=\lambda\}$$

is a smooth graph in a neighborhood of x_0. A unit normal vector of $\Sigma_{t_0}^{\lambda,\phi}$ at point x_0 is

$$\nu^{\phi}(x_0,t_0)=\frac{D\phi}{|D\phi|}(x_0,t_0).$$

On the other hand, x_0 belongs to the smooth Jordan level line $\Sigma_{t_0}^{\lambda,u}$ of u. By the local maximum condition at point (x_0,t_0) the two graphs $\Sigma_{t_0}^{\lambda,\phi}$ and $\Sigma_{t_0}^{\lambda,u}$ are tangent at x_0 and do not intersect in a small neighborhood of the point. Therefore, the unit normal vectors of these curves coincide up to their sign. We set

$$\nu^{u}(x_0,t_0)=\frac{D\phi}{|D\phi|}(x_0,t_0).$$

Furthermore, for short times $t\in(t_0-\delta,t_0+\delta)$ with $\delta>0$ small enough, the λ level set of $\phi(\cdot,t)$ denoted by

$$\Sigma_{t}^{\lambda,\phi}=\{x\in\Omega_t;\phi(x,t)=\lambda\}$$

remains a smooth graph in a neighborhood of x_0. By the maximum condition (6.11), $\Sigma_t^{\lambda,\phi}$ stays on the same side of $\Sigma_t^{\lambda,u}$ (see Figure 6.4.1).

To fix ideas, suppose that for points x close enough to $\Sigma_{t_0}^{\lambda,u}$, $u(x)>\lambda$ in the interior domain bounded by the level line $\Sigma_{t_0}^{\lambda,u}$. Then the $\lambda-$level line of the test function $\Sigma_{t_0}^{\lambda,\phi}$ lies locally outside the same domain. In addition, the normal vectors $\nu^u(x_0,t_0)$ and $\nu^{\phi}(x_0,t_0)$ point inwards the interior domain bounded by the level line $\Sigma_{t_0}^{\lambda,u}$.

2. We consider now the backwards locations $x(t)$ on the curves $\Sigma_t^{\lambda,u}$ of the point $x_0\in\Sigma_{t_0}^{\lambda,u}$, curves which represent the curve shortening evolutions of some level line $\Sigma_0^{\lambda,u}$. Let $\nu(x(t),t)$ be the unit inward vector at point x_0 of the level line $\in\Sigma_{t_0}^{\lambda,u}$. The vector points in the direction of $x_0-x(t)$ and hence there exists $d(x(t),t)$ such that

$$x(t)=x_0-d(x(t),t)\nu(x(t),t) \tag{6.12}$$

By the smoothness property $(P1)$ of Theorem 6.3.1,

$$\lim_{t\nearrow t_0}\nu(x(t),t)=\nu^u(x_0,t_0).$$

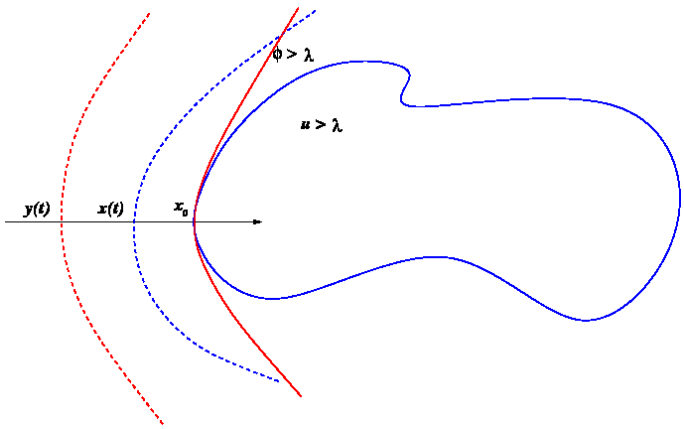

Figure 6.4: The level line $\Sigma_t^{\lambda,\phi}$ (in red) stays on the same side of the level line $\Sigma_t^{\lambda,u}$ (in blue). For $t < t_0$, we consider the backwards locations $x(t)$ of the point x_0 on the level lines $\Sigma_t^{\lambda,u}$ as well as the intersections $y(t)$ of the normal direction with the level lines $\Sigma_t^{\lambda,\phi}$ of the test function.

Let $y(t)$ be the intersection point of the outward normal direction $-\nu(x(t),t)$ (we take here into account that we have considered upper level sets, i.e. ν^ϕ points inwards) with the level curve $\Sigma_t^{\lambda,\phi}$ (situated outside $\Sigma_{t_0}^{\lambda,u}$). Then there exists $d(y(t),t)$ such that

$$y(t) = x_0 - d(y(t),t)\nu(x(t),t) \tag{6.13}$$

and $D\phi(y(t),t) \neq 0$, since $\Sigma_t^{\lambda,\varphi}$ remains a local graph for short times. From the implicit function theorem we deduce that $y(t)$ is uniquely defined and varies smoothly in time. Thus the following limit exists:

$$\lim_{t \nearrow t_0} \frac{y(t) - x_0}{t - t_0} = \frac{\partial y}{\partial t}(t_0).$$

Furthermore, since $\Sigma_t^{\lambda,\phi}$ stays on the same side of $\Sigma_t^{\lambda,u}$ we have

$$d(x(t),t) \leq d(y(t),t).$$

Taking the inner product with $\nu(x(t,)t)$ in equations (6.12) and (6.13) and dividing by $t < t_0$, the previous inequality implies that

$$\langle \frac{x(t) - x_0}{t - t_0}, \nu(x(t),t)\rangle \leq \langle \frac{y(t) - x_0}{t - t_0}, \nu(x(t),t)\rangle.$$

Passing to the limits as $t \to t_0$ we have

$$\langle \frac{\partial x}{\partial t}(t_0), \nu^u(x_0,t_0)\rangle \leq \langle \frac{\partial y}{\partial t}(t_0), \nu^u(x_0,t_0)\rangle \tag{6.14}$$

and taking into account that (CS) gives

$$\langle \frac{\partial x}{\partial t}(t_0), \nu^u(x_0,t_0)\rangle = k^u(x_0,t_0) \tag{6.15}$$

we get

$$k^u \leq \langle \frac{\partial y}{\partial t}(t_0), \nu^u(x_0, t_0)\rangle.$$

But $\Sigma^u_{t_0}$ and $\Sigma^\phi_{t_0}$ are ordered by inclusion and meet at point x_0. Thus, their curvatures at x_0 are ordered

$$k^\phi(x_0, t_0) \leq k^u(x_0, t_0).$$

On the other hand, from the regularity of the test function and the fact that $D\phi(x_0, t_0) \neq 0$ the curvature at x_0 can be expressed as

$$k^\phi(x_0, t_0) = -\mathrm{div}(\frac{D\phi}{|D\phi|})(x_0, t_0)$$

Consequently

$$-\mathrm{div}(\frac{D\phi}{|D\phi|})(x_0, t_0) \leq \langle \frac{\partial y}{\partial t}(t_0), \nu^u(x_0, t_0)\rangle. \tag{6.16}$$

3. The sequence of points $y(t)$ found before belongs to the $\lambda-$level set of the test function, thus we have

$$\phi(y(t), t) = \lambda, \text{ for } t \in (t_0 - \delta, t_0].$$

Differentiating this identity with respect to t one gets for $t = t_0$

$$\langle \frac{\partial y}{\partial t}(t_0), D\phi(x_0, t_0)\rangle + \phi_t(x_0, t_0) = 0.$$

But at the touching point x_0 the normal vector to $\Sigma^{\lambda,\phi}_{t_0}$ can be expressed as

$$\frac{D\phi}{|D\phi|}(x_0, t_0) = \nu^u(x_0, t_0).$$

Consequently the equality above at point (x_0, t_0) becomes

$$\phi_t(x_0, t_0) = -|D\phi|(x_0, t_0)\langle \frac{\partial y}{\partial t}(x_0, t_0), \nu^u(x_0, t_0)\rangle$$

which by inequality (6.16) implies

$$\phi_t(x_0, t_0) \leq |D\phi|\mathrm{div}(\frac{D\phi}{|D\phi|})(x_0, t_0)\rangle.$$

□

Remark 6.4.2. *If a point x_0 is a collapsing point at time t_0, then*

$$u(x, t) = \lambda, \forall\, t \in [t_0, t_0 + \delta)$$

Therefore the test function φ satisfies $D\phi(x_0, t_0) = 0$.

Lemma 6.4.3. *Let x_0 belong to a level line $\Sigma^{\lambda,u}_{t_0}$ of the function $u(\cdot, t_0)$. Let ϕ be a test function such that $D\phi(x_0, t_0) = 0$, $D^2\phi(x_0, t_0) = 0$. Then ϕ satisfies $\phi_t(x_0, t_0) \leq 0$.*

Proof. By Remark 6.4.1 we can assume that the test function has the form $\phi(x,t) = f(x) + g(t)$. By assumption, for every (x,t) in a neighborhood of (t_0, x_0) we have

$$u(x,t) - f(x) - g(t) \leq u(x_0,t_0) - f(x_0) - g(t_0). \tag{6.17}$$

1. Assume first that $\Sigma^{\lambda,u}_{t_0}$ is not reduced to a point and say it is the curve shortening evolution of the original level line $\Sigma^{\lambda,u}_0$. Denote by $\Sigma^{\lambda,u}_t$ the intermediate evolutions for $0 < t < t_0$. Consider, as before, for short times $t \in (t_0 - \delta, t_0]$ the points $x(t)$ belonging to $\Sigma^{\lambda,u}_t$ such that $x(t) \to x_0$ as $t \to t_0$. Since $u(x(t),t) = u(x_0,t_0)$ from inequality (6.17) we get

$$g(t_0) - g(t) \leq f(x(t)) - f(x_0). \tag{6.18}$$

However, since the level line evolves by curve shortening, we also have

$$x(t) = x_0 + (t - t_0)k(x_0,t_0)\nu(x_0,t_0) + o(t - t_0). \tag{6.19}$$

Substituting this asymptotic expansion in (6.18) and recalling that $Df(x_0,t_0) = 0$ yields

$$g'(t_0)(t_0 - t) \leq o(t_0 - t),$$

which implies $g'(t_0) \leq 0$. Since $g'(t_0) = \phi_t(x_0,t_0)$, this proves the announced statement.

2. The only case not treated by the above argument is when x_0 is the collapsing point of some level line $\Sigma^{\lambda,u}_t$. Accordingly, t_0 is its collapsing time. In this case, the level line does not have a normal direction at (x_0,t_0) and consequently equation (6.19) is not valid anymore.

Nevertheless, by Theorem 6.3.1, property $(P3)$, for short times $t \in (t_0 - \delta, t_0)$ the points $x(t)$ lie approximatively on a circle of radius $R(t)$ respectively, with $R(t_0) = 0$. Thus

$$|x(t) - x_0| \simeq \sqrt{2(t_0 - t)}. \tag{6.20}$$

Substituting this asymptotic expansion in (6.18) and taking into account that $Df(x_0,t_0) = 0$ and $D^2 f(x_0,t_0) = 0$ we obtain

$$g'(t_0)(t_0 - t) \leq o(t_0 - t),$$

which implies again $g'(t_0) \leq 0$. □

The Level Lines Shortening can be extended by density to an operator acting on the class of Lipschitz functions.

Corollary 6.4.1. *For each $u \in Lip(\Omega)$ consider a uniform approximation by very simple functions $u_0^n \in \mathcal{VS}(\Omega)$ and define its LLS evolution by*

$$LLS(t)u_0(x) = \lim_{n\to\infty} \left(LLS(t)u_0^n(x)\right),$$

Then the limit is well defined and is a solution of (MCM) with initial data u_0.

Proof. From the previous theorem we know that the LLS evolutions of the very simple functions u_0^n

$$u^n(\cdot,t) = LLS(t)u_0^n$$

are solutions of the mean curvature equation. By the comparison principle we know that

$$\max_{x\in\Omega}(u^n(x,t)-u^m(x,t)) \le \max_{x\in\Omega}(u_0^n(x)-u_0^m(x)).$$

Since the sequence of very simple functions is uniformly convergent, we deduce that for each $t>0$, the family $\{LLS(t)u_0^n\}_n \subset \mathscr{VS}(\Omega)$ is a Cauchy sequence in the $||\cdot||_\infty$ norm. By the stability properties of viscosity solutions, the limit function

$$u(x,t) = \lim_{n\to\infty} u^n(x,t)$$

is also a viscosity solution of (MCM) and hence satisfies $Lip(u(\cdot,t)) \le Lip(u_0)$. □

6.4.2 Affine Curvature Motion

Similarly, one can connect the affine shortening

$$\frac{\partial x}{\partial t} = k^{1/3}\nu, \tag{AS}$$

where $\nu(\cdot,t)$ is the inner unit normal vector of the curve $x(\cdot,t)$ and $k(\cdot,t)$ the signed scalar curvature corresponding the choice of $\nu(\cdot,t)$, with the affine curvature motion

$$\begin{cases} u_t = |Du|\big(\mathrm{curv}(u)\big)^{1/3}, & \text{in } \mathbb{R}^2\times[0,\infty) \\ u(\cdot,0)=u_0, & \text{on } \mathbb{R}^2. \end{cases} \tag{ACM}$$

In the definition of these nonlinear evolutions, for $x\in\mathbb{R}$, $x^{1/3}$ stands for $\mathrm{sgn}(x)|x|^{1/3}$.

Theorem 6.4.2. *Let $u_0\in\mathscr{F}(\Omega)$. Its Level Lines Affine Shortening evolution*

$$u(x,t) = LLAS(t)u_0(x), \forall\, x\in\mathbb{R}^2, \forall\, t\in[0,\infty)$$

is a viscosity solution for (ACM) with initial data u_0.

Proof. The proof of Theorem 6.4.1 is purely geometric, thus the same arguments apply for level lines affine shortening.

1. When $D\phi(x_0,t_0)\neq 0$ we need to estimate from above the right hand side of

$$\phi_t(x_0,t_0) = -|D\phi|(x_0,t_0)\langle\frac{\partial y}{\partial t}(x_0,t_0), \nu^u(x_0,t_0)\rangle.$$

The proof is literally the same up to inequality (6.14)

$$\langle\frac{\partial x}{\partial t}(t_0), \nu^u(x_0,t_0)\rangle \le \langle\frac{\partial y}{\partial t}(t_0), \nu^u(x_0,t_0)\rangle.$$

The only difference it makes with the previous proof is when (AS) comes into play. More precisely the evolution equation (6.15) at the maximum point (x_0,t_0) should be replaced by an

affine shortening evolution

$$\langle \frac{\partial x}{\partial t}(t_0), v^u(x_0,t_0)\rangle = \big(k^u(x_0,t_0)\big)^{1/3} \tag{6.21}$$

On the other hand $k^\phi(x_0,t_0) \leq k^u(x_0,t_0)$ which implies

$$\big(k^\phi(x_0,t_0)\big)^{1/3} = \mathrm{sgn}(k^\phi)|k^\phi(x_0,t_0)|^{1/3} \leq \mathrm{sgn}(k^u)|k^u(x_0,t_0)|^{1/3} = \big(k^u(x_0,t_0)\big)^{1/3}$$

But for the test function ϕ, $k^\phi(x_0,t_0) = -\mathrm{curv}(\phi)(x_0,t_0)$. Hence

$$-(\mathrm{curv}(\phi))^{1/3} \leq \langle \frac{\partial y}{\partial t}(t_0), v^u(x_0,t_0)\rangle.$$

from where we deduce the desired viscosity inequality.

2. For the case $D\phi(x_0,t_0) = 0$ and $D^2\phi(x_0,t_0) = 0$ it is sufficient to replace the asymptotic expansions (6.19) by

$$x(t) = x_0 + (t-t_0)\big(k(x_0,t_0)\big)^{1/3} v(x_0,t_0) + o(t-t_0). \tag{6.22}$$

respectively (6.20) by

$$|x(t) - x_0| \simeq \sqrt[\frac{4}{3}]{\frac{4}{3}(t_0 - t)}. \tag{6.23}$$

This concludes the proof. □

6.5 Conclusion

We have defined in this chapter the continuous Level Lines Shortening, as the Curve Shortening operator acting simultaneously and independently on all the level lines of a bilinear interpolated image. Furthermore, this operator has been extended to flat areas and functions with a special topological structure, that we termed *very simple functions*. The Level Lines (Affine) Shortening evolution of a very simple function turns out to be a viscosity solution of the mean curvature motion (MCM), respectively affine curvature motion (ACM), setting thus forth an explicit connection between the geometric curve evolution and the analytical PDE evolution.

The method does not apply for 3D hypersurfaces, principally because of the topological changes interfeering during the evolution. It is however readable from the proof that the results remain true for any increasing function of the curvature. We would therefore like to use the result for monotonous powers of curvature in order to arrive asymptotically to the simoultanoeus erosion-dilation, which has been an open problem for the last twenty years.

We describe in the next chapter the discrete Level Lines Shortening Algorithm and show it performs accurate sub-pixel evolution by mean curvature motion. The main goal of the implementation is to obtain and move level lines with arbitrarily high sub-pixel precision, overcoming thus all the drawbacks of finite difference schemes based on pixel approximations.

CHAPTER 7

Level Lines Shortening Algorithm. Accurate Curvature Estimates

It is interesting thus to follow the intellectual truths of analysis in the phenomena of nature. This correspondence [...] makes one of the greatest charms attached to mathematicall speculations.

Pierre-Simon Laplace (1749-1827)

Abstract: This chapter describes the discrete *Level Lines Shortening (LLS)* Algorithm and its variant the *Level Lines Affine Shortening (LLAS)*. The numerical chain starts from a digital image, proceeds to the level lines extraction and to their independent evolution by discrete *Curve Shortening* or *Affine shortening* and ends up with an image reconstruction from the evolved level lines. Following [CM10a], a fast numerical method for extracting the topographic map is presented. We complete here their work with a fast inverse algorithm, of image reconstruction from a family of l evel lines (at arbitrary resolution), provided it is embedded in a tree structure. We show that LL(A)S provides an accurate visualization tool of image curvatures that we term *an Image Curvature Microscope*. As an application we present some illustrative example of image restoration and visualization. Noise, JPEG artifacts, and aliasing will be shown to be nicely smoothed out by the subpixel curvature motion. [1]

Résumé : Ce chapitre présente l'algorithme discret de *Level Lines Shortening (LLS)* et sa variante *Level Lines Affine Shortening (LLAS)*. Le schéma numérique part d'une image pour laquelle on extrait toutes ses lignes de niveau, applique un *Curve Shortening* ou *Affine Shortening* discret, indépendamment pour chaque ligne de niveau, et reconstruit une nouvelle image à partir des ces évolutions. Suivant [CM10a], nous présentons une méthode numérique rapide pour extraire la carte topographique. Nous complétons leur travail avec un algorithme inverse, de reconstruction d'une image à partir d'une famille arbitraires de lignes de niveau, organisées dans une structure d'arbre. Nous montrons que LL(A)S fourni un outil précis de visualisation des courbures, que nous appelons un *Microscope des Courbures d'une Image*. Comme application, nous montrons quelques exemples significatifs de restauration et visualisation d'images. Notamment, l'évolution sous-pixélienne peut servir pour réduire le bruit, les artefacts JPEG et l'aliasing dans les images.

[1] This corresponds to the article *An Image Curvature Microscope*, to appear in SIAM Multiscale Modeling and Simulation, joint work with Pascal Monasse and Jean-Michel Morel. [CMM11]

Contents

7.1 Introduction

Caselles, Coll and Morel [CCM96] discussed the physical generation process of images as a combination of occlusions, transparencies and contrast changes. Subsequently, they defined [CCM99] a contrast invariant representation of digital images in terms of a topographic map, proposed several vizualization strategies and established some stability results of the topographic map under digitization. The main objects of their analysis were the *level lines* of an image, as the boundaries of its level sets.

A study by Kronrod in 1950 shows that if the function u is continuous, then the isolevels sets $\{u = \lambda\}$ are endowed with a tree structure when ordered by inclusion. These isolevel sets are not necessarily curves; they are curves, however, if u has continuous first derivatives. Monasse et al. [CCM03] extended Kronrod's result for lower semicontinuous and upper semicontinuous functions and proved that the rees of upper and lower level sets can be merged into a single one, called *the tree of shapes*.

This representation is well suited for shape analysis and recognition, since it is based on the geometrical information of images. In particular, for block and bilinear image interpolations the level lines have the following properties: they are composed of a finite number of rectifiable Jordan curves, and they are nested. However, since the level lines of digital images (zero order interpolates) suffer from pixelization effect, shapes cannot be accurately described and thus bilinear level lines are prefered.

Based on this image representation, we describe an Euclidian and affine invariant evolution of an image by mean curvature and affine curvature, operating directly on level lines. The discrete Level Lines Shortening algorithm starts from a digital image, proceeds to the level lines extraction and to their independent evolution by discrete curve shortening or affine shortening and ends up with an image reconstruction from the evolved level lines. In addition, it provides an accurate visualization tool of image curvatures computed on the smoothed level lines. This, hopefully, advances Attneave's program and yields what we shall term a *curvature image microscope*, since level lines have floating coordinates and the image can be reconstructed from them at any precision. The above described numerical chain was outlined in [KM99] and also in [LMMM03] where shape recognition algorithms were explored. The chain will be completed here with a subpixel image reconstruction from an arbitrary tree of level lines, which results in a powerful visualization tool.

There is something slightly paradoxical in smoothing an image to see it better. Nevertheless, noise, JPEG artifacts, and aliasing (pixelization effects) will be shown to be nicely smoothed out by the subpixel curvature motion. As anticipated by Attneave, the level line evolution eliminates the erratic curvatures and yields a curvature more conform to our multiscale contour perception. Finally the level line visualization (after smoothing) reveals many hidden image details which can be zoomed in, thanks to the grid independent representation of the image by its level lines. The resulting algorithm is fast and can be tested on line[1] [2].

This chapter describes in detail the discrete Level Lines Shortening (LLS) Algorithm and its variant the Level Lines Affine Shortening (LLAS). In particular, the bilinear interpolation of gray level images is described. Then, following [CM10a], a fast numerical method for extracting the topographic map is presented. We complete here the work with a fast inverse algorithm, of image reconstruction from a family of level lines (at arbitrary resolution), provided it is embedded in a tree structure. The Image Curvature Microscope is described in section §7.4 where many numerical comparisons are performed. Section §7.5 is devoted to illustrative experiments on a choice of image parts containing contours, shapes and textures.

[21] http://www.ipol.im/pub/algo/cmmm_image_curvature_microscope/

7.2 The Level Lines Shortening Algorithm

We set forth a grid independent evolution of a digital image by curvature motion, which corresponds precisely to the analytical framework presented in Chapter 6. This image processing algorithm, *Level Lines Shortening* (LLS) or *Level Lines Affine Shortening* (LLAS), first extracts all level lines of a digital image, with a number of levels sufficient to grant an exact reconstruction of the initial image. Then the algorithm simulates an image evolution by moving independently and simultaneously all of its level lines by curve shortening (CS) (resp. affine curve shortening (AS)). The evolved image is eventually reconstructed from its evolved level lines. We have just seen in Chapter 6 that the image reconstructed from the evolved level lines is a viscosity solution of the mean curvature motion (MCM) (resp. affine curvature motion (ACM)) provided that the level lines at almost all levels evolve by curve shortening (resp. affine shortening).

The level lines (affine) shortening chain LL(A)S, described in Algorithm 7, is based on a topological structure, the inclusion tree of level lines as a full and non-redundant representation of an image, and on a topological property, the monotonicity of curve shortening with respect to inclusion. The hierarchy of the level lines is therefore maintained while performing the smoothing. Thus, the reconstruction can start with the largest level line, namely the frame of the image, and continue by filling from top to bottom in this inclusion the interior of each level line. At each step the lamina bounded by the current level line is filled in with its own level, and these levels are updated when passing to its descendants.

Algorithm 7: Level Lines Shortening (LL(A)S) Algorithm

Input: Original Image u_0.

Output: The LL(A)S evolution of u_0 at scale t: $u(\cdot, t)$.

1 Extract the tree of level lines $\{\Sigma_0^{\lambda,i}\}_{i\in F_\lambda,\lambda}$;

2 **for** *Level line* $\Sigma_0^{\lambda,i}$ **do**

3 $\quad \Sigma_t^{\lambda,i}$ = Discrete Curve/Affine Shortening of $(\Sigma_0^{\lambda,i})$;

4 **for** *Evolved Level line* $\Sigma_t^{\lambda,i}$ **do**

5 $\quad$ fill the interior of level line $\Sigma_t^{\lambda,i}$.

LLAS is illustrated in Figure 7.1. From left to right we perform each step of the numerical chain. The level lines were extracted at half-integer gray values and were chosen with a quantization step $q = 4$. The Moisan affine plane curve evolution [Moi98] is then applied independently to all level lines, at *renormalized scale* $s = 4$. This scale is chosen so that a circle with radius $r = 4$ (where the unit is given by the length of a pixel edge) disappears at scale $s = 4$. This normalization by the result is numerically important for comparing numerical schemes with very different settings. A new image which has exactly these curves as level lines is finally reconstructed. The result is by Theorem 6.4.1 an affine invariant curvature motion (ACM) of the original image. The rest of this section is devoted to several crucial details of LL(A)S regarding the level lines extraction, their evolution, and the reconstruction algorithm.

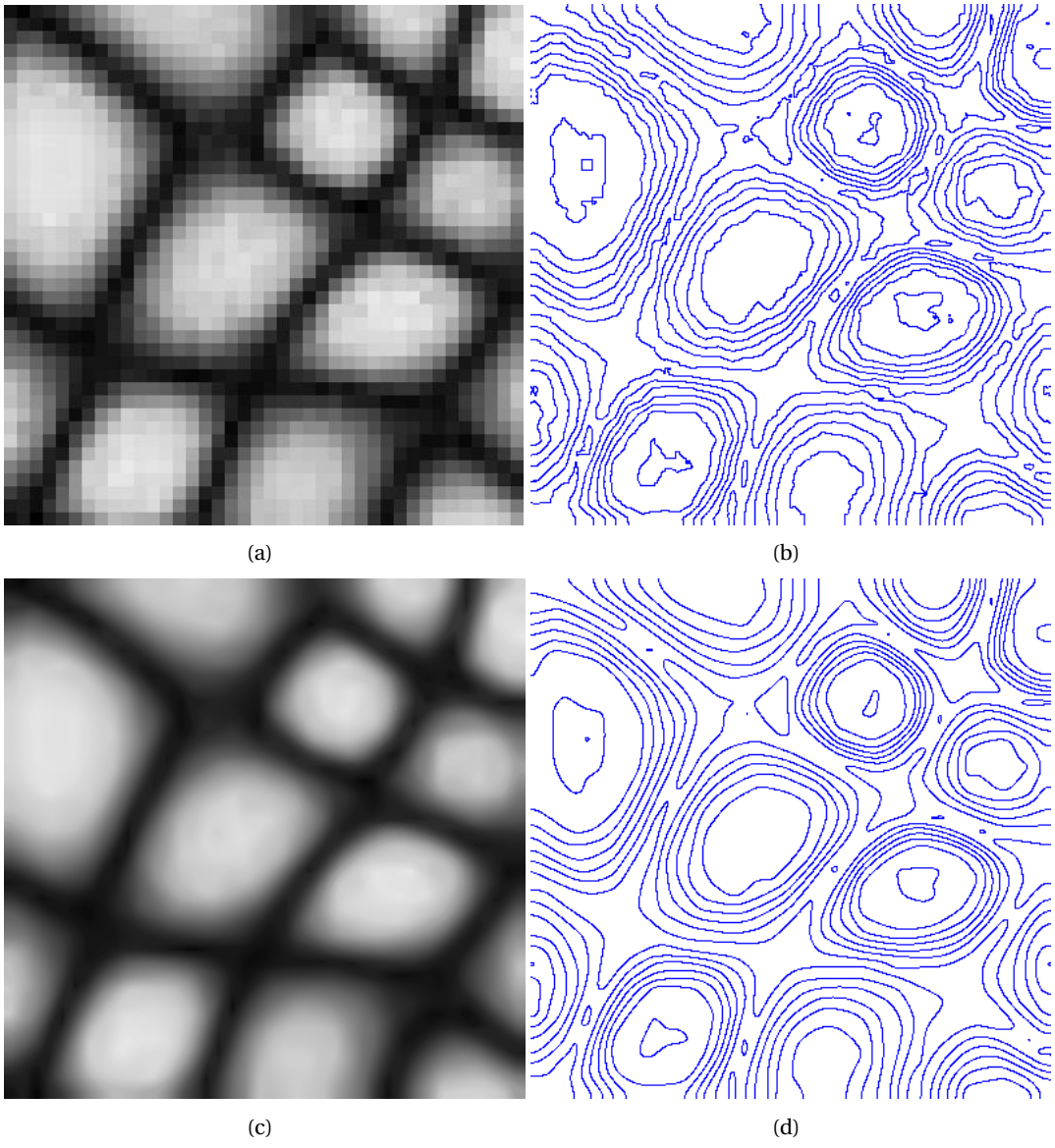

(a) (b)

(c) (d)

Figure 7.1: Illustration of the LL(A)S numerical chain. (a) Original image. (b) Bilinear level lines extraction. (d) Simultaneous and independent smoothing of level lines by affine shortening. (c) Image reconstructed from shortened level lines.

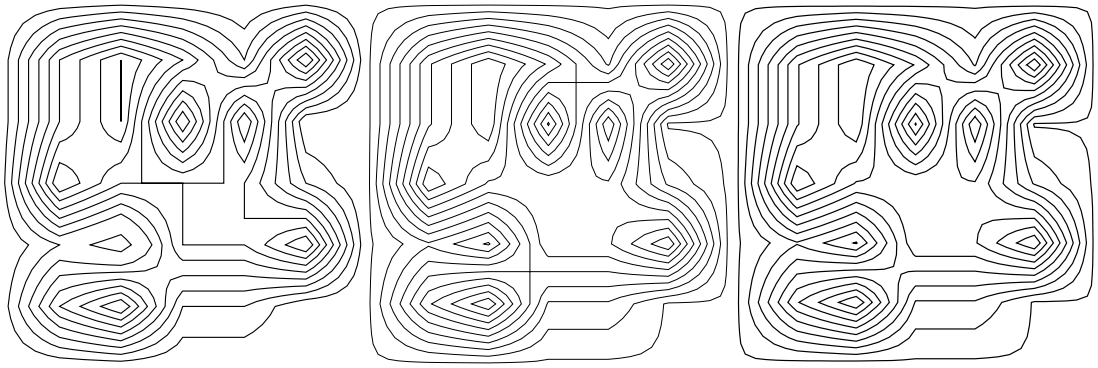

Figure 7.2: Gray levels for a piecewise bilinearly interpolated image. Three different sets of level lines were computed. Left: gray levels from 10 to 100 with step 10. Observe how some of the level lines (the ones at gray level 70) follow the dual edges, producing an effect similar to pixelization. Middle: level lines were computed at gray levels different from those of the original image but we get 90^o crossings between level lines due to the presence of a saddle point. Nevertheless, these saddle points will always appear inside the dual pixels and the curves never go along the grid of the digital image. Right: gray level 11 to gray level 91 with quantization step 10. Pixelization effect no longer arises since level lines are computed at gray levels different from those of the original image.

7.2.1 Bilinear Interpolation

The simplest image interpolation that preserves its continuity is the bilinear interpolation on the dual pixels. (A dual pixel is any square whose vertices are centers of contiguous pixels). The bilinear interpolation in the dual pixel is written in the form

$$u_0(x,y) = axy + bx + cy + d$$

where the parameters a,b,c,d are computed from the values taken at the four vertices of the dual pixel, which are normal pixel values. The bilinear interpolated image is the concatenation of the bilinear interpolations on all dual pixels; it is continuous, but its gradient may present discontinuities.

7.2.1.1 Bilinear Level Lines

The equation for a level line at level λ of the bilinear interpolated image inside a dual pixel can be written

$$a(x-x_s)(y-y_s) + (\lambda_s - \lambda) = 0$$

or

$$bx + cy + (d-\lambda) = 0.$$

In the first case, level lines are pieces of hyperbola, of asymptotes $x = x_s, y = y_s$. When $\lambda = \lambda_s$ the level line consists of two orthogonal straight lines crossing at the saddle point (x_s, y_s), provided this point is inside the dual pixel. In the second case, level lines are straight lines. This may lead to visual pixelization effects, for instance when level lines pass through the center of a pixel and follow a dual-edge (see Figure 7.2). This phenomenon will be attenuated by taking for λ only half-integer values (given that the digital image has integer values).

7.2.1.2 The Inclusion Tree

One can decompose an interpolated image into its level lines at predefined levels. A fast algorithm, the Fast Level Set Transform (FLST) performing the decomposition into a tree of shapes, is described in [CM10a] and [MG98]. The image is parsed into a set of parametric Jordan curves. This set is ordered in a tree structure, induced by the geometrical inclusion.

We say that a curve Σ^{λ_1} is a *child* of the curve Σ^{λ_2} and we denote

$$\Sigma^{\lambda_1} \prec \Sigma^{\lambda_2}$$

if its interior is included in the interior of the latter. In addition, each curve has an assigned tag ± 1 according to whether it is the boundary of a connected component of a lower level set ($\mathrm{sgn}(\Sigma^{\lambda}) = -1$) or upper level set ($\mathrm{sgn}(\Sigma^{\lambda}) = +1$).

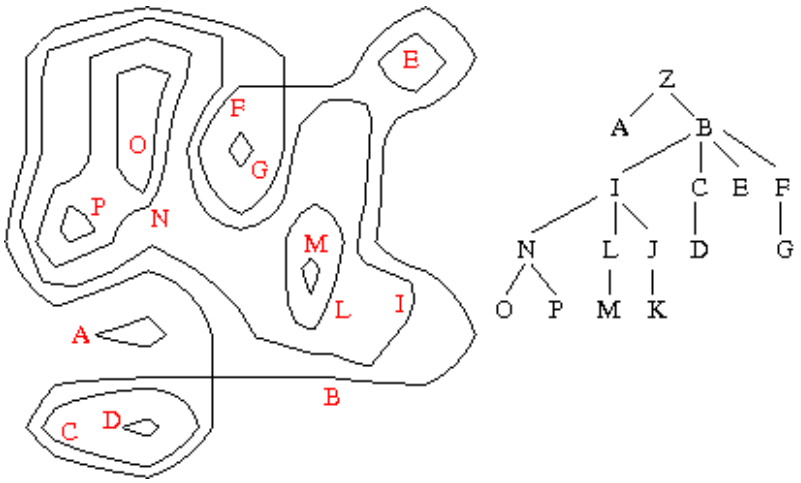

Figure 7.3: Tree of bilinear level lines.

For each gray level $\lambda \in \mathbb{N}+1/2$ there corresponds a finite set F^{λ} of level lines $\{\Sigma_0^{\lambda,i}\}_{i\in F^{\lambda}}$. Each level line $\Sigma_0^{\lambda,i}$ is stored as a set of ordered points leaving the level line interior on the left hand side. Thus, the tree of level lines is given by a finite set of *tagged* polygonal lines, indexed by half-integer gray values

$$\mathcal{T}_0 = \{\Sigma_0^{\lambda,i}; i \in F^{\lambda}, \lambda \in \mathbb{N}+1/2\}. \tag{7.1}$$

An inclusion tree of bilinear level lines is displayed in Figure 7.3.

7.2.2 Direct Extraction Algorithm of Bilinear Level Lines

We describe a simple algorithm for the extraction of level lines of a bilinear interpolated image, alternative to the Fast Level Set Transform. This algorithm requires a quantization avoiding initial levels of the image. The algorithm is in two phases: it first extracts the bilinear level lines then it orders them in a tree.

[2] This section is taken from [CM10a] and it was added here for the reader's convenience.

7.2.2.1 Extraction

The *extraction* of a level line relies on these observations:

1. the level line is not a regional extremum, so that an orientation can be chosen, for example leaving the interior of the level line on the left hand-side;
2. the level line meets dual edges at non endpoints, so that when we 'enter' a dual pixel by a dual edge, we can compute from which other dual edge to 'exit'.

Considering we get into the dual pixel through some dual edge, the exit dual edge is in front, on the left or on the right depending on the value of λ with respect to levels at both other corners of the dual pixel. We may store for the line only its list of intersections with dual edges.

To avoid extracting several times the same level line, we put markers at all intersection points of extracted level lines with dual edges. The algorithm starts by considering all dual edges at the boundary of the image. If a level of interest λ is between the levels at endpoints of the dual edge, we follow the level line, marking intersection points with dual edges. We then close the level line by the shortest path along the image boundary. Finally we do the same for interior dual edges. For them, we detect closure by checking the marker at exit dual edges.

7.2.2.2 Ordering the Level Lines in a Tree

To build the tree structure of the extracted level lines, we consider all intersection points of level lines with vertical edgels and order them. While scanning a column of dual edges, we are in the interior domain of a level line if we have crossed it an odd number of times. If we meet a level line that has no parent yet, its parent has to be the last level line we are in. For the root, we add the boundary of the image as a level line to the list L at the beginning.

Let L be the list of level lines. To describe the intersection y of a level curve Σ_{id}, having index id in the list L, with dual edge at column $i+0.5$, we use the triplet (i, y, id). The main idea used in the ordering algorithm is to look for the innermost shapes that we denote generically by Σ. The arrow $\Sigma \leftarrow \tilde{\Sigma}$ shorlty says that we set the curve Σ to be now $\tilde{\Sigma}$. And finally, we denote the parent of a level line by $Parent(\Sigma)$.

Algorithm 8: Ordering the level lines in a tree.

Input: List L of bilinear level lines Σ
Output: Fill tree structure

```
1 Collect all (i, y, id) in array V;
2 Order V lexicographically by key (i, y);
3 Σ ← ∅;
4 for all (i, y, id) ∈ V do if Σ = Σ_id then
5     Σ ← Parent(Σ);
6     else if Σ ≠ ∅ and Parent(Σ_id) = ∅ then
7         set Σ_id as a child of Σ;
8         Σ ← Σ_id.
```

This algorithm relies on the fact that the quantization is chosen so that each level line crosses dual edges, but does not contain any. For this, it is sufficient that it avoids the levels at the centers of pixels (the initial data). In particular, regional extrema of the image cannot be extracted by the algorithm.

7.2.3 Independent Evolution of All Level Lines

As already described, the affine shortening is numerically defined as an alternate filter of affine erosion and affine dilation. Up to re-sampling issues, the scheme is monotonous with respect to geometrical inclusion and therefore the tree structure of the level lines is preserved. It consists of a finite set of Jordan curves, denoted by

$$\mathscr{T}_n = \{\Sigma_n^{\lambda,i}; i \in F^\lambda, \lambda \in \mathbb{N} + 1/2\}. \tag{7.2}$$

Figure 7.1.(c) displays the affine evolution, using Moisan's robust algorithm [Moi98], of the level lines appearing in Figure 7.1.(b). As can be observed, the curves become smoother, oscillations due to the grid reduce, and curves with small perimeter vanish. The inclusion tree structure is clearly preserved under the affine shortening evolution. The same chain applies to the curve shortening by the Mackworth-Mokhtarian scheme [MM92]. With a fine enough curve sampling it is consistent with the curve shortening and therefore also numerically monotone.

7.2.3.1 The Fattening Effect

Bilinear level lines can present self-intersections at image saddle points. In that case, LLS develops a non-empty interior, meaning that two distinct touching curves instantly tear apart, and that the space liberated becomes a flat region with a grey level equal to the level line value. Thus the level line "fattens". This effect is easily explained by considering the classic evolution of the level curves just above and just below the saddle curve.

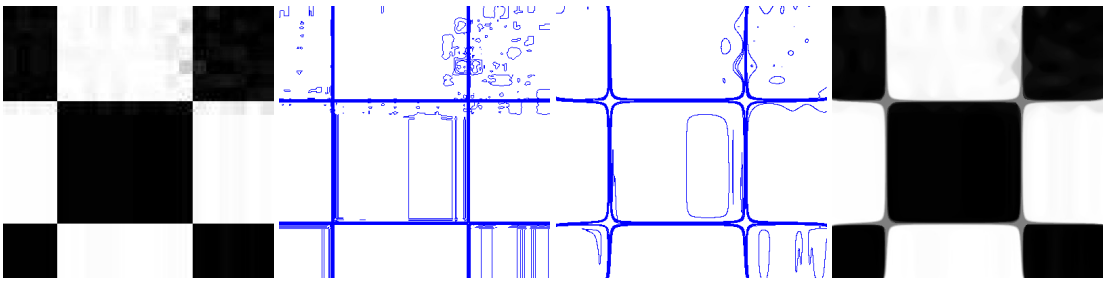

Figure 7.4: Fattening effect. From left to right: the original image and its extracted level lines with quantization step $s = 16$, their independent evolution by affine shortening at renormalized scale $l = 8$ and the image reconstructed from the evolved level lines. Observe that distinct, touching level lines tear apart and non-empty interiors appear at the saddle points. At these points four squares, two black, two white, meet initially by their corners. After evolution, fattened grey regions are liberated by the retraction of the square level lines surrounding the black and the white squares.

Let Σ^μ be a level line passing through a saddle point (see Figure 7.4). Assume that the curve is the limit of level lines from above and from below. More precisely, suppose (e.g.) that

for slightly higher levels λ the interiors of level lines Σ^λ include the interior of Σ^μ and that for smaller levels each connected component of the interior of Σ^μ contains the interiors of Σ^λ (this is always the case if u_0 is a bilinear interpolation). Then the exterior curve will evolve as the limit of the level lines surrounding it from the outside and simultaneously all interior (touching) Jordan curves will evolve as the monotone limits of interior level lines. Consequently, they will tear apart from the exterior curves, thus liberating a flat region.

7.2.4 Image Reconstruction from a Tree of Level Lines

The algorithm described in this section performs an exact image reconstruction from a topographic map, i.e. from an arbitrary family of Jordan curves organized in a tree structure with respect to geometrical inclusion.

The reconstruction starts from a topographic map, namely a family of discrete level lines (typically obtained after (affine) curve shortening) $\{\Sigma^{\lambda,i}\}_{i\in F^\lambda,\lambda\in\Lambda}$ organized in an inclusion tree structure. This tree is walked down (parent before children) and the interior of the current level line is filled in with its level λ. Using that order, each level line interior is painted before its descendants, ensuring that its private pixels are at the correct level while non-private pixels get painted over by the children. This yields an exact reconstruction for any digital image u_d from its level lines at half-integer levels.

Theorem 7.2.1. *Let $\mathcal{T} = \{\Sigma^{\lambda,i}; i \in F^\lambda, \lambda \in \mathbb{N} + 1/2\}$ be the tree of bilinear level lines associated to u_d. For every x let λ be such that $x \in Int(\Sigma^\lambda)$ and $\forall \Sigma^{\tilde{\lambda}} \prec \Sigma^\lambda$, $x \notin Int(\Sigma^{\tilde{\lambda}})$ and define*

$$\tilde{u}_d(x) = \begin{cases} \lambda - 1/2, \ if sgn(\Sigma^\lambda) = -1 \\ \lambda + 1/2, \ if sgn(\Sigma^\lambda) = +1 \end{cases}$$

Then $u_d \equiv \tilde{u}_d$.

A closed curve Σ is stored as a set of ordered points $\{P_k(x_k, y_k)\}_{1\le k\le N}$ with N depending on Σ. The real numbers x_k and y_k are the floating point coordinates of the vertex number k of the polygon Σ. We need to fill in all pixels with integral coordinates (j, i) inside the polygon. To avoid any ambiguity, the algorithm secures that y_k is never an integer by translating when necessary Σ by a tiny amount ε vertically or horizontally, at the price of a minor numerical uncertainty in the reconstructed image. The filling in of each curve is performed by a fast ray casting algorithm described below.

7.2.4.1 Polygon Intersections with the Grid

The goal of Algorithm 9, which is a preliminary to the filling algorithm, is to find the intersections of the polygonal level line with all horizontal lines $y = i$. For any given i the intersection is in fact the intersection of a segment $[P_k P_{k+1}]$ of the polygon with the line $y = i$. These intersections are ordered by their abscissas so that $x_1^i \le x_2^i \le \cdots \le x_p^i$, where p is even because Σ is a closed curve. This gives a simple and fast decision rule: a pixel (j, i) is surrounded by the polygon if and only if j is within an odd interval $[x_{2k+1}^i, x_{2k+2}^i]$.

Algorithm 9: Intersections of a polygon Σ with the grid

Input: Vertices $P_k(x_k, y_k)$ of polygon Σ
Output: For each i, the ordered list L^i of points of Σ on the line of equation $y = i$

```
for all i do L^i ← ∅;
for all segments [P_k P_{k+1}] do
    for i ∈ [y_k, y_{k+1}] ∩ ℕ do
        (x, i) ← [P_k P_{k+1}] ∩ {y = i};
        Insert x in L^i;
for all i do sort list L^i
```

7.2.4.2 Filling the Interior

Line by line all odd intervals on L^i are enumerated and filled in with level $\lambda \pm 1/2$ at all pixels with ordinate i whose abscissa is inside such an interval, as shown in Algorithm 10.

Algorithm 10: Filling polygon Σ

Input: Sorted lists L^i of intersections of Σ with lines $\{y = i\}$, level λ
Output: Pixels inside polygon Σ are at level $\lambda \pm 1/2$, pixels outside unchanged

```
for all i do
    for all x^i_{2k+1} ∈ L^i do
        for j ∈ ℕ ∩ [x^i_{2k+1}, x^i_{2k+2}] do
            pixel (j, i) ← λ ± 1/2
```

Due to the inclusion principle it is possible to go from the $2D$ topology of the level lines to the $1D$ topology on a dual edge and conversely. Suppose that two or more level lines belonging to different gray levels intersect a dual edge, leaving the same data points outside and inside: denote them P_{in} and P_{out} (Figure 7.5(a)). Then the restored gray value at P_{out} is the gray value associated to the largest shape ordered by inclusion which leaves the pixel outside, whereas P_{in} belongs to the smallest shape that includes the pixel. If curves with different orientation cross the same dual edge it is enough to update the gray value at P_{in}. This conforms to our choice of filling the interiors of the lines in the order given by the level line inclusion tree.

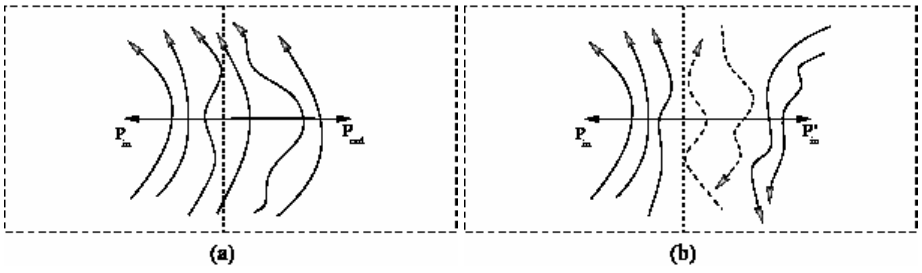

Figure 7.5: The level line topology is reflected in the $1D$ ordering of their intersections with dual edges.

Numerical examples of image reconstruction from the tree of evolved level lines are displayed in Figure 7.1 and Figure 7.4.

7.3 Numerical Properties of the LLS Numerical Chain

7.3.1 Fixed Point Property

The filling algorithm itself is a stand alone *image reconstruction* method, working for every family of curves endowed with levels and a tree inclusion structure. To check its consistency, it is enough to take any digital image u_0, to extract its level lines at quantized gray levels, with quantization step $s = 1$ but without applying any evolution. Then the digital image is reconstructed exactly from its level line tree by the filling algorithm.

7.3.2 Local Comparison Principle and Regularity

The order preserving property or *inclusion principle* is the main structural requirement of a level line evolution algorithm. It basically prevents the crossing of two different level curves and therefore permits the construction of a unique image having a prescribed set of level lines. Some level lines may present multiple crossings at saddle points, in which case the level lines shortening develops a non-empty interior. The phenomenon is due to an instantaneous tearing apart of two distinct, touching curves. Any level curve with self-contact points develops a non-empty interior by CS (curve shortening), which implies the formation of a flat area (see Figure 7.6.).

We compare in the following the LLS algorithms with the FDSs for mean curvature given by Guichard et al. in [GM97]. The finite difference schemes (FDS) tested here have been optimized by its authors It creates new grey levels and blurs out the edges. It is true that the full contrast invariance of an FDS is restored by its stack filter. Nevertheless, spurious diffusions occur around the image extrema and at *T-junctions* or *X-junctions*. At saddle points both algorithms create new extrema, and therefore spurious level lines. Only LLS resolves this issue, by separately evolving the level lines and then reconstructing the image.

Figure 7.6 compares various implementations of the mean curvature motion on a checkerboard image (a) with calibration of the numerical scales. The left images of each pair show the evolutions of the image by the various implementations of mean curvature motion, while the right ones display a zoom at the X-junction and the corresponding level lines. The iterated median filter (a) instantaneously stops and leaves the checkerboard invariant. This may look fine, but it is not consistent with curvature motion. LLS (b) is performed with a 1D gaussian kernel of standard deviation $\sigma = 2$. The level lines are encoded with a $p = 5$ points per pixel precision and displayed with a $s = 4$ quantization step, starting at an offset $o = 96$. The figure next shows the effect of FDS (c) at normalized scale $l = 3$, the FDS stack filter (d) at normalized scale $l = 3$, and finally the LLS evolution with the same normalized scale. At $X - junctions$, both FDS and the FDS stack filter create spurious diffusions, while LLS doesn't. With LLS a grey region develops at the junction, because level lines corresponding to different gray levels instantly tear apart. This is not necessarily gratifying perceptually, but it is mathematically consistent.

Figures 7.7 and 7.8 on a binary fingerprint put in evidence the failures of FDSs. Up to some critical scale, FDS stack filters restore the correct topology, but in case of fast diffusions they break off as well. Oscillating ridges with high gradient amplitudes make it difficult to keep separated the various connected components during the smoothing process. A visual

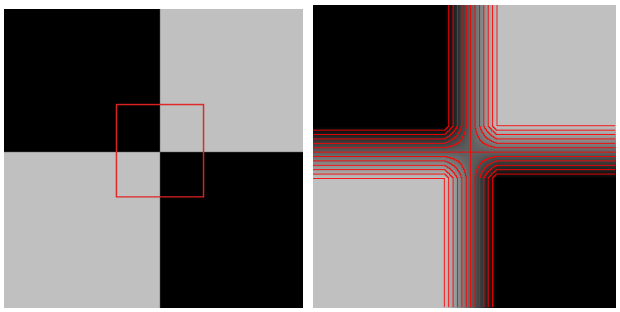

(a)

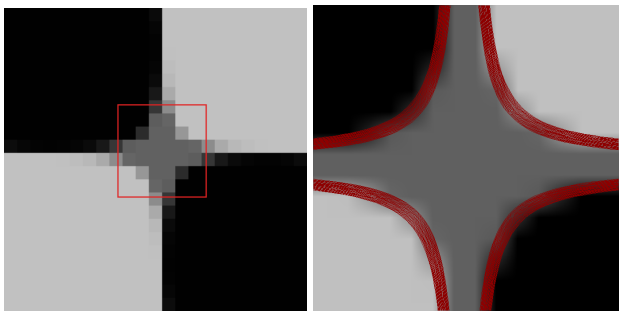

(b)

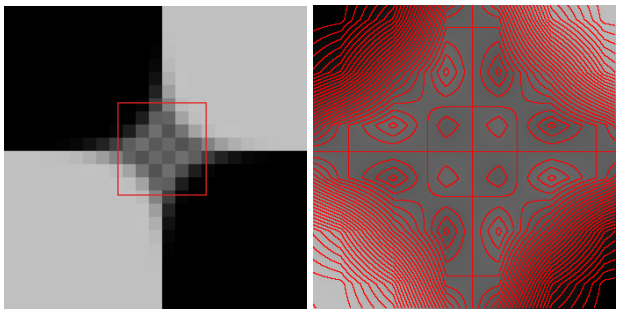

(c)

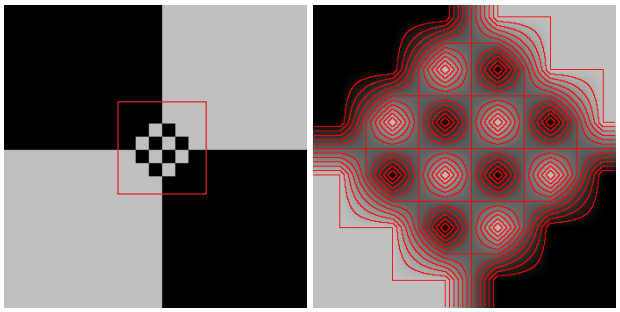

(d)

Figure 7.6: The four pairs present various implementations of the mean curvature motion on a checkerboard image (left column) and zooms at an X-junction, with its level lines overprinted on the image (right). From top to bottom : (a). original image (the zoom is by bilinear interpolation), (b). Level lines shortening, (c). Finite difference scheme, (d) FDS stack filter. Only LLS does not create new extrema.

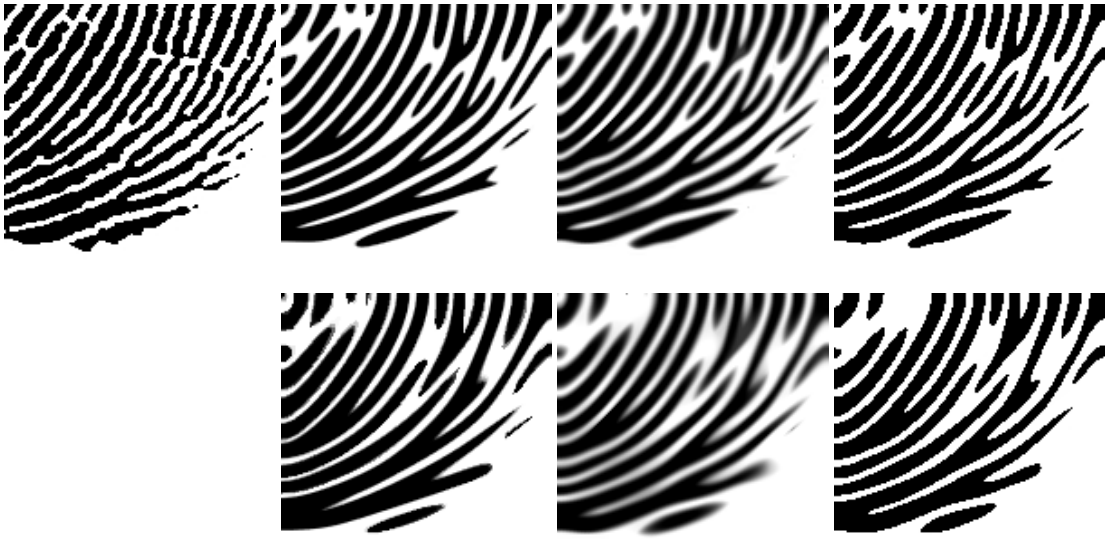

Figure 7.7: Various implementations of the affine curvature motion. the original image is displayed alone in the left column. In the other columns, from left to right: LLAS, FDS and FDS-stack filter at renormalized scales $l = 4$ (top) and $l = 8$ (bottom). In the case of the affine curvature scale space, the gradient amplitude keeps down ridge diffusion, unlike the mean curvature scale space. In general the affine smoothing performs better than the curvature motion (compare with Figure 7.8).

Figure 7.8: Various implementations of the mean curvature motion. Are compared (from left to right): LLS, FDS, the FDS-stack filter and the median filter at renormalized scales $l = 4$ (top) and $l = 8$ (bottom). Up to some critical scale, the stack filters restore the correct topology, but in case of fast diffusions they break off as well. Observe that spurious diffusion mixing the ridges occurs in all cases except LLS, which tears apart ridges and emphasizes crossovers. A comparison with Figure 7.7 shows that the affine curvature schemes perform all better than their analogous curvature schemes.

comparison of these two figures proves abundantly that the affine curvature is a much better shape preserver than the curvature motion.

7.3.3 JPEG Artifacts Reduction on Color Images

The prevailing JPEG 1992 image coding format aims at compressing images while maintaining acceptable image quality. This is achieved by dividing the image in 8×8 pixels blocs and applying a discrete cosine transform (DCT) on the partitioned image. The resulting coefficients are quantized. In particular the less significant coefficients are set to zero. This process causes several types of artifacts such as Gibbs oscillations, staircase noise along curving edges, and checkerboard patterns (which are nothing but cosine functions). The phenomenon is illustrated in Figure 7.9. LLS seems to be a useful postprocessing technique for JPEG artifact reduction. In color images LLS is applied independently to each color channels.

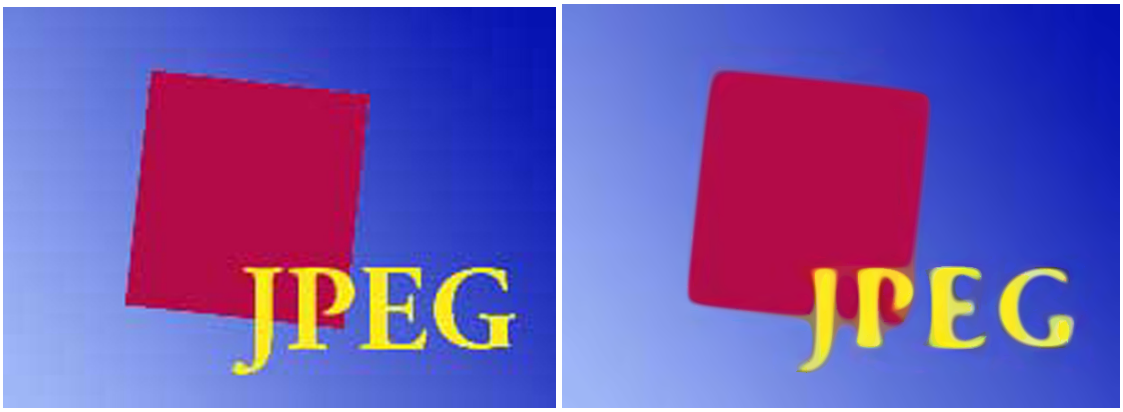

(a) (b)

Figure 7.9: (a). Original image, suffering of JPEG artifacts such as Gibbs oscillations, staircase noise along curving edges and checkerboarding. (b). LLAS is applied separately to each RGB channel. Although diffusions occur at junctions, LLAS considerably reduces these artifacts.

7.3.4 Accurate Mean Curvature Evolution

The main goal of the implementation is to obtain and move level lines with arbitrarily high sub-pixel precision. Indeed, level lines are encoded as polygons whose vertices have double precision coordinates. Moving simultaneously level lines extracted with high sample precision allows straight level lines with high gradient to stand still with LLS, whereas they are diffused by FDS, even in its stack variant.

The phenomenon is shown in Figure 7.10 on a photograph of one of Botticelli's paintings. Are displayed the original detail (left column) and the differences in absolute value between the original and its evolutions by LLS (middle column) and by the FDS stack filter (right column). The FDS stack filter was applied at normalized scale $l = 2$ and the LLS evolution at an equivalent normalized scale. For FDS the level lines were quantized at half integer levels with a step $s = 1$ and extracted with $p = 5$ points per pixel. Zooms of the highlighted regions in the original image show fast diffusions of shapes for stack FDS, even though the curvature is zero.

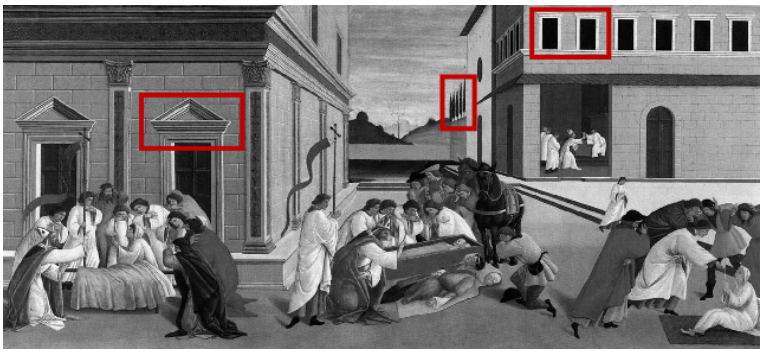

(a)

(b)

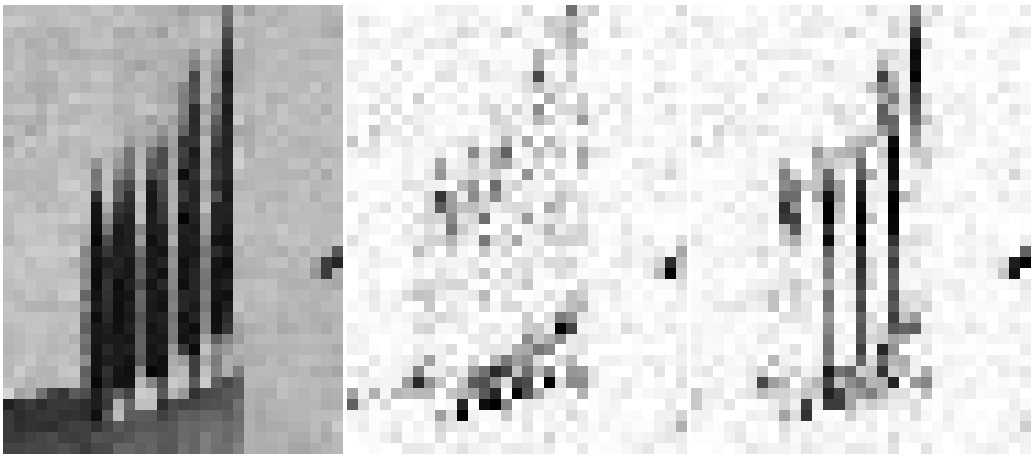

(c)

(d)

Figure 7.10: Zooms on three highlighted details in the painting "Three miracles of St. Zenobius" by Sandro Botticelli (Left). Middle column: the differences in absolute value between the original image and the evolutions by level line shortening. Right: same result, after applying the FDS stack filter. Even though the curvature is zero, the FDS stack filter lets level lines with high gradient evolve, while with LLS straight lines stand still.

See for example the window frames (b) the trees in the background (c) or the finely textured bricks (d).

7.4 An Image Curvature Microscope

Whenever we talk about curvatures in a digital image, we actually refer to the curvatures of the level lines associated to the image. Yet, most curvature computation algorithms are based on finite difference schemes (FDS) with formula (5.1). But with FDSs, the curvature depends on the gray values of a whole neighborhood. Consequently, high oscillations along transverse level lines do appear.

For the sake of precision, curvatures should be computed directly on level lines and not on a discrete grid. A polygonal line approximation followed by uniform and fine sampling allows one to compute reliable curvatures, but only after level line smoothing. This smoothing is necessary because the initial level lines present oscillations due to the initial aliasing and to the interpolation itself. Thus curvatures wouldn't correspond to our visual perception. But, more fundamentally, the perception of curvature is and must be multiscale. The striking difference between an FDS result and an LLS result is displayed in Figure 7.11. With LLS, the curvature is

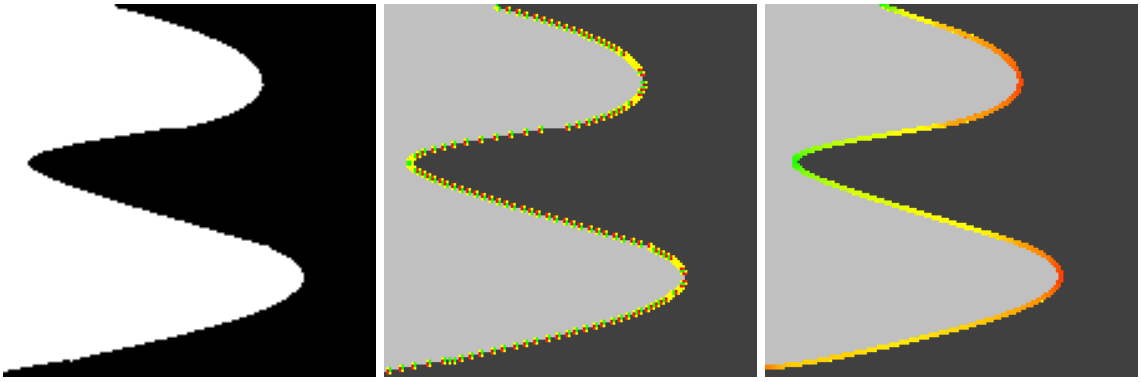

(a) (b) (c)

Figure 7.11: The curvature color display rule. Zero curvatures are displayed in yellow, positive curvatures are shown in a gradation from yellow to red, and negatives from yellow to green. The initial image (a) had its curvatures computed in two different ways: by an FDS by formula (5.1) (b), and by LLS (c). In the first case the curvature presents oscillations, whereas the second result is coherent with our perception.

computed at each vertex of each level line. A curvature image is then created by associating to each dual pixel an average of all curvatures computed in it.

7.4.1 Discrete curvature for a polygonal line

We recall that each level line is stored as a set of ordered points

$$\Sigma = \{P_i(x_i, y_i)\}_{i=0..n}, \text{ with } P_0 = P_n.$$

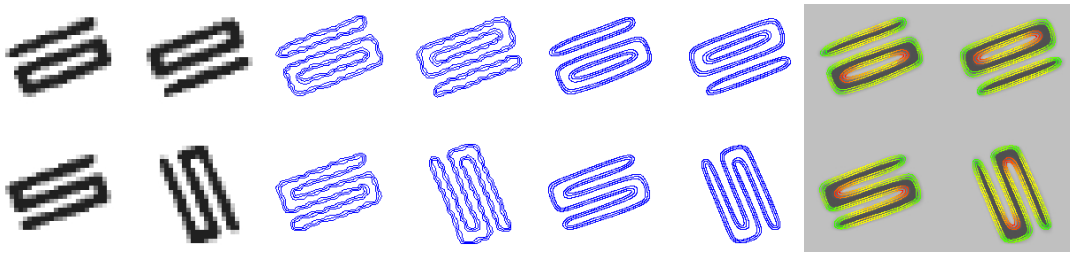

(a) (b) (c) (d)

Figure 7.12: The curvature map numerical chain: (a) original image, (b) level lines, uniformly sampled, (c) evolved level lines, (d) curvature image.

The simplest discrete scalar curvature k_i computed at each vertex P_i is obtained by taking the triple (P_{i-1}, P_i, P_{i+1}) and computing k_i as the inverse of the circumscribed radius R_i of this triangle. Set $\overrightarrow{u_i} = (u_i^1, u_i^2) = \overrightarrow{P_{i-1}P_i}$ and its length $u_i = |\overrightarrow{P_{i-1}P_i}|$, respectively $\overrightarrow{v_i} = (v_i^1, v_i^2) = \overrightarrow{P_{i-1}P_{i+1}}$, with the corresponding length $v_i = |\overrightarrow{P_{i-1}P_{i+1}}|$. Then

Lemma 7.4.1. *The curvature at vertex P_i is given by*

$$k_i = 2\frac{u_i^1 u_{i+1}^2 - u_i^2 u_{i+1}^1}{u_i u_{i+1} v_i}. \tag{7.3}$$

7.4.2 Curvature map

The algorithm computing the curvature map of any digital image is based on LLS. The image level lines at given quantization levels are first extracted, then uniformly sampled with fine sub-pixel step, and smoothed by affine or curve shortening. Curvatures are then computed at each vertex of each level curve and associated to the dual pixels containing the vertex. A curvature image is eventually created by attributing to each dual pixel the average of all curvatures computed in it.

Algorithm 11: Curvature map

Input: Original Image u_0.
Output: Curvatures u_0 at scale t: $u(\cdot, t)$.

```
Extract the tree of level lines {Σ_0^{λ,i}}_{i∈F_λ;λ};
Sample uniformly each level line Σ_0^{λ,i}
for Level line Σ_0^{λ,i} do
    Σ_t^{λ,i} = Curve Shortening Flow (Σ_0^{λ,i});
for Σ_t^{λ,i} = {P_i(x_i, y_i)}_{i=0..n} do
    k_i = 1/R_i;
for each dual pixel do
    k = mean(k_{i_1}, k_{i_2}, ..., k_{i_m}).
```

Topological curvatures and scalar curvatures can be computed as well. Indeed, the information encoded in the tree enables the computation of signed curvatures, where the sign is

either given by the gradient ascent, or by the topological orientation of the curve. In the first case, the curvature changes sign when the grey scale is reverted. Indeed, $\mathrm{curv}(-u) = -\mathrm{curv}(u)$. Thus, a black disk and a white disk on grey background have opposite curvatures. The topological curvature is instead invariant to contrast changes. But it is nonlocal, since its sign depends on the global curve topology and not on the local curve shape. Figure 7.13 illustrates the difference on a famous Julesz texture discrimination experiment. On the left image, a preattentively undiscriminate texture pair. The "10" in random orientations surround a square made of "S". The middle image shows the scalar curvature defined by formula (5.1). This curvature is identical for both shapes. The topological curvature (right) changes because the "0" have an interior circle missing in the "S". This proves that our perception does not compute the topological curvature. If it did, we would discriminate the two textures.

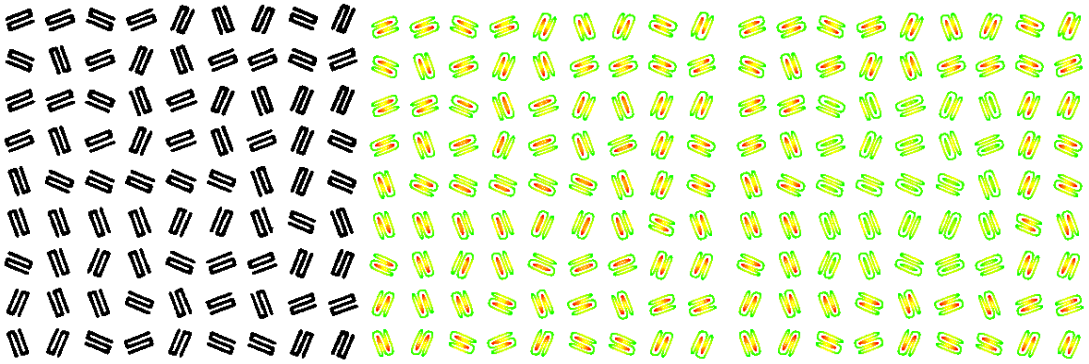

(a) (b) (c)

Figure 7.13: (a) Original image, Julesz pair of undiscriminate textures (b). Signed curvatures, no discrimination (c). Topological curvatures: probably not computed in our perception, it would discriminate the texture pair.

7.4.3 Comparison with FDSes

One could object that the above shortcomings of FDSs can be fixed by interpolating the image on a very thin grid. All schemes being consistent eventually should give similar results. The comparison would be fair because the LLS method actually starts with a subpixel level line description, equivalent to sampling on a finer grid. Nevertheless, curvature computation by FDS wouldn't work satisfactorily, even after a finer interpolation, and even if the smoothing has been done by LLS, which has the advantage of being less diffusive.

To prove this, we run an FDS and LLS on a very simple geometric image, as displayed in Figure 7.14. The FDS was the scheme implemented in [17], which creates minimal smoothing. The LLS was the affine level line motion, whose algorithm can now be tested online. The Level Lines Affine Shortening Algorithm was applied to the original image at the normalized scale $l = 2$. In Figure 7.14 the curvature map is estimated by a direct computation on the shortened level lines and compared to the curvature map computed on the smoothed image by the FDS (approximating the directional derivative $u_{\xi\xi}$ with a 3×3 scheme). On the other hand an FDS with grid refinement was tested in Figure 7.15. The image was zoomed in by a factor $Z = 2$ using bilinear interpolation. The finite difference scheme for the affine curvature motion was

run and the curvatures computed by FDS, before and after smoothing.

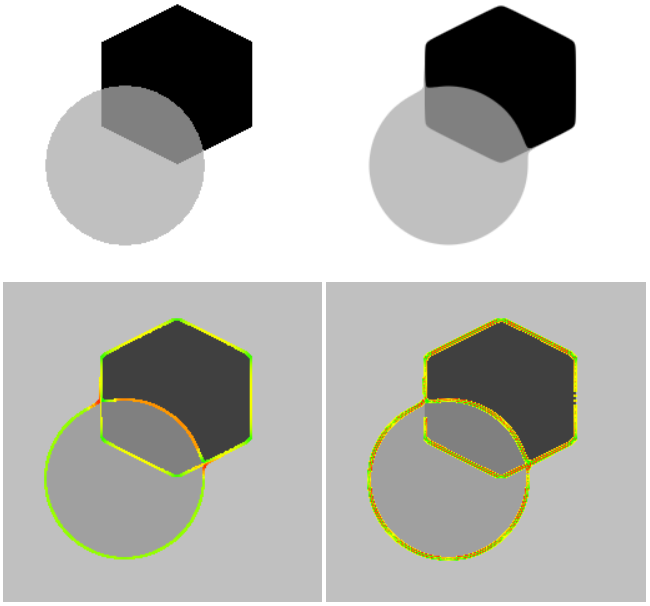

Figure 7.14: From top to bottom and left to right: the original image and its filtering by LLAS at normalized scale $l = 2$; the curvature map estimated by a direct computation on the shortened level lines, as well as the curvature map computed on the LLAS image by FDS.

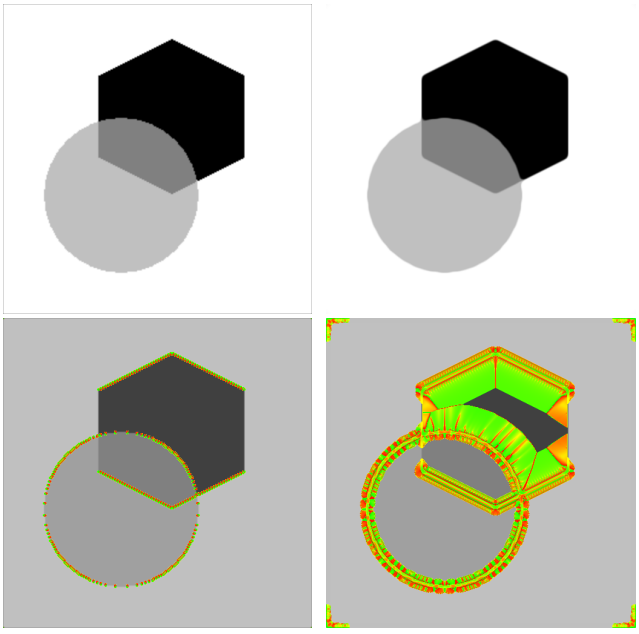

Figure 7.15: From top to bottom and left to right: the original image sampled on a thinner grid using a bilinear zoom by a factor $Z = 2$ and its filtering by FDS for affine curvature motion at renormalized scale $l = 4$; the corresponding curvature maps of the images (before and after FDS filtering), computed with a 3×3 stencil, as before.

As can be seen by comparing Figures 7.14 and 7.15, the difference between both *smoothed images* can be perceived by the human eye as a slight blur with the FDS, due to the diffusion term in the FDS. Note however (by comparing the lower -right images in both figures) that a large diffusion occurs after several iterations of the finite differences scheme. Of more concern, however, is the fact that wrong curvatures appear everywhere with the FDS: see how red and green color alternate on all boundaries. With LLS, in contrast, the computed curvatures are coherent with the geometry.

7.4.4 Curvature Microscope

By performing a scaled zoom on the considered image one can expect to have one level line passing through each dual pixel, and thus to observe more and more exactly the curvatures at microscopic scale. *The fact that all level lines are polygons with real coordinates allows one to zoom in the image at an arbitrary resolution.* This is necessary to explore visually the intricacy of the local image structure. Hence the name of *curvature microscope* given to the final visualization.

Since the curve shortening is only defined for closed curves, a rule is needed for the level lines finishing on the image border. One could close these lines by joining their endpoints by (e.g.) a geodesic on the image boundary. But such junctions would create strong curvatures at the meeting points of the level lines with the image frame. To avoid this phenomenon a standard extrapolation is performed by flipping the image left and right, up and down and extending it in that way by a wide band.

For better rendering, the curvature map is printed over the smoothed image and the latter is attenuated (its gray values are concentrated around 128). Curvature values shade from red to green as follows: positive curvatures scale from red down to yellow; negative ones go down from yellow to green. Thus yellow means a small curvature. The image curvature microscope is a complex visualization tool dealing with three scale space parameters

1. the zooming factor;
2. the quantization step of the level lines;
3. the renormalized smoothing scale (the scale l at which a circle of radius $r = l$ vanishes).

These parameters vary according to the total variation and the gradient amplitude of the image and therefore cannot be *a priori* fixed for any type of image. However, the zooming factor is proportional to the renormalized smoothing scale. The quantization step can be fixed once for all.

(a)

(b)

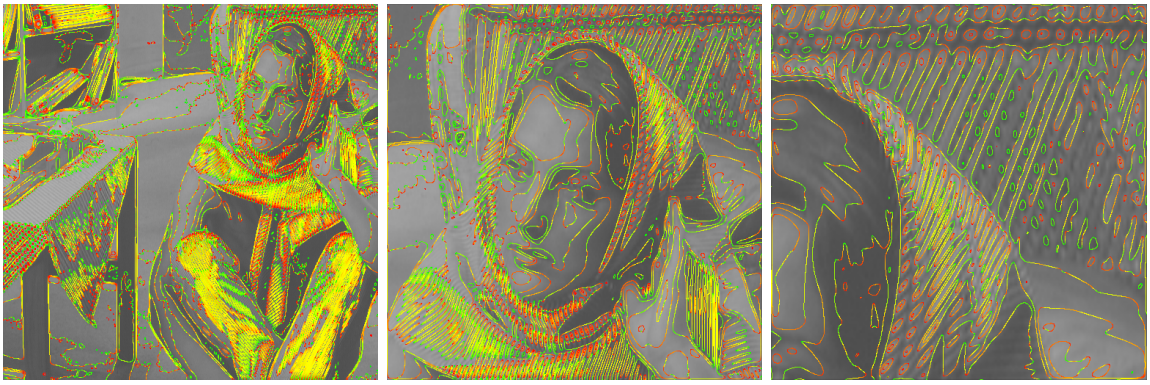

(c)

Figure 7.16: Image curvature microscope. (a) the original image, 2X zoom and 4X zoom of the up-right corner; (b) curvature map computed on the original level lines with a quantization step $s = 36$; (c) curvature map computed on shortened level lines at normalized scales $l = 1$, $l = 2$, and $l = 4$ (the zoom factor must be equal to the normalized smoothing scale). The left column permits to observe the curvature densities. A zoom is necessary to observe the single curvatures. The middle column and right column focus more and more on shape and texture details.

7.5 Image Restoration and Vizualization

After processing the pixelized level lines become accurate curves with sub-pixel control points, whose curvature can be faithfully computed. Thus the whole chain can be viewed as a numerical preprocessing before further numerical analysis and feature extraction. But there is also a strong interest in the direct visualization of the level lines and of the microscopic curvature map of an image. The following gallery on a variety of image details illustrates the recovery of shapes freed from their aliasing, JPEG, and noise artifacts.

7.5.1 Founding Example: Attneave's cat

Short time smoothing reveals useful invariant features (curvature extrema, inflection points, angles and junctions). Therefore, as pointed out by Attneave, objects are represented with great economy and striking fidelity by marking the points at which their contours change direction maximally. In Figure 7.17, the head of the Attneave cat is scanned and processed by LLAS. Before filtering, the curvature values reflect essentially the pixel staircases: positive and negative curvatures in red and green alternate along contours. A visual inspection shows that, after LLAS, the level curves can be easily segmented into concave and convex parts, separated by flat parts (in yellow).

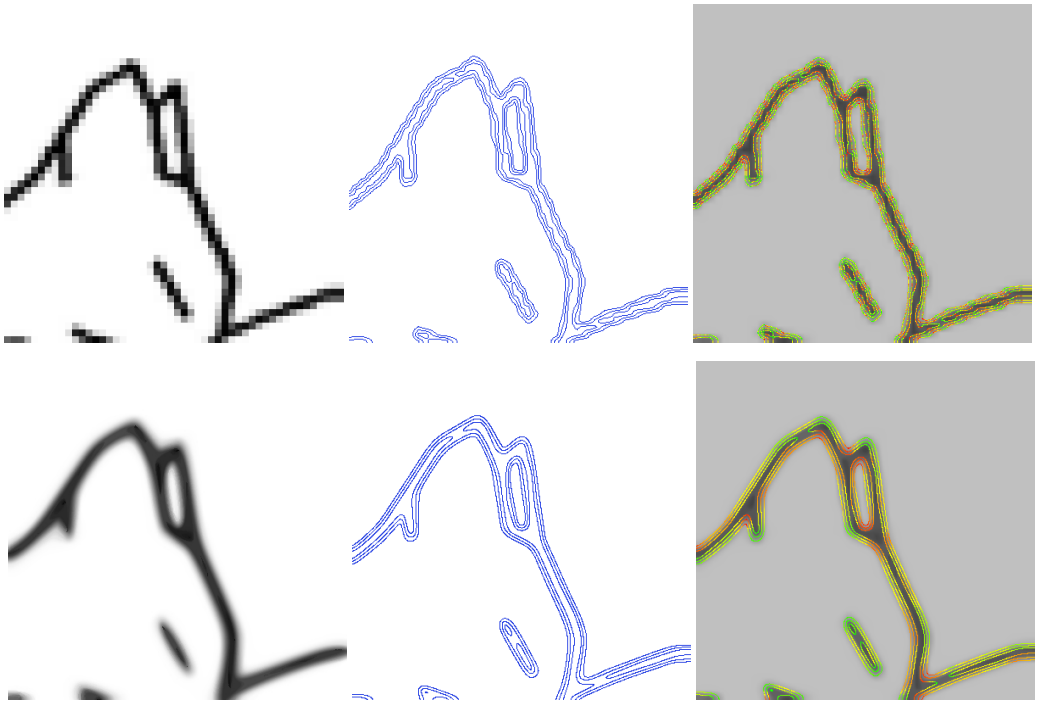

Figure 7.17: Part of Attneave cat, its corresponding level lines and curvatures. LLAS evolution, smoothed level lines and curvature map after filtering.

7.5.2 Geometric Shapes

The same improvements can be demonstrated on the geometric drawings of Figures 7.18, 7.19 and 7.20. A straight oblique line appears serrated because of its pixel representation. Thus the right angle that it forms with another line is simply lost in clutter: there are locally right angles everywhere.

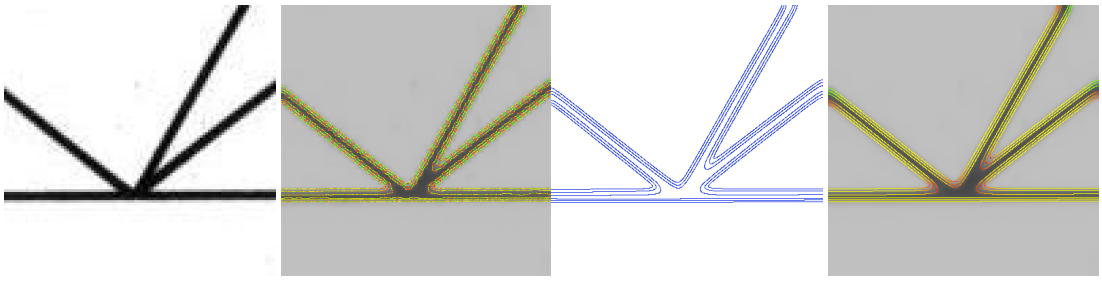

Figure 7.18: Image and corresponding curvatures, smoothed level lines and curvatures after LLAS filtering.

When a curve stops onto another curve, T-junctions or Y-junctions are created. In such cases, our perception tends to interpret the interrupted curve as the boundary of some object undergoing occlusion. In the image on the left of Figure 7.19, which is a typical Kanizsa experiment demonstrating our layered perception, one tends to see a grey rectangle on top of a black polygon. The T-junctions creating this layered illusion can be detected by their adjacent positive and negative curvatures. Note that a short time smoothing is necessary to extract these meaningful curvatures from the clutter of oscillating curvatures due to the staircase effect.

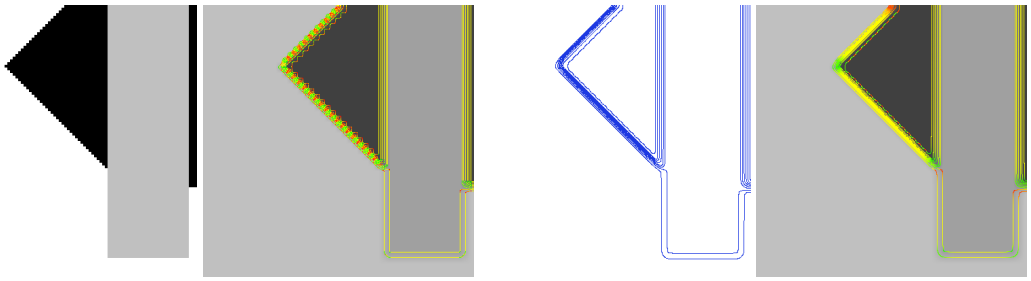

Figure 7.19: Original image, non-filtered curvatures, smoothed level lines by LLAS and curvature map.

Another series of typical experiments was dedicated by Kanizsa to the transparency illusion, by which, in presence of X-junctions, our perceptions infers the presence of two objects on top of each other, the upper one being transparent. For instance the left image of Figure 7.20 is spontaneously described by viewers as a grey transparent disk in front of a black wedge. Kanizsa [Kan79] pointed out the paradox of such a description, which sees two objects where there are in fact four regions with different grey levels. The local configuration responsible for the transparency illusion is the X-junction, seen as the apparent crossing of the boundaries of the disk and of the black wedge. As illustrated after applying LLAS to the figure, X junctions can be detected as a particular configuration of adjacent negative, positive, and zero curvatures.

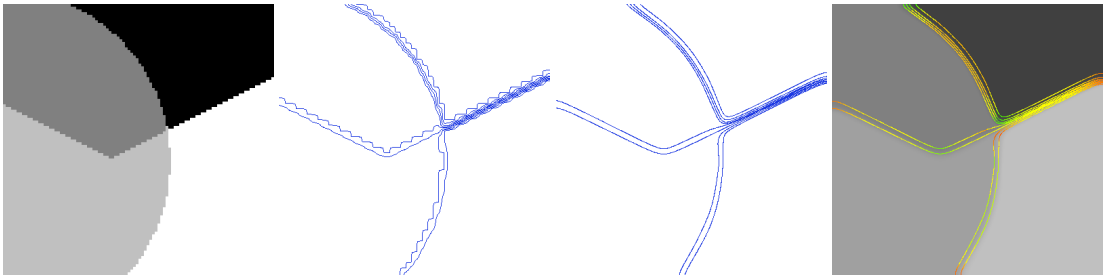

Figure 7.20: Original image and extracted bilinear level lines, smoothed level lines and curvature map.

7.5.3 Graphics and Aliasing

Aliasing due to pixelization is common in scanned documents. As illustrated by all experiments, LLAS can be used for a graphic quality improvement smoothing contours. This is actually done at the cost of smoothing out corners and junctions, but this smoothing is necessary to single them out as the stable peaks of curvature. All in all, in most zoomed-in figures the improvement is manifest, starting with the laughing mouse of Figure 7.21.

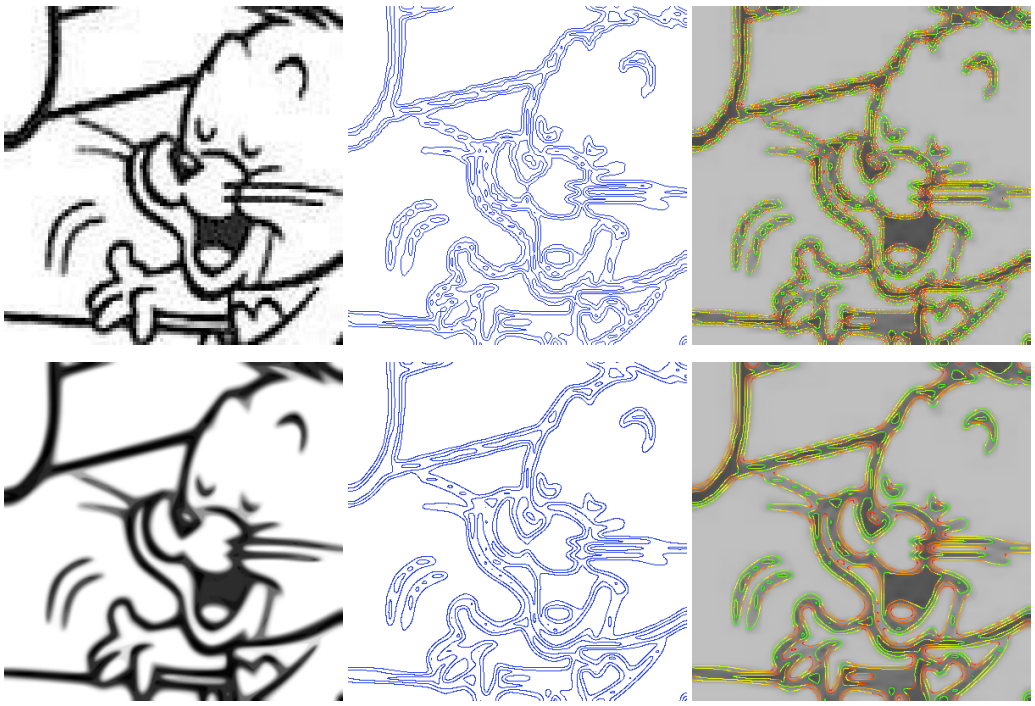

Figure 7.21: Top: original image, its corresponding level lines and curvatures. Bottom: LLAS evolution, smoothed level lines and curvature map after filtering.

A decent recovery is possible even with badly pixelized shapes such as the one reproduced in Figure 7.22. This drawing is not perfectly restored because of the fattening effect at junctions, but it definitely improves on the original, and opens the way to a geometric analysis that would be impossible on the original.

But the example in Figure 7.23 demands the impossible. Although some undulating curves

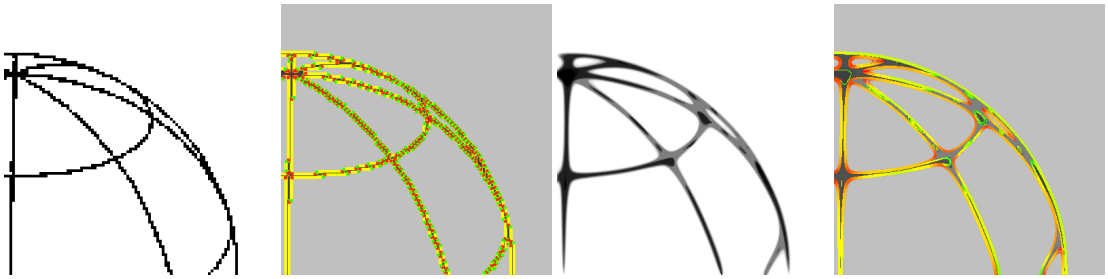

Figure 7.22: Original image and its corresponding curvatures. LLAS evolution and curvature map after filtering.

still may be figured out by an intelligent viewer, the figure locally is nothing but a checkerboard at pixel size. Thus the curvature motion removes all squares, black and white, and creates a huge fattening effect.

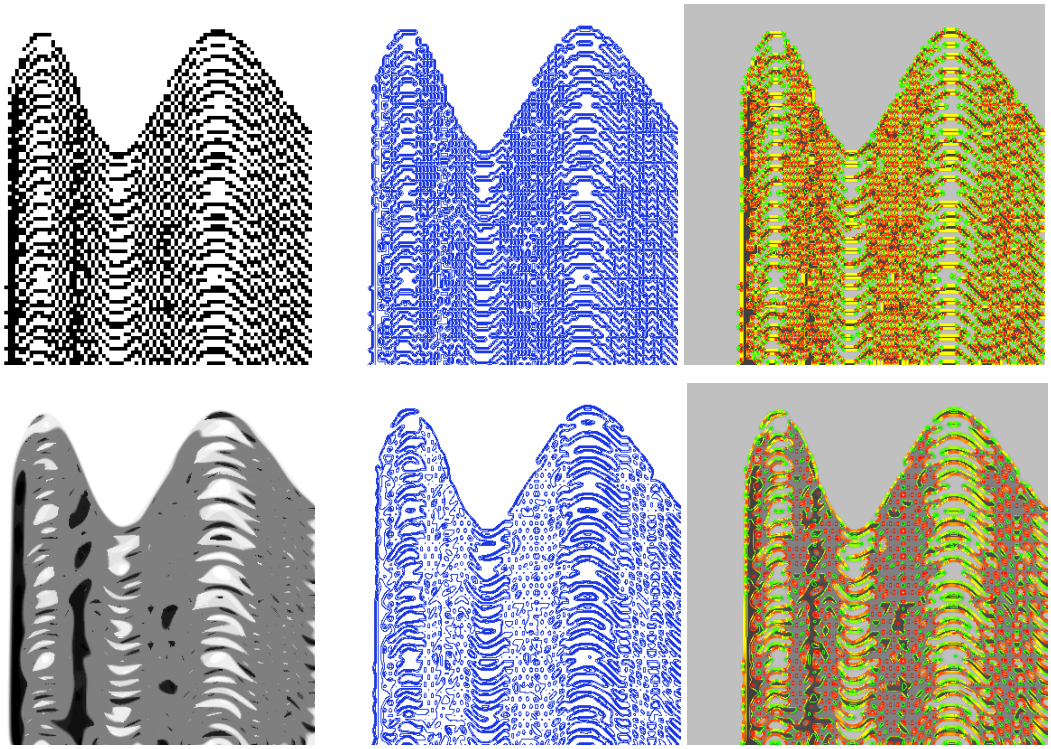

Figure 7.23: Top: original image, its corresponding bilinear level lines and curvatures. Bottom: LLAS evolution, smoothed level lines and curvature map after filtering.

7.5.4 Pre-attentively Undiscriminable Textons

Julesz conjectured in his second texture perception theory [Jul81] that two different textures cannot be pre-attentively discriminated if they have the same texton density. For instance the Julesz patterns in Figure 7.24 are different, but have the same "texton densities", namely the same number of bars, corners, and terminators. After filtering, the microscopic curvature

map will permit to compute a density of positive, negative and zero curvatures.

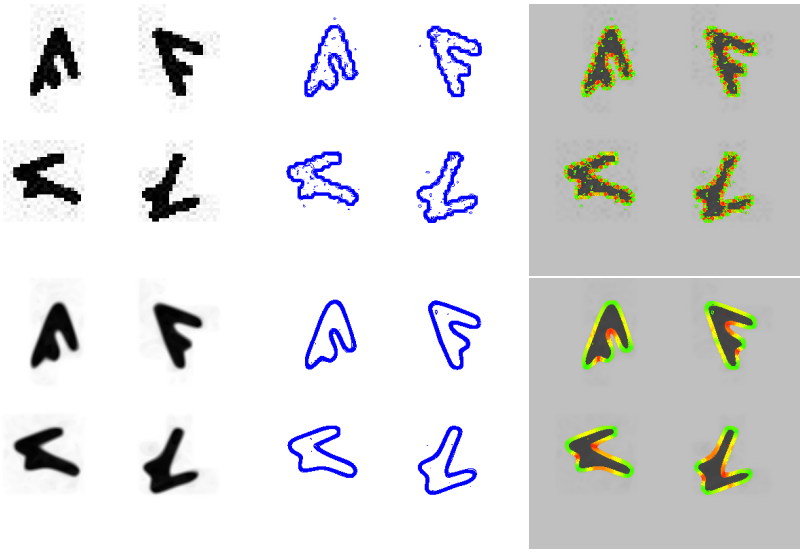

Figure 7.24: Top: original image, its corresponding level lines and curvatures. Bottom: LLAS evolution, smoothed level lines and curvature map after filtering.

7.5.5 Bacteria Morphologies

Bacteria shapes are determined by the bacterial cell wall and cytoskeleton. The curvature is an intrinsic geometrical descriptor, useful for shape discrimination. In Figure 7.25 we display bacterial morphologies and the corresponding curvature map. Bacteria porosities are characterized by strong curvature oscillations, whereas the borders of bacterial shapes present smooth curvature variations. In microbiology, many tasks involve the counting of geometrically simple objets. An accurate curvature filter permits to make curvature statistics.

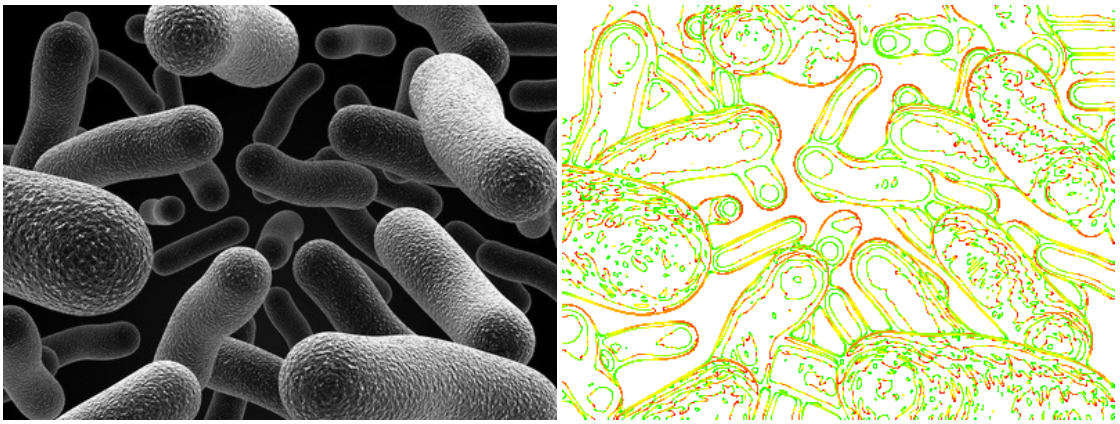

(a) (b)

Figure 7.25: (a). Original image (b). Curvature Map

7.5.6 Topography

Digital elevation models represent ground surface topography. Gray levels indicate ground elevation (lightest shades for highest elevations) and therefore the image level lines are true level lines. As can be seen in Figure 7.26, the set of level lines of a digital image is a natural representation of the shape contents, because it provides topological information invariant to contrast changes. The bilinear interpolation is the most local of continuous interpolations preserving the order between the gray levels of the image. Because the interpolation is continuous, level lines with different gray levels never touch. However, they are concatenations of pieces of hyperbolae and straight segments and hence present oscillations along transverse contours. A short time smoothing reduces the oscillations and straightens up the edges. The remaining curvature extrema after filtering become relevant as geometric shape descriptors.

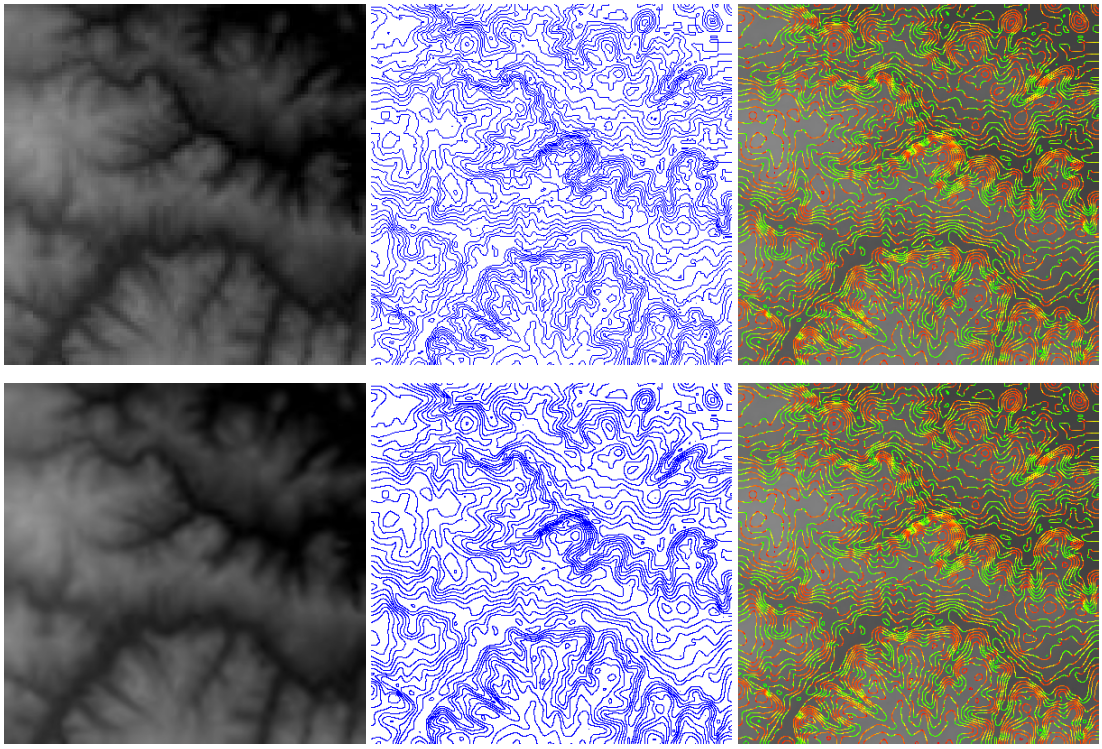

Figure 7.26: Top: digital elevation map, its corresponding level lines (for once a real topographic map) and non-filtered curvature map. Bottom: smoothed image, affine smoothed level lines and filtered curvature map.

The fragment of scanned map in Figure 7.27 is exemplary, in its amount of ringing, aliasing, and JPEG artifacts. Such graphic images are satisfactorily restored with short time affine smoothing. The essential ingredient in restoring graphic image, is to remove the lines distortion without creating new level lines. This requirement is respected to the letter by LL(A)S, which only smooths out existing level lines.

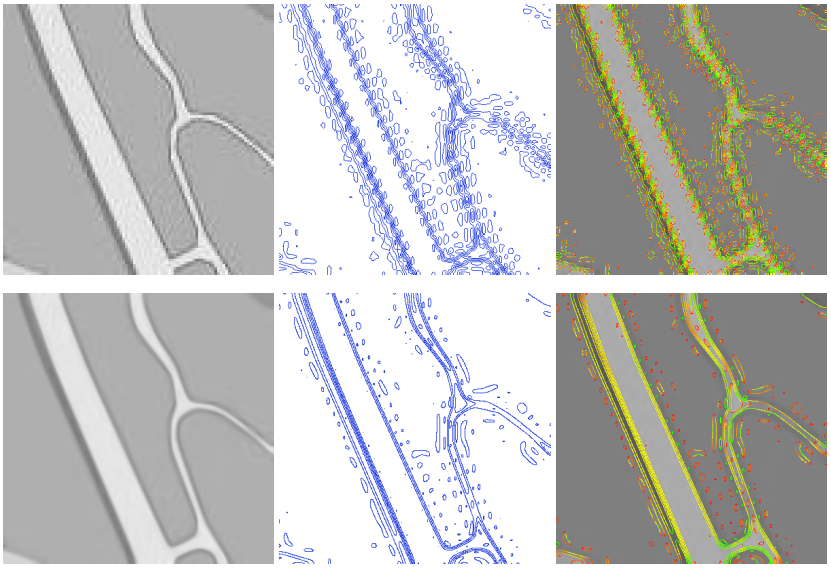

Figure 7.27: Top: Piece of map with roads and its corresponding level lines and curvature map before filtering; smoothed image, shortened level lines and curvature map after filtering.

7.5.7 Textures

Figures 7.28 and 7.29 illustrate the potential use of LLAS to restore the image micro-geometry and to facilitate the identification of smoothly varying shapes in a texture.

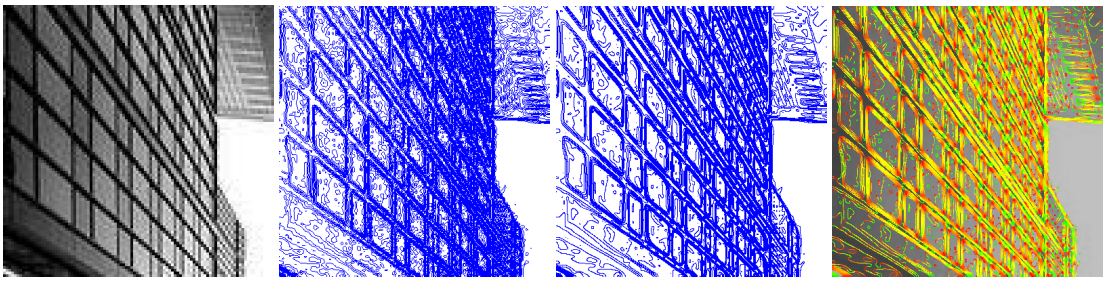

Figure 7.28: Original image, extracted level lines, smoothed level lines and curvature map.

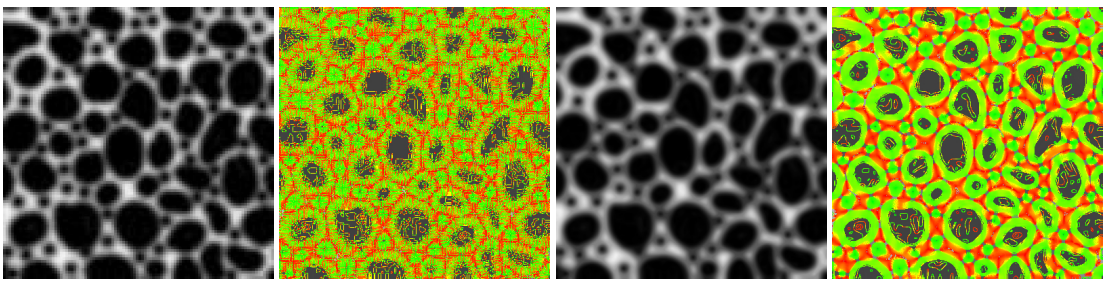

Figure 7.29: Original image and its curvature map, filterd image and its curvature map.

7.5.8 Paintings

Even on details of paintings, this geometric analysis can be relevant. As already mentioned, the LLAS evolution can be used for noise reduction and picture restoration. In Figure 7.30 the desaliasing successfully restores the paint strokes and improves for example the perception of the pearls and of their shadows.

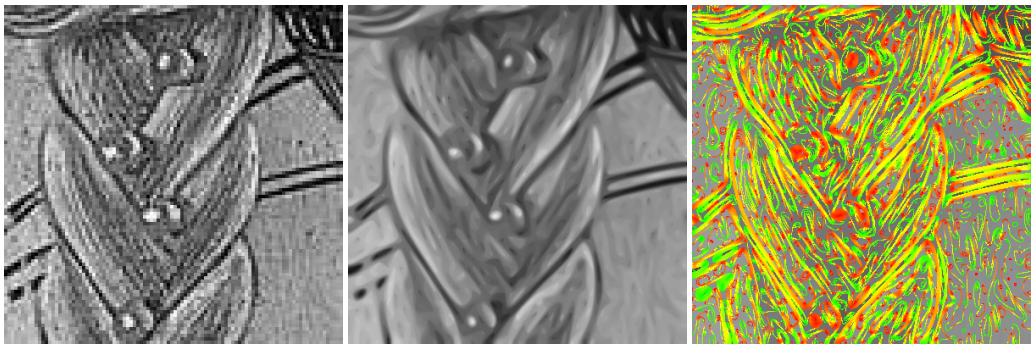

Figure 7.30: Original photo-painting, LLAS evolution and curvature map after filtering.

Leonardo's portrait of Mona Lisa is remarkable for its *sfumato* technique of soft shaded modeling. The stylistic motifs are reflected in the fact that level lines fall widely apart like if it were a very blurry image. The experiment of Figure 7.31 demonstrates the amazing sparsity of visual information in the Mona Lisa.

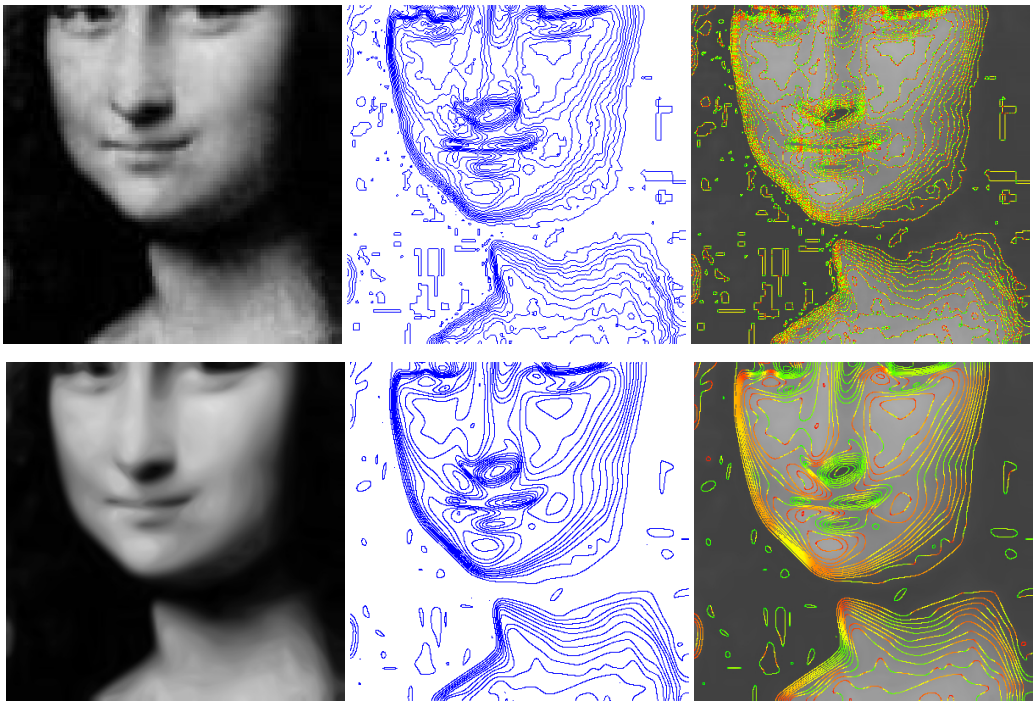

Figure 7.31: Extraction with zoom of *Mona Lisa* photograph, its corresponding level lines and curvatures. LLAS evolution, affine smoothed level lines and curvature map after filtering.

7.5.9 Text Processing

The same good effects are observable with pixelized written text. After the application of LLAS the image in Figure 7.32 retrieve a curvature signature that is obviously usable for handwriting recognition. To that aim the *causality* of the process is essential: no creation of new levels and no creation of new curvatures.

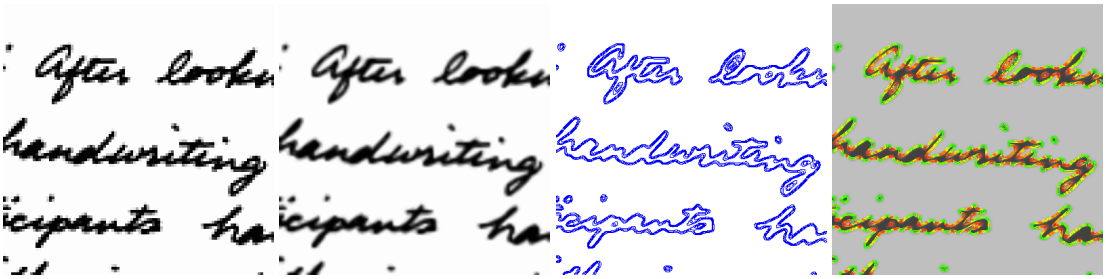

Figure 7.32: Original image, LLAS evolution, smoothed level lines and curvature map after filtering.

7.5.10 Fingerprints Restoration and Discrimination

Minutiae such as cores, bifurcations and ridge endings characterize uniquely fingerprints. Their detection requires a careful smoothing, particularly to avoid a spurious diffusion mixing the ridges. The main objective of smoothing is to sieve the curvature extrema. Indeed, many are present everywhere on the ridge borders before smoothing. The main objective of smoothing is to sieve the curvature extrema, which allow the fingerprint discrimination. LLAS

Figure 7.33: Original fingerprint, Level Lines Affine Shortening and its Curvature map.

removes these ridge border oscillations and provides a smooth version of the fingerprint on which the curvature map locates its characteristic points. Observe in Figure 7.33 that the subpixel smoothing tears apart ridges and emphasizes crossovers, unlike pixel evolutions, when ridge endings shrink fast, and islands and crossovers diffuse.

7.6 Conclusion

Full contrast invariance can be restored by the stack filters based on finite difference schemes but they are not sufficient at any scale. Numerical motions based on pixel approximation are quantized, and in particular blind to small curvatures. This drawback was overcome by evolving independently the level curves of the image and by reconstructing from them a new image which has exactly these level lines.

The first outcome of the Level lines Shortening algorithm is the evolved image, which presents some sort of denoising, simplification, and desaliasing. But the main outcome is an accurate curvature estimate on all level lines. As a visualization tool, the fact that all level lines are polygons with real coordinates allows to zoom in the image at an arbitrary resolution. This is necessary to explore visually the intricacy of the local image structure. Hence the name of *curvature microscope* given to the final visualization.

There is no chance whatsoever of extending the approach proposed here to 3D images. In 3D the level surfaces evolving by curvature motion can generate singularities. They cannot be efficiently parameterized. The state of the art is therefore to use the Osher-Sethian level set method. Thanks to Grayson's theorem, the 2D case has a very peculiar structure which has been taken advantage of.

Bibliography

[AB86] H. Asada and M. Brady. The curvature primal sketch. *IEEE Transactions on Pattern Analysis and Machine Intelligence*, 8(1):2–14, 1986. 13, 131

[AGLM93] L. Alvarez, F. Guichard, P.-L. Lions, and J.-M. Morel. Axioms and fundamental equations of image processing. *Arch. Rational Mech. Anal.*, 123(3):199–257, 1993. 13, 132, 134

[AM99] L. Alvarez and J.-M. Morel. Formalization and computational aspects of image analysis. *Acta Numerica*, pages 1–59, 1999. 140

[Ama03] Anna Lisa Amadori. Nonlinear integro-differential evolution problems arising in option pricing: a viscosity solutions approach. *Differential Integral Equations*, 16(7):787–811, 2003. 36, 47

[App04] David Applebaum. Lévy processes—from probability to finance and quantum groups. *Notices Amer. Math. Soc.*, 51(11):1336–1347, 2004. 26

[App09] David Applebaum. *Lévy processes and stochastic calculus*, volume 116 of *Cambridge Studies in Advanced Mathematics*. Cambridge University Press, Cambridge, second edition, 2009. 26

[Ari06] Mariko Arisawa. A new definition of viscosity solutions for a class of second-order degenerate elliptic integro-differential equations. *Ann. Inst. H. Poincaré Anal. Non Linéaire*, 23(5):695–711, 2006. 37, 47

[Ari07] Mariko Arisawa. Corrigendum for the comparison theorems in: "A new definition of viscosity solutions for a class of second-order degenerate elliptic integro-differential equations" [Ann. Inst. H. Poincaré Anal. Non Linéaire **23** (2006), no. 5, 695–711; mr2259613]. *Ann. Inst. H. Poincaré Anal. Non Linéaire*, 24(1):167–169, 2007. 37, 47

[AST98] S. B. Angenent, G. Sapiro, and A. Tannenbaum. On the affine heat flow for non-convex curves. *J. Amer. Math. Soc.*, 11:601–634, 1998. 149

[AT96] Olivier Alvarez and Agnès Tourin. Viscosity solutions of nonlinear integro-differential equations. *Ann. Inst. H. Poincaré Anal. Non Linéaire*, 13(3):293–317, 1996. 2, 36, 47

[Att54] F. Attneave. Some informational aspects of visual perception. *Psychological review*, 61(3):183–193, 1954. 13, 130

[ATW93] Fred Almgren, Jean E. Taylor, and Lihe Wang. Curvature-driven flows: a variational approach. *SIAM J. Control Optim.*, 31(2):387–438, 1993. 20

[Bar94] Guy Barles. *Solutions de viscosité des équations de Hamilton-Jacobi*, volume 17 of *Mathématiques & Applications (Berlin) [Mathematics & Applications]*. Springer-Verlag, Paris, 1994. 46

[BBP97] Guy Barles, Rainer Buckdahn, and Etienne Pardoux. Backward stochastic differential equations and integral-partial differential equations. *Stochastics Stochastics Rep.*, 60(1-2):57–83, 1997. 36

[BCI11] Guy Barles, Emmanuel Chasseigne, and Cyril Imbert. Hölder continuity of solutions of second-order non-linear elliptic integro-differential equations. *J. Eur. Math. Soc. (JEMS)*, 13(1):1–26, 2011. 8, 9, 40, 65, 78, 79, 87, 97

[BDL01] Martino Bardi and Francesca Da Lio. Propagation of maxima and strong maximum principle for viscosity solutions of degenerate elliptic equations. I. Convex operators. *Nonlinear Anal.*, 44(8, Ser. A: Theory Methods):991–1006, 2001. 46

[BDL03] Martino Bardi and Francesca Da Lio. Propagation of maxima and strong maximum principle for viscosity solutions of degenerate elliptic equations. II. Concave operators. *Indiana Univ. Math. J.*, 52(3):607–627, 2003. 46

[BG95] Guy Barles and Christine Georgelin. A simple proof of convergence for an approximation scheme for computing motions by mean curvature. *SIAM J. Numer. Anal.*, 32(2):484–500, 1995. 131, 138, 162

[BI08] Guy Barles and Cyril Imbert. Second-order elliptic integro-differential equations: viscosity solutions' theory revisited. *Ann. Inst. H. Poincaré Anal. Non Linéaire*, 25(3):567–585, 2008. 3, 35, 37, 47, 82, 88

[BK05a] Richard F. Bass and Moritz Kassmann. Harnack inequalities for non-local operators of variable order. *Trans. Amer. Math. Soc.*, 357(2):837–850 (electronic), 2005. 38, 81

[BK05b] Richard F. Bass and Moritz Kassmann. Hölder continuity of harmonic functions with respect to operators of variable order. *Comm. Partial Differential Equations*, 30(7-9):1249–1259, 2005. 38

[BKR01] Fred Espen Benth, Kenneth Hvistendahl Karlsen, and Kristin Reikvam. Optimal portfolio selection with consumption and nonlinear integro-differential equations with gradient constraint: a viscosity solution approach. *Finance Stoch.*, 5(3):275–303, 2001. 37

[BL02] Richard F. Bass and David A. Levin. Harnack inequalities for jump processes. *Potential Anal.*, 17(4):375–388, 2002. 38

[Bou66] Nicolas Bourbaki. *Elements of mathematics. General topology. Part 1*. Hermann, Paris, 1966. 152

[Bra78] Kenneth A. Brakke. *The motion of a surface by its mean curvature*, volume 20 of *Mathematical Notes*. Princeton University Press, Princeton, N.J., 1978. 149

[BS91] G. Barles and P. M. Souganidis. Convergence of approximation schemes for fully nonlinear second order equations. *Asymptotic Analysis*, 4:271–283, 1991. 140, 141

[BS01] G. Barles and P. E. Souganidis. Space-time periodic solutions and long-time behavior of solutions to quasi-linear parabolic equations. *SIAM J. Math. Anal.*, 32(6):1311–1323 (electronic), 2001. 3, 12

[BSS93] G. Barles, H. M. Soner, and P. E. Souganidis. Front propagation and phase field theory. *SIAM J. Control Optim.*, 31(2):439–469, 1993. 14, 150

[Cao03] F. Cao. *Geometric Curve Evolution and Image Processing*. Number 1805 in Lecture Notes in Mathematics. Springer Verlag, February 2003. 138

[CC93] Luis A. Caffarelli and Antonio Córdoba. An elementary regularity theory of minimal surfaces. *Differential Integral Equations*, 6(1):1–13, 1993. 20

[CC95] Luis A. Caffarelli and Xavier Cabré. *Fully nonlinear elliptic equations*, volume 43 of *American Mathematical Society Colloquium Publications*. American Mathematical Society, Providence, RI, 1995. 39

[CCM96] V. Caselles, B. Coll, and J.-M. Morel. A Kanizsa program. *Progress in Nonlinear Differential Equations and their Applications*, 25:35–55, 1996. 15, 132, 172

[CCM99] Vicent Caselles, Bartomeu Coll, and Jean-Michel Morel. Topographic maps and local contrast changes in natural images. *Int. J. Comput. Vision*, 33:5–27, September 1999. 172

[CCM03] Ballester Coloma, Vicent Caselles, and Pascal Monasse. The tree of shapes of an image. volume 9, pages 1–18, 2003. 173

[CCV] Luis Caffarelli, Chi Hin Chan, and Alexis Vasseur. Regularity theory for nonlinear integral operators. preprint. 38, 81

[CEL84] M. G. Crandall, L. C. Evans, and P.-L. Lions. Some properties of viscosity solutions of Hamilton-Jacobi equations. *Trans. Amer. Math. Soc.*, 282(2):487–502, 1984. 149

[CGG91] Yun Gang Chen, Yoshikazu Giga, and Shun'ichi Goto. Uniqueness and existence of viscosity solutions of generalized mean curvature flow equations. *J. Differential Geom.*, 33(3):749–786, 1991. 13, 131, 134, 149, 162

[Cha04] Antonin Chambolle. An algorithm for mean curvature motion. *Interfaces Free Bound.*, 6(2):195–218, 2004. 20

[CI90] Michael G. Crandall and Hitoshi Ishii. The maximum principle for semicontinuous functions. *Differential Integral Equations*, 3(6):1001–1014, 1990. 2, 37, 47

[CIL92] Michael G. Crandall, Hitoshi Ishii, and Pierre-Louis Lions. User's guide to viscosity solutions of second order partial differential equations. *Bull. Amer. Math. Soc. (N.S.)*, 27(1):1–67, 1992. 2, 37, 47, 134, 149

[Cio] Adina Ciomaga. On the strong maximum principle for second order nonlinear parabolic integro - differential equations. *submitted*. 5, 79

[CL83] Michael G. Crandall and Pierre-Louis Lions. Viscosity solutions of Hamilton-Jacobi equations. *Trans. Amer. Math. Soc.*, 277(1):1–42, 1983. 13, 149

[CL96] Michael G. Crandall and Pierre-Louis Lions. Convergent difference schemes for nonlinear parabolic equations and mean curvature motion. *Numer. Math.*, 75(1):17–41, 1996. 140, 141

[CLM+08] Frédéric Cao, José-Luis Lisani, Jean-Michel Morel, Pablo Musé, and Frédéric Sur. *A theory of shape identification*, volume 1948 of *Lecture Notes in Mathematics*. Springer-Verlag, Berlin, 2008. 14

[CM] Adina Ciomaga and Jean-Michel Morel. A proof of equivalence between level lines shortening and curvature motion in image processing. *submitted*. 147

[CM02] F. Cao and L. Moisan. Geometric computation of curvature driven plane curve evolutions. *SIAM Journal on Numerical Analysis*, pages 624–646, 2002. 138

[CM10a] V. Caselles and P. Monasse. *Geometric Description of Images as Topographic Maps*, volume 1984 of *Lecture Notes in Mathematics*. Springer, 2010. 16, 18, 150, 153, 171, 173, 177

[CM10b] Adina Ciomaga and Marco Mondelli. Image filtering techniques based on finite difference schemes for mean curvature motion and affine morpological scale space. *Image Processing On Line Journal*, 2010. 140

[CMM10] Adina Ciomaga, Pascal Monasse, and Jean-Michel Morel. Level lines shortening yields an image curvature microscope. In *Proceedings of the International Conference on Image Processing, ICIP 2010, September 26-29, Hong Kong, China*, pages 4129–4132, 2010. 15

[CMM11] Adina Ciomaga, Pascal Monasse, and Jean-Michel Morel. An image curvature microscope. *SIAM Multiscale Modeling and Simulation*, page to appear, 2011. 171

[CMMM] Adina Ciomaga, Lionel Moisan, Pascal Monasse, and Jean-Michel Morel. Image restoration and vizualization by curvature motions. *Image Processing On Line Journal*, submitted. 16, 151

[CN08] A. Chambolle and M. Novaga. Implicit time discretization of the mean curvature flow with a discontinuous forcing term. *Interfaces Free Bound.*, 10(3):283–300, 2008. 20

[Cov08] Jérôme Coville. Remarks on the strong maximum principle for nonlocal operators. *Electron. J. Differential Equations*, pages No. 66, 10, 2008. 8, 46, 48

[CRS10] L. Caffarelli, J.-M. Roquejoffre, and O. Savin. Nonlocal minimal surfaces. *Comm. Pure Appl. Math.*, 63(9):1111–1144, 2010. 20, 81

[CS09] Luis Caffarelli and Luis Silvestre. Regularity theory for fully nonlinear integro-differential equations. *Comm. Pure Appl. Math.*, 62(5):597–638, 2009. 8, 12, 38, 81

[CV10] Luis A. Caffarelli and Alexis Vasseur. Drift diffusion equations with fractional diffusion and the quasi-geostrophic equation. *Ann. Math.*, 2(3):1903 – 1930, 2010. 99

[DG57] Ennio De Giorgi. Sulla differenziabilità e l'analiticità delle estremali degli integrali multipli regolari. *Mem. Accad. Sci. Torino. Cl. Sci. Fis. Mat. Nat. (3)*, 3:25–43, 1957. 38, 81

[DL04] Francesca Da Lio. Remarks on the strong maximum principle for viscosity solutions to fully nonlinear parabolic equations. *Commun. Pure Appl. Anal.*, 3(3):395–415, 2004. 8, 46

[ES91] L. C. Evans and J. Spruck. Motion of level sets by mean curvature. I. *J. Differential Geom.*, 33(3):635–681, 1991. 13, 15, 131, 134, 149, 150, 162

[Eva93] Lawrence C. Evans. Convergence of an algorithm for mean curvature motion. *Indiana Univ. Math. J.*, 42(2):533–557, 1993. 131, 138

[Gag83] Michael E. Gage. An isoperimetric inequality with applications to curve shortening. *Duke Math. J.*, 50(4):1225–1229, 1983. 148

[Gag84] M. E. Gage. Curve shortening makes convex curves circular. *Invent. Math.*, 76(2):357–364, 1984. 148

[Gag90] Michael E. Gage. Curve shortening on surfaces. *Ann. Sci. École Norm. Sup. (4)*, 23(2):229–256, 1990. 148

[GG92] Yoshikazu Giga and Shun'ichi Goto. Motion of hypersurfaces and geometric equations. *J. Math. Soc. Japan*, 44(1):99–111, 1992. 149

[GH86] M. Gage and R. S. Hamilton. The heat equation shrinking convex plane curves. *J. Differential Geom.*, 23(1):69–96, 1986. 14, 133, 148, 155

[GM97] F. Guichard and J.-M. Morel. Partial differential equations and image iterative filtering. In I. S. Duff et al., editor, *The State of the Art in Numerical Analysis*, Inst. Math. Appl. Conf. Ser., New Ser. 63, pages 525–562. Institute of Mathematics and its Applications (IMA), Oxford Univ. Press, 1997. 140, 144, 182

[GM00] F. Guichard and J.-M. Morel. Image iterative smoothing and P.D.E.'s. Book in preparation, 2000. 139, 162, 163

[GM02] Maria Giovanna Garroni and Jose Luis Menaldi. *Second order elliptic integro-differential problems*, volume 430 of *Chapman & Hall/CRC Research Notes in Mathematics*. Chapman & Hall/CRC, Boca Raton, FL, 2002. 34

[Gra87] Matthew A. Grayson. The heat equation shrinks embedded plane curves to round points. *J. Differential Geom.*, 26(2):285–314, 1987. 14, 131, 133, 148, 155

[Gra89] Matthew A. Grayson. Shortening embedded curves. *Ann. of Math. (2)*, 129(1):71–111, 1989. 148

[GS] Nestor Guillen and Russell Schwab. Aleksandrov-bakelman-pucci type estimates for integro-differential equations. preprint. 12

[Hui84] Gerhard Huisken. Flow by mean curvature of convex surfaces into spheres. *J. Differential Geom.*, 20(1):237–266, 1984. 149

[IL90] H. Ishii and P.-L. Lions. Viscosity solutions of fully nonlinear second-order elliptic partial differential equations. *J. Differential Equations*, 83(1):26–78, 1990. 2, 8, 9, 37, 40, 47, 78, 87

[Imb05] Cyril Imbert. A non-local regularization of first order Hamilton-Jacobi equations. *J. Differential Equations*, 211(1):218–246, 2005. 37, 38, 47

[Ish89] Hitoshi Ishii. On uniqueness and existence of viscosity solutions of fully nonlinear second-order elliptic PDEs. *Comm. Pure Appl. Math.*, 42(1):15–45, 1989. 2, 37, 47, 149

[Ish95] H. Ishii. A generalization of the Bence, Merriman and Osher algorithm for motion by mean curvature. In *Curvature flows and related topics (Levico, 1994)*, volume 5 of *GAKUTO Internat. Ser. Math. Sci. Appl.*, pages 111–127. Gakkōtosho, Tokyo, 1995. 131, 138

[Jen88] Robert Jensen. The maximum principle for viscosity solutions of fully nonlinear second order partial differential equations. *Arch. Rational Mech. Anal.*, 101(1):1–27, 1988. 2, 37, 47

[JK05] Espen R. Jakobsen and Kenneth H. Karlsen. Continuous dependence estimates for viscosity solutions of integro-PDEs. *J. Differential Equations*, 212(2):278–318, 2005. 3, 37, 47

[JK06] Espen R. Jakobsen and Kenneth H. Karlsen. A "maximum principle for semicontinuous functions" applicable to integro-partial differential equations. *NoDEA Nonlinear Differential Equations Appl.*, 13(2):137–165, 2006. 2, 37, 47

[JLS88] R. Jensen, P.-L. Lions, and P. E. Souganidis. A uniqueness result for viscosity solutions of second order fully nonlinear partial differential equations. *Proc. Amer. Math. Soc.*, 102(4):975–978, 1988. 149

[Jul81] B. Julesz. Textons, the elements of texture perception, and their interactions. *Nature*, 290(5802):91–97, 1981. 196

[Kan79] G. Kanizsa. *Organization in Vision: Essays on Gestalt Perception*. Praeger, 1979. 194

[Kas09] Moritz Kassmann. A priori estimates for integro-differential operators with measurable kernels. *Calc. Var. Partial Differential Equations*, 34(1):1–21, 2009. 38, 81

[KM99] G. Koepfler and L. Moisan. Geometric multiscale representation of numerical images. In *Proc. of the Second International Conference on Scale Space Theories in Computer Vision*, volume 1682 of *Lecture Notes in Computer Science*, pages 339–350, Corfu, Greece, 1999. Springer. 173

[KM02] Z. Krivá and K. Mikula. An adaptive finite volume scheme for solving nonlinear diffusion equations in image processing. *Journal of Visual Communication and Image Representation*, 13(1-2):22–35, 2002. 138

[KN10] Alexander Kiselev and Fedor Nazarov. A variation on a theme of Caffarelli and âĂŕVasseur. 166(1):31–39, 2010. 99

[KvD86] J. J. Koenderink and A. J. van Doorn. Dynamic shape. *Biological Cybernetics*, 53:383–396, 1986. 138

[LMMM00] J.-L. Lisani, L. Moisan, P. Monasse, and J.-M. Morel. Affine invariant mathematical morphology applied to a generic shape recognition algorithm. In *Proceedings of the International Symposium of Mathematical Morphology*, Palo Alto, CA, 2000. Available at `http://pascal.monasse.free.fr/index.html`. 137, 153

[LMMM03] J.L. Lisani, L. Moisan, P. Monasse, and J.M. Morel. On the theory of planar shape. *SIAM Multiscale Modeling and Simulation*, 1(1):1–24, 2003. 173

[LMR01] J.L. Lisani, P. Monasse, and L. Rudin. Fast shape extraction and applications. Technical Report 2001-16, CMLA, ENS Cachan, 2001. 153

[LS05] P.L. Lions and P.E. Souganidis. Homogenization of degenerate second-order pde in periodic and almost periodic environments and applications. *Ann. Inst. H. Poincaré Nonlinear Ann.*, 22(5):667–677, 2005. 12

[LV] Papanicolaou G. Lions, P. L. and S.R.S. Varadhan. Homogenization of Hamilton-Jacobi equations. unpublished work. 4, 12

[MBO92] B. Merriman, J. Bence, and S. Osher. Diffusion generated motion by mean curvature. *J. E. Taylor, Editor, Computational Crystal Growers Workshop*, pages 73–83, 1992. 131, 138

[MC10] Marco Mondelli and Adina Ciomaga. On finite difference schemes for curvature motions. *Proceedings of the International Conference on Image Processing*, 2010. 140

[MG98] P. Monasse and F. Guichard. Fast computation of a contrast invariant image representation. *IEEE Trans. on Image Proc*, 9:860–872, 1998. 15, 17, 132, 177

[MM86] A. Mackworth and F. Mockhtarian. Scale-based description and recognition of planar curves and two-dimensional shapes. *IEEE Trans. Pattern Analysis and Machine Intell.*, 8(1):34–43, 1986. 14, 131, 133

[MM92] A. Mackworth and F. Mockhtarian. A theory of multiscale, curvature-based shape representation for planar curves. *IEEE Trans. Pattern Analysis and Machine Intell.*, 14:789–805, 1992. 133, 136, 179

[Moi98] Lionel Moisan. Affine plane curve evolution: a fully consistent scheme. *IEEE Trans. Image Process.*, 7(3):411–420, 1998. 14, 132, 136, 174, 179

[MS87] P. Maragos and R. W. Schafer. Morphological filters. Part II: Their relations to median, order-statistic, and stack filters. *IEEE Trans. Acoust. Speech Signal Process.*, 35:1170–1184, 1987. 144

[MŠ99] Karol Mikula and Daniel Ševčovič. Solution of nonlinearly curvature driven evolution of plane curves. *Appl. Numer. Math.*, 31(2):191–207, 1999. 137

[MŠ01] Karol Mikula and Daniel Ševčovič. Evolution of plane curves driven by a nonlinear function of curvature and anisotropy. *SIAM J. Appl. Math.*, 61(5):1473–1501 (electronic), 2001. 137

[MSC+06] P. Musé, F. Sur, F. Cao, Gousseau Y., and Morel J.-M. An a contrario decision method for shape element recognition. *International Journal of Computer Vision*, 69:295–315, 2006. 137

[Nas58] J. Nash. Continuity of solutions of parabolic and elliptic equations. *Amer. J. Math.*, 80:931–954, 1958. 38, 81

[Nir53] Louis Nirenberg. A strong maximum principle for parabolic equations. *Comm. Pure Appl. Math.*, 6:167–177, 1953. 46

[NR97] Gawtum Namah and Jean-Michel Roquejoffre. Convergence to periodic fronts in a class of semilinear parabolic equations. *NoDEA Nonlinear Differential Equations Appl.*, 4(4):521–536, 1997. 3

[Obe06] Adam M. Oberman. Convergent difference schemes for degenerate elliptic and parabolic equations: Hamilton-Jacobi equations and free boundary problems. *SIAM J. Numer. Anal.*, 44(2):879–895 (electronic), 2006. 139

[OS88] S. Osher and J. A. Sethian. Fronts propagating with curvature-dependent speed: algorithms based on Hamilton-Jacobi formulations. *J. Comput. Phys.*, 79(1):12–49, 1988. 13, 131, 143, 149

[Pha98] Huyên Pham. Optimal stopping of controlled jump diffusion processes: a viscosity solution approach. *J. Math. Systems Estim. Control*, 8(1):27 pp. (electronic), 1998. 37

[PS97] F. Pollick and G. Sapiro. Constant affine velocity predicts the 1/3 power law of planar motion perception and generation. *Vision Research*, 37(3):347–353, 1997. 136

[Say91a] Awatif Sayah. Équations d'Hamilton-Jacobi du premier ordre avec termes intégro-différentiels. I. Unicité des solutions de viscosité. *Comm. Partial Differential Equations*, 16(6-7):1057–1074, 1991. 2, 36, 47

[Say91b] Awatif Sayah. Équations d'Hamilton-Jacobi du premier ordre avec termes intégro-différentiels. II. Existence de solutions de viscosité. *Comm. Partial Differential Equations*, 16(6-7):1075–1093, 1991. 2, 36, 47

[SCB97] Guillermo Sapiro, Albert Cohen, and Alfred M. Bruckstein. A subdivision scheme for continuous-scale B-splines and affine-invariant progressive smoothing. *J. Math. Imaging Vision*, 7(1):23–40, 1997. 136

[Sch] Russell Schwab. Stochastic homogenization for some nonlinear integro-differential equations. preprint. 12

[Ser82] J. Serra. *Image Analysis and Mathematical Morphology*. Academic Press, San Diego, CA, 1982. 144

[Set99] J. A. Sethian. *Level set methods and fast marching methods*, volume 3 of *Cambridge Monographs on Applied and Computational Mathematics*. Cambridge University Press, Cambridge, second edition, 1999. Evolving interfaces in computational geometry, fluid mechanics, computer vision, and materials science. 149

[Sila] Luis Silvestre. Hölder estimates for advection fractional-diffusion equations. preprint. 11, 99

[Silb] Luis Silvestre. On the differentiability of the solution to an equation with drift and fractional diffusion. preprint. 11, 99

[Sil06] Luis Silvestre. Hölder estimates for solutions of integro-differential equations like the fractional Laplace. *Indiana Univ. Math. J.*, 55(3):1155–1174, 2006. 8, 81

[Sme03] Peter Smereka. Semi-implicit level set methods for curvature and surface diffusion motion. *J. Sci. Comput.*, 19(1-3):439–456, 2003. Special issue in honor of the sixtieth birthday of Stanley Osher. 143

[Son86a] Halil Mete Soner. Optimal control with state-space constraint. I. *SIAM J. Control Optim.*, 24(3):552–561, 1986. 2, 36, 47

[Son86b] Halil Mete Soner. Optimal control with state-space constraint. II. *SIAM J. Control Optim.*, 24(6):1110–1122, 1986. 2, 36, 47

[Son93] Halil Mete Soner. Motion of a set by the curvature of its boundary. *J. Differential Equations*, 101(2):313–372, 1993. 14, 150

[ST93a] G. Sapiro and A. Tannenbaum. Affine invariant scale space. *IJCV*, 11(1):25–44, 1993. 14, 132, 134, 149

[ST93b] Guillermo Sapiro and Allen Tannenbaum. On invariant curve evolution and image analysis. *Indiana Univ. Math. J.*, 42(3):985–1009, 1993. 134, 149

[ST94] Guillermo Sapiro and Allen Tannenbaum. On affine plane curve evolution. *J. Funct. Anal.*, 119(1):79–120, 1994. 134, 149

[Woy01] Wojbor A. Woyczyński. Lévy processes in the physical sciences. In *Lévy processes*, pages 241–266. Birkhäuser Boston, Boston, MA, 2001. 66

Vita

Adina Giorgiana Ciomaga was born in Huşi, Romania, on March 24^{th} 1983. She graduated from the University *Alexandru Ioan Cuza* Iaşi, Romania in June 2006. She got her Masters degree in *Mathematics, Vision and Learning* in September 2007 at *Ecole Normale Superieure de Cachan* and her Masters degree in *Fundamental Mathematical Structures* at the University *Alexandru Ioan Cuza* Iaşi, in February 2009. In October 2007, she started her PhD Thesis at *Ecole Normale Superieure de Cachan*, France. Starting September 2011, she will be a postdoc at *the University of Chicago*.